12-2012

Hydrothermal Chemistry of the M(I,II)/PAHA/Anion System

Kari Ann Darling
Syracuse University

ABSTRACT

This research encompasses the detailed investigation of the design and synthesis of metal organic framework (MOF) materials involving the M(I,II)/ polyazaheterocycle/anion system in order to expand our understanding of the principles which render the chemistry more controllable and predictable. In addition, this research investigates the development of properties in these classes of compounds. Furthermore, it has been demonstrated that hydrothermal reaction conditions of stoichiometry, pH, and temperature can influence the identity of the products.

The structural versatility of the M(I,II)/polyazaheterocycle/anion system for M = Cu(I,II), Co(II), Ni (II), Zn (II), and Cd(II) and where the anion is F^-, Cl^-, I^-, OH^-, SO_4^{2-}, or PO_4^{3-}, is a reflection of the many structural determinants at play. These include factors such as: (i) the variety of coordination polyhedra available to the metal, (ii) variable modes of coordination associated with the azole(ate) ligands, (iii) the role of functional substituents on the azolate moiety, (iv) the incorporation and coordination preferences of secondary anionic components (X^{n-} or XO_m^{n-}) and (v) the variable incorporation of solvent molecules.

The structural chemistry of these materials is quite complex, as evidenced by the range of component substructures observed including a range of chains, layers, frameworks, and embedded metal/azolate clusters. In addition, many of the products exhibited interesting magnetic properties. While a number of recurring structural motifs have been observed, the remarkable array of structures of materials in this study underlines the difficulty in predicting product composition and the challenge in rational design of framework materials. It is anticipated that the continued elaboration of a structural data base for these complex hierarchical materials will evolve into a structural systematic.

Hydrothermal Chemistry of the M(I,II)/Polyazaheteroaromic/Anion System: Structural Consequences of Coordinating Anions

By

Kari A. Darling

B.S. Lake Superior State University, 2008

DISSERTATION

Submitted in partial fulfillment of the requirements for the

Degree of Doctor of Philosophy in Chemistry

In the Graduate School of Syracuse University

December 2012

ACKNOWLEDGEMENTS

This work would not have been possible without the guidance, support, and patience of Professor Jon Zubieta. His intellect and character provide a constant source of inspiration.

In addition, the Zubieta Lab has provided a welcoming and enlightening atmosphere to embark on this journey. I owe them my most sincere gratitude.

Above all else, I thank my family, who make this experiement of life worthwhile.

Table of Contents

List of Figures

List of Tables

Chapter 1: Introduction

1.1 Introduction

Coordination polymers, a term that first appeared in the 1960's,[1] are defined as metal-ligand compounds that extend infinitely in one-, two-, or three-dimensions via covalent metal-ligand bonding. These hybrid organic-inorganic materials, often referred to as metal organic frameworks or MOFs, are constructed from metal nodes or clusters bridged by organic linkers and are often shown to have high surface areas, tunable pore sizes, and tunable surfaces.[4] **(see Figure 1.1)**. The last two decades have witnessed exponential growth in the syntheses and studies of these materials and, given the diversity of organic molecules, MOFs can exhibit a plethora of structures and properties, giving them a wide array of potential applications.[2-22] Because such materials are usually formed by self-assembly, however, the resulting structures are often quite difficult to control and understand as compared to conventional organic chemistry.

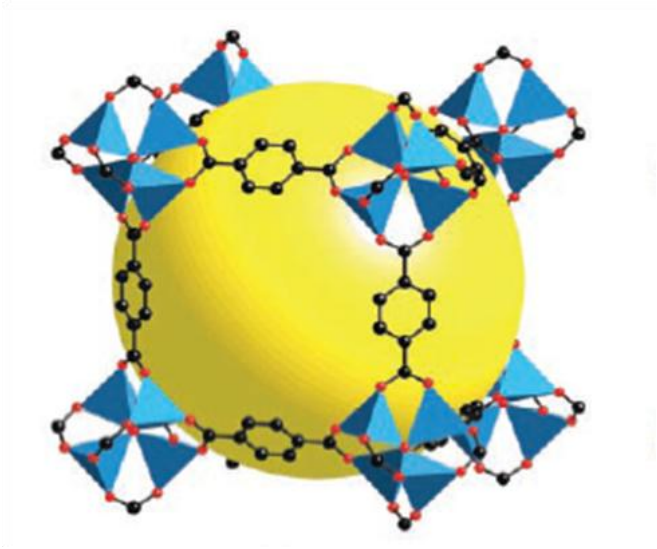

Figure 1.1: A MOF composed of zinc acetate building units and dicarboxylate linker ligands.[4]

The synthetic rules and mechanisms of metal organic frameworks require exploration so as to gain control over design and eventually function of the resulting products. However, while

organic chemists possess incredible control over synthesis on a molecular scale, predictable synthesis of hybrid composites remains a "synthetic wasteland" in the words of Roald Hoffman.[23] Hoffman states that because control of synthesis of framework solid state materials remains an elusive task, it is an important growth point for future study.

Coordination polymers not only represent a creative approach to design of new materials for structural research purposes, but as noted, the unusual and often improved features of these hybrid inorganic-organic materials give rise to numerous applications.[2-22] Since these materials are composed of metal ions or clusters that are connected through molecular bridges, properties inherent to both the inorganic and organic components may be manifested. The inorganic ions or clusters offer magnetic, optical, and dielectric properties as well as thermal stability and mechanical hardness, while manipulation of the organic component allows for tailoring and functionalization of the products.[2-22] The result is a synergistic combination of properties from both the inorganic as well as the organic moieties, giving rise to materials with enhanced or even novel properties and function for use in technological applications in areas as diverse catalysis, gas storage, drug delivery, luminescence, magnetism, imaging, and chemical separations.[21] It is no surprise, then, that chemists wish to control and rationally design these materials to introduce or enhance functionality.

1.2 Early Developments of Metal Organic Frameworks

Over the decades, countless solids have been described that contain metal ions linked by organic molecular moieties. This collection of materials has been coined metal-organic frameworks, with much overlap between hybrid organic-inorganic materials, coordination polymers, and organic-containing zeolite analogs. Simply stated, MOFs are coordination-based, crystalline compounds in which metal center nodes are bridged by organic ligands to create a

network structure (**see Figure 1.2**). [24-40] First generation research of MOFs began with simple self-assembly of molecules with metallic centers, largely due to the foundational work of researchers such as Hoskins and Robson,[41,42] who in 1990 reported a design approach to the construction of MOFs using organic molecular ligands and metal ions. This unique combination of organic and inorganic chemistry, two fields often considered separate, has experienced massive growth since the 1990's, as evidenced by the vast number and scope of research papers devoted to this field. [24-40]

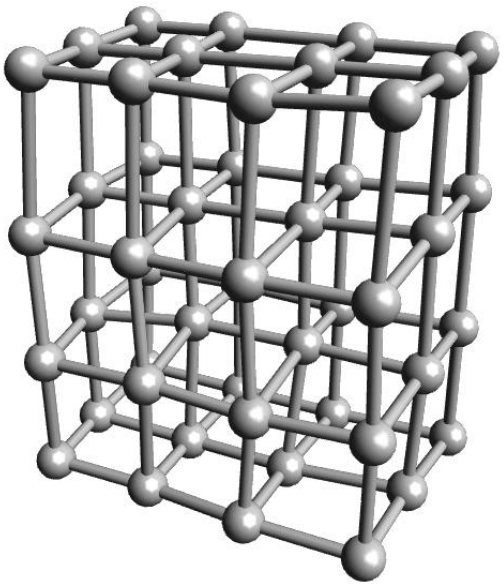

Figure 1.2: A scheme of a MOF, a coordination-based, crystalline compounds in which metal center nodes are bridged by organic ligands to create a network structure.

Second generation research in the field is characterized by the introduction of rigid secondary building units in some form of organic linker.[40] It is this combination and potential synergistic interaction of the two components of a MOF that provides promise for a wide variety of properties and applications (**see Figure 1.3**). Design and synthesis of compounds begins with selection of these two building units where functionality can arise from either the organic or inorganic entities, or even from the nature of connection between them. In this way, MOFs

posses a high degree of synthetic flexibility which gives rise to a potential to tune their properties. Interest in using these materials in fields such as gas storage, separation, luminescence, and catalysis is therefore rapidly accelerating.[43-64] Steps toward these applications have been reached with several MOF materials now being manufactured and sold as commercial products.[64]

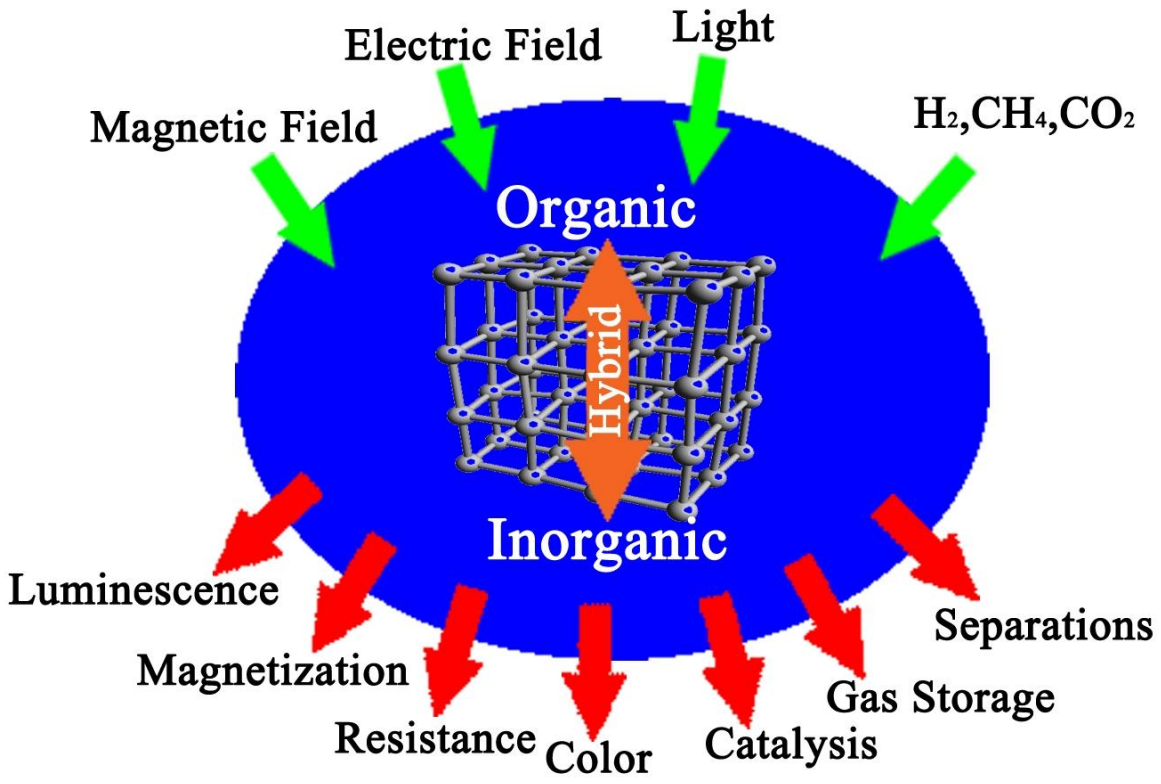

Figure 1.3: Multifunctionality of Metal Organic Frameworks.

MOFs often show symmetrical, aesthetically pleasing chemical structures, many being derived from naturally occurring minerals. To reverse-engineer a target structure from nature, understanding of the underlying geometric principles is fundamentally important. In MOFs, building blocks are carefully chosen to retain certain properties and, in many cases, the vertice connectivity is a large determinant of the product's properties. The design of a material with

specific properties with control over connectivity as well as functionality is therefore a general goal of this research, where it is hoped that the potential for rational design inherent in these materials will result in superior properties.

John Maddox, in a quite famous Nature editorial published in 1988 states, "It remains in general impossible to predict the structure of even the simplest crystalline solids from their known composition".[65] While Maddox's statement regarding problems with crystal structure and design is still true, recent empirical approaches to exploit known and reproducible structural building blocks as a synthetic strategy are seeing success.[66] This 'reticular synthesis' design approach was originally proposed by Yaghi[66] and colleagues and has played a huge part in the development of a systematic study of frameworks in an attempt to determine the effect that slight structural modifications can have on product MOFs. While serendipity admittedly plays a role in the discovery of MOFs with useful properties, it is often times true that once the synthesis of a MOF with useful properties is established, it is possible to reproduce that synthesis using similar building blocks[67,68] and use this as a starting point for a generation of a library of materials with tunable properties.

1.3 Properties and Applications of Metal Organic Frameworks

MOFs are known for their high surface areas, tunable pore size, and tunable surfaces.[69-73] The construction of porous materials with maintained structural stability is one of the most important goals of the synthesis of MOFs and, although porosity is an interesting feature in its own right, a truly functional material must possess a combination of properties. Porous MOFs find applications in a wide array of areas including: ion exchange, gas storage, gas separation, and molecular sieving.[74-95]

1.3.1 Gas Storage

Hydrogen and methane are attractive alternatives to fossil fuels but realistic methods of storage remain problematic. Following the pioneer work of Kitagawa et al.[96,97], open framework materials have shown promise as sorptive materials, resulting in applications in hydrogen or methane gas storage.[98-105] In designing sorptive materials many factors must be taken into consideration such as pore size, pore shape, surface area, and chemical composition. For instance, it has been concluded that along with the necessity of a high surface area, for MOFs to be useful sorbents small interdigiated pores are also desirable.[106] In addition, the inner surface should contain functional groups or open metal sites that can interact with guest molecules.

The Department of Energy has set a goal for hydrogen storage density at near-ambient temperature and amenable pressures at 5.5% by weight by 2017.[107] In order to achieve this, the framework should have a high surface area as well as a high enthalpy of adsorption. The highest H_2 storage capacity reported so far for a MOF is 99.5 mg g^{-1} at 77 K and 56 bar,[108] but these values decrease dramatically at room temperature due to low interaction energies between the H_2 molecules and the framework material. To increase framework surface interaction with hydrogen, a better understanding of the guest-host relationship is needed. In addition, the effects of framework density, catenation, ligand functionalization, and MOF active metal sites[109] on the adsorption process is currently being explored, but developing materials that meet this ambitious DOE goal remains a serious challenge.

1.3.2 Gas Separation

Adsorptive separation is a process by which a mixture is separated based on differences in adsorption/desorption behavior. MOFs have been studied for purposes of separation of molecules based upon both size, as well as adsorptive separation mechanisms.[110-113] Gases in

particular are quite difficult to separate, especially when they have similar radii. Framework materials have the ability to assist in interaction between a guest molecule and the inner surface of the material, giving them significant advantages over zeolites and activated carbon.

MOF materials may also be designed to have fine-tuned pore sizes[114] and surfaces, allowing for synthesis of materials with specific interactions with guest molecules. In addition, the frameworks of MOFs can be flexible in response to the introduction of guest molecules. Materials with this ability to structurally transform, while retaining structural integrity, are quite interesting with regard to adsorptions.[115-119] Such structural flexibility can result in selective guest adsorption, and therefore superior separation properties, which would be difficult to obtain with a more rigid porous material.

1.3.3 Sequestration of Carbon Dioxide

Rising levels of CO_2 in the atmosphere, as a result of emissions from human origins, remains of great environment concern. The addition of CO_2 capture systems to coal-burning plants could reduce this emission. Many current technologies for CO_2 capture, such as zeolites, activated carbon, and aqueous alkanolamine solutions,[120-122] have a large energy price[123] and the development of new materials with proper physical and chemical properties to reduce this cost are quite desirable. A number of performance factors should be considered in the design of CO_2 capture material including high selectivity for pure CO_2, high density storage, and stability during both the capture and regeneration process.[124]

MOFs inherent tunability[114] make them excellent candidates for next-generation carbon dioxide capture materials and some key aspects related to their adsorption of CO_2 include capacity for CO_2, enthalpy of adsorption, and selectivity of CO_2 combined with low regeneration energy. [120,121,125-131] Currently, common strategies for enhancing these properties in MOFs

involve functionalizing the inner surface with nitrogen bases and other strongly polarizing organic functional groups and introduction of exposed metal sites.[132-138]

1.3.4 Catalysis

Catalysis is the acceleration or deceleration of a chemical reaction by means of a substance which is not consumed in the overall reaction. Most solid catalysts are primarily inorganic materials, with vanadyl pyrophosphates, vanadyl phosphates, and microporous zeolites being well known examples.[139-150] Increased interest in environmentally friendly technologies, as well as the economic benefits of catalysis, has led to interest in the development of novel catalysts. Recently, there has been growing interest in the exploitation of MOFs as heterogeneous catalysts and recent reports show promising potential.[151] The objective of such research is not to replace zeolites as the most commonly used industrial catalysts, but rather to fill a number of gaps, such as enantioselective catalysis.[151]

Currently, chiral chemicals are generally prepared using homogenous catalysts, which have a variety of limitations including separation and reuse problems and decrease in activity. Selection of an organic building unit for design and synthesis of a chirally-active MOF may provide a solution to this problem. Evans *et al.* recently reported a homochiral lanthanide-based material that could be used as heterogeneous catalysts in the ring opening of meso-carboxylic acid anhydrides and cyanosilylation of aldehydes.[152] The Kitagawa group recently demonstrated that highly catalytically active MOFs can be synthesized by controlling the functional groups lining the inner channels and therefore the stabilization of intermediates in the catalytic cycle.[153] Post-synthetic modification of existing MOFs to induce chirality is also a growing area of research and maybe be quite useful in synthesis of enantioselective catalysis.[154]

1.3.5 Magnetism

As previously stated in Section 1.2, hybrid organic microporous materials are often constructed from transition metal ions or clusters and as a result of the metal's electron configuration, these materials may have interesting magnetic and optical properties depending quite strongly on the identity and interaction of both the organic linker as well as the metallic center. As magnetic materials find use in memory storage devices, interest in development of materials with increased density and efficiency is quite intense. Hybrid organic-inorganic materials often have paramagnetic centers and such materials have found application in semiconductors, metal conductors, and superconductors[155-158] where delocalized and localized electrons coexist in paramagnetic centers. Of great interest is the development of compounds that exhibit two or more magnetic phenomena, such as ferro-, ferri-, and canted antiferromagnetism.[159,160] In addition, the ability to transition from low spin to high spin as a function of external stimuli such as temperature, pressure, or light is also appealing.[161-167]

Incorporation of a paramagnetic metal or open-shell organic ligands is not enough to render a material magnetic. For a compound to be magnetic, connection between moment carriers must be within interaction range, rendering MOFs excellent candidates for magnetically interesting materials. The majority of magnetic frameworks to date contain first row transition metals, although magnetism can also be introduced by the incorporation of guest molecules with a nonmagnetic framework. The interactions that lead to magnetism often result in a wide range of other phenomena including conductivity and optical properties and this combination can render the material as multifunctional with applications in optical sensors or semiconductors, respectively. This multifunctionality is a general goal of novel MOF materials, as noted previously.

1.3.6 Optical Properties

In addition to their magnetic potential, MOFs provide an avenue for crystal engineering optically-active compounds and MOFs exhibiting photoluminescence and fluorescence have seen attention in recent years.[168-171] Luminescent MOFs are quite promising as multifunctional materials for chemical sensors, LEDs, and biomedicine.[172-184] One advantage of MOFs is the ability to simultaneously tune both the inorganic and organic components where light emission in these compounds can arise from either component individually or through their connection.[185-189] The introduction of guest molecules into the framework that can emit or induce luminescence provides yet another avenue for development of optically active MOFs.[190,191] Again, preparation of multifunctional MOFs is a general goal and the porosity of MOFs allows for reversible storage of guest molecules,[192-194] setting these hybrid materials apart from traditional organic or inorganic luminescent materials. This luminescence, combined with their permanent porosity, could find applications in chemical sensors in environmental and biological systems.

1.4 Coordination Chemistry of Materials of the Type M(I,II)/Polyazaheterocycle

Protypical examples of MOF-based materials are constructed from metal nodes or clusters linked through polyfunctional ligands, with carboxylates, polypyridyl, and organophosphonate linkers seeing the most development though the efforts of researcher such as Yaghi, Ferey, and Kitagawa.[195-203] Other ligand types of variable tether lengths, different charge-balance requirements, additional functional groups, and combination and placement of different donor groups are also of interest to further investigate the structural chemistry and resulting properties of the composite materials. Compounds featuring N-donor polyazaheteroaromatic ligands such as pyrazole, imidazole, and triazole (**see Figure 1.4**) have

been largely explored in recent years in the design of organic-inorganic hybrid materials due to a variety of desirable features common in this family of ligands.[204-216]

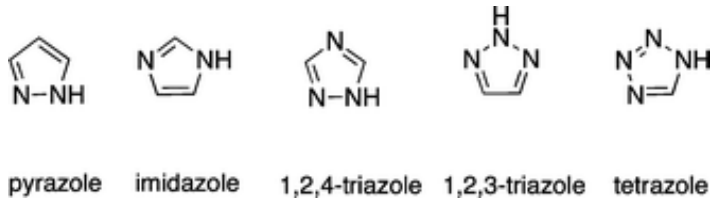

Figure 1.4: Common polyazaheteroaromatic ligands (azolates).

These five-membered ring ligands feature a number of nitrogen donor groups and can exist as both neutral and anionic, resulting in a variety of possible coordination modes and unusual structural diversity. Deprotonation of the ligand not only results in the ability for all nitrogen atoms to coordinate with metal ions, but also further increases the basicity of the donors, resulting in a high thermal and chemical stability of products, an important issue for practical applications of coordination polymers. This family of ligands has proven to be attractive in the construction of complex hybrid architectures due to this ability to bridge multiple metal centers combined with their super exchange capacity, and their often facile derivitization to allow introduction of additional functionality.[204-216]

As an organic building unit, 1,2,4 triazole can serve to bridge metal centers via N1,N2 coordination, resulting in one-dimensional chains as common building units. The N4 nitrogen of the ligand then serves as another point of attachment and provides expanded dimensionality of the products, with the two-dimensional [Cu(trz)][217] being a prototypical example (**see Figure 1.5**). In addition to the rich structural chemistry that results from these numerous coordination sites, triazolate-containing transition metal coordination compounds tend to exhibit interesting magnetic and optical properties.[231,232] Furthermore, the synthesis of materials with close

interaction between closed d shell cations such as Cu(I) and Zn(II) provides an avenue for synthesis frameworks with luminescent properties.

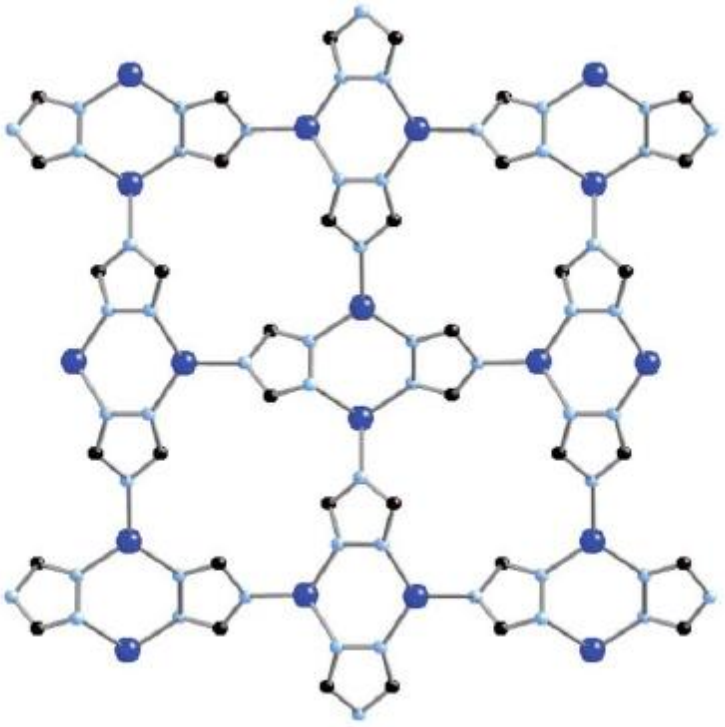

Figure 1.5: The two dimensional [Cu(trz)].

Previous studies in the Zubieta group of the chemistry of triazole with transition metal cations focused on materials of the general type: (i) M(I,II)/triazolate and (ii) M(I,II)/triazolate/anion,[204-216] where the anion could include a halogen, hydroxide, oxyanion, or a more complex metal oxide cluster. Over the course of these studies, it was determined that the identity of the anion has dramatic consequences over both the structure and properties of the products and that a focus on the effects of anion incorporation is desirable in indentifying structural trends in these compounds.

A quite simple example of the structural consequences of anion incorporation is found comparing the structures of [Cu(trz)] and $[Cu_3(trz)_3\text{-}(OH)_3(H_2O)_4]$.[217] The 2D network of [Cu(trz)] consists of $\{Cu_2(trz)_2\}$ clusters linked through the N4 position of triazolate.

Incorporation of hydroxide anion into the second structure, however, results in a dramtically different structural motif for $[Cu_3(trz)_3\text{-}(OH)_3(H_2O)_4]$ (**see Figure 1.6a**). In this case the three dimensional material contains trinuclear $\{Cu_3(\mu\text{-}OH)(trz)_3(OH)_2(H_2O)_4\}$ building units (**see Figure 1.6b**). Within the triangular unit the Cu sites are bridged by N1,N2 triazolates as well as a triply bridging central oxy group. The adjacent trinuclear units are linked through the N4 triazolate donors.

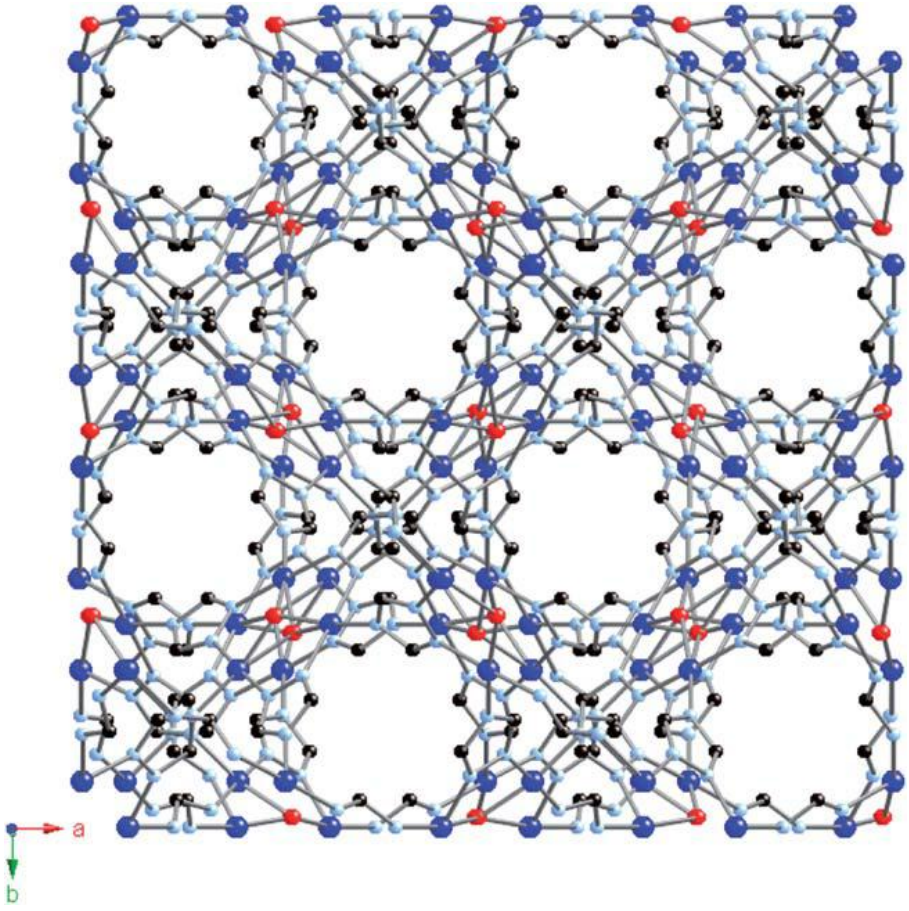

(a)

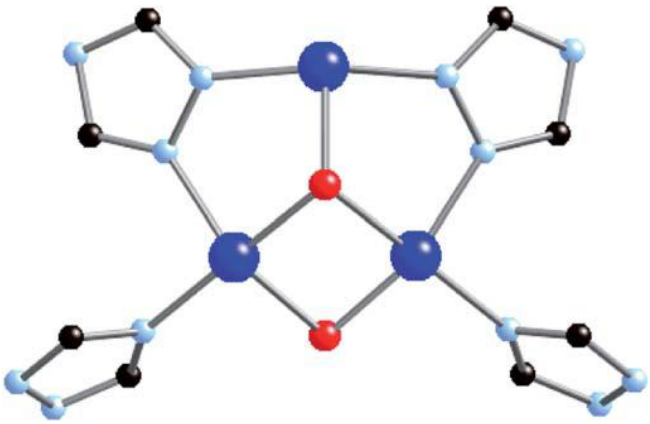

(b)

Figure 1.6: (a) The three dimensional structure of $[Cu_3(trz)_3\text{-}(OH)_3(H_2O)_4]$, emphasizing the void volume. (b) The trinuclear $\{Cu_3(\mu\text{-}OH)(trz)_3(OH)_2(H_2O)_4\}$ building units of $[Cu_3(trz)_3\text{-}(OH)_3(H_2O)_4]$.

The range of component substructures revealed by these materials includes layers, chains, clusters, cages and even three dimensional frameworks (**see Figure 1.7**)[217] and this is reflected in the physical properties of the products. For materials of the type Cu(II)/triazole/anion, magnetism is consistent with fitting models based upon building units of the composite material (whether it be triangular units, linear triangular units, pentamer units, 1D chains, etc).

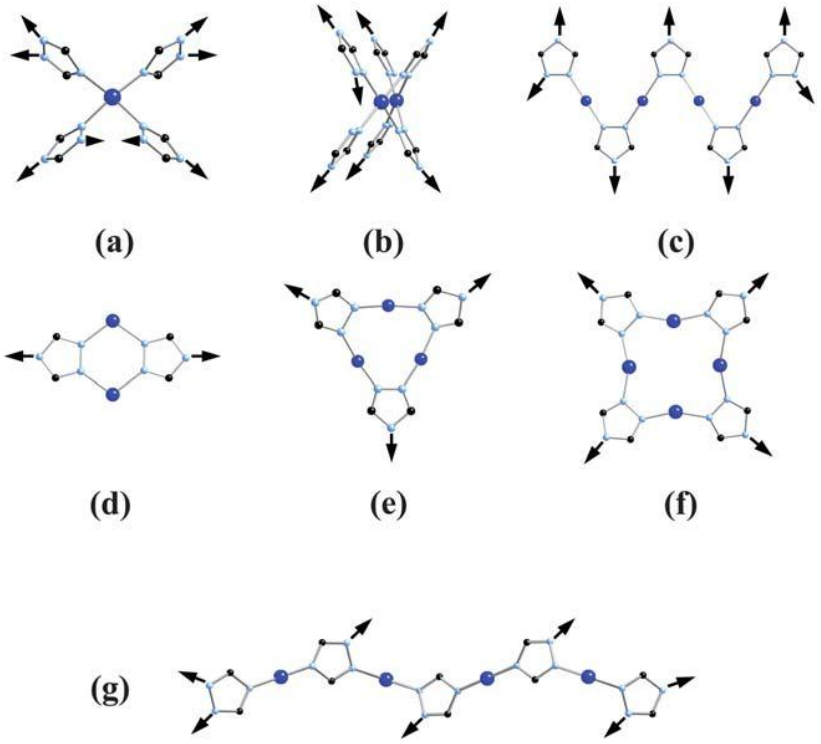

Figure 1.7: Common coordination modes of triazolate, resulting in a variety of different cluster, chain, layer, and even framework building units.

1.5 Hybrid Materials of the M(I,II)/Polyazaheterocycle/Anion System

As an extension of the structural study of the M(I,II)/triazole and M(I,II)/triazole/anion systems, focus on the structural chemistry of materials featuring 4-pyridyl tetrazole, which can be considered an extended analog of triazole, is desired. The additional nitrogen donors of the derivatized tetrazolate linker ligand allows for a variety of different bridging modes. For instance, the pyridyltetrazole (ate) ligand has been shown to adopt a variety of coordination and bridging modes ranging from monodentate terminal to bridging through one pyridyl and four tetrazolate nitrogen donors (**see Figure 1.8**).

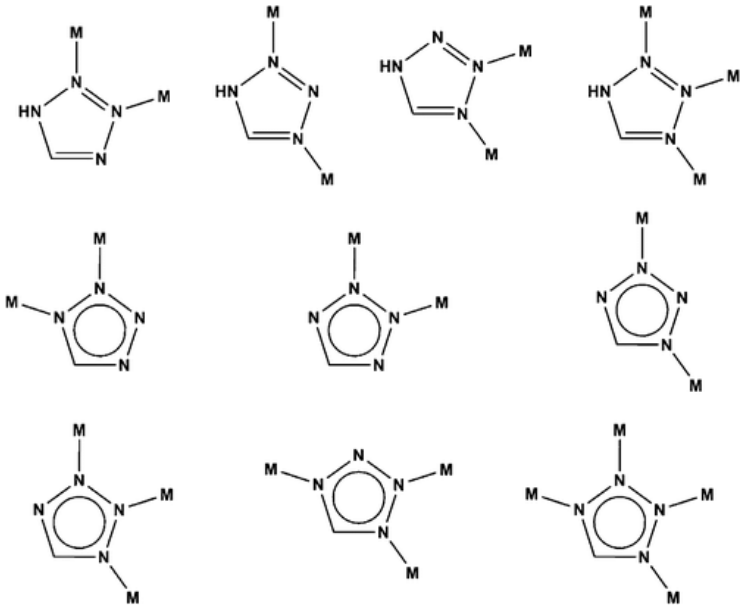

(a)

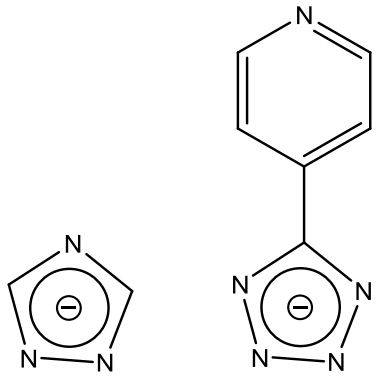

(b)

Figure 1.8: (a) The variety of different possible coordination modes of tetrazolate ligands; (b) 4- pyridyltetrazole as an extended analog of 1,2,4- triazole.

1.5.1 Azolate Moities with Functionalized Substituents

The structural consequences of modification of the pyridyl nitrogen donor location and the replacement of a pyrazine group for the pyridyl substituent can also be examined, where the ligands can adopt a variety of bridging and chelating modes. Synthesis of a ligand that replaces a pyridyl ring with a carboxylate functionality is also attractive in that this multi-functional ligand

could serve to bridge the gap between the growing fields of carboxylate and azolate chemistry. Furthermore, in a study analogous of that to frameworks containing carboxylate linker ligands, the secondary building unit (in the case a tetrazolate-containing secondary building unit or SBU) could be expanded by insertion of tethering groups, and therefore result in expansion of the coordination domain of the ligand (**see Figure 1.9**).

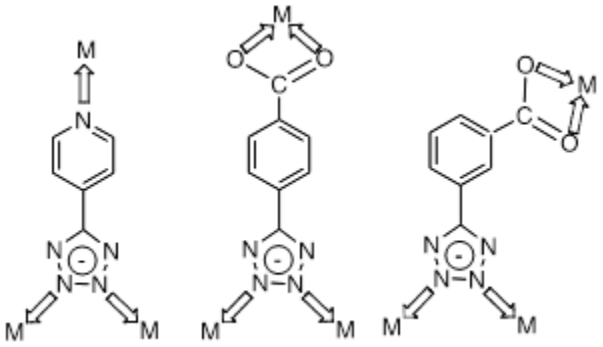

(a)

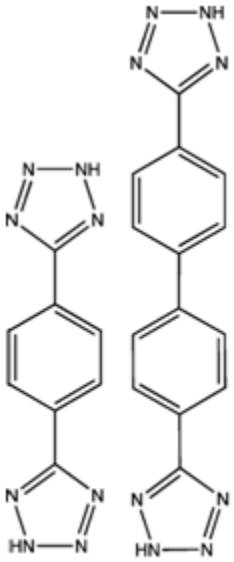

(b)

Figure 1.9: (a) Replacement of a pyridyl ring with a carboxylate functionality as a multi-functional ligand. (b) Expansion of the coordination domain of a tetrazolate ligand through insertion of tethering groups.

1.5.2 Incorporation of an Anionic Component

An array of architectures and substructures are observed for M(II)/triazolate materials which is further enhanced by the introduction of auxiliary coordinating anions, whether simple halides X^- or pseudohalides (such as CN^-) or oxyanions. The synergism of bridging triazolate and the observed effectiveness of the anionic components in adopting bridging modes provides complex, highly dimensional materials and suggests the need for a paralleled investigation of the structural consequences of the introduction of a variety of different charge balancing subunits as well. Materials featuring anions including F^-, Cl^-, I^-, OH^-, SO_4^{2-}, or PO_4^{3-} are desirable, where the incorporation of the secondary anionic component is predicted to have dramatic structural consequences on the products due to the tendency of these anionic components to adopt a variety of different coordination modes.

As only a small region of space has been investigated in transition metal/azolate coordination chemistry, a more systematic and thorough structural study is necessary if common structural motifs are to be identified. This could be further elaborated through investigation of additional factors such as: (i) the identity of and variety of coordination polyhedra available to the metal, (ii) variable modes of coordination associated with the azole(ate) ligands, (iii) the role of functional substituents on the azolate moiety, (iv) the incorporation and coordination preferences of secondary anionic components (X^{n-} or XO_m^{n-}) and (v) the variable incorporation of solvent molecules. It is possible that a variety of structural trends may be realized and also that more complicated variants could exist.

1.6 Hydrothermal Synthesis

Hydrothermal synthesis is an effective method for the preparation of x-ray quality single crystals of hybrid organic-inorganic materials. In the temperature domain of conventional

hydrothermal methods, the reactants are solubilized while retaining their structural features in the product phases.[233-240] Hydrothermal reactions, typically carried out in the temperature range 120-200 ^{o}C under autogenous pressure, exploit the self assembly of the product from soluble precursors. The reduced viscosity of water under these conditions enhances diffusion processes so that solvent extraction of solids and crystal growth from solution are favored. Since problems associated with different solubilities of organic and inorganic starting materials are minimized, a variety of precursors may be introduced, as well as a number of organic and/or inorganic structure-directing or charge-balancing reagents. Several reaction parameters including temperature, time, pH, stoichiometry, and presence of a mineralizer are easily varied.

1.7 General Research Considerations

The scope of this research encompasses the detailed investigation of the design, synthesis, and structural influence of a secondary anionic component on the structure and connectivity of hybrid organic-inorganic materials of the M(I,II)/polyazaheterocycle/anion system. In addition to the structural chemistry, magnetic properties were also examined. The structural versatility of this family of compounds is a reflection of the many structural determinants at play including the identity and coordination environment of the transition metal cation, the variety of coordination modes associated with the azolate moiety, the role of additional functional groups on the ligand, the variable coordination modes of anion components, and the hydrothermal reaction parameters themselves. Our understanding of both synthetic conditions as well as design strategies of solid state materials remains rudimentary and further exploration of the synthetic conditions outlined above is essential. It is hoped that by further adding to the library of hybrid organic-inorganic materials, an understanding of the mechanisms governing these complex systems may be attained. It is by this effort that we seek to one day

predict products based upon rational design strategy so as to tune materials for specific applications.

1.8 References

1. Bailar, J.C. Preparative Inorganic Reaction; Interscience: New York, **1964**.
2. Chen, B.; Ockwig, N.W.; Millward, A.R.; D.S. Contreras, D.S.; O.M. Yaghi, O.M., *Angew. Chem., Int. Ed.* **2005**, *44*, 4745.
3. Janiak, C., *Dalton Trans.* **2003**, 2781-2804, and references therein.
4. Eddaoudi, M.; Kim, J.; Rosi, N.; Vodak, D.; Wachter, J.; O'Keeffe, M.; Yaghi, O. M. *Science* **2002**, *295*, 469.
5. Zou, R.; Abdel-Fattah, A. I.; Xu, H.; Zhao, Y.; Hickmott, D. D. *CrystEngComm* **2010**, *12*, 1337.
6. Ma, S. Q.; Zhou, H. C. *Chem. Commun*. **2010**, *46*, 44.
7. Wang, Z.; Chen, G.; Ding, K. L. *Chem. Rev.* **2009**, *109*, 322.
8. Isaeva, V. I.; Kustov, L. M. *Pet. Chem.* **2010**, *50*, 167.
9. Ma, L. Q.; Abney, C.; Lin, W. B. *Chem. Soc. Rev.* **2009**, *38*, 1248.
10. Corma,A.;Garcia,H.;Xamena, F.X. L. *Chem. Rev.* **2010**, *110*, 4606.
11. Farrusseng, D.; Aguado, S.; Pinel, C. *Angew. Chem., Int. Ed.* **2009**, *48*, 7502.
12. Liu, Y.; Xuan, W. M.; Cui, Y. *Adv. Mater.* **2010**, *22*, 4112.
13. Zhao,D.; Yuan,D.Q.; Zhou,H.C. *Energy Environ. Sci.* **2008**, *1*, 222.
14. Hu, Y. H.; Zhang, L. Adv. Mater. **2010**, *22*, E117.
15. Murray, L. J.;Dinca,M.; Long, J.R. *Chem. Soc. Rev.* **2009**, *38*, 1294.
16. Dinca, M.; Long, J. R. *Angew. Chem., Int. Ed.* **2008**, *47*, 6766.
17. Hedin, N.; Chen, L. J.; Laaksonen, A. *Nanoscale* **2010**, *2*, 1819.
18. Choi, S.; Drese, J. H.; Jones, C. W. *ChemSusChem* **2009**, *2*, 796.

19. Ferey, G.; Serre, C.; Devic, T.; Maurin, G.; Jobic, H.; Llewellyn, P. L.; De Weireld, G.; Vimont, A.; Daturi, M.; Chang, J.-S. *Chem. Soc. Rev.* **2011**, *40*, 550.

20. Huxford, R. C.; Della Rocca, J.; Lin, W. B. *Curr. Opin. Chem. Biol.* **2010**, *14*, 262.

21. Li, J. R.; Kuppler, R. J.; Zhou,H.C.*Chem. Soc. Rev.* **2009**, *38*, 1477.

22. Phan, A.; Doonan, C. J.; Uribe-Romo, F. J.; Knobler, C. B.; O'Keeffe, M.; Yaghi, O. M. *Acc. Chem. Res*. **2010**, *43*, 58.

23. Hoffman, R. *Scientific American*, Feb. **1993**, 65-73

24. Kitagawa, S.; Noro, S., *Compr. Coord. Chem. II* **2004**, *7*, 231.

25. Yaghi, O.M.; O'Keeffe, M.; Ockwig, N.W.; Chae, H.K.; Eddaoudi, M.; Kim, J., *Nature* **2003**, *423*, 705.

26. James, S.L., *Chem. Soc. Rev*. **2003**, *32*, 276.

27. Rao, C.N.R.; Natarajan, S.; Vaidhyanathan, R., *Angew. Chem., Int. Ed*. **2005**, *43*, 1466.

28. Kitagawa, S.; Kitaura, R.; Noro, S.-I., *Angew. Chem., Int. Ed*. **2004**, *43*, 2334.

29. Papaefstathiou, G.S.; MacGillivray, L.R., *Coord. Chem. Rev*. **2003**, *246*, 169.

30. Papaefstathiou, G.S.; MacGillivray, L.R., *Coord. Chem. Rev*. **2003**, *246*, 169.

31. Finn, R.C.; Haushalter, R.C.; Zubieta, J., *Prog. Inorg. Chem*. **2003**, *51*, 421.

32. Vioux, A.; LeBideau, J.; Mutin, P.H.; Leclercq, D., *Top. Curr. Chem*. **2004**, *232*, 145.

33. Clearfield, A., Curr. Opin. Solid State Mater. Sci. **2003**, 6, 495.

34. Clearfield, A., *Prog. Inorg. Chem*. **1998**, *47*, 371.

35. Alberti, G. in *Comprehensive Supramolecular Chemistry*, J.L. Atwood, J.E.D. Davies, D.D. MacNicol and F. Vogtle, ed., Pergamon Press, New York, **1996**, vol. 7, G. Alberti, T. Bein, ed. 151.

36. Ferey, G., *Chem. Mater*. **2001**, *13*, 3084.

37. Farrusseng, D.; Aguado, S.; Pinel, C., *Angew. Chem., Int. Ed*. **2009**, *48*, 7502–7513.

38. Zheng, B.; Bai, J.; Duan, J.; Wojtas, L.; Zaworotko, M.J., *J. Am. Chem. Soc*. **2011**, *133*, 748.

39. Sumida, K.; Brown, C.R.; Herm, Z.R.; Chavan, S.; Bordiga, S.; Long, J.R., *Chem. Commun*. **2011**, *47*, 1157.

40. Eddaoudi, M.; Moler, D.B.; Li, H.L.; O'Keefe, M.; Yaghi, O.M., *Acc. Chem. Res.* **2001**, *34*, 319-330.

41. Hoskins, B. F.; Robson, R.; *J. Am. Chem. Soc*., **1990**, *112*, 1546-1554

42. Robson, R.; Abrahams, F.; Liu, J.P.; *ACS Symp. Ser.* **1992**, *499*, 256-271

43. Chen, B.; Ockwig, N.W.; Millward, A.R.; D.S. Contreras, D.S.; O.M. Yaghi, O.M., *Angew. Chem., Int. Ed*. **2005**, *44*, 4745.

44. Rowsell, J.L.C.; Yaghi, O.M., *Angew. Chem., Int. Ed*. **2005**, *44*, 4670.

45. Bradshaw, D.; Claridge, J.B.; Cussen, E.J.; Prior, T.J.; Rosseinsky, M.J., *Acc. Chem. Res*. **2005**, *38*, 273.

46. Rosseinsky, M.J., *Microporous Mesoporous Mater*. **2004**, *73*, 15.

47. Cingolani, A.; Galli, S.; Masciocchi, N.; Pandolfo, L.; Pettinari, C.; Sironi, A., *J. Am. Chem. Soc*. **2005**, *127*, 6144.

48. Ohmori, O.; Kawano, M.; Fujita, M., *Angew. Chem., Int. Ed*. **2005**, *44*, 1962.

49. Lee, E.Y.; Jang, S.Y.; Suh, M.P., *J. Am. Chem. Soc*. **2005**, *127*, 6374.

50. Noro, S.-I.; Kitagawa, S.; Kondo, M.; Seki, K., *Angew. Chem., Int. Ed*. **2000**, *39*, 2081.

51. Wang, Z.; Zhang, B.; Kurmoo, M.; Green, M.A.; Fujiwara, H.; Otsuka, T.; Kobayashi, H., *Inorg. Chem*. **2005**, *44*, 1230.

52. Kim, H.; Suh, M.P., *Inorg. Chem*. **2005**, *44*, 810.

53. Sudik, A.C.; Millward, A.R.; Ockwig, N.W.; Cote, A.P.; Kim, J.; Yaghi, O.M., *J. Am. Chem. Soc*. **2005**, *127*, 7110.

54. Kitaura, R.; Kitagawa, S.; Kubtoa, Y.; Kobayashi, T.C.; Kindo, K.; Mita, Y.; Matsuo, A.; Kobayashi, M.; Chang, H.-C.; Ozawa, T.C.; Suzuki, M.; Sakata, M.; Takata, M., *Science* **2002**, *298*, 2358.

55. Bradshaw, D; Prior, T.J.; Cussen, E.J.; Claridge, J.B.; Rosseinsky, M.J., *J. Am. Chem. Soc*. **2004**, *126*, 6106.

56. Kepert, C.J.; Prior, T.J.; Rosseinsky, M.J., *J. Am. Chem. Soc*. **2000**, *122*, 5158.

57. Halder, G.J.; Kepert, C.J.; Moubaraki, B.; Murray, K.S.; Cashion, J.D., *Science* **2002**, *298*, 1762.

58. Evans, O.R.; Ngo, H.L.; Lin, W., *J. Am. Chem. Soc*. **2001**, *123*, 10395.

59. Sanchez, C.; Lebeau, B.; Chaput, F.; Boilet, J.P., *Adv. Mater*. **2003**, *15*, 1969.

60. Evans, O.R.; Lin, W., *Chem. Mater*. **2001**, *13*, 3009.

61. Jannasch, P., Curr. Opin. Colloid Interface Sci. **2003**, 8, 96.

62. Javaid, A.; Hughey, M.P.; Varutbangkul, V.; Ford, D.M., *J. Membr. Sci*. **2001**, *187*, 141.

63. Honma, I.; Nomura, S.; Nakajima, H., *J. Membr. Sci*. **2001**, *185*, 83.

64. Rowsell, J.L.C.; Millward, A.R.; Park, K.S.; Yaghi, O.M., *J. Am. Chem. Soc*. **2004**, *126*, 5666.

65. Maddox,J.; *Nature* **1988**, *335*, 201.

66. Yaghi, O. M.; O'Keeffe, M.; Ockwig, N. W.; Chae, H. K.; Eddaoudi, M.; Kim, J. *Nature* **2003**, *423*, 705.

67. O'Keeffe, M. *Chem. Soc. Rev.* **2009**, *38*, 1215.

68. Zhao, D.; Timmons, D. J.; Yuan, D.; Zhou, H.-C. *Acc. Chem. Res.* **2011**, *44*, 123.

69. James, S. L. *Chem. Soc. Rev*. **2003**, *32*, 276.

70. Rowsell, J. L. C.; Yaghi, O. M. *Microporous Mesoporous Mater.* **2004**, *73*, 3.

71. Natarajan, S.; Mahata, P. *Chem. Soc. Rev.* **2009**, *38*, 2304.

72. Long, J. R.; Yaghi, O. M. *Chem. Soc. Rev.* **2009**, *38*, 1213.

73. Meek, S. T.; Greathouse, J. A.; Allendorf, M. D. *Adv. Mater.* **2011**, *23*, 249.

74. Czaja,A.U.;Trukhan,N.;Muller,U.*Chem. Soc. Rev.* **2009**, *38*, 1284.

75. Kuppler, R. J.; Timmons, D. J.; Fang, Q. R.; Li, J. R.; Makal, T. A.; Young, M. D.; Yuan, D. Q.; Zhao, D.; Zhuang, W. J.; Zhou, H. C. Coord. Chem. Rev. **2009**, 253, 3042.

76. Zou, R.; Abdel-Fattah, A. I.; Xu, H.; Zhao, Y.; Hickmott, D. D. *CrystEngComm* **2010**, *12*, 1337.

77. Ma, S. Q.; Zhou, H. C. *Chem. Commun.* **2010**, *46*, 44.

78. Liu, Y.; Xuan, W. M.; Cui, Y. *Adv. Mater.* **2010**, *22*, 4112.

79. Zhao,D.; Yuan,D.Q.; Zhou,H.C. *Energy Environ. Sci.* **2008**, *1*, 222.

80. Hu, Y. H.; Zhang, L. *Adv. Mater.* **2010**, 22, E117.

81. Murray, L. J.;Dinca,M.; Long, J.R. *Chem. Soc. Rev.* **2009,** *38*, 1294.

82. Dinca, M.; Long, J. R. *Angew. Chem., Int. Ed.* **2008**, *47*, 6766.

83. Hedin, N.; Chen, L. J.; Laaksonen, A. *Nanoscale* **2010**, *2*, 1819.

84. Choi, S.; Drese, J. H.; Jones, C. W. *ChemSusChem* **2009**, *2*, 796.

85. Ferey, G.; Serre, C.; Devic, T.; Maurin, G.; Jobic, H.; Llewellyn, P. L.; De Weireld, G.; Vimont, A.; Daturi, M.; Chang, J.-S. *Chem. Soc. Rev.* **2011**, *40*, 550.

86. D'Alessandro, D. M.; Smit, B.; Long, J. R. Angew. Chem., Int. Ed. **2010**, 49, 6058.

87. Li, J. R.; Ma, Y.; McCarthy, M. C.; Sculley, J.; Yu, J.; Jeong, H. K.; Balbuena, P. B.; Zhou, H. C. *Coord. Chem. Rev.* **2011**, *255*, 1791.

88. Horcajada, P.; Serre, C.; Vallet-Regi, M.; Sebban, M.; Taulelle, F.; Ferey, G. *Angew. Chem., Int. Ed*. **2006**, *45*, 5974.

89. Huxford, R. C.; Della Rocca, J.; Lin, W. B. Curr. Opin. *Chem. Biol.* **2010**, *14*, 262.

90. Li, J. R.; Kuppler, R. J.; Zhou,H.C.*Chem. Soc. Rev*. **2009**, *38*, 1477.

91. Custelcean, R.; Moyer, B. A. *Eur. J. Inorg. Chem.* **2007**, 1321.

92. Liu, D. H.; Zhong, C. L. *J. Mater. Chem.* **2010**, *20*, 10308.

93. Cychosz, K. A.; Ahmad, R.; Matzger, A. *J. Chem. Sci.* **2010**, *1*, 293.

94. Phan, A.; Doonan, C. J.; Uribe-Romo, F. J.; Knobler, C. B.; O'Keeffe, M.; Yaghi, O. M. *Acc. Chem. Res.* **2010**, *43*, 58.

95. Keskin, S.; van Heest, T. M.; Sholl, D. S. *ChemSusChem* **2010**, *3*, 879.

96. Noro, S.; Kitagawa, S.; Seki, K., *Angew. Chem Int. Ed.,* **2000**, *39*, 2082-2084

97. Kondo, M.; Yoshitomi, T.; Kitagawa, S.; *Angew. Chem Int. Ed.*, **1997**, *36*, 1725-1727

98. Sculley, J.; Yuan, D.; Zhou, H.-C. *Energy Environ. Sci.* **2011**, *4*, 2721.

99. Lin, X.; Champness, N. R.; Schr€oder, M. *Top. Curr. Chem.* **2010**, *293*, 35.

100. Hu, Y. H.; Zhang, L. *Adv. Mater*. **2010**, *22*, E117.

101. Ma, S.; Zhou, H.-C. *Chem. Commun*. **2010**, *46*, 44.

102. Han, S. S.; Mendoza-Cortes, J. L.; Goddard, W. *A. Chem. Soc. Rev*. **2009**, *38*, 1460.

103. Murray, L. J.; Dinc_a, M.; Long, J. R. *Chem. Soc. Rev.* **2009**, *38*, 1294.

104. Dinca, M.; Long, J. R. *Angew. Chem., Int. Ed.* **2008**, *47*, 6766.

105. Lin, X.; Jia, J.; Hubberstey, P.; Schr€oder, M.; Champness, N. R. *CrystEngComm* **2007**, *9*, 438.

106. Belof, J. L.; Ster, A.C.; Eddaoudi, M.; Space, B.; *J. Am. Chem. Soc.*, **2007**, *129*, 15202-15210

107. *Multi-Year Research, Development and Demonstration Plan: Planned Program Activities for 2011-201:Technical Plan,* United States Department of Energy. http://www1.eere.energy.gov/hydrogenandfuelcells/ storage/current_technology.html.

108. Farha, O. K.; Yazaydin, A. O.; Eryazici, I.; Malliakas, C. D.; Hauser, B. G.; Kanatzidis, M. G.; Nguyen, S. T.; Snurr, R. Q.; Hupp, J. T. *Nat. Chem*. **2010**, *2*, 944.

109. Suh, M. P.; Hye J.P.; Prasad, T.K.; Lim, D. *Chem. Rev.* **2012**, *112*, 782–835 and references therein

110. Li, J.-R.; Kuppler, R. J.; Zhou, H.-C. *Chem. Soc. Rev.* **2009**, *38*, 1477.

111. Keskin, S.; van Heest, T. M.; Sholl, D. S. *ChemSusChem* **2010**, *3*, 879.

112. Li, J.-R.;Ma, Y.;McCarthy,M. C.; Sculley, J.; Yu, J.; Jeong, H.-K.; Balbuena, P. B.; Zhou, H.-C. *Coord. Chem. Rev.* **2011**, *255*, 1791.

113. Morris, R. E.; Wheatley, P. S. *Angew. Chem., Int. Ed.* **2008**, *47*, 4966.

114. Rowsell, J. L. C.; Yaghi, O. M. *J. Am. Chem. Soc.* **2006**, 128, 1304.

115. Bradshaw, D.; Claridge, J. B.; Cussen, E. J.; Prior, T. J.; Rosseinsky, M. *J. Acc. Chem. Res.* **2005**, *38*, 273.

116. Horike, S.; Shimomura, S.; Kitagawa, S. *Nat. Chem.* **2009**, *1*, 695.

117. Uemura, K.; Matsuda, R.; Kitagawa, S. *J. Solid State Chem.* **2005**, *178*, 2420.

118. Bureekaew, S.; Shimomura, S.; Kitagawa, S. *Sci. Technol. Adv. Mater*. **2008**, 9.

119. Serre, C. *Actual. Chim.* **2008**, 15.

120. Rochelle, G. T. *Science* **2009**, *325*, 1652.

121. Cejka, J.; Corma, A.; Zones, S. *Zeolites and Catalysis: Synthesis, Reactions and Applications;* Wiley-VCH: Weinheim, Germany, **2010**.

122. Plaza, M. G.; García, S.; Rubiera, F.; Pis, J. J.; Pevida, C. *Chem. Eng. J.* **2010**, *163*, 41.

123. Haszeldine, R. S. *Science* **2009**, *325*, 1644.

124. Sumindai, K.; *Chem. Rev.* **2012**, *112*, 724–781 and references therein

125. Kitagawa, S.; Kitaura, R.; Noro, S.-I. *Angew. Chem., Int. Ed.* **2004**, *43*, 2334.

126. Ferey, G. *Chem. Soc. Rev.* **2008**, *37*, 191.

127. Lee, J. Y.; Farha, O. K.; Roberts, J.; Scheidt, K. A.; Nguyen, S. T.; Hupp, J. T. *Chem. Soc. Rev.* **2009**, *38*, 1450.

128. Murray, L. J.; Dinc_a, M.; Long, J. R. *Chem. Soc. Rev.* **2009**, *38*, 1294.

129. Kuppler, R. J.; Timmons, D. J.; Fang, Q.-R.; Li, J.-R. M.; T., A.;Young, M. D.; Yuan, D.; Zhao, D.; Zhuang, W.; Zhou, H.-C. Coord. Chem. Rev. **2009**, 253, 3042.

130. Farrusseng, D.; Aguado, S.; Pinel, C. *Angew. Chem., Int. Ed.***2009**, *48*, 7502.

131. Corma, A.; García, H.; Llabr_es, i; Xamena, F. X. *Chem. Rev.* **2010**, *110*, 4606.

132. Banerjee, R.; Furukawa, H.; Britt, D.; Knobler, C.; O'Keefe, M.; Yaghi, O. M. *J. Am. Chem. Soc.* **2009**, *131*, 3875.

133. Banerjee, R.; Phan, A.; Wang, B.; Knobler, C.; Furukawa, H.; O'Keefe, M.; Yaghi, O. M. *Science* **2008**, *319*, 939

134. Vimont, A.; Goupil, J.-M.; Lavalley, J.-C.; Daturi, M.; Surble, S.; Serre, C.; Millange, F.; F_erey, G.; Audebrand, N. *J. Am. Chem. Soc.* **2006,** *128*, 3218.

135. Dinca, M.; Long, J. R. *Angew. Chem., Int.* Ed. **2008**, *47*, 6766.

136. Zhou, W.; Wu, H.; Yildirim, T. *J. Am. Chem. Soc.* **2008**, *130*, 15268.

137. Dietzel, P. D. C.; Besikiotis, V.; Blom, R. *J. Mater. Chem.* **2009**, *19*, 7362.

138. Chen, B.; Xiang, S.; Qian, G. *Acc. Chem. Res*. **2010**, *43*, 1115.

139. Centi, G.; Trifiro, F.; Ebner, J.R.; Franchetti, V.M. *Chem. Rev.* **1988**, *88*, 55.

140. Centi, G. (Ed.), "Vanadyl Pyrophosphate Catalysts," *Catalysis Today*, vol. *16*, Elsevier, Amsterdam, **1993**.

141. Sananes, M.T.; Hutchings, G.J.; Volta, J.-C. *J. Chem. Soc. Chem. Comm.* **1995,** 243.

142. Sananes, M.T.; Hutchings, G.J.; Volta, J.-C. *J. Catal.* **1995**, *154*, 253.

143. HTlderich, W.; Hesse, M.; and Naumann, F., *Angew. Chem.* **1988**, *100*, 232 – 251; *Angew. Chem. Int. Ed. Engl.* **1988**, 27, 226 – 246.

144. Tanski, J.M.; and Wolczanski, P.T., *Inorg. Chem.* **2001**, *40*, 2002-2033.

145. Gomez-Lor, B.; GutiYrrez-Puebla, E.; Iglesias, M.; Monge, M.A.; Ruiz-Valero, C.; and Snejko, N., *Inorg. Chem.* **2002**, *41*, 2429–2432.

146. Tannenbaum, R., *Chem. Mater.* **1994**, *6*, 550–555.

147. Tannenbaum, R., *J. Mol. Catal. A* **1996**, *107*, 207 – 215.

148. Feinstein-Jaffe, I.; and Efraty, A., *J. Mol. Catal.* **1987**, *40*, 1–7.

149. Naito, S.; Tanibe, T.; Saito, E.; Miyao, T.; and Mori, W., *Chem. Lett.* **2001**, 1178 – 1179.

150. Xing, B.; Choi, M-F.; and Xu, B., *Chem. Eur. J.* **2002**, *8*, 5028 – 5032.

151. Corma, A.; Garcia, H. Xamena, *Chem Rev*., **2010**, *110*, 4606-4655 and references therein.

152. Evans, O.R.; Ngo, H.L.; and Lin, W.B., *J. Am. Chem. Soc*., **2011**, *123*, 10395-1039.

153. Hasegawa, S.; Horike, S.; and Kitagawa, S., *J. Am. Chem. Soc.*, **2006**, *128*, 16416-16417.

154. Seo, J.S.; Whang, D.; and Kim, K., *Nature*, **2006**, *404*, 982-986.

155. Clemente-León, M.; Coronado, E.; Galán-Mascarós, J. R.; Giménez-Saiz, C.; Gómez-García, C. J.; Ribera, E.; Vidal-Gancedo, J.; Rovira, C.; Canadell, E.; and Laukhin, V.N., *Inorg. Chem.* **2001**, *40*, 3526-3533.

156. Mori, H.; Hirabayashi, I.; Tanaka, S.; Mori, T.; and Manyama, Y., *Synth. Met.* **1995**, *70*, 789-790.

157. Coronado, E.; Falvello, L. R.; Galán-Mascarós, J. R.; Giménez-Saiz, C.; Gómez- García, C. J.; Laukhin, V. N.; Pérez-Benítez, A.; Rovira, C.; andVeciana, J., *Adv. Mater.* **1997**, *9*, 984-987.

158. Kurmoo, M.; Graham, A. W.; Day, P.; Coles, S. J.; Hursthouse, M. B.; Caulfield, M.; Singleton, J.; Ducasse, L.; and Guionneau, P., *J. Am. Chem. Soc.* **1995**, *117*, 12209-12217.

159. Kobayashi, H.; Sato, A.; Arai, E.; Akutsu, H.; Kobayashi, A.; and Cassoux, P., *J. Am. Chem. Soc.* **1997**, *119*, 12392-12393.95.

160. Mathonière, C.; Nuttall, C. J.; Carling, S.G.; and Day, P., *Inorg. Chem.* **1996**, *35*, 1201–1206.

161. Gutlich, P.; Garcia, Y.; and Goodwin, H.A., *Chem. Soc. Rev*., **2000**, *29*, 419.

162. Halder, G.J.; Kepert, C.J.; Moubaraki, B.; Murray, K.S.; and Cashion, J.D., *Science*, **2002**, *298*, 1762.

163. Kahn, O.; and Martinez, C.J., *Science*, **1998**, *279*, 44.

164. Bonhommeau, S.; Molna´r, G.; Galet, A.; Zwick, A.; Real, J-A.; McGarvey, J.J.; and Bousseksou, A., *Angew. Chem., Int. Ed.*, **2005**, *44*, 4069.

165. Bousseksou, A.; Molna´r, G.; and Matouzenko, G., *Eur. J. Inorg. Chem.*, **2004**, 4353.

166. Real, J-A.; Gaspar, A.B.; Niel, V.; and Munoz, M.C., *Coord. Chem. Rev.*, **2003**, *236*, 121.

167. Kahn, O., *Molecular Magnetism*; VCH: New York, **1993**.

168. Piguet, C.; and Bunzli, J.C., *Chem Soc Rev*., **2005**, *34*, 1048-1077

169. Allendorf, M.D.; Bauer, C.A.; and Houk, R. J. T., *Chem Soc Rev*., **2009**, *38*, 1330-1352

170. Rocha, J.; Carlos, L.D.; and Ananias, D., *Chem Soc rev*., **2011**, *40*, 926-940

171. Vasudevan, K. V., *Dalton Trans*., **2010**, *39*, 776-786

172. Janiak, C., *Dalton Trans*. **2003**, 2781.

173. Cahill, C. L.; de Lill, D. T.; and Frisch, M., *CrystEngComm* **2007**, *9*, 15.

174. Suh, M.; Cheon, Y.; and Lee, E., *Coord. Chem. Rev.* **2008**, *252*, 1007.

175. Maspoch, D.; Ruiz-Molina, D.; and Veciana, *J. Chem. Soc. Rev.* **2007**,*36*, 770.

176. Rocha, J.; Carlos, L. D.; Paz, F. A. A.; and Ananias, D., *Chem. Soc. Rev.***2011**, *40*, 926.

177. Allendorf, M. D.; Bauer, C. A.; Bhakta, R. K.; and Houk, R. J. T., *Chem. Soc. Rev.* **2009**, *38*, 1330.

178. Chen, B.; Xiang, S.; and Qian, G., *Acc. Chem. Res.* **2010**, *43*, 1115.

179. Meek, S.T.; Greathouse, J.A.; and Allendorf, M.D., *Adv. Mater.* **2011**, *23*, 249.

180. Shekhah, O.; Liu, J.; Fischer, R. A.; and W€oll, C., *Chem. Soc. Rev*.**2011**, *40*, 1081.

181. Ferey, G., *Chem. Soc. Rev.* **2008**, *37*, 191.

182. Silva, C. G.; Corma, A.; and Garcia, H., *J. Mater. Chem.* **2010**, *20*, 3141.

183. Kuppler, R. J.; Timmons, D. J.; Fang, Q.-R.; Li, J.-R.; Makal, T. A.; Young, M. D.; Yuan, D.; Zhao, D.; Zhuang, W.; and Zhou, H.-C., *Coord. Chem. Rev*. **2009**, *253*, 3042.

184. Janiak, C.; and Vieth, J. K., *New J. Chem*. **2010**, *34*, 2366.

185. Takashima, Y.; Martinez, M.; and Kitagawa, S., *Nat Commun*., **2011**, *2*, 168

186. Zhao, B.; Chen, X.-Y.; Cheng, P.; Liao, D.-Z.; Yan, S.-P.; and Jiang, Z.-H., *J. Am. Chem. Soc.* **2004**, *126*, 15394.

187. Liu, W.; Jiao, T.; Li, Y.; Liu, Q.; Tan, M.; Wang, H.; and Wang, L., *J. Am. Chem. Soc.* **2004**, *126*, 2280.

188. Chen, B.; Wang, L.; Zapata, F.; Qian, G.; and Lobkovsky, E. B., *J. Am. Chem. Soc.* **2008**, *130*, 6718.

189. Chen, B.; Wang, L.; Xiao, Y.; Fronczek, F. R.; Xue, M.; Cui, Y.; and Qian, G., *Angew. Chem., Int. Ed.* **2009**, *48*, 500.

190. Wong, K. L.; Law, G. L.; Yang, Y. Y.; Wong, W. T. *Adv. Mater*. **2006**, *18*, 1051.

191. Harbuzaru, B.V.; Corma, A.; Rey, F.; Atienzar, P.; Jorda, J. L.; Garcia, H.; Ananias, D.; Carlos, L.D.; and Rocha, J., *Angew. Chem., Int. Ed*. **2008**, *47*, 1080.

192. Chen, B.; Yang, Y.; Zapata, F.; Lin, G.; Qian, G.; and Lobkovsky, E. B., *Adv. Mater.* **2007**, *19*, 1693.

193. Jiang, H.-L.; Tatsu, Y.; Lu, Z.-H.; and Xu, Q., *J. Am. Chem. Soc*. **2010**, *132*, 5586.

194. Takashima, Y.; Martinez, V. M.; Furukawa, S.; Kondo, M.; Shimomura, S.; Uehara, H.; Nakahama, M.; Sugimoto, K.; and Kitagawa, S., *Nat. Comms*. **2011**, *2*, 168

195. *Metal Phosphonate Chemistry*, Clearfield, A.; and Demadis, K.D., eds., RSC Publishing, Cambridge, UK, **2012**.

196. Ferey, G.; Serre, C.; Devic, T.; Maurin, G.; Jobic, H.; Llewellyn, P.L.; De Weireld, G.; Vimont, A.; Daturi, M.; and Chang, J.-S., *Chem. Soc. Rev*. **2011**, *40*, 550.

197. Hijikata, Y.; Horike, S.; Sugimoto, M.; Sato, H.; Matsuda, R.; and Kitagawa, S., *Chem.–Eur. J*. **2011**, *17*, 5138.

198. Noro, S.; and Kitagawa, S., *Supramolecular Chemistry of Organic-Inorganic Hybrid Materials*, Rurack, K.; and Martinez-Manez, R., ed., **2010**, 235.

199. Bloch, E.D.; Britt, D.; Lee, C.; Doonan, C.J.; Uribe-Romo, F.J.; Furukawa, H.; Long, J.R.; and Yaghi, O.M., *J. Am. Chem. Soc*. **2010**, *132*, 14382

200. Moulton, B.; and Zaworotko, M.J., *Curr. Opin. Solid State Mater. Sci*. **2002**, *6*, 117.

201. Wang, C.; and Lin, W., *J. Am. Chem. Soc.* **2011**, *133*, 4232–4235.

202. Choi, H.J.; Dinca; and Long, J.R., *J. Am. Chem. Soc.* **2008**, *130*, 7848.

203. Sava, D.F.; Kravtsov, V. Ch.; Nouar, F.; Wojtas, L.; Eubank, J.F.; and Eddaoudi, M., *J. Am. Chem. Soc.* **2008**, *130*, 3768.

204. Beckmann, U.; and Brooker, S., *Coord. Chem. Rev*. **2003**, *245*, 17.

205. Haasnoot, J.G., *Coord. Chem. Rev*. **2000**, *200*, 131.

206. Hellyer, R.M.; Larsen, D.S.; and Brooker, S., *Eur. J. Inorg. Chem*. **2009**, 1162.

207. Zhang, J.-P.; and Chen, X.-M., *Chem. Commun*. **2006**, 1689.

208. Steel, P.J., *Coord. Chem. Rev*. **1990**, *106*, 227.

209. Potts, K.T., *Chem. Rev*. **1961**, *61*, 87.

210. Dawe, L.N.; and Thompson, L.K., *Dalton Trans*. **2008**, 3610.

211. Zhang, J.-P.; Lin, Y.-Y.; Huang, X.-C.; and Chen, X.-M., *J. Am. Chem. Soc*. **2005**, *127*, 5495.

212. Zhang, J.-P.; Zheng, S.-L.; Huang, X.-C; and Chen, X.-M., *Angew. Chem., Int. Ed*. **2004**, *43*, 206.

213. Ferrer, S.; Lloret, F.; Bertomeu, I.; Alzuet, G.; Borras, J.; Garcia-Granda, S.; Liu-González, M.; and Haasnoot, J.G., *Inorg. Chem*. **2002**, *41*, 5821.

214. Zhou, J.-H.; Cheng, R.-M.; Song, Y.; Li, Y.-Z.; Yu, Z.; Chen, X.-T.; Xue, Z.-L.; and You, X.-Z., *Inorg. Chem*. **2005**, *44*, 8011 and references therein.

215. Zhang, J.-P.; Lin, Y.-Y.; Zhang, W.-X.; and Chen, X.-M., *J. Am. Chem. Soc*. **2005**, *127*, 14162.

216. Zhang, D.-C.; Lu, W.-G.; Jiang, L.; Feng, X.-L.; and Lu, T.-B., *Cryst. Growth Des*. **2010**, *10*, 739.

217. Ouellette, W.; Jones, S.; and Zubieta, J., *CrystEngComm*. **2011**, *13*, 4457.

218. Ouellette, W.; Darling, K.; Prosvirin, A.; Whitenack, K.; Dunbar, K.R.; and Zubieta, J., *Dalton Trans.* **2011**, *40*, 12288.

219. Hagrman, P.J.; Bridges, C.; Greedan, J.E.; and Zubieta, J., *J. Chem. Soc. Dalton Trans.* **1999**, 2901.

220. Hagrman, D.; and Zubieta, J., *Chem. Commun.* **1998**, 2005.

221. Ouellette, W.; Yu, M.H.; O'Connor, C.J.; Hagrman, D.; and Zubieta, J., *Angew. Chem., Int. Ed*. **2006**, *45*, 3497.

222. Ouellette, W.; Prosvirin, A.V.; Valeich, J.; Dunbar, K.R.; and Zubieta, J., *Inorg. Chem*. **2007**, *46*, 9067.

223. Ouellette, W.; Galán-Mascarós, J.R.; Dunbar, K.R.; and Zubieta, J., *Inorg. Chem*. **2006**, *45*, 1909.

224. Ouellette, W.; Prosvirin, A.V.; Chieffo, V.; Dunbar, K.R.; Hudson, B.; and Zubieta, J., *Inorg. Chem*. **2006**, *45*, 9346.

225. Chesnut, D.J.; Kusnetzow, A.; Birge, R.; and Zubieta, J., *Inorg. Chem*. **1999**, *38*, 5484.

226. Ouellette, W.; Hudson, B.S.; and Zubieta, J., *Inorg. Chem*. **2007**, *46*, 4887.

227. Ouellette, W.; Liu, H.; O'Connor, C.J.; and Zubieta, J., *Inorg. Chem*. **2009**, *48*, 4655.

228. Ouellette, W.; and Zubieta, J., *Chem. Commun*. **2009**, 4533.

229. Ouellette, W.; Prosvirin, A.V.; Whitenack, K.; Dunbar, K.R.; and Zubieta, J., *Angew. Chem., Int. Ed*. **2009**, *48*, 2140.

230. Ouellette, W.; Jones, S; and Zubieta, J., *CrystEngComm*. **2011**, *13*, 4457.

231. Kahn, O.; and Martinez, C.J., *Science* **1998**, *279*, 44 and references therein.

232. Krober, J.; Audie`re, R.; Claude, R.; Codjovi, E.; Kahn, O.; Haasnoot, J.G.; Grolie`re, F.; Jay, C.; Bousseksou, A.; Linare`s, J.; Varret, F.; and Gonthier-Vassal, A., *Chem. Mater.* **1994**, *6*, 1404.

233. Whittingham, M.S., Current Opinion Solid State & Mater. Sci. **1996**, *1*, 227.

234. Gopalakrishnan, J., *Chem. Mater.* **1995**, *7*, 1265.

235. Fing, S.; and Xu, R., *Acc. Chem. Res.* **2001**, *34* 239.

236. Rabenau, A., *Angew. Chem., Int. Ed.* Engl. **1985**, 24, 1026.

237. Weller, M.; and Dann, S.E., Current Opinion Solid State & Mater. Sci. **1998**, 3, 137.

238. Laudise, P.A., *Chem. Eng. News* **1987**, Sept. 28, pp. 30-43.

239. Stein, A.; Keller, S.W.; and Mallouk, T.E., *Science* **1993**, *289*, 1558.

240. J. Zubieta, Solid-State Methods, Hydrothermal. In Comprehensive Coordination Chemistry II; J.A McCleverty, T.J. Meyer, Elsevier Science: New York, **2004**; Vol. 1, pp 697-709.

Chapter 2: Solid State Coordination Chemistry of Copper with Pyridyltetrazoles. Structural Consequences of Incorporation of Coordinating Anions.

2.1 Introduction

The contemporary interest in metal organic frameworks (MOFs) reflects their structural diversity and vast compositional range, which leads to applications in separation, catalysis and preeminently gas storage.[1-7] As mentioned in Chapter 1, although the most prominent ligands used in the construction of MOFs have been carboxylate and polypyridyl ligands,[8-10] polyazaheteroaromatic ligands (azolates) such as imidazolate, pyrazolate, triazolate and tetrazolate have been exploited recently in the design of novel hybrid materials.[11-28] This class of ligands affords the ability to bridge metal sites, as well as a super exchange capacity reflected in the unusual magnetic properties of their complexes. In addition, azolate ligands are readily derivatized to provide bridging ligands with additional functionality.

As part of our investigations into the design of hybrid organic-inorganic materials from molecular building blocks, we studied the hydrothermal chemistry of triazole with various transition metal cations.[12, 29-38] In the course of these studies, we noted that 4-pyridyltetrazolate (4-pyrtet) may be naively considered as an expanded analogue of 1,2,4-triazolate (trz), as shown in **Scheme 1**, an observation that led to a significant spatial expansion of the framework and accessible void volume in $[Cu_3(OH)_3(4\text{-pt})_3(DMF)_4]$ compared to $[Cu_3(OH)_3(trz)_3(H_2O)_4]$.

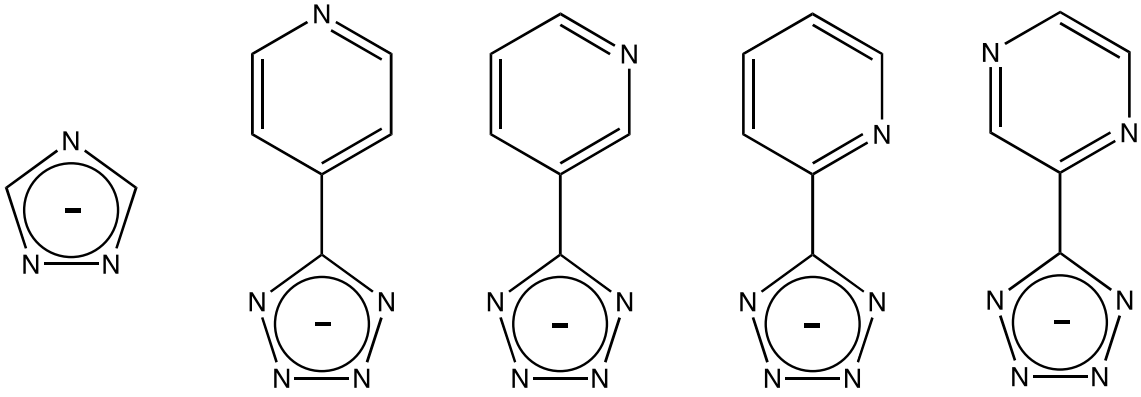

Scheme 1

It was also noted in the studies of metal-triazolates, that coordinating anions, such as halides, sulfate, and phosphate can dramatically influence the structures and properties of the hybrid materials. These observations encouraged us to explore the chemistry of copper-pyridyltetrazole with various anionic components. We report the structures of the two-dimensional parent compound [Cu(3-pyrtet)$_2$] (**1**), the reduced species [Cu(4-pyrtet)] (**2**) and the dimethylformamide inclusion product [Cu(4-pyrtet)]•0.5DMF (**3**•0.5DMF), as well as the halide derivatives [$CuCl_2$(4-Hpyrtet)]•0.5H_2O (**4**•0.5H_2O), [Cu_2I_2(4-Hpyrtet)] (**5**) and [H_2en]$_{0.5}$[$CuCl_2$(prztet)] (**6**) and the acetylacetonate analogue [Cu(acac)(4-pyrtet)] (**7**) (where Hpyrtet = pyridyltetrazole; Hprztet = pyrazinetetrazole; acac = acetylacetonate; H_2en = ethylenediammonium cation).

2.2 Results and Discussion

2.2.1 Syntheses

While the classical hydrothermal literature is concerned with the synthesis of zeolites and metal phosphates,[45,46] the technique has now been extended to the routine synthesis of metal oxides and organic-inorganic composite materials.[47-50] Hydrothermal syntheses are conventionally carried out in water at 120-250 ^oC at autogenous pressure. Product composition depends on a number of critical conditions, including pH of the medium, temperature and hence pressure, the presence of structure-directing cations, and the use of mineralizers. Since a variety of cationic and anionic components may be present in solution, those of appropriate size, geometry and charge to fulfill crystal packing requirements may be selected from the mixture in the crystallization process. The technique thus exploits "self-assembly" of a solid phase from soluble precursors at moderate temperatures. Compounds **1-7** were synthesized using such conventional hydrothermal methods. At these temperature ranges, the reactants are solubilized

while retaining their structural features in the product phases, exploiting the self assembly of products from these soluble precursors. It is noteworthy that compounds **2**, **3**, and **5** contain reduced copper, although Cu(II) starting materials were used in the syntheses. Reduction of Cu(II) to Cu(I) is observed in hydrothermal reactions in the presence of nitrogenous ligands.

2.2.2 X-Ray Crystal Structures

The parent compounds [Cu(3-pyrtet)$_2$] (**1**) and [Cu(4-pyrtet)] (**2**) reveal the consequences of the location of the pyridyl nitrogen on the moiety attached to the tetrazole unit and of reduction from Cu(II) to Cu(I).

As shown in **Figure 2.1**, the two dimensional structure of **1** is composed of Cu(II) square pyramids defined by two nitrogen donators from the pyridyl moieties and two nitrogens of the tetrazolate functionality. In this case, the 3-pyridyltetrazole ligand is present in the deprotonated form, linking two Cu(II) sites through one pyridyl and one tetrazolate nitrogen, resulting in layers propagating parallel to the *ab*-plane. In contrast, [Cu(4-pyrtet)] (**2**) (**Figure 2.2**) consists of pairs of Cu(I)(units bridged buy N2,N3 bonded tetrazolate groups. The geometry of the Cu(I) is trigonal planar, composed of two bridging nitrogen donors from the tetrazolate unit and a nitrogen from the pyridyl ring. In this case, the 4-pyridyltetrazole ligand is again deprotonated and links pairs of Cu(I) units into a two dimensional layer.

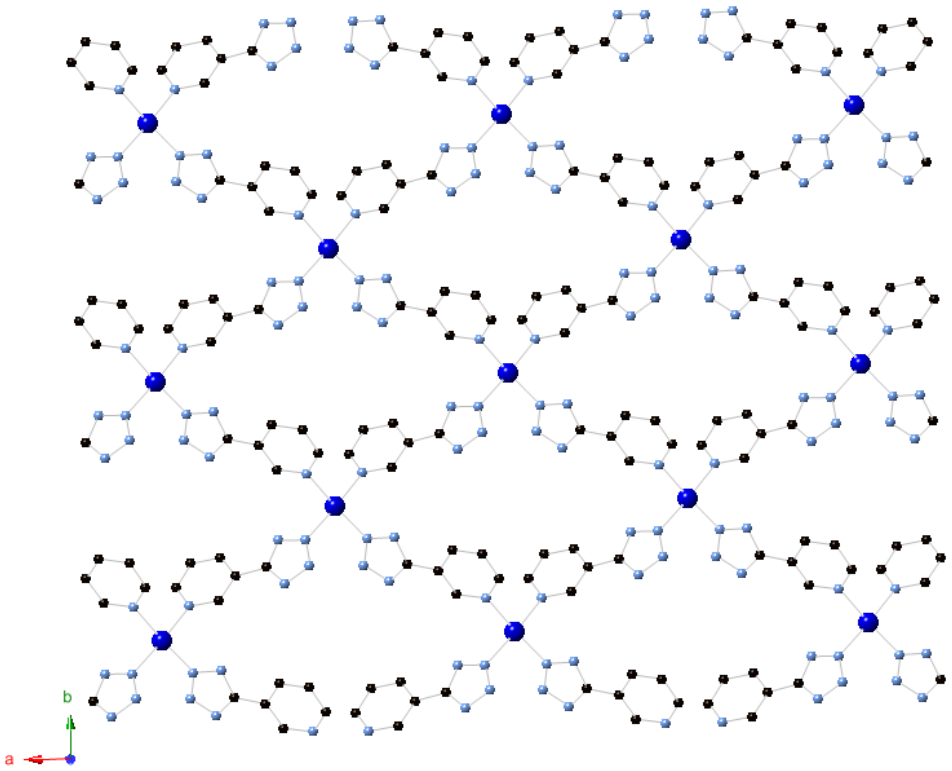

Figure 2.1: A ball and stick representation of the structure of [Cu(3-pyrtet)$_2$] (**1**), viewed normal to the *ab* plane. Color scheme: Copper, dark blue square spheres; nitrogen, light blue spheres; carbon, black spheres. This color scheme is used throughout the figures.

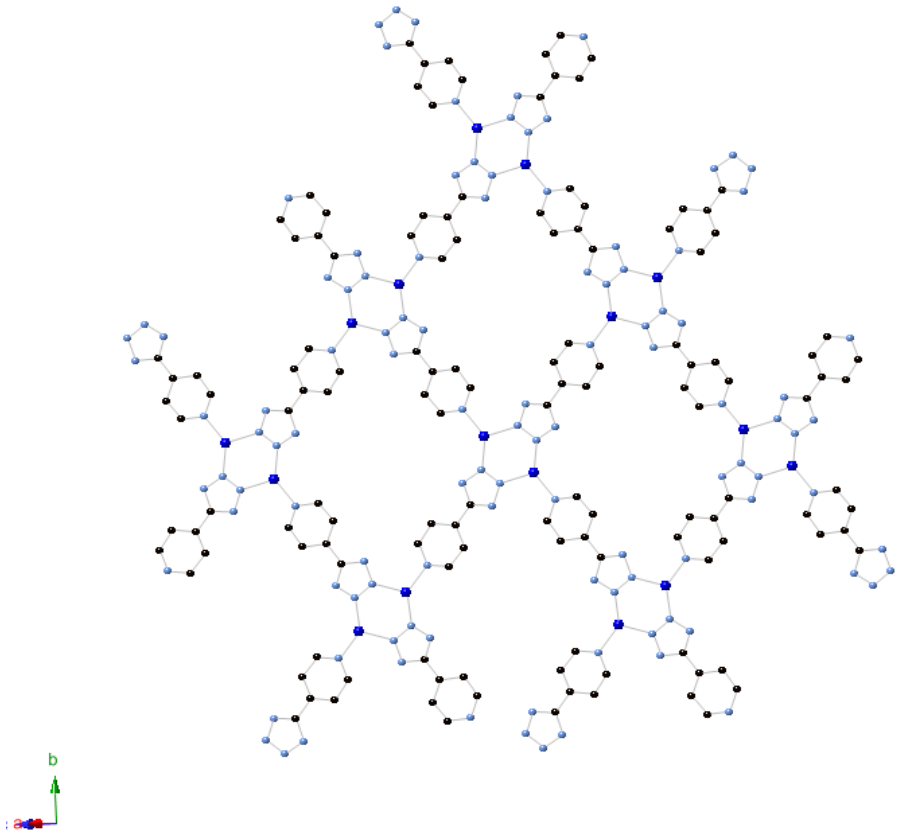

Figure 2.2: A ball and stick representation of the two-dimensional structure of [Cu(4-pyrtet)] (**2**).

As shown in **Figure 2.3**, the structure of [Cu(4-pyrtet)]•0.5DMF (**3**•0.5DMF) is three-dimensional. A binuclear $\{Cu_2(4\text{-pyrtet})_4\}$ cluster provides the secondary building unit (SBU) for the extended structure. The unit consists of two Cu(I) sites exhibiting distorted tetrahedral $\{CuN_4\}$ geometry defined by three tetrazolate nitrogen donors and a pyridyl donor. These SBUs are fused into a chain of N1,N2,N3 bridged copper sites propagating parallel to the crystallographic *a*-axis. Each copper site of a chain is additionally bonded to a pyridyl nitrogen of a 4-pyridyl-tetrazolate ligand bridging to an adjacent chain. In this fashion, each chain is linked to four adjacent chains. The connectivity pattern produces a grid in projection onto the *bc*

plane with channels of approximate dimensions 10Å x 15Å running parallel to the *a*-axis. The DMF molecules of crystallization occupy these cavities.

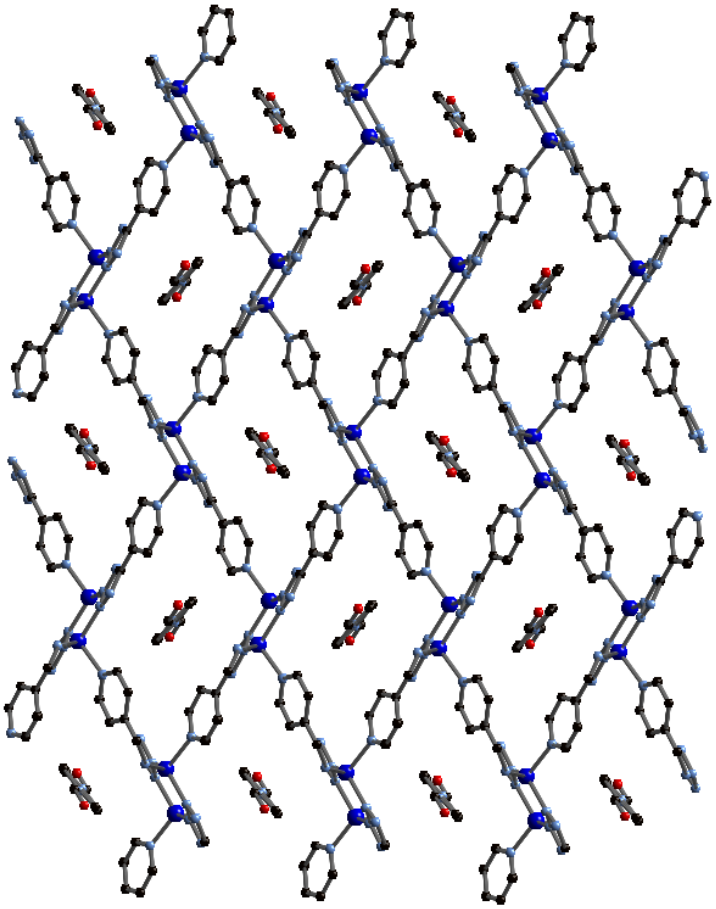

(a)

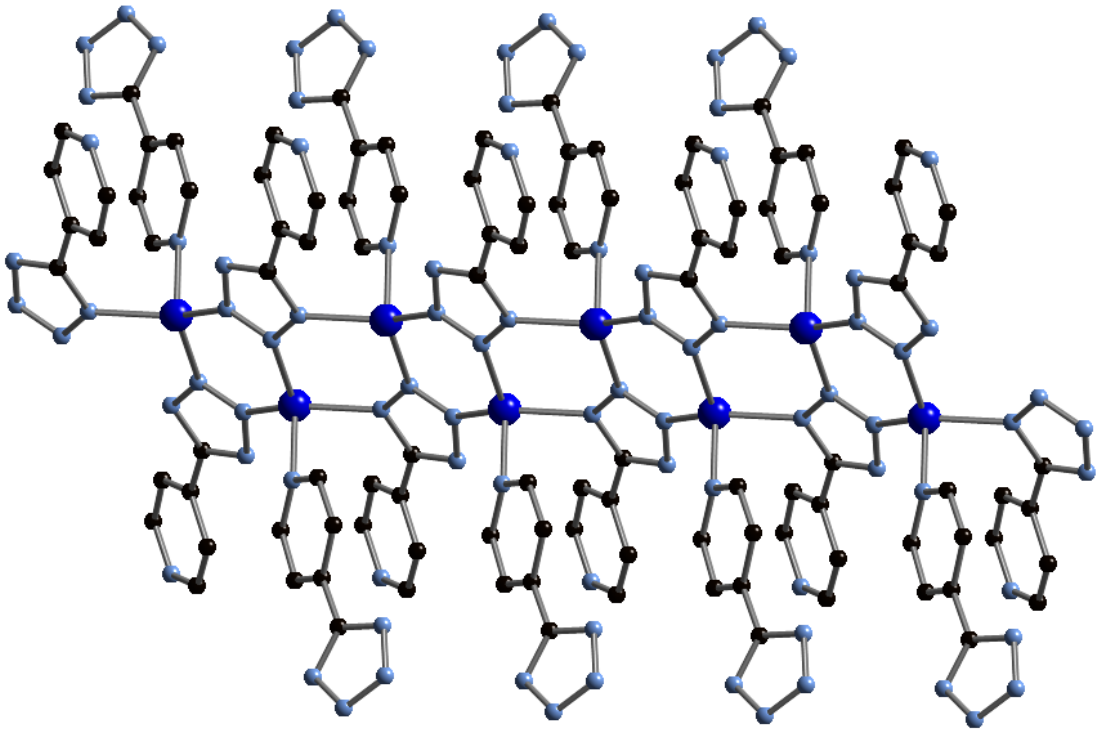

(b)

Figure 2.3: (a) A view of the three-dimensional structure of [Cu(4-pyrtet)]•0.5 DMF (**3**•0.5 DMF), viewed normal to the *bc* plane and showing the channels occupied by the DMF molecules of crystallization. Oxygen donors illustrated as red spheres. (b) A view of the Cu(I)-4-pyridyltetrazolate chain motif parallel to the *a*-axis.

The structural consequences of introducing simple anionic components are demonstrated by structures of $[CuCl_2(4\text{–Hpyrtet})]\bullet 0.5H_2O$ (**4**•$0.5H_2O$), $[Cu_2I_2(4\text{-Hpyrtet})$ (**5**) and [Cu(acac)(4-pyrtet)] (**7**). The structure of the Cu(II) derivative **4**•$0.5H_2O$, shown in **Figure 2.4**, is one-dimensional, consisting of a chain of chloride and N2,N3 tetrazole bridged metal sites, propagating parallel to the *a*-axis. Each copper site exhibits $\{CuCl_4N_2\}$ distorted octahedral geometry, with the equatorial plane defined by four μ^2-chloride ligands and two tetrazole nitrogen donors in the axial positions. The 4-pyridyltetrazole ligand is present as the neutral 4-

Hpyrtet with the pyridyl nitrogen as the protonation site. The structure of **4** is reminiscent of the chain structure adopted by the triazole species $[CuCl_2(Htrz)]$.[51]

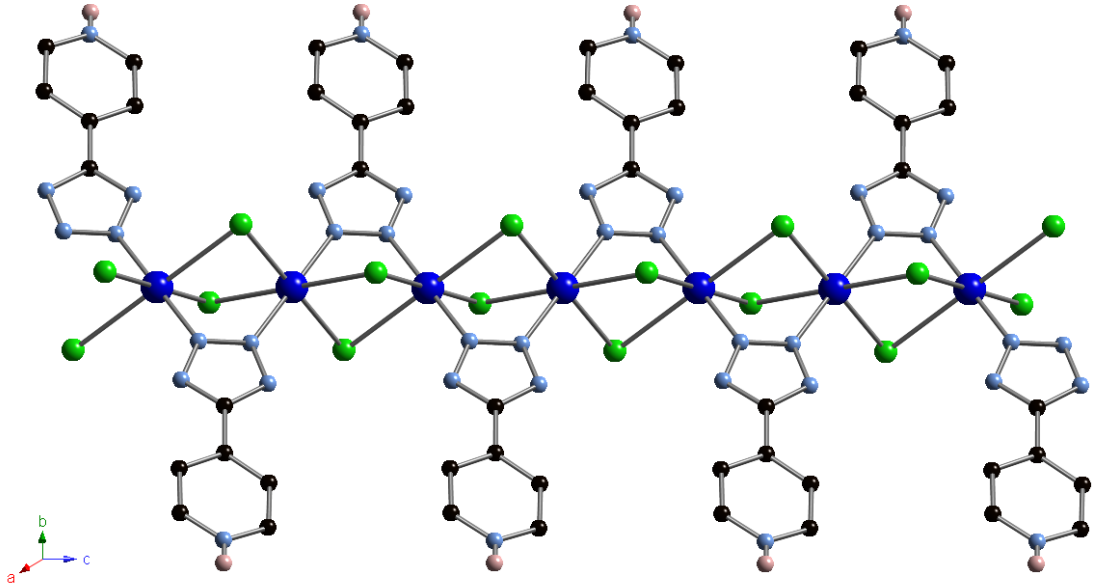

Figure 2.4: The one-dimensional structure of $[CuCl_2(4\text{-}Hpyrtet)]\bullet 0.5H_2O$ (**4**$\bullet 0.5H_2O$). Chlorine atoms shown as green spheres; the hydrogen atom bound to the pyridyl nitrogen shown as a pink sphere.

The structural influence of the substituent attached to the tetrazole moiety is apparent in the one-dimensional structure of the pyrazine-tetrazole derivative $[H_2en]_{0.5}[CuCl_2(prztet)]$ (**6**) (en = ethylenediamine). As shown in **Figure 2.5**, the structure consists of $\{CuCl_2(prztet)\}^{n-}_n$ chains and discrete ethylenediammonium cations. In contrast to the neutral chain of **4**, that of **6** exhibits an alternating pattern of copper sites bridged only by two μ^2-chlorides and of copper sites bridged only by the N1,N2 nitrogen donors of the tetrazolate units. As a result, each Cu center possesses distorted octahedral $\{CuCl_3N_3\}$ geometry, with two bridging chlorides and a terminal chloride donor in a meridional arrangement, two tetrazolate nitrogen donors, and a pyrazine

nitrogen ligand. Each 4-prztet ligand chelates to one copper site and bridges to a second. The Cu···Cu distances alternate between 3.700(1)Å and 4.081(1)Å for the μ^2-chloride bridged pair and the tetrazolate bridged pair, respectively.

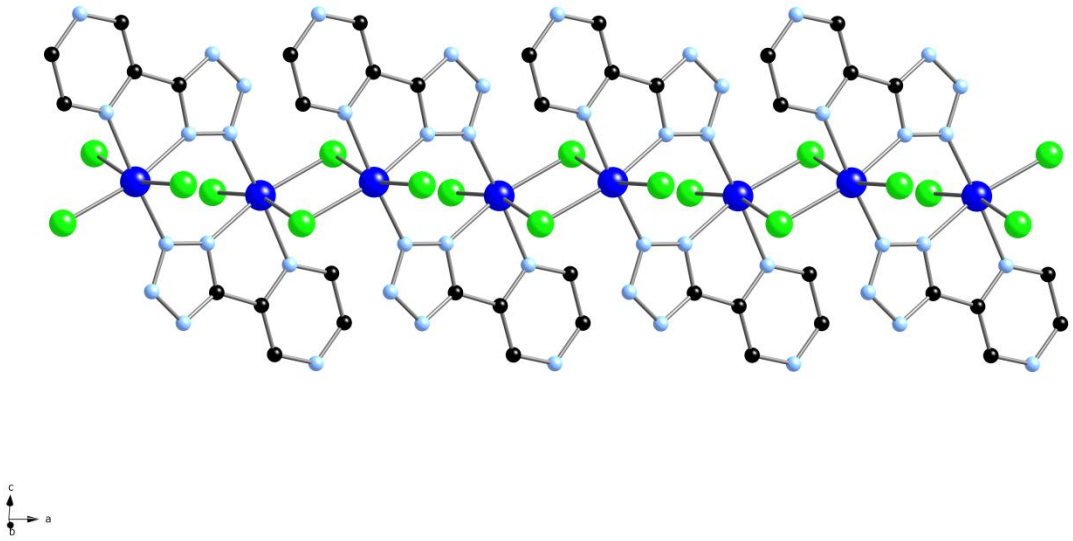

Figure 2.5: A view of the one-dimensional structure of the anion of $[H_2en]_{0.5}[CuCl_2(prztet)]$ (**6**).

In contrast to the one-dimensional, Cu(II) based structures of the chloride derivatives **4** and **6**, the iodide-containing phase $[Cu_2I_2(4\text{-Hpyrtet})]$ (**5**) is two-dimensional and contains exclusively Cu(I) sites. As shown in **Figure 2.6**, the structure consists of $\{CuI\}_n$ puckered layers in the *ac*-plane with 4-Hpyrtet ligands projecting from either face into the interlamellar domain. The distorted tetrahedral $\{CuI_3N\}$ geometry at each Cu(I) site is defined by three μ^3-bridging iodine donors of the layer and a tetrazole nitrogen donor. Pairs of copper sites are bridged by N1,N2 bonded tetrazole groups. The connectivity within the $\{CuI\}_n$ layers generates a pattern of fused $\{Cu_3I_3\}$ rings.

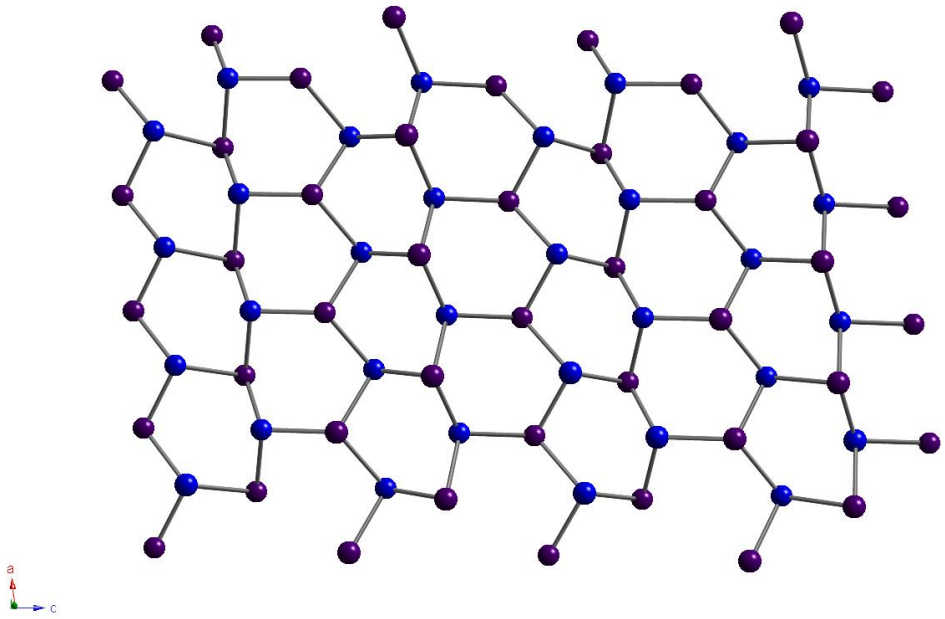

(a)

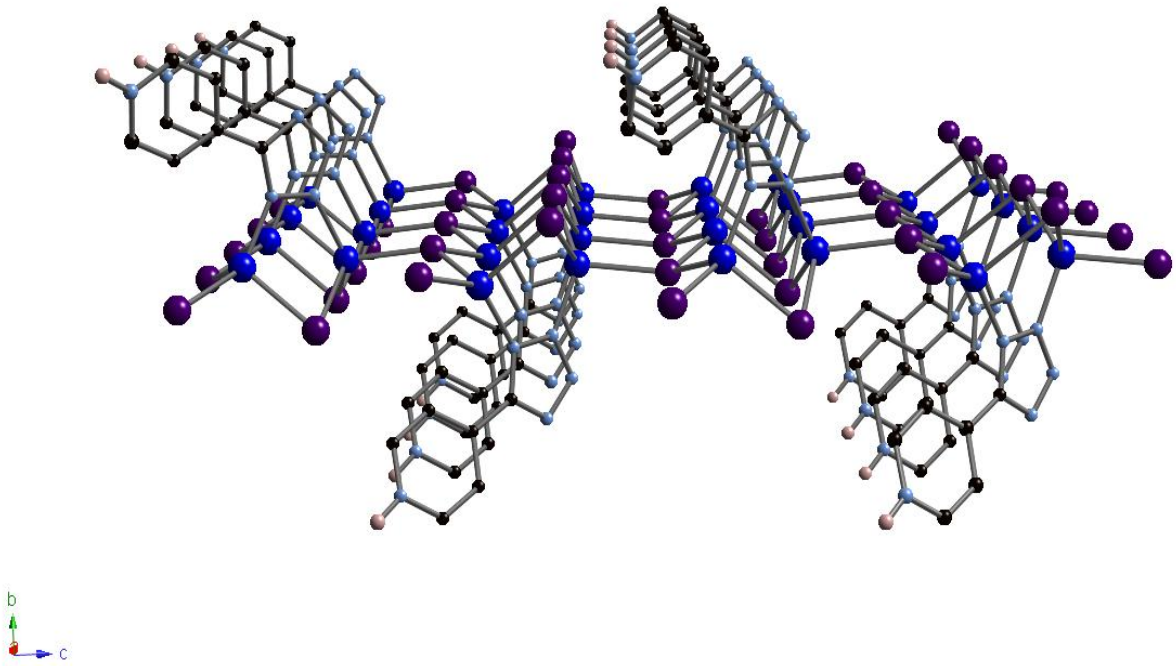

(b)

Figure 2.6: (a) A view of the two-dimensional structure of $[Cu_2I_2(4\text{-Hpyrtet})]$ (**5**) along the *a* crystallographic axis. (b) A view of the $\{CuI\}_n$ layer of 5 in the *ac* plane.

As shown in **Figure 2.7**, the acetylacetonate derivative [Cu(acac)(4-pyrtet)] (**7**) is two dimensional, with the layers propagating parallel to the *bc*-plane. The SBU consists of a binuclear unit of distorted octahedral $\{CuO_2N_4\}$ sites with the $\{Cu_2(azole)_2\}$ planar core. The coordination geometry at each Cu(II) site is defined by the oxygen donors of a chelating acetylacetonate ligand, two tetrazolate nitrogen donors and two pyridyl nitrogen donors. Each binuclear building block is thus associated with four 4-pyrtet ligands which project from the unit with relative angles of *ca*. 90^o to link to four adjacent SBUs, producing a grid-like connectivity pattern. The dimensions of the channels propagating parallel to the (111) direction are *ca.* 10 x 10Å. The acac groups project into the interlamellar space.

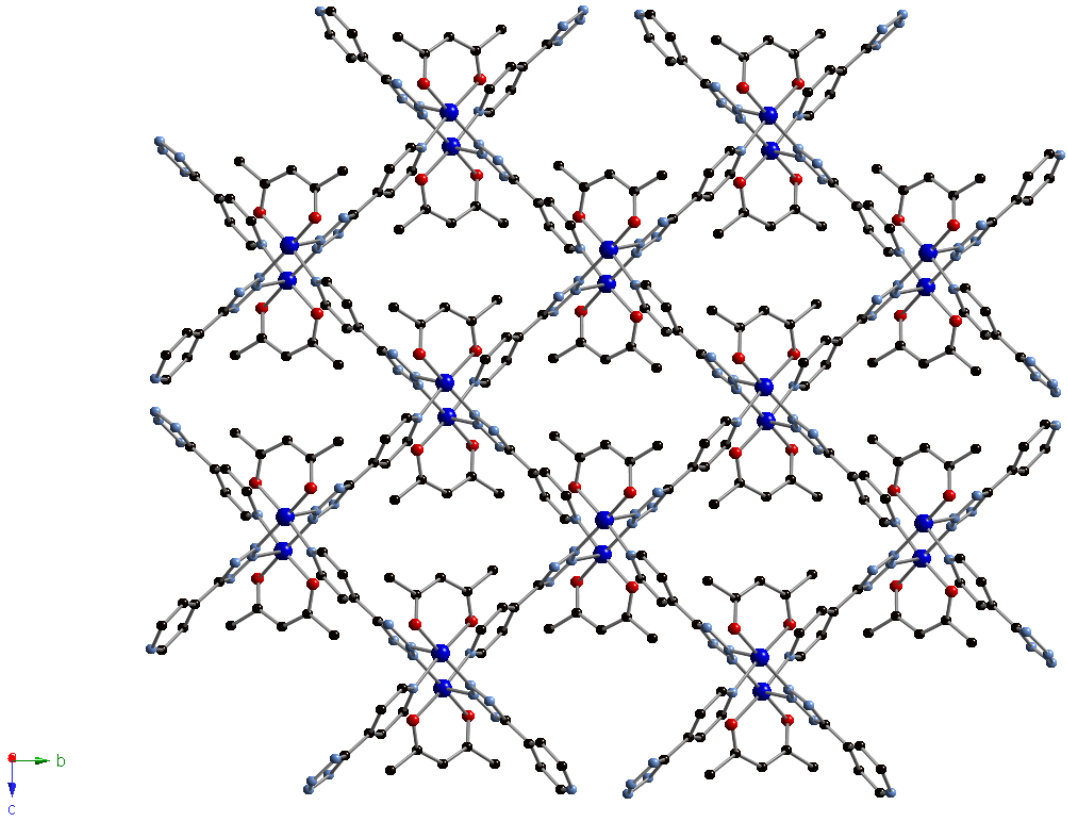

(a)

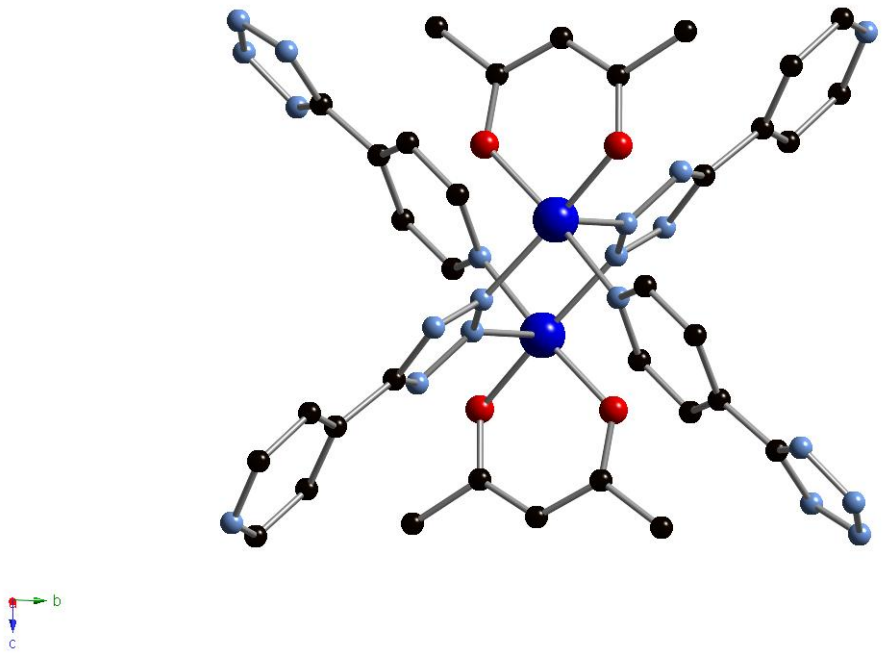

(b)

Figure 2.7: (a) The two-dimensional structure of [Cu(acac)(4-pyrtet)] (7) in the *bc* plane. (b) The binuclear $\{Cu_2(acac)_2(4\text{-pyrtet})_4\}$ secondary building unit of **7**.

2.3 Conclusions

Hydrothermal synthesis provides a proven and effective path to the preparation of coordination polymers incorporating a variety of metals, organic ligands, and inorganic anions leading to a wealth of novel coordination chemistry and structural motifs. This study focused on the copper/pyridyltetrazole system in the presence of a variety of anions which could potentially be incorporated into the overall structure.

The influence of reaction conditions is quite apparent in the compositions of compounds **1**-**3** which fail to incorporate an anionic component. Compounds **1** and **2** were prepared using copper acetate as the copper source in the presence of arsenic trioxide. This produced the two-dimensional $[Cu(3\text{-pyrtet})_2]$ (**1**) and the three-dimensional [Cu(4-pyrtet)] (**2**). That the

compounds differ both in dimensionality and copper oxidation state is an unexpected and unpredictable result. When the reaction is carried out in DMF rather than water, the two-dimensional Cu(I) species [Cu(4-pyrtet)]•0.5DMF (**3**•0.5DMF) is isolated.

On the other hand, chloride incorporation was achieved in the one-dimensional [$CuCl_2$(4-Hpyrtet)]•0.5H_2O (**4**•0.5H_2O) using conventional hydrothermal methods. However, the tetrazole group of the ligand is protonated in this case. A one-dimensional material is also isolated with pyrazinetetrazole as ligand, $[Hen]_{0.5}[CuCl_2(prztet)]$ (**6**). In contrast to **4**, the tetrazolate ligand is deprotonated in this case. Iodide incorporation occurs with concomitant reduction of copper in [Cu_2I_2(4-Hpyrtet)] (**5**). The acetylacetonate derivative **7** is two-dimensional with a common grid-like network structure.

The structural versatility of the copper/pyridyltetrazole system is rather remarkable and reflects the facile reduction of copper under hydrothermal conditions, the variability in metal coordination polyhedra, the protonation state of the ligand, and the ability of the pyridyltetrazole (ate) ligand to adopt a variety of coordination modes ranging from monodentate terminal to bridging through one pyridyl and four tetrazolate nitrogen donors. While predictability remains elusive as a result of these factors, the continuing expansion of the structural database may provide recurring secondary building blocks and common structural motifs.

2.4 Experimental Section

2.4.1 Materials and General Procedures

The ligands pyrazinetetrazole, 4- and 3-pyridyltetrazole were prepared by the "click" chemistry approach using zinc catalysis in aqueous solution or by the use of modified montmorillonite K-10.[38-40] All other chemicals were used as obtained without further

purification: copper acetate monohydrate, copper acetylacetonate, copper chloride dihydrate, copper iodide, arsenic trioxide, and dimethylformamide were purchased from Aldrich. All hydrothermal syntheses were carried out in 23 mL poly-(tetrafluoroethylene)-lined stainless steel containers under autogenous pressure. The reactants were stirred briefly, and the initial pH was measured before heating. Water was distilled above 3.0MX in-housing using a Barnstead model 525 Biopure distilled water center. The initial and final pH values of each reaction were measured using color pHast sticks.

2.4.1.1 Synthesis of [Cu(3-pyrtet)$_2$] (1)

A mixture of copper acetate monohydrate (136 mg, 0.684 mmol), 3-pyridyltetrazole (50 mg, 0.342 mmol), arsenic trioxide (129 mg, 0.684 mmol), and H_2O (10.00 g, 556 mmol) in the mole ratio 2.00:1.00:2.00:1626 was stirred briefly before heating to 150°C for 72 hours (initial and final pH values of 3.0 and 2.5, respectively). Dark blue block crystals of **1**, suitable for X-ray diffraction, were isolated in 50% yield. Anal. Calcd. for $C_{12}H_8CuN_{10}$: C, 40.5; H, 2.25; N, 39.3. Found: C, 40.3; H, 2.33; N, 39.2.

2.4.1.2 Synthesis of [Cu(4-pyrtet)] (2)

A mixture of copper acetate monohydrate (136 mg, 0.684 mmol), 4-pyridyltetrazole (50 mg, 0.342 mmol), arsenic trioxide (129 mg, 0.684 mmol), and H_2O (10.00 g, 556 mmol) in the mole ratio 2.00:1.00:2.00:1626 was stirred briefly before heating to 150°C for 72 hours (initial and final pH values of 3.0 and 2.5, respectively). Dark blue block crystals of **2**, suitable for X-ray diffraction, were isolated in 60% yield. Anal. Calcd. for $C_6H_4CuN_5$: C, 34.3; H, 1.91; N, 33.4. Found: C, 34.4; H, 1.84; N, 33.4.

2.4.1.3 Synthesis of [Cu(4-pyrtet)]•0.5DMF (1•0.5DMF) (3)

A mixture of copper acetate monohydrate (136 mg, 0.684 mmol), 4-pyridyltetrazole (50 mg, 0.342 mmol), and DMF (5 mL, 680 mmol) in the mole ratio 2.00:1.00:1704 was stirred briefly before heating to 120°C for 48 hours. Dark blue block crystals of **3**, suitable for X-ray diffraction, were isolated in 40% yield. Anal. Calcd for $C_{7.5}H_{7.5}N_{5.5}CuO_{0.5}$: C, 36.6; H, 3.05; N, 31.3. Found: C, 35.9; H, 2.99; N, 31.6.

2.4.1.4 Synthesis of [$CuCl_2$(4-Hpyrtet)]•0.5H_2O (4•0.5H_2O)

A mixture of copper chloride dihydrate (116 mg, 0.684 mmol), 4- pyridyltetrazole (50 mg, 0.342 mmol), and H_2O (10.00 g, 556 mmol) in the mole ratio 2.00:1.00:1626 was stirred briefly before heating to 150°C for 72 hours (initial and final pH values of 3.5 and 3.3, respectively). Blue plate crystals of **4**, suitable for X-ray diffraction, were isolated in 30% yield. Anal. Calcd for $C_6H_6N_5CuCl_2O_{0.5}$: C, 24.8; H, 2.06; N, 24.1. Found: C, 24.9; H 2.25; N, 23.8.

2.4.1.5 Synthesis of [Cu_2I_2(4-Hpyrtet)] (5)

A mixture of copper iodide (129 mg, 0.684 mmol), 4- pyridyltetrazole (50 mg, 0.342 mmol), and H_2O (10.00 g, 556 mmol) in the mole ratio 2.00:1.00:1626 was stirred briefly before heating to 150°C for 72 hours (initial and final pH values of 3.3 and 2.7, respectively). Blue plate crystals of **5**, suitable for X-ray diffraction, were isolated in 30% yield. Anal. Calcd. for $C_6H_5Cu_2I_2N_5$: C, 13.6; H, 0.95; N,13.3. Found: C, 13.5; H, 0.88; N, 13.2.

2.4.1.6 Synthesis of [H_2en]$_{0.5}$[$CuCl_2$(prztet)] (6)

A mixture of copper chloride dihydrate (116 mg, 0.684 mmol), 4- pyridyltetrazole (50 mg, 0.342 mmol), and H_2O (10.00 g, 556 mmol) in the mole ratio 2.00:1.00:1626 was stirred briefly before heating to 200°C for 72 hours (initial and final pH values of 3.3 and 3.3,

respectively). Blue block crystals of **6**, suitable for X-ray diffraction, were isolated in 20% yield. Anal. Calcd. for $C_6H_8Cl_2CuN_7$: C, 23.0; H, 2.56; N, 31.3. Found: C, 23.2; H, 2.32; N, 30.9.

2.4.1.7 Synthesis of [Cu(acac)(4-pyrtet)] (7)

A mixture of copper acetylacetonate (180 mg, 0.684 mmol) 4-pyridyltetrazole (50 mg, 0.342 mmol), and H_2O (10.00 g, 556 mmol) in the mole ratio 2.00:1.00:1626 was stirred briefly before heating to 150°C for 72 hours (initial and final pH values of 3.3 and 2.9, respectively). Clear blue block crystals of **7**, suitable for X-ray diffraction, were isolated in 40% yield. Anal Calcd. for $C_{11}H_{11}CuN_5O_2$: C, 42.7; H, 3.56; N, 22.7. Found: C, 42.4; H, 3.67; N, 22.5.

2.4.2 X-Ray Crystallography

Structural measurements were performed on a Bruker-AXS SMART-CCD diffractometer at low temperature (90 K) using graphite-monochromated Mo-Ka radiation (Mo K_α = 0.71073A˚).[41] The data were corrected for Lorentz and polarization effects and absorption using SADABS.[42,43] The structures were solved by direct methods. All non-hydrogen atoms were refined anisotropically. After all of the non-hydrogen atoms had been located, the model was refined against $\mathbf{F}^2$, initially using isotropic and later anisotropic thermal displacement parameters. Hydrogen atoms were introduced in calculated positions and refined isotropically. Neutral atom scattering coefficients and anomalous dispersion corrections were taken from the *International Tables*, Vol. C. All calculations were performed using SHELXTL crystallographic software packages.[44]

Crystallographic details have been summarized in **Table 2.1**. Atomic positional parameters, full tables of bond lengths and angles, and anisotropic temperature factors are available in the Supplementary Materials. Selected bond lengths and angles are given in **Table 2.2**.

Table 2.1: Summary of crystal data for the structures of [Cu(3-pyrtet)$_2$] (**1**), and [Cu(4-pyrtet)] (**2**) [Cu(4-pyrtet)]•0.5DMF (**3**•0.5DMF), [$CuCl_2$(4 –Hpyrtet)]•0.5H_2O (**4**•0.5H_2O), [Cu_2I_2(4-Hpyrtet)] (**5**), [H_2en]$_{0.5}$[$CuCl_2$(prztet)] (**6**), and [Cu(acac)(4-pyrtet)] (**7**).

Compound	1	2	3	4
Formula	$C_{12}H_8CuN_{10}$	$C_6H_4CuN_5$	$C_{7.5}H_{7.5}CuN_{5.5}O_{0.5}$	$C_6H_6Cl_2CuN_5O_{0.5}$
Formula weight	355.83	209.69	246.22	290.60
Crystal System	Monoclinic	Monoclinic	Monoclinic	Monoclinic
Space group	C2/c	P21/c	P21/c	C2/c
a (Å)	15.467(4)	3.550(7)	5.814(7)	9.613(11)
b (Å)	11.275(3)	17.71(4)	16.880(2)	19.653(2)
c (Å)	7.094(2)	13.212(3)	8.9663(11)	6.909(8)
α (°)	90	90	90	90
β (°)	94.811(6)	90.136(7)	94.078(2)	113.158(2)
γ (°)	90	90	90	90
V (Å3)	1232.8	830.8(3)	877.80(19)	952.30(19)
Z	4	4	4	4
Dcalc (mg/m3)	1.917	1.677	1.84	2.02
μ (mm-1)	1.791	2.576	2.458	2.824
T (K)	98	98	98	98
Wavelength (Å)	0.71073	0.071073	0.71073	0.71073
R1	0.0314	0.0630	0.0698	0.0427
wR2	0.0812	0.2053	0.1432	0.1052

Compound	5	6	7
Formula	$C_6H_5Cu_2I_2N_5$	$C_6H_8Cl_2CuN_7$	$C_{11}H_{11}CuN_5O_2$
Formula weight	528.03	311.6	308.79
Crystal System	Monoclinic	Triclinic	Monoclinic
Space group	Cc	P-1	P21/n
a (Å)	4.142(3)	6.251(5)	9.185(8)
b (Å)	18.727(12)	8.432(6)	13.461(11)
c (Å)	13.686(9)	10.308(8)	10.741(9)
α (°)	90	71.87(10)	90
β (°)	97.30(10)	85.561(10)	101.18(2)
γ (°)	90	82.965(10)	90
V (Å3)	1053.21(12)	512.13(7)	1302.8(19)
Z	4	2	4
Dcalc (mg/m3)	3.33	1.995	1.574
μ (mm-1)	9.871	2.634	1.681
T (K)	98	98	98
Wavelength (Å)	0.71073	0.71073	0.71073
R1	0.0193	0.0507	0.048
wR2	0.0456	0.1226	0.0964

Table 2.2: Selected bond lengths and angles for [Cu(3-pyrtet)$_2$] (**1**), and [Cu(4-pyrtet)] (**2**), [Cu(4-pyrtet)]•0.5DMF (**3**•0.5DMF), [$CuCl_2$(4 –Hpyrtet)]•0.5H_2O (**4**•0.5H_2O), [Cu_2I_2(4-Hpyrtet) (**5**), [H_2en]$_{0.5}$[$CuCl_2$(prztet)] (**6**), [Cu(acac)(4-pyrtet)] (**7**).

1		5	
Cu(1)-N(2)	2.0009(19)	I(1)-Cu(2)	2.5691(6)
Cu(1)-N(2)	2.0010(19)	I(1)-Cu(1)	2.6370(6)
Cu(1)-N(5)	2.0577(19)	I(1)-Cu(2)	2.6548(6)
Cu(1)-N(5)	2.0577(19)	I(2)-Cu(1)	2.5772(6)
N(2)-Cu(1)-N(5)	170.09(8)	I(2)-Cu(1)	2.6755(7)
N(2)-Cu(1)-N(5)	170.09(8)	I(2)-Cu(2)	2.7044(6)
2		Cu(1)-N(2)	2.021(4)
Cu(1A)-N(2)	1.927(10)	Cu(2)-N(1)	2.019(4)
Cu(1A)-N(1)	1.970(10)	I(1)-Cu(1)-I(2)	114.44
Cu(1A)-N(3)	2.038(11)	I(2)-Cu(1)-N(2)	124.15
N(2)-Cu(1A)-N(1)	135.9(4)	I(1)-Cu(1)-N(2)	105.87
N(2)-Cu(1A)-N(3)	111.9(4)	N(1)-Cu(2)-I(1)	130.43
N(1)-Cu(1A)-N(3)	112.1(4)	I(2)-Cu(2)-I(1)	97.48
3		N(1)-Cu(2)-I(2)	104.35
Cu(1)-N(3)	1.993(4)	6	
Cu(1)-N(2)	2.025(5)	Cu(1)-N(2)	1.993(3)
Cu(1)-N(1)	2.087(4)	Cu(1)-N(1)	2.027(3)
Cu(1)-N(5)	2.096(5)	Cu(1)-N(5)	2.060(3)
4		Cu(1)-Cl(1)	2.2589(10)
Cu(1)-N(1)	2.000(3)	Cu(1)-Cl(2)	2.553(2)
Cu(1)-N(1)	2.000(3)	N(2)-Cu(1)-N(5)	171.83(13)
Cu(1)-Cl(1)	2.3004(7)	N(1)-Cu(1)-Cl(1)	165.93(9)
Cu(1)-Cl(1)	2.3004(7)	Cl(1)-Cu(1)-Cl(2)	165.455
Cl(1)-Cu(1)-Cl(1)	180	7	
N(1)-Cu(1)-N(1)	179.999(1)	Cu(1)-O(1)	1.913(2)
		Cu(1)-O(2)	1.944(2)
		Cu(1)-N(1)	2.010(3)
		Cu(1)-N(5)	2.025(3)
		Cu(1)-N(2)	2.291(3)
		O(2)-Cu(1)-N(5)	169.49(10)
		O(1)-Cu(1)-N(1)	169.80(10)

2.5 Supplementary Materials

Additional material is available from the Cambridge Crystallographic Data Centre. CCDC No. 875439-875445 comprises the final atomic coordinates for all atoms, thermal parameters, and a complete listing of bond distances and angles for compounds **1-7** respectively.

2.6 Acknowledgement

This work was supported by a grant from the National Science Foundation, CHE-0907787.

2.7 References

1. Janiak, C.; and Vieth, J.K.; *New J. Chem.*, *34*, **2010**, 2366.
2. Sachdeva, S.; Lee, A.; and Jeeng, H.-K., *Ind. Eng. Chem. Res.*, DOI: 10.1021/ie 202038m.
3. Ohmori, O.; Kawao, M.; and Frijita, M., *Angew. Chem. Int. Ed.*, *47*, **2008**, 1994.
4. Hagashi, H.; Coté, A.P.; Furukawa, H.; O'Keeffe, M.; and Yaghi, O.M., *Nat. Mater.*, **2007**, *6*, 501.
5. Murray, L.J.; Dinca, M.; and Long, J.R., *Chem. Soc. Rev.*, *38*, **2009**, 1294.
6. Metal-Organic Frameworks, Applications from Catalysis to Gas Storage, Farrusseng, D.; ed., Wiley-VCH Verlag GmbH & Co. KGaA, Weinheim, Germany.
7. Stock, N.; and Biswas, S.; *Chem. Rev.*, dx.doi, org/10.1021/cr200304e.
8. Cheetham, A.K.; Rao, C.N.R.; and Feller, R.K., *Chem. Commun.*, **2006**, 4780.
9. Rao, C.N.R.; Natajaran, S.; Vaidhzanathan, R.; *Angew. Chem. Int. Ed.*, **2004**, *43*, 1466.
10. Tranchemontage, D.J.; Ni, Z.; O'Keeffe, M.; Yaghi, O.M.; *Angew. Chem. Int. Ed.*, 47, **2008**, 5136.
11. Zhang, J.-P.; Zhang, Y.-B.; Lin, J.-B.; and Chen, X.-M., *Chem. Rev.*, dx.doi.org/10.1021/cr2001398.
12. Ouellette, W.; Jones, S.; and Zubieta, J., *Cryst. Eng. Comm.*, **2011**, *13*, 4457.
13. Juricek, M.; Kouwer, P.H.J.; and Rowan, A.E., *Chem. Commun.*, **2011**, *47*, 8740.
14. Zhoa, H.; Qu, Z.-R.; Ye, H.-Y.; and Xiong, R.-G., *Chem. Soc. Rev.*, **2008**, *37*, 84.
15. Beckmann, U.; and Brooker, S., *Coord. Chem. Rev.*, **2003**, *17*, 245.
16. Haasnoot, J.G., *Coord. Chem. Rev.*, **2000**, 200, 131/
17. Hellyer, R.M.; Larsen, D.S.; Brooker, S.; and Eur. J., *Inorg. Chem.*, **2009**, 1162.

18. Zhang, J.-P.; and Chen, X.-M., *Chem. Commun.*, **2006**, 1689.

19. Steel, P.J., *Coord. Chem. Rev.*, **1990**, *106*, 227.

20. Potts, K.T., *Chem. Rev.*, **1961**, *61*, 87.

21. Dawe, L.N.; and Thompson, L.K., *Dalton Trans.*, **2008**, 3610.

22. Zhang, J.-P.; Lin, Y.-Y.; Huang, X.-C.; and Chen, X.-M., *J. Am. Chem. Soc.*, **2005**, *127*, 5495.

23. Zhang, J.-P.; Zheng, S.-L.; Huang, X.-C.; and Chen, X.-M., *Angew. Chem., Int. Ed.*, **2004**, *43*, 206.

24. Ferrer, S.; Lloret, F.; Bertomeu, I.; Alzuet, G.; Borras, J.; Garcia-Granda, S.; Liu-González, M.; and Haasnoot, J.G., *Inorg. Chem.*, **2002**, *41*, 5821.

25. Zhou, J.-H.; Cheng, R.-M.; Song, Y.; Li, Y.-Z.; Yu, Z.; Chen, X.-T.; Xue, Z.-L.; and You, X.-Z., *Inorg. Chem.*, **2005**, *44*, 8011 and references therein.

26. Zhang, J.-P.; Lin, Y.-Y.; Zhang, W.-X.; and Chen, X.-M., *J. Am. Chem. Soc.*, **2005**, *127*, 14162

27. Zhang, D.-C.; Lu, W.-G.; Jiang, L.; Feng, X.-L.; Lu, T.-B., *Cryst. Growth Des.*, **2010**, *10*, 739.

28. Ouellette, W.; Yu, M.H.; O'Connor, C.J.; Hagrman, D.; and Zubieta, J., *Angew. Chem., Int. Ed.*, **2006**, *45*, 3497.

29. Ouellette, W.; Prosvirin, A.V.; Valeich, J.; Dunbar, K.R.; and Zubieta, J., *Inorg. Chem.*, **2007**, *46*, 9067.

30. Ouellette, W.; Galán-Mascarós, J.R.; Dunbar, K.R.; and Zubieta, J., *Inorg. Chem.*, **2006**, *45*, 1909.

31. Ouellette, W.; Prosvirin, A.V.; Chieffo, V.; Dunbar, K.R.; Hudson, B.; and Zubieta, J., *Inorg. Chem.*, **2006**, *45*, 9346.

32. Chesnut, D.J.; Kusnetzow, A.; Birge, R.; and Zubieta, J., *Inorg. Chem.*, **1999**, *38*, 5484.

33. Ouellette, W.; Hudson, B.S.; and Zubieta, J., *Inorg. Chem.*, **2007**, *46*, 4887.

34. Ouellette, W.; Liu, H.; O'Connor, C.J.; and Zubieta, J., *Inorg. Chem.*, **2009**, *48*, 4655.

35. Ouellette, W.; and Zubieta, J., *Chem. Commun.*, **2009**, 4533.

36. Ouellette, W.; Prosvirin, A.V.; Whitenack, K.; Dunbar, K.R., and Zubieta, J., *Angew. Chem., Int. Ed.*, **2009**, *48*, 2140.

37. Ouellette, W.; Darling, K.; Prosvirin, A.; Whitenack, K.; Dunbar, K.R.; and Zubieta, J., *Dalton Trans.*, **2011**, *40*, 12288.

38. (a) Demko, P.Z.; and Sharpless, K.B., *J. Org. Chem.*, **2001**, *66*, 7945; (b) Hirno, F.; Demko, P.Z.; Noodleman, L.; and Sharpless, K.B., *J. Am. Chem. Soc.*, **2002**, *124*, 12210.

39. Tao, J.; Ma, Z.-J.; Huang, R.-B.; and Zhang, L.-S., *Inorg. Chem.*, **2004**, *43*, 6133.

40. Chermahini, A.N.; Teimouri, A.; and Moaddeli, A., *Heteroatom. Chem.*, **2011**, *22*, 168.

41. SMART, Data Collection Software, version 5.630, Bruker-AXS Inc., Madison, WI, **1997-2002**.

42. SAINT Plus, Date Reduction Software, version 6.45A, Bruker-AXS Inc., Madison, WI, **1997-2002**.

43. Sheldrick, G.M., SADABS, University of Göttingen, Göttingen, Germany, **1996**.

44. SHELXTL PC, version 6.12, Bruker-AXS Inc., Madison, WI, **2002**.

45. Barrer, R.M., Hydrothermal Chemistry of Zeolites, Academic Press, London, **1982**.

46. Lobachev, A.N.; and Archand, G.D., Crystallization Processes Under Hydrothermal Conditions, Consultants Bureau, New York, **1973**.

47. Whittingham, M.S., *Curr. Opin. Solid State Mater. Sci.*, **1996**, *1*, 227.

48. Laudise, R.A., *Chem. Eng. News*, **1987**, *65*, 30.

49. Gopalakrishnan, J., *Chem. Mater.*, **1995**, *7*, 1265.

50. Zubieta, J., Solid-State Methods, Hydrothermal. In Comprehensive Coordination Chemistry II; McCleverty, J.A.; Meyer, T.J.; Elsevier Science: New York, **2004**; Vol. 1, pp 697-709.

51. Jarvis, J.A., *Acta Crystallogr.*, **1962**, *15*, 964

Chapter 3: Solid State Coordination Chemistry of Cobalt(II) with Carboxyphenyltetrazoles

3.1 Introduction

As stated previously, solid state coordination chemistry applies fundamental principles of metal-ligand complexation to the design of extended materials, often adopting a bottom-up or building block approach.[1,2] Most prominent among materials of this type are the metal organic frameworks (MOFs) that are constructed from metal or metal cluster nodes linked through dipodal or multipodal ligands. The significant structural diversity and compositional range of MOFs are reflected in applications to separation, gas storage, catalysis and molecular electronics.[3-9] While MOFs have generally been designed by exploiting carboxylate and polypyridyl ligands,[10-12] polyazaheteroaromatic ligands (azolates), of which imidazolate, pyrazolate, triazolate and tetrazolate are representative, have become more prominent in recent years.[13] Azolates exhibit a variety of bridging modes between metals, a superexchange ability that results in unusual magnetic properties of the complexes and facile derivatization to provide multipodal ligands with additional functionality.

In the course of our studies of the hydrothermal chemistry of coordination polymers,[14,31-40] we noted that functionalizing tetrazole with a pyridyl substituent (**Scheme 1**) provided a considerable expansion of the accessible void volume in the copper(II)/pyridyltetrazolate material in comparison with the copper(II)/tetrazolate parent phase. Encouraged by these results, we have investigated other functionalized tetrazoles, including 3- and 4-carboxyphenyltetrazole ($HtrzphCO_2H$). In this article, we report the structure of tetra-butylammonium salt of the ligand $[Bu_4N][4\text{-}HtrzphCO_2]$ (**1**), the molecular complex $[Co(3\text{-}trzphCO_2H)_2(H_2O)_4]\bullet 6H_2O$ (**2**), and the three-dimensional materials $[Co(3\text{-}trzphCO_2)]$ (**3**), $[Co(4\text{-}trzphCO_2)(H_2O]$ (**4**) and $[Co_2)(SO_4)(OH)(3\text{-}trzphCO_2H)]$ (**5**).

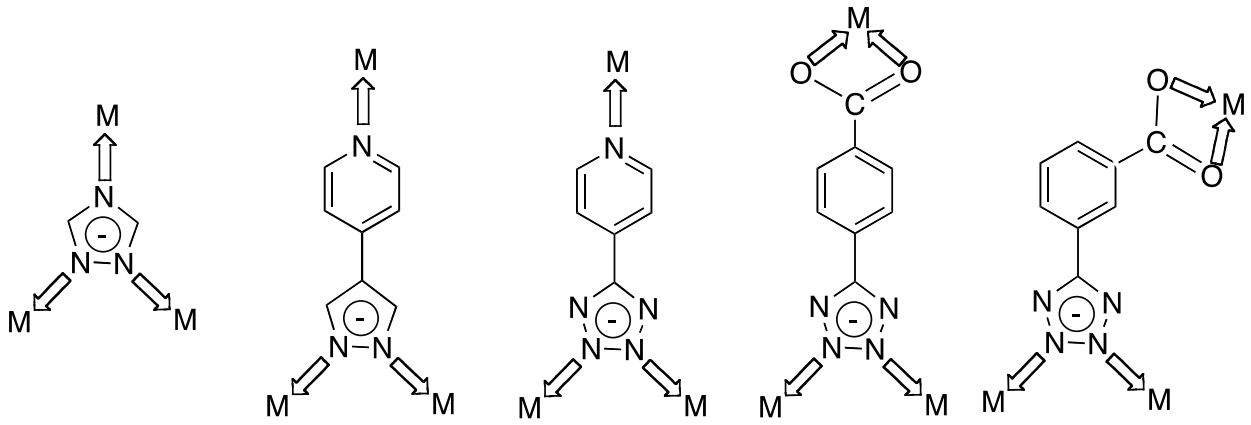

Scheme 1

3.2 Results and Discussion

3.2.1 Syntheses

While the classical hydrothermal literature is concerned with the synthesis of zeolites and metal phosphates [48,49] the technique has now been extended to the routine synthesis of metal oxides and organic-inorganic composite materials.[50-53] Hydrothermal syntheses are conventionally carried out in water at 120-250 ^{o}C at autogenous pressure. Product composition depends on a number of critical conditions, including pH of the medium, temperature and hence pressure, the presence of structure-directing cations, and the use of mineralizers. Since a variety of cationic and anionic components may be present in solution, those of appropriate size, geometry and charge to fulfill crystal packing requirements may be selected from the mixture in the crystallization process. The technique thus exploits "self-assembly" of a solid phase from soluble precursors at moderate temperatures.

The tetraalkylammonium salt of 4-carboxyphenyltetrazole was isolated from the hydrothermal reaction of 4-carboxyphenyltetrazole in the presence of n-Bu_4NOH and $CoSO_4$ in an attempt to prepare a Co-containing material under basic conditions. The reaction mixtures for

compounds **2-5** consisted of the appropriate metal salt and the carboxyphenyltetrazole at the autogenous pH value of ca. 4.1; these were heated at temperatures of 150 to 200 ^{o}C for 3 days. Attempts to prepare the compounds by more conventional (non-hydrothermal) methods proved unsuccessful.

3.2.2 X-ray Structural Studies

The structure of the tetra-butylammonium salt of 4-carboxyphenyltetrazole ($HtrzphCO_2H$) is shown in **Figure 3.1**. The final electron difference map clearly establishes a carboxyl oxygen O2 on the protonation site, an observation consistent with the C-O2 bond distance of 1.318(3)Å and the C-O1 bond distance of 1.217(3)Å. While the tetrazolate group is deprotonated, there is hydrogen bonding between the N3 tetrazolate of one $(trzphCO_2H)^-$ anion and the O2 of a neighboring anion, with N3···O2 and N3···H distances of 2.599(3)Å and 1.630(3)Å, respectively, and an O2-H···N3 angle of 168.64(17)^{o}. The hydrogen bonding links adjacent anions to form chains parallel to the crystallographic *c*-axis.

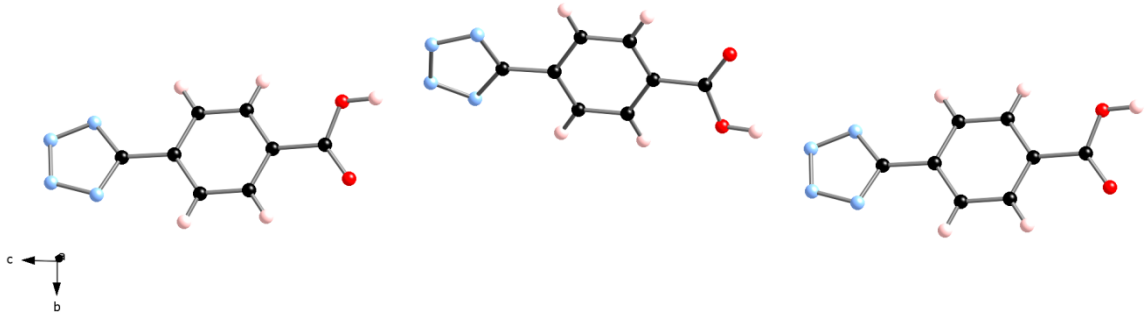

Figure 3.1: A ball-and-stick view of the hydrogen bonding between $(trzphCO_2H)^-$ molecular anions to provide a chain parallel to the *c*-axis in the structure of $(Bu_4N)(4\text{-}trzphCO_2H)$ (**1**).

The structure of molecular species $[Co(3\text{-}trzphCO_2H)_2(H_2O)_4]$ (**2**), shown in **Figure 3.2**, displays distorted octahedral geometry at *trans*-CoN_2O_4 center. The average Co-O bond distance to the equatorial aqua ligands is unexceptional at 2.011(4)Å, while the axial Co-N distances are 2.111(3)Å and 2.126(3)Å. The C-O distances for C-O(H) and C = O of 1.219(5)Å and 1.210(5)Å, respectively, are consistent with protonation of the carboxyl groups.

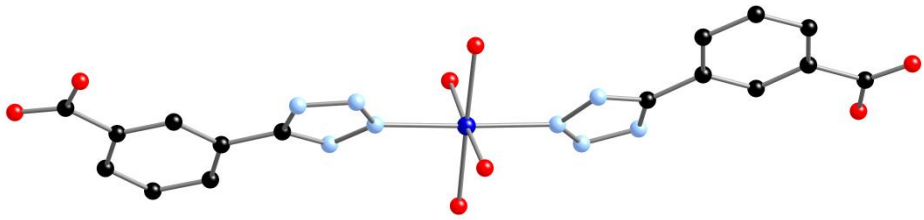

Figure 3.2: A ball-and-stick representation of the molecular structure of $[Co(H_2O)_4(3\text{-}trzphCO_2H)_2]$ (**2**), showing the carboxyl protonation sites. Color scheme: cobalt, dark blue spheres; oxygen, red spheres; nitrogen, blue spheres; carbon, black spheres; hydrogen, pink spheres. The color scheme is used throughout the figures.

As shown in **Figure 3.3**, the structure of $[Co(3\text{-}trzphCO_2)]$ (**3**) is three-dimensional. The fundamental building block is the tetrahedral $\{Co(II)O_2N_2\}$ site that emerges from the bonding of a Co(II) center to donors from four $trzphCO^{2-}$ ligands. This results in a grid-like pattern of carboxylate-bridged chains parallel to the *a*-axis, intersecting with tetrazolate-bridged chains along the *c*-axis in the projection onto the *ac* plane (**Figure 3.3b**). These layers are connected to adjacent layers through the $trzphCO_2^{2-}$ ligands, each of which bonds to four cobalt sites, two through the N1,N4 donors of the tetrazolate group and two through the carboxylate oxygen donors in an *anti-syn* coordination mode.[54,55]

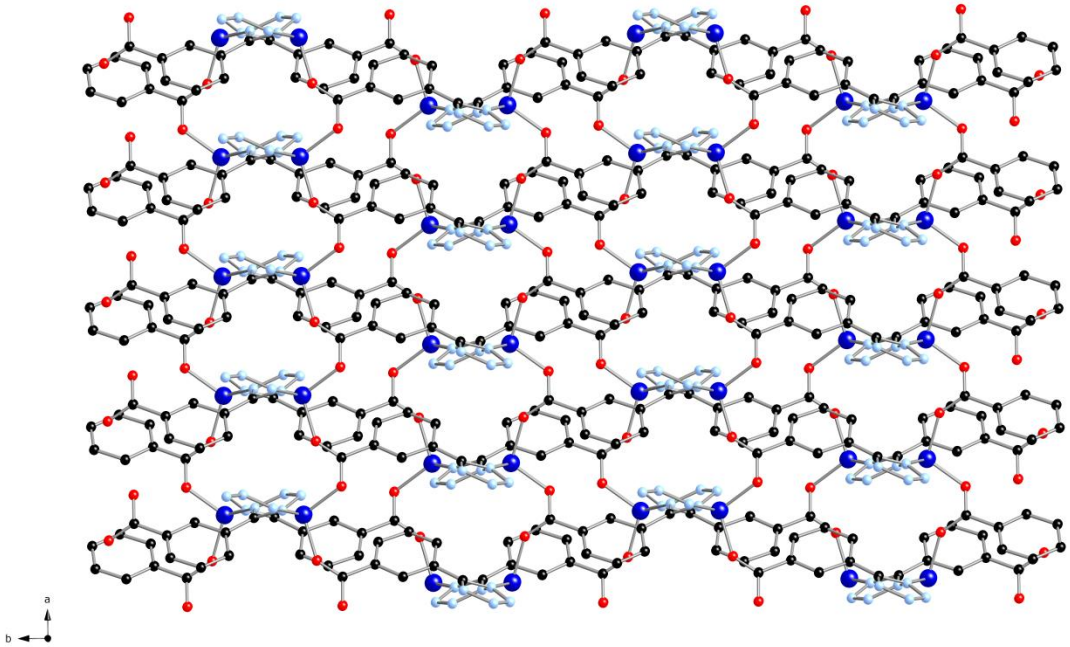

(a)

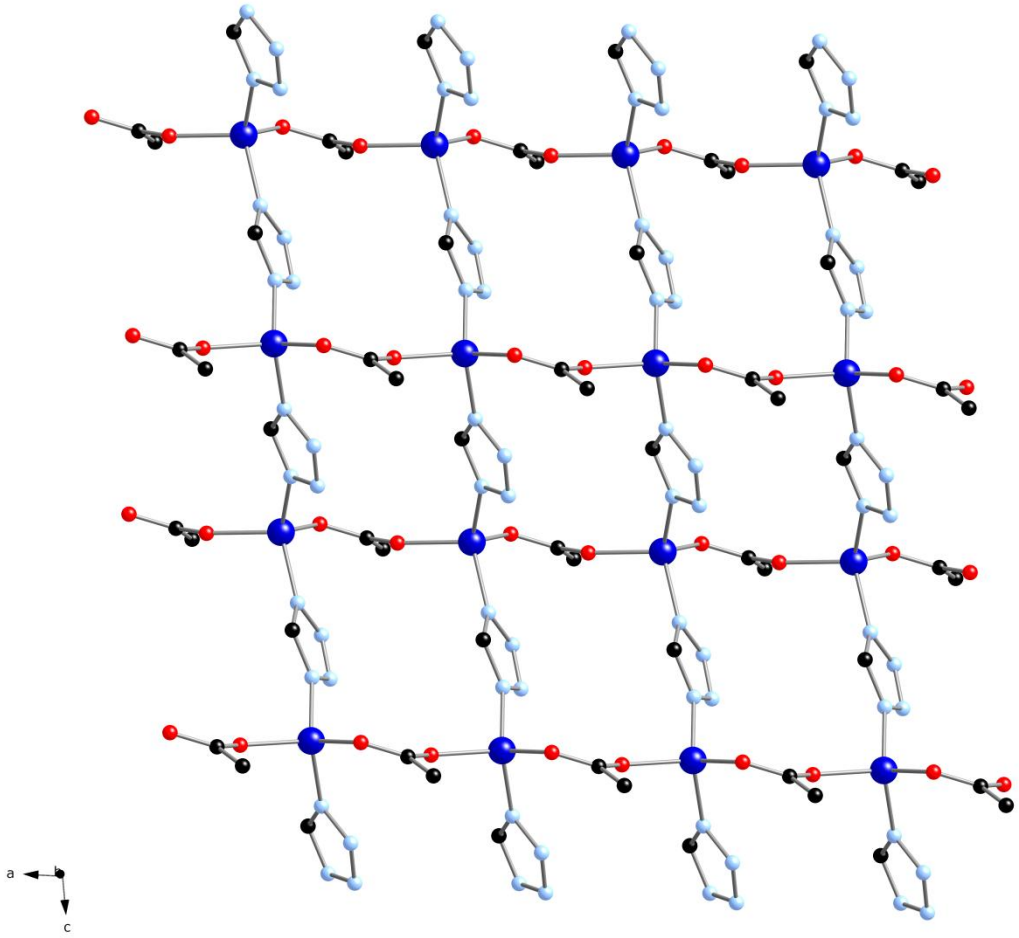

(b)

Figure 3.3: (a) A view of the three-dimensional pillared layer structure of [Co(3-trzphCO_2)] (**3**) normal to the *ab* plane. (b) A view of the {Co(tetrazolate)(carboxylate)}$_n$ layers of **3**, showing the {Co(tetrazolate)} chain substructures linked through RCO_2^- groups.

The hydrated analogue [Co(4-trzphCO_2)(H_2O)] (**4**) is also three-dimensional, as shown in **Figure 3.4**. The structure may be described as layers of tetrazolate-bridged Co(II) sites in the *bc* plane, linked through the phenylcarboxylate groups that project above and below the plane, into the overall framework or pillared layer structure.

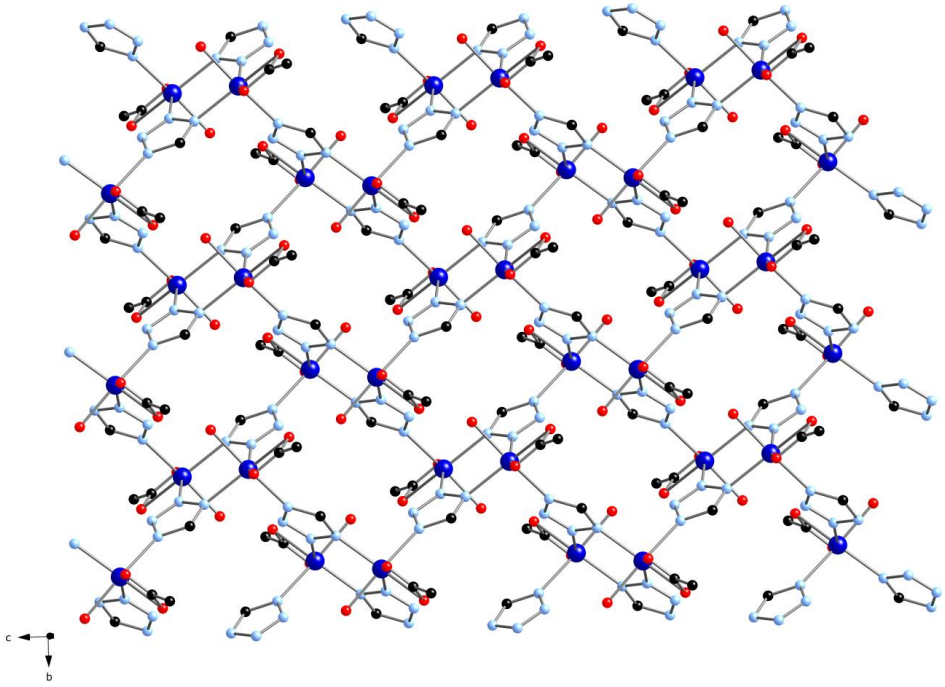

(a)

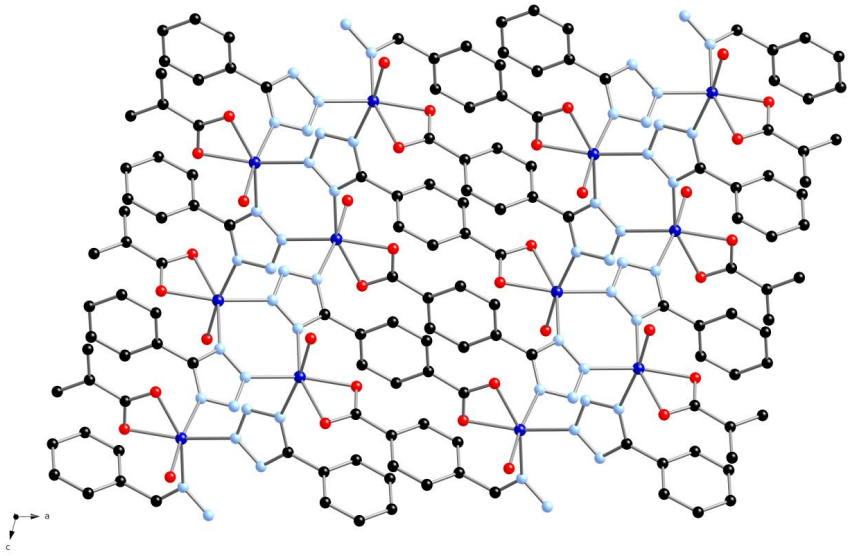

(b)

Figure 3.4: (a) A view of the layer substructure of the three-dimensional [Co(4-trzphCO_2) (H_2O)] (4) in the *bc* plane, showing the {Co(tetrazolate)} two-dimensional connectivity through μ^3-tetrazolate coordination. (b) A view of the structure of 4, normal to the *ac* plane, showing the pillaring of the {Co(tetrazolate)} layers through the (-$C_6H_5CO_2^-$) substituents to establish the overall three-dimensional connectivity.

The Co(II) sites exhibit distorted *facial* $\{CoN_3O_3\}$ coordination geometry through bonding to tetrazolate nitrogen donors from three trzphCO_2^{2-} ligands, a bidentate chelating carboxylate group from a fourth ligand and an aqua ligand. Each tetrazolate moiety bridges three cobalt sites through the N1,N2,N4 sites. Consequently, the trzphCO_2^{2-} ligands bridge three cobalt sites of one layer to a cobalt center of an adjacent layer.

Within the layers there are binuclear $\{Cu_2(azole)_2\}$ secondary building units (SBUs) adopting a six connect pattern.[56] The aqua ligands adopt the *anti*-orientation with respect to the $\{Co_2N_4\}$ plane of this binuclear building block. The layer is two cobalt octahedra thick, and the aqua groups project into the intralamellar domain. The distinct connectivity pattern also aligns the $\{Co_2(azole)_2\}$ planes of adjacent binuclear units at right angles, rather than providing a planar grid of $\{Co_2(azole)_2\}$ groups.

The structure of $[Co_2(SO_4)(OH)(3\text{-trzph}CO_2H)]$ (**5**), while also three-dimensional, illustrates the consequences of introducing the coordinating sulfate anion (**Figure 3.5**). This framework may be described in terms of several substructures. The most evident are the ribbons of Co(II)-tetrazolate groups running parallel to the *b*-axis. These ribbons are linked in turn through sulfato-groups to produce $\{Co_2(azole)(SO_4)\}_n$ layers parallel to the *ab* plane. These layers are connected through the phenylcarboxylate groups along the *c*-axial direction to complete the three-dimensional connectivity.

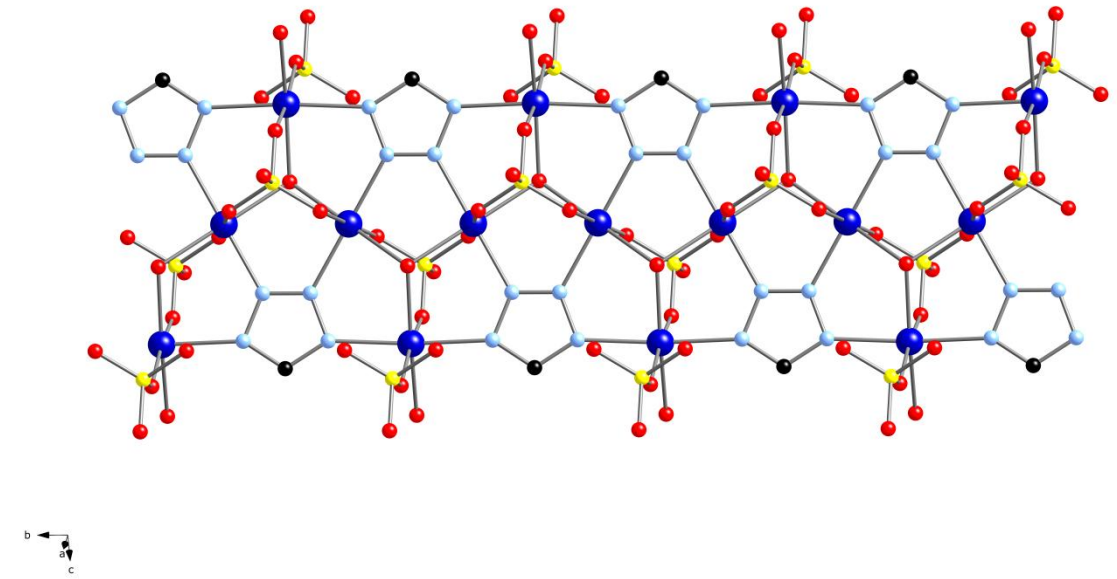

(a)

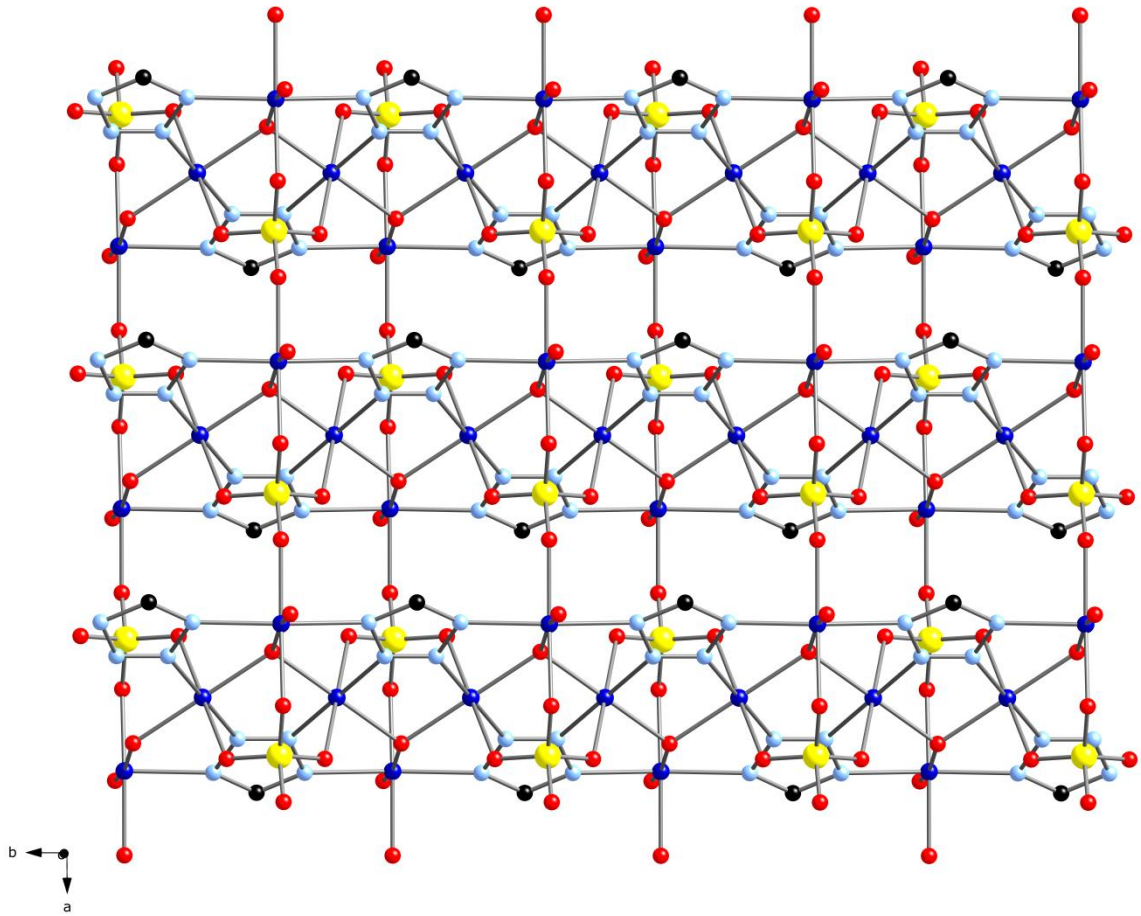

(b)

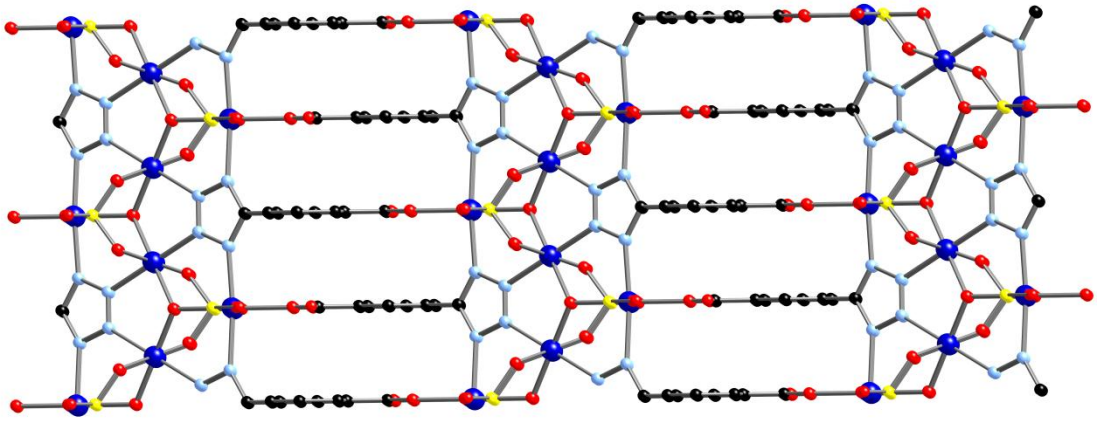

(c)

Figure 3.5: (a) The $\{Co_2(tetrazolate)(OH)(SO_4)\}_n$ chain substructure of $[Co_2(SO_4)(OH)(3\text{-}trzphCO_2H)]$ (**5**), showing the μ^4-tetrazolate bridging motif and the fused $\{Co_3(\mu^3\text{-}OH)(tetrazolate)_3\}^{2+}$ secondary building units. Color scheme: as above with sulfur as yellow spheres. (b) The linking of $\{Co_2(tetrazolate)(OH)(SO_4)\}_n$ chains through $(SO_4)^{2-}$ groups to produce layers parallel to the *ab* plane. Color scheme: as above with sulfur as yellow spheres. (c) The linking of the $\{Co_2(tetrazolate)(OH)(SO_4)\}_n$ layers through $(\text{-}C_6H_5CO_2H)$ groups into a pillared layer, three-dimensional structure. Color scheme: as above with sulfur as yellow spheres.

Within the cobalt-azole ribbon, we observe the common trinuclear secondary building unit $\{Co_3(azole)_3(OH)\}^{2+}$. Such $\{M_3(azole)_3(OH)\}^{n+}$ substructures are common features of triazolate-based materials, such as $[Fe_3(Htrz)_3(HSO_4)(SO_4)_2(OH)]$, $[Ni_3(trz)_3(OH)_3(H_2O)_4]$ and $[Cu_3(trz)_3(OH)_3(H_2O)_4]$.[57,58] The triangular SBU consists of three Co(II) sites, bridged through three azole ligands and a central μ^3-hydroxy group. The cobalt triad is capped on one face by an O,O′,O′′-bridging sulfate group. Each trinuclear SBU shares cobalt sites with two adjacent SBUs to form a ribbon of tetrazolate bridged Co(II) centers. Each tetrazolate group bridges four cobalt sites and links three SBU triads.

There are two distinct cobalt environments, both with *trans* $\{CoN_2O_4\}$ coordination geometry. The first exhibits bonding to nitrogen donors from two tetrazolate ligands, two oxygen donors from sulfato groups triply-bridging with the ribbon, and two hydroxy ligands. The second site bonds to two tetrazolate nitrogen donors, a single hydroxy group, an oxygen donor from the capping sulfato group, an oxygen donor from a sulfato group sharing a single vertex with the ribbon containing the cobalt center, and a carboxylate oxygen. These latter oxygen donors project above and below the planes of the $\{Co_2(tetrazole)(OH)(SO_4)\}_n$ slabs and serve to connect the planes through the phenylcarboxy residues. The carboxyl group is monodentate and protonated at the pendant oxygen, as suggested by C-O distances of 1.221(15)Å and 1.323(16)Å for the C = O(Co) and C-OH bond lengths, respectively.

3.2.3 Structural Observations

Polyazaheterocyclic ligands, in general, are attractive groups for the design of hybrid materials, by virtue of their ability to bridge multiple metal sites, and a super-exchange capacity reflected in the magnetic properties of the complexes. In the specific case of tetrazolate, the anionic ligand can bridge two, three or four metal sites to provide a variety of secondary building units. Compounds **3**, **4** and **5** exhibit one form of bridging bidentate coordination, three and four metal bridging, respectively, demonstrating that minor variation in hydrothermal conditions can result in dramatic structural consequences.

The structural chemistry is further expanded upon introduction of additional functional groups, such as 4-pyridyl or 3- and 4-carboxyphenyl substituents. As previously noted,[14] 4-pyridyltetrazolate can function in the N2,N3-bridging mode to provide an expanded analogue to the triazolate ligand (**Scheme 1**). The 4-carboxyphenyl-tetrazolate ligand could in principle

provide a similar connectivity pattern. However, in this study, the coordination modes adopted are quite different and result in novel and unexpected structural types.

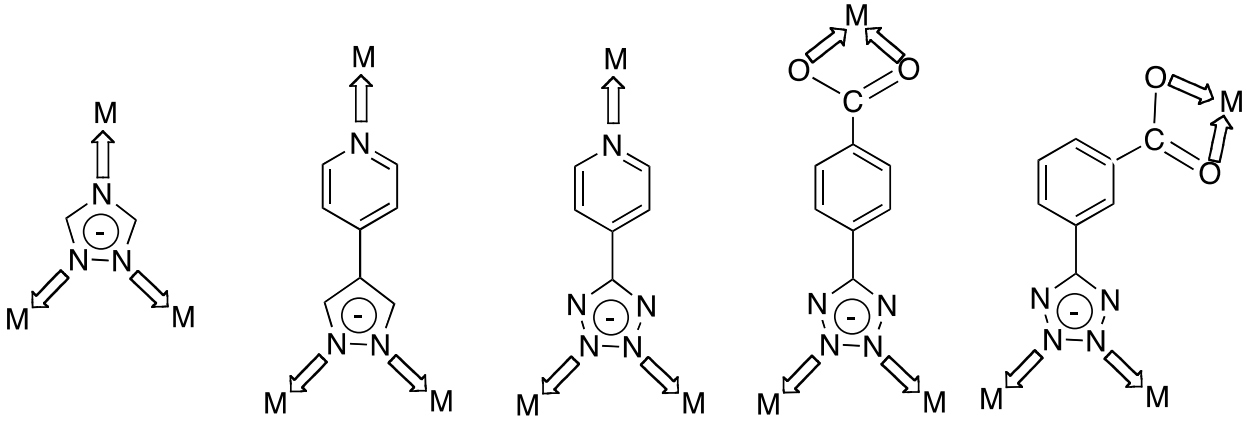

Scheme 1

However, as noted above, the triangular $\{M_3(azole)_3(OH)\}$ SBU is observed in the structure of **5**, although as part of a Co(II)-tetrazolate ribbon rather than as ligand bridged triads. The structural significance of coordinating anions is also apparent in the structure of **5** where the sulfato groups provide capping and bridging groups for the triad units. While a triangular SBU with sulfate coordination is also observed for $[Fe_3(Htrz)_3(HSO_4)(SO_4)_2(OH)]$, the trinuclear building block is quite distinct from that adopted by that of **5** (**Scheme 2**). Once again, these observations reinforce the unpredictability of structures of materials prepared in the hydrothermal domain, particularly when potentially multidentate ligands are present.

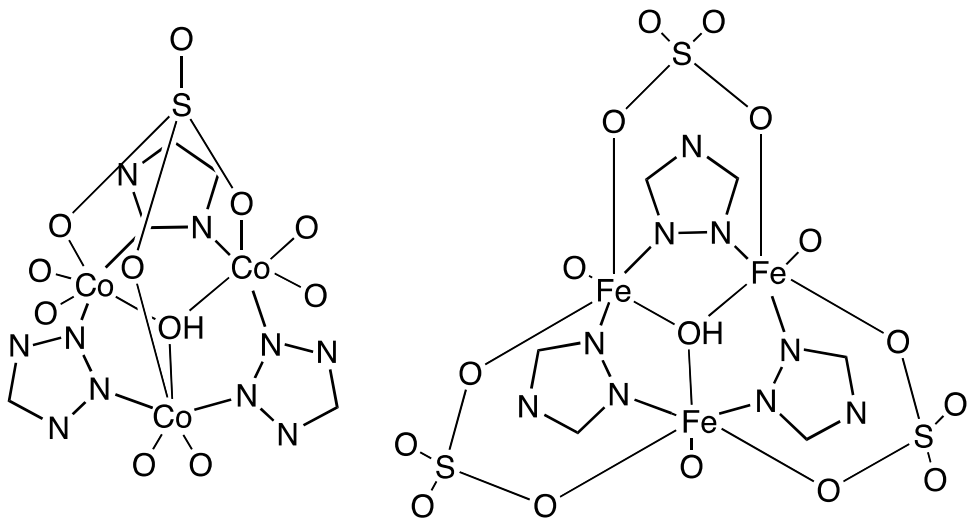

Scheme 2

3.3 Conclusions

Hydrothermal syntheses has been exploited to prepare four Co(II)/carboxyphenyltetrazolate phases, one of which, **2**, is molecular while **3-5** are three-dimensional. The compounds of this study exhibit a range of tetrazolate bonding patterns: through a single nitrogen donor in **2**, bridging bidentate coordination in **3**, bridging to three metal sites in **4**, and bridging to four metal sites in **5**.

The structures are further enhanced through participation of the carboxylate groups in bonding to the Co(II) sites. As noted previously,[32,59] the incorporation of secondary anion components, specifically sulfate in compound **5**, can have dramatic and unpredictable structural consequences. The evolving chemistry of materials of the general class M(II)/derivatized azolate/XO_4^{n-} (X= S, n = 2; X = P, n = 3; X = V, n = 3) continues to provide a wealth of unusual structural types exhibiting a variety of secondary building units. The persistence of such SBU's and their predictable incorporation into extended structures remain elusive goals.

3.4 Experimental Section

3.4.1 Materials and General Procedures

The ligands 3-, and 4- carboxyphenyltetrazole were prepared by the "click" chemistry approach using zinc catalysis in aqueous solution or by the use of modified montmorillonite K-10 [41-43]. All other chemicals were used as obtained without further purification: cobalt nitrate hexahydrate, cobalt chloride hexahydrate, cobalt sulfate heptahydrate, and tetrabutylammonium hydroxide were purchased from Aldrich. All hydrothermal syntheses were carried out in 23 mL poly-(tetrafluoroethylene)-lined stainless steel containers under autogenous pressure. The reactants were stirred briefly, and the initial pH was measured before heating. Water was distilled above 3.0MX in-housing using a Barnstead model 525 Biopure distilled wager center. The initial and final pH values of each reaction were measured using color pHast sticks.

3.4.1.1 Synthesis of $(Bu_4N)(4\text{-}trzphCO_2H)$ (1)

A mixture of cobalt sulfate heptahydrate (280 mg, .996 mmol), 4-carboxyphenyltetrazole (75 mg, .395 mmol), tetrabutylammonium hydroxide (102.5 mg, .395 mmol) and H_2O (10.00 g, 556 mmol) in the mole ratio 2.52:1.00:1.00:1626 was stirred briefly before heating to 180 ^oC for 72 hours (initial and final pH values of 3.0 and 2.7, respectively). Clear colorless block crystals of **1**, suitable for X-ray diffraction, were isolated in 10% yield. Anal. Calcd. for $C_{24}H_{41}N_5O_2$: C, 66.7; H, 9.50; N, 16.2. Found: C, 66.8; H, 9.21; N, 16.1.

3.4.1.2 Synthesis of $[Co(3\text{-}trzphCO_2H)_2(H_2O)_4 \bullet 6H_2O]$ (2)

A mixture of cobalt chloride hexahydrate (280 mg, 1.18 mmol), 3-carboxyphenyltetrazole (75mg, .395 mmol), and H_2O (10.00 g, 556 mmol) in the mole ratio

3.00:1.00:1626 was stirred briefly before heating to 150 ^{o}C for 72 hours (initial and final pH values of 3.5 and 3.3, respectively). Clear pink block crystals of **2**, suitable for X-ray diffraction, were isolated in 20% yield. Anal. Calcd. for $C_{16}H_{30}CoN_8O_{14}$: C, 31.1; H, 4.86; N, 18.1. Found: C, 29.7; H, 4.73; N, 17.9.

3.4.1.3 Synthesis of [Co(3-trzphCO$_2$)] (3)

A mixture of cobalt chloride hexahydrate (280 mg, .962 mmol), 3-carboxyphenyltetrazole (75 mg, .395 mmol), and H_2O (10.00 g, 556 mmol) in the mole ratio 3.00:1.00:1626 was stirred briefly before heating to 200 ^{o}C for 72 hours (initial and final pH values of 3.5 and 3.3, respectively). Clear pink block crystals of **3**, suitable for X-ray diffraction, were isolated in 20% yield. Anal. Calcd. for $C_8H_4CoN_4O_2$: C, 38.9; H, 1.62; N, 22.7. Found: C, 39.0; H, 1.47; N, 22.5.

3.4.1.4 Synthesis of [Co(4-trzphCO$_2$)(H$_2$O)] (4)

A mixture of cobalt nitrate hexahydrate (200 mg, .687 mmol), 4-carboxyphenyltetrazole (75 mg, .395 mmol), and H_2O (10.00 g, 556 mmol) in the mole ratio 2.00:1.00:1626 was stirred briefly before heating to 150 ^{o}C for 72 hours (initial and final pH values of 3.3 and 2.7, respectively). Clear dark pink plate crystals of **4**, suitable for X-ray diffraction, were isolated in 30% yield. Anal. Calcd. for $C_8H_6CoN_4O_3$: C, 36.2; H, 2.26; N, 21.1. Found: C, 36.4; H, 2.44; N, 20.9.

3.4.1.5 Synthesis of [Co$_2$(SO$_4$)(OH)(3-trzphCO$_2$H)] (5)

A mixture of cobalt sulfate heptahydrate (280 mg, 0.970 mmol), 3-carboxyphenyltetrazole (75 mg, .395 mmol), and H_2O (10.00 g, 556 mmol) in the mole ratio 3.00:1.00:1626 was stirred briefly before heating to 150 ^{o}C for 72 hours (initial and final pH

values of 3.0 and 2.5, respectively). Clear pink block crystals of **5**, suitable for X-ray diffraction, were isolated in 20% yield. Anal. Calcd. for $C_8H_6Co_2N_4O_7S$: C, 22.9; H, 1.43; N, 13.3. Found: C, 23.2; H, 1.55; N, 13.3.

3.4.2 X-Ray Crystallography

Structural measurements were performed on a Bruker-AXS SMART-CCD diffractometer at low temperature (90 K) using graphite-monochromated Mo-Ka radiation (Mo K_α = 0.71073A^o).[44] The data were corrected for Lorentz and polarization effects and absorption using SADABS.[45,46] The structures were solved by direct methods. All non-hydrogen atoms were refined anisotropically. After all of the non-hydrogen atoms had been located, the model was refined against F^2, initially using isotropic and later anisotropic thermal displacement parameters. Hydrogen atoms were introduced in calculated positions and refined isotropically. Neutral atom scattering coefficients and anomalous dispersion corrections were taken from the *International Tables*, Vol. C. All calculations were performed using SHELXTL crystallographic software packages.[47]

Crystallographic details have been summarized in **Table 3.1**. Atomic positional parameters, full tables of bond lengths and angles, and anisotropic temperature factors are available in the Supplementary Materials. Selected bond lengths and angles are given in **Table 3.2**.

Table 3.1: Summary of crystal data for the structures of (Bu_4N)[4-trzphCO_2H] (**1**), [Co(3-trzphCO_2H)$_2$(H_2O)$_4$]·6H_2O (**2**), [Co(3-trzphCO_2)] (**3**), [Co(4-trzphCO_2)(H_2O)] (**4**), and [Co_2(SO_4)(OH)(3-trzphCO_2H)] (**5**).

Compound	1	2	3	4	5
Formula	$C_{24}H_{41}N_5O_2$	$C_{16}H_{30}CoN_8O_{14}$	$C_8H_4CoN_4O_2$	$C_8H_6CoN_4O_3$	$C_8H_6Co_2N_4O_7S$
Formula weight	431.62	617.41	247.08	265.1	420.10
Crystal System	Orthorhombic	Monoclinic	Monoclinic	Monoclinic	Monoclinic
Space group	Pbca	P21/c	P21/c	P21/c	P21/m
a (Å)	15.1187(12)	6.947(10)	4.9452(7)	12.0643(10)	6.4544(13)
b (Å)	16.1083(13)	28.203(3)	17.033(2)	7.3225(6)	6.6011(13)
c (Å)	21.4947(17)	13.215(2)	10.3554(15)	10.1654(8)	13.914(3)
α (°)	90	90	90	90	90
β (°)	90	114.00(10)	98.707(2)	106.352(2)	93.838
γ (°)	90	90	90	90	90
V ($Å^3$)	5234.7(7)	2365.3	862.2(2)	861.70(12)	591.5(2)
Z	8	4	4	4	2
D_{calc} (mg/m^3)	1.095	1.734	1.903	2.043	2.425
μ (mm-1)	0.071	0.816	1.971	1.988	3.299
T (K)	98(2)	98(2)	98(2)	98(2)	98(2)
Wavelength (Å)	0.71073	0.71073	0.71073	0.71073	0.71073
R_1	0.0773	0.0819	0.0368	0.0692	0.1015
wR_2	0.1308	0.1813	0.0828	0.1373	0.2064

Table 3.2: Selected bond lengths and angles for $[Co(3\text{-}trzphCO_2H)_2(H_2O)_4]\cdot 6H_2O$ (**2**), $[Co(3\text{-}trzphCO_2)]$ (**3**), $[Co(4\text{-}trzphCO_2)(H_2O)]$ (**4**), and $[Co_2(SO_4)(OH)(3\text{-}trzphCO_2H)]$ (**5**).

2		3	
Co(1)-O(2)	1.992(4)	N(1)-Co(1)	1.986(2)
Co(1)-O(3)	2.002(4)	O(1)-Co(1)	1.9422(17)
Co(1)-O(4)	2.005(4)	Co(1)-N(4)	1.999(2)
Co(1)-O(1)	2.030(3)	O(2)-Co(1)	1.9551(18)
Co(1)-N(5)	2.111(4)	N(1)-Co(1)-N(2)	177.81(10)
Co(1)-N(1)	2.126(4)	N(4)-Co(1)-N(5)	178.19(10)
O(2)-Co(1)-O(4)	176.74(17)		
O(3)-Co(1)-O(1)	178.94(16)	5	
N(5)-Co(1)-N(1)	178.08(14)	Co(2)-O(4)	2.075(13)
		Co(2)-O(4)	2.075(13)
4		Co(2)-N(1)	2.083(9)
Co(1)-O(1)	2.056(3)	Co(2)-O(3)	2.090(8)
Co(1)-O(90)	2.109(4)	Co(2)-O(3)	2.090(8)
Co(1)-N(2)	2.137(4)	Co(1)-O(2)	2.055(12)
Co(1)-N(1)	2.165(4)	Co(1)-O(1)	2.064(11)
Co(1)-N(4)	2.180(4)	Co(1)-O(5)	2.106(11)
Co(1)-O(2)	2.249(3)	Co(1)-O(4)	2.105(19)
O(1)-Co(1)-N(2)	166.70(15)	Co(1)-N(2)	2.169(10)
O(90)-Co(1)-N(4)	171.66(15)	O(2)-Co(1)-O(1)	167.5(4)
N(1)-Co(1)-O(2)	167.78(14)	O(4)-Co(2)-O(4)	180.0(14)
		O(5)-Co(1)-O(4)	167.3(7)
		N(2)-Co(1)-N(2)	173.1(5)
		N(1)-Co(2)-N(1)	180.0(3)

3.5 Supplementary Materials

Additional material available from the Cambridge Crystallographic Data Centre, CCDC No. CCDC 873554-873558, comprises the final atomic coordinates for all atoms, thermal parameters, and a complete listing of bond distances and angles, for compounds **1-5**, respectively.

3.6 Acknowledgement

This work was supported by a grant from the National Science Foundation, CHE-0907787.

3.7 References

1. Hagrman, P.J.; Hagrman, D.; and Zubieta, J., *Angew Chem.*, Int. Ed. Engl., **1999**, *38*, 2639.
2. Hagrman, P.J.; Hagrman, D.; and Zubieta, J., Perspectives in the solid state coordination chemistry of the molybdenum oxides, in Polyoxometalate Chemistry, M.T. Pope and A. Muller, eds., Kluwer Academic Publ., Dordrecht, The Netherlands, **2001**, pp. 269-300.
3. Janiak, C.; and Vieth, J.K., *New J. Chem.* **2010**, *34*, 2366.
4. Sachdeva, S.; Lee, A.; and Jeong, H.-K., *Ind. Eng. Chem. Res.*, DOI: 10.1021/ie 202038m.
5. Ohmori, O.; Kawano, M.; and Fujita, M., *Angew. Chem.*, Int. Ed. **2008**, *48*, 1994.
6. Hagashi, H.; Coté, A.P.; Furukawa, G.; O'Keeffe, M.; and Yaghi, O.M., *Nat. Mater.*, **2007**, *6*, 501.
7. Murray, L.J.; Dinca, M.; and Long, J.R., *Chem. Soc. Rev.*, **2009**, *38*, 1294.
8. Metal-Organic Frameworks, Applications from Catalysis to Gas Storage, Farrusseng, D., ed., Wiley-VCH Verlag GmbH & Co KGaA, Weinheim, Germany.
9. Stock, N.; and Biswas, S., *Chem. Rev.*, dx.doi, org/10.1021/cr200304e.
10. Cheetham, A.K.; Rao, C.N.R.; and Feller, R.K., *Chem. Commun.*, **2006**, *47*, 80.
11. Rao, C.N.R.; Natajaran, S.; and Vaidhzanathan, R., *Angew. Chem.*, Int. Ed. **2004**, *43*, 1466.
12. Tranchemontage, D.J.; Ni, Z.; O'Keeffe, M.; and Yaghi, O.M., *Angew. Chem.*, Int. Ed. **2008**, *47*, 5136.
13. Zhang, J.-P.; Zhang, Y.-B.; Lin, J.-B.; and Chen, X.-M., *Chem. Rev.*, dx.doi.org/10.1021/ cr200139g.

14. Ouellette, W.; Jones, S.; and Zubieta, J., *Cryst. Eng. Comm.*, **2011**, *13*, 4457.

15. Juricek, M.; Kouwer, P.H.J.; and Rowan, A.E., *Chem. Commun.*, **2011**, *47*, 8740.

16. Zhoa, H.; Qu, Z.-R.; Ye, H.-Y.; and Xiong, R.-G., *Chem. Soc. Rev.*, **2008**, *37*, 84.

17. Beckmann, U.; and Brooker, S., *Coord. Chem. Rev.*, **2003**, *17*, 245.

18. Haasnoot, J.G., *Coord. Chem. Rev.*, **2000**, *200*, 131.

19. Hellyer, R.M.; Larsen, D.S.; and Brooker, S., *Eur. J. Inorg. Chem.*, **2009**, 1162.

20. Zhang, J.-P.; and Chen, X.-M., *Chem. Commun.*, **2006**, 1689.

21. Steel, P.J., *Coord. Chem. Rev.*, **1990**, *106*, 227.

22. Potts, K.T., *Chem. Rev.*, **1961**, *61*, 87.

23. Dawe, L.N.; and Thompson, L.K., *Dalton Trans.*, **2008**, 3610.

24. Zhang, J.-P.; Lin, Y.-Y.; Huang, X.-C.; and Chen, X.-M., *J. Am. Chem. Soc.*, **2005**, *127*, 5495.

25. Zhang, J.-P.; Zheng, S.-L.; Huang, X.-C.; and Chen, X.-M., *Angew. Chem., Int. Ed.*, **2004**, *43*, 206.

26. Ferrer, S.; Lloret, F.; Bertomeu, I.; Alzuet, G.; Borras, J.; Garcia-Granda, S.; Liu-González, M.; and Haasnoot, J.G., *Inorg. Chem.*, **2002**, 5821.

27. Ferrer, S.; Lloret, F.; Bertomeu, I.; Alzuet, G.; Borras, J.; Garcia-Granda, S.; Liu-González, M.; and Haasnoot, J.G., *Inorg. Chem.*, **2002**, 5821.

28. Zhou, J.-H.; Cheng, R.-M.; Song, Y.; Li, Y.-Z.; Yu, Z.; Chen, X.-T.; Xue, Z.-L.; and You, X.-Z., *Inorg. Chem.* **2005**, *44*, 8011 and references therein.

29. Zhang, J.-P.; Lin, Y.-Y.; Zhang, W.-X.; and Chen, X.-M., *J. Am. Chem. Soc.*, **2005**, *127*, 14162.

30. Zhang, D.-C.; Lu, W.G.; Jiang, L.; Feng, X.L.; and Lu, T.-B., *Cryst. Growth Des.*, **2010**, 10, 739.

31. Ouellette, W.; Yu, M.H.; O'Connor, C.J.; Hagrman, D.; and Zubieta, J., *Angew. Chem.*, Int. Ed. **2006**, *45*, 3497.

32. Ouellette, W.; Prosvirin, A.V.; Valeich, J.; Dunbar, K.R.; and Zubieta, J., *Inorg. Chem.*, **2007**, *46*, 9067.

33. Ouellette, W.; Galán-Mascarós, J.R.; Dunbar, K.R.; and Zubieta, J., *Inorg. Chem.*, **2006**, *45*, 1909.

34. Ouellette, W.; Prosvirin, A.V.; Chieffo, V.; Dunbar, K.R.; Hudson, B.; and Zubieta, J., *Inorg. Chem.*, **2006**, *45*, 9346.

35. Chesnut, D.J.; Kusnetzow, A.; Birge, R.; and Zubieta, J., *Inorg. Chem.*, **1999**, *38*, 5484.

36. Ouellette, W.; Hudson, B.S.; and Zubieta, J., *Inorg. Chem.*, **2007**,*46*, 4887.

37. Ouellette, W.; Liu, H.; O'Connor, C.J.; and Zubieta, J., *Inorg. Chem.*, **2009**, *48*, 4655.

38. Ouellette, W.; and Zubieta, J., *Chem. Commun.*, **2009**, 4533.

39. Ouellette, W.; Prosvirin, A.V.; Whitenack, K.; Dunbar, K.R.; and Zubieta, J., *Angew. Chem.*, Int. Ed. **2009**, *48*, 2140.

40. Ouellette, W.; Darling, K.; Prosvirin, A.; Whitenack, K.; Dunbar, K.R.; and Zubieta, J., *Dalton Trans.*, **2011**, *40*, 12288.

41. (a) Demko, P.Z.; and Sharpless, K.B., *J. Org. Chem.*, **2001** 66 7945; (b) Hirno, F.; Demko, P.Z.; Noodleman, L.; and Sharpless, K.B., *J. Am. Chem. Soc.*, **2002**, *122*, 12210.

42. Tao, J.; Ma, Z.-J.; Huang, R.-B.; and Zhang, L.-S., *Inorg. Chem.*, **2004**, *43*, 6133.

43. Chermahini, A.N.; Teimouri, A.; and Moaddeli, A., *Heteroatom Chem.*, **2011**, *22*, 168.

44. SMART, Data Collection Softward, version 5.630, Bruker-AXS Inc., Madison, WI, (**1997**-**2002**).

45. SAINT Plus, Data Reduction Software, version 6.45A, Bruker-AXS Inc., Madison, WI (**1997**-**2002**).

46. Shldrick, G.M., SADABS, University of Göttingen, Göttingen, Germany, **1996**.

47. SHELXTL PC, version 6.12, Bruker-AXS Inc., Madison, WI, **2002**.

48. Barrer, R.M., Hydrothermal Chemistry of Zeolites, Academic Press, London, **1982**.

49. Lobachev, A.N.; and Archand, G.D., Crystallization Processes Under Hydrothermal Conditions, Consultants Bureau, New York, **1973**.

50. Whittingham, M.S., *Curr. Opin. Solid State Mater. Sci.*, **1996**, *1*, 227.

51. Laudise, R.A., *Chem. Eng. News*, **1987**, *65*, 30.

52. Gopalakrishnan, J., *Chem. Mater.*, **1995**, *7*, 1265.

53. Zubieta, J., Solid-State Methods, Hydrothermal. In Comprehensive Coordination Chemistry II; McCleverty, J.A.; and Meyer, T.J., Elsevier Science: New York, **2004**, 1 697-709.

54. Appleton, T.G.; Byriel, K.A.; Garrett, J.M.; Hall, J.R.; Kennard, C.H.L.; Mathieson, M.T.; and Stranger, R., *Inorg. Chem.*, **1995**, *34*, 8646.

55. Wei, P.-R.; Li, Q.; Leung, W.P.; and Mak, T.C.W., *Polyhedron*, **1997**, *16*, 897.

56. Li, Z.; Li, M.; Zhan, S.-Z.; Huang, X.-C.; Ng, S.W.; and Li, D., *Cryst. Eng. Comm.*, **2008**, *10*, 978.

57. Ouellette, W.; Prosvirin, A.V.; Valeich, J.; Dunbar, K.R.; and Zubieta, J., *Inorg. Chem.*, **2007**, *46*, 9067.

58. Ouellette, W.; Yu, M.H.; O'Connor, C.J.; Hagrman, D.; and Zubieta, J., *Angew. Chem.*, Int. Ed. Eng., **2006**, *45*, 3497.

59. Darling, K.; Ouellette, W.; Prosvirin, A.; Freund, S.; Dunbar, K.R.; and Zubieta, J., *Cryst. Growth Des.*, approved.

Chapter 4: One- and Two-dimensional Coordination Polymers of Substituted Tetrazoles with Cadmium(II)

4.1 Introduction

As noted in Chapter 1, polyazaheteroaromatic compounds such as pyrazole, imidazole, triazole and tetrazole in their anionic forms have elicited considerable contemporary interest as bridging ligands between transition metal ions for the preparation of 1-D, 2-D and 3-D coordination polymers and for the isolation of a variety of molecular cluster complexes.[1-15] Of the azole ligands, the tetrazolate ligand has been shown to adopt a variety of coordination modes, as shown in **Scheme 1**.

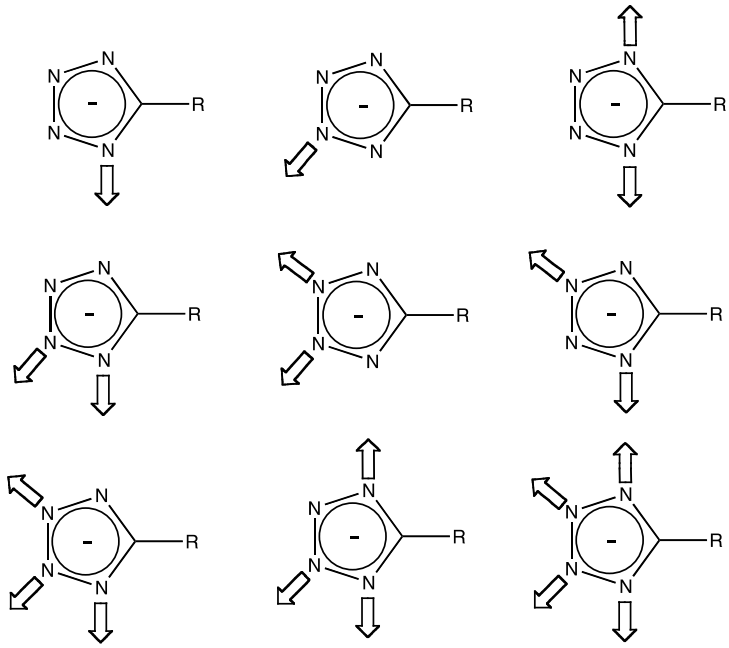

Scheme 1

In the course of our investigations of the coordination chemistry of polyazaheteroaromatic ligands with transition metals,[16-25] we have investigated the consequences of additional functional group substituents, such as pyridine and pyrazine, on the structural chemistry of metal-tetrazole (**Scheme 2**). Since cadmium-azole materials exhibit both unusual structures and luminescent properties,[27-30] we have investigated the chemistry of Cd(II) with 4-pyridyltetrazole, 2-pyridyltetrazole and pyrazinetetrazole. We report the structures of the two

dimensional $[Cd(4\text{-}Hpyrtet)_2(OH)_2]$ (**1**) and the analogous $[M(4\text{-}pyrtet)_2(H_2O)_2]$ (M = Co(**2**), Cu(**3**)), the one-dimensional [CdCl(2-pyrtet)(DMF)] (**4**), the two-dimensional $[Cd_4Cl_6(pyrztet)_2(DMF)_4]$ (**5**), and the three-dimensional $[Cd_3(N_3)_4(4\text{-}pyrtet)_2(H_2O)_2]$ (**6**).

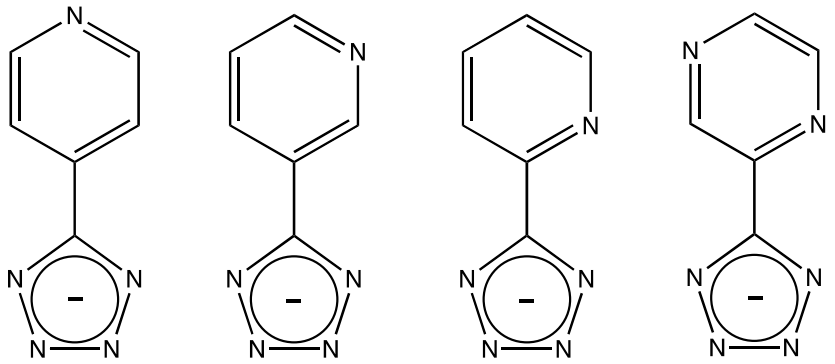

Scheme 2

4.2 Results and Discussion

4.2.1 Syntheses

The isolation of compounds **1**-**6** demonstrates the range of synthetic methods that can be exploited in the preparation of coordination polymers. Compounds **1-3** were synthesized using conventional hydrothermal methods, which have been extensively explored in the synthesis of hybrid materials. At these temperature ranges, the reactants are solubilized while retaining their structural features in the product phases, exploiting the self assembly of products from these soluble precursors.[38-43] Compounds **4** and **5** were prepared from the room temperature reaction of the appropriate cadmium salts with 2-pyridyltetrazole and pyrazinetetrazole in dimethylformamide as solvent, a common synthetic approach for similar systems.[22] The synthesis of **6** exploited the *in situ* preparation of 4-pyridyltetrazole from 4-pyridinecarbonitrile and sodium azide in the presence of a cadmium(II) salt. The *in situ* preparation of

pyridinetetrazoles from the appropriate pyridinecarbonitrile and sodium azide under hydrothermal conditions has been described previously.[44]

4.2.2 X-Ray Structural Studies

The two-dimensional structure of $[Cd(4\text{-Hpyrtet})_2(OH)_2]$ (**1**) is shown in **Figure 4.1**. The structure is constructed from the linking of distorted $\{CdO_2N_4\}$ octahedra through the dipodal 4-pyridyltetrazole ligands. The Cd(II) coordination environment consists of an equatorial plane defined by *trans* oriented N1 donors from two tetrazole ligands and two pyridyl donors from a second pair of 4-Hpyrtet ligands, with hydroxy ligands occupying the axial position. Each Cd(II) site is linked to four adjacent sites through the 4-Hpyrtet bridging ligands, a connectivity that produces a grid pattern with intralamellar cavities with edges defined by the 4-Hpyrtet ligands. The hydroxy ligands project into the cavities. The 4-Hpyrtet ligand is present in the neutral state with the N3 site of the tetrazole unit as the protonation site.

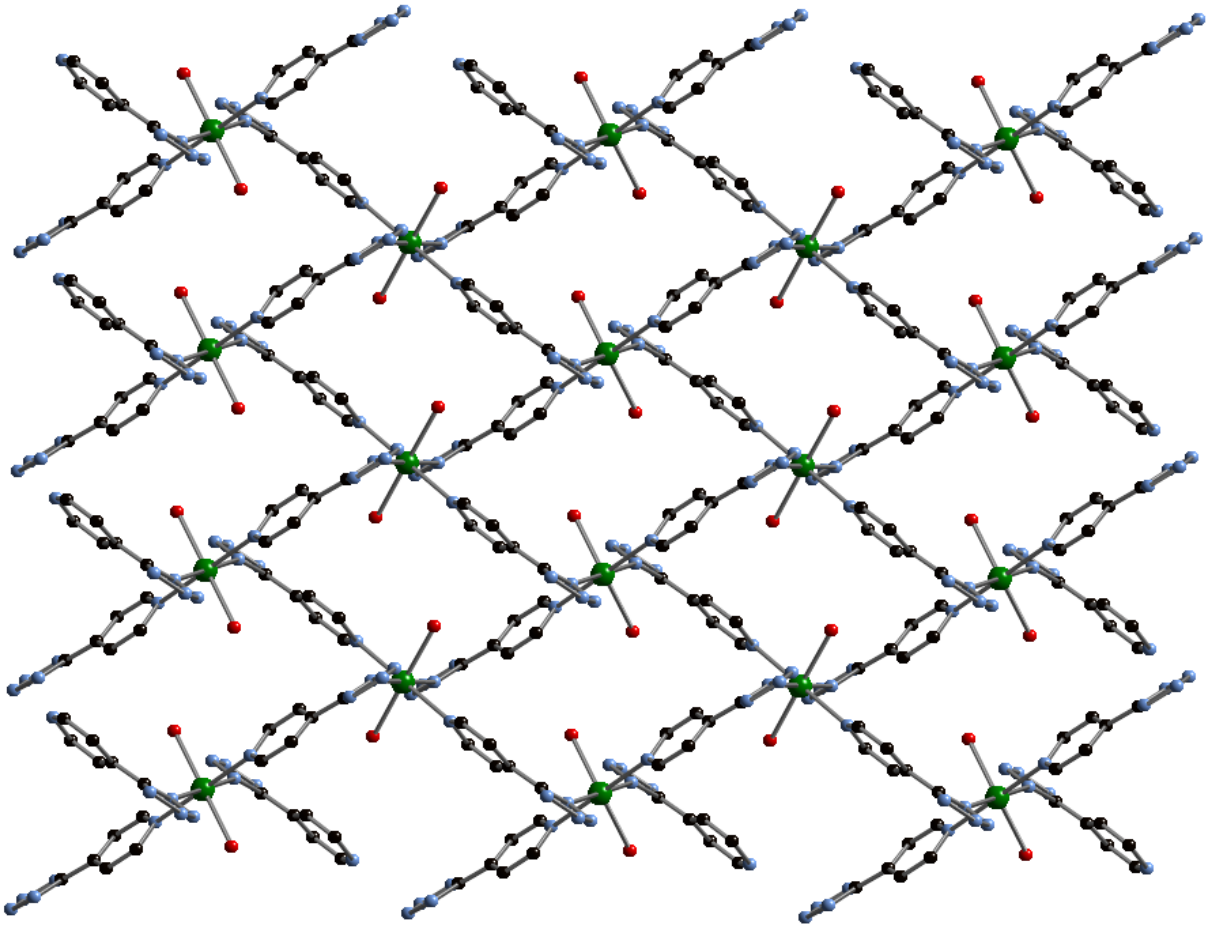

Figure 4.1: Ball and stick representation of the two-dimensional structure of [Cd(4-Hpyrtet)$_2$(OH)$_2$] (**1**). Color scheme: Cd, green, oxygen, red; nitrogen, light blue; carbon black.

The structure of compound **1** is reminiscent of that previously reported for [Cd(NCS)$_2$(4-Hpypz)$_2$] (H-pypz = pyridylpyrazole).[45] In the case of the thiocyanide derivative, one nitrogen of each pyrazole group is also protonated, and the thiocyanide ligands are directed into the intralamellar cavities in much the same fashion as that observed for compound **1**.

The cobalt(II) and copper analogues [Co(4-pyrtet)$_2$(H$_2$O)$_2$] **(2)** and [Cu(4-pyrtet)$_2$(H$_2$O)$_2$] (**3**), shown in **Figure 4.2**, exhibit grossly similar structures to that of **1**. However, in contrast to

the bonding in **1**, the distorted octahedral $\{MO_2N_4\}$ building units of **2** and **3** involve bonding through the N2-tetrazolate donor, rather than N1 as is the case for **1**. The structural consequence of this difference in coordination modes is that the tetrazolate bound ligands in **1** fold their planes toward the {HO-Cd-OH} bond axis, while those of **2** and **3** project outward from the $\{MN_4\}$ plane. As a result, while the hydroxy ligands of **1** project into the intralamellar grids, the aqua ligands of **2** and **3** project from either surface of the $\{M(4\text{-pyrtet})_2\}_n$ layer into the interlamellar domain. In the structures of **2** and **3**, the water molecules of adjacent layers interdigitate and the interlayer separation is 3.78Å and 3.39Å, respectively. In the case of the cadmium compound **1**, the bulky 4-pyrtet ligands project above and below the mean plane requiring a larger interplanar separation of 7.18Å.

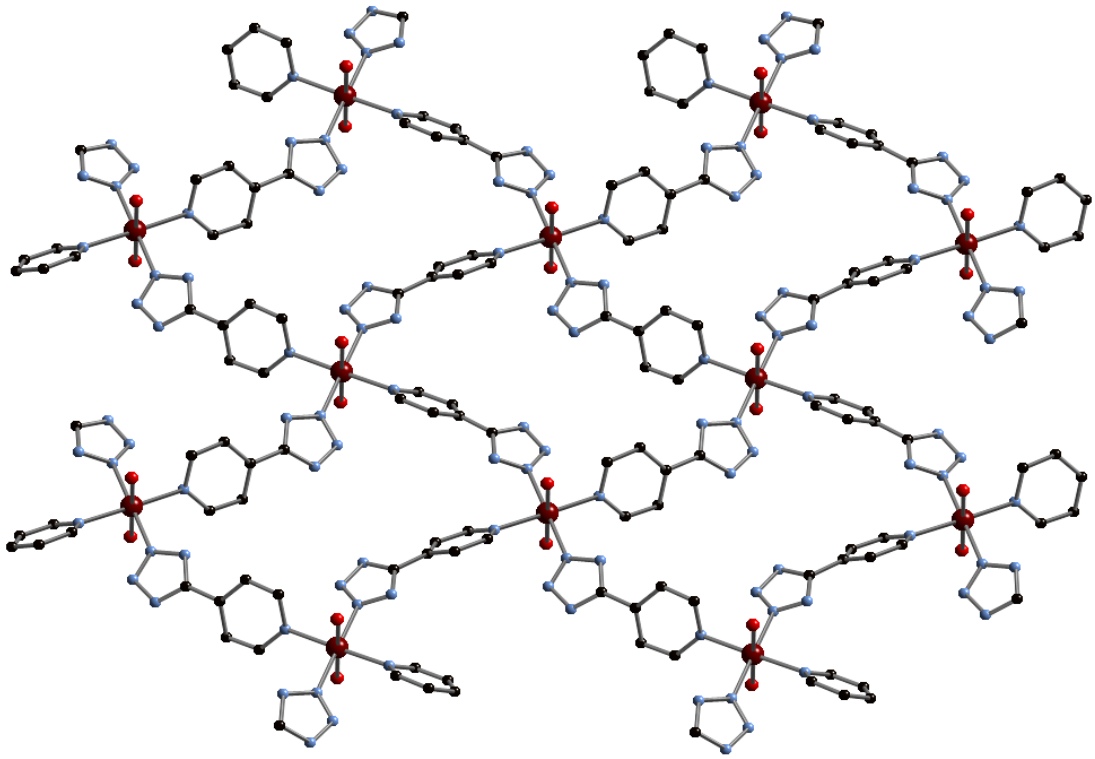

Figure 4.2: Ball and stick representation of the two-dimensional structure of $[Co(4\text{-pyrtet})_2(H_2O)_2]$ (**2**). Color scheme as for **Figure 4.2.1** with Co shown as brown spheres.

As shown in **Figure 4.3**, the structure of the 2-pyridyltetrazolate derivative [CdCl(2-pyrtet)(DMF)] (**4**) is one-dimensional. The structure may be described as a $\{Cd(2\text{-pyrtet})\}_n^{n+}$ ribbon with chloride and DMF ligands projecting above and below the ribbon. The structure contains the recurrent $\{M_2(azolate)_2\}$ planar building block, with these binuclear SBU fusing into the chain propagating parallel to the *a*-axis. The Cd(II) sites exhibit distorted octahedral $\{CdClON_4\}$ coordination with an equatorial plane defined by three tetrazolate nitrogen donors and a pyridyl ligand and the axial positions occupied by a DMF oxygen donor and a terminal chloride. Each 4-pyrtet ligand bridges three Cd sites through N1,N2,N3-coordination and chelates to one of these sites through additional coordination of the pyridyl nitrogen.

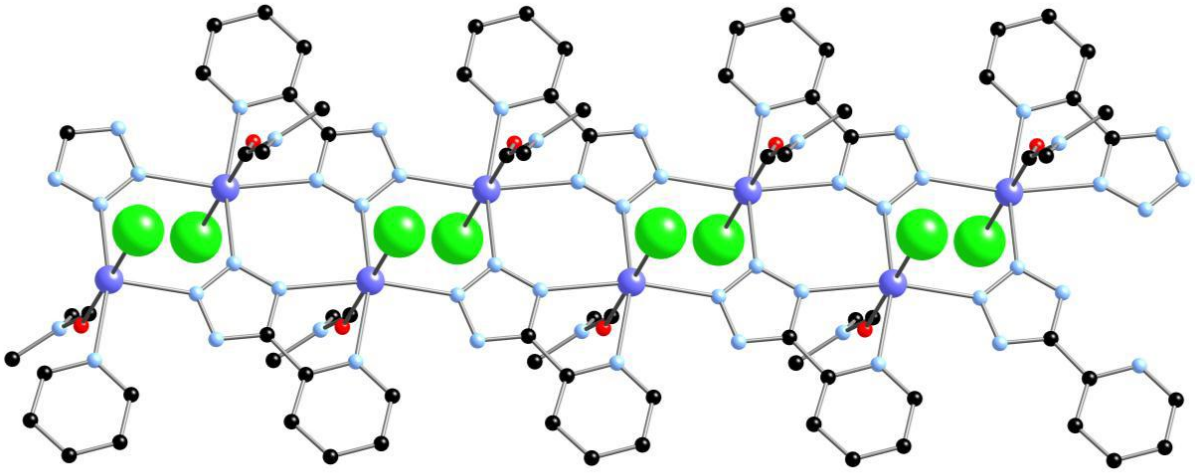

Figure 4.3: The one-dimensional structure of [CdCl(2-pyrtet)(DMF)] (**4**). Color scheme as for **Figure 4.1** with Cd shown as blue spheres and Cl as large light green spheres.

The structure of the pyrazinetetrazolate derivative, $[Cd_4Cl_6(prztet)_2(DMF)_4]$ (**5**), is two-dimensional, as shown in **Figure 4.4**. The structure is constructed from tetranuclear chloride bridged secondary building units $\{Cd_4Cl_6\}$ that are linked into chains propagating parallel to the

crystallographic *a*-axis through tetrazolate groups. These chains are in turn linked through the pyrazine substituents to provide the two-dimensional connectivity. There are two distinct Cd(II) coordination geometries. The central pair of cadmium sites of the tetrad exhibit distorted octahedral $\{CdCl_4ON\}$ geometry, bonding to four chloride atoms, the oxygen donor of a DMF and a pyrazine nitrogen donor. The equatorial plane may be defined by three chloride and the pyrazine nitrogen, while the fourth chloride ligand and the DMF occupy the axial positions. The two peripheral cadmium sites of the tetrad exhibit $\{CdCl_2ON_3\}$ coordination, defined by two tetrazole nitrogen donors, a pyrazine nitrogen and a chloride in the equatorial plane, with the axial positions occupied by a second chloride and the oxygen donor of a DMF molecule.

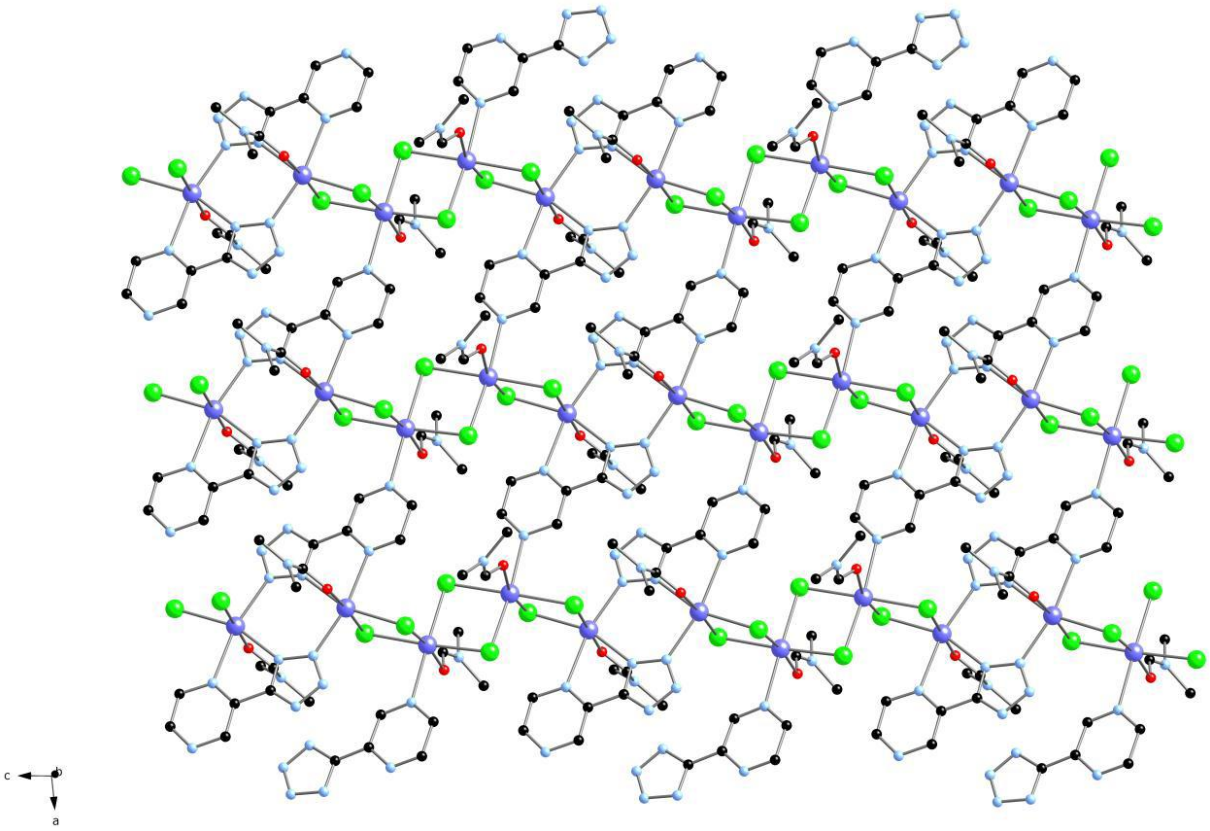

(a)

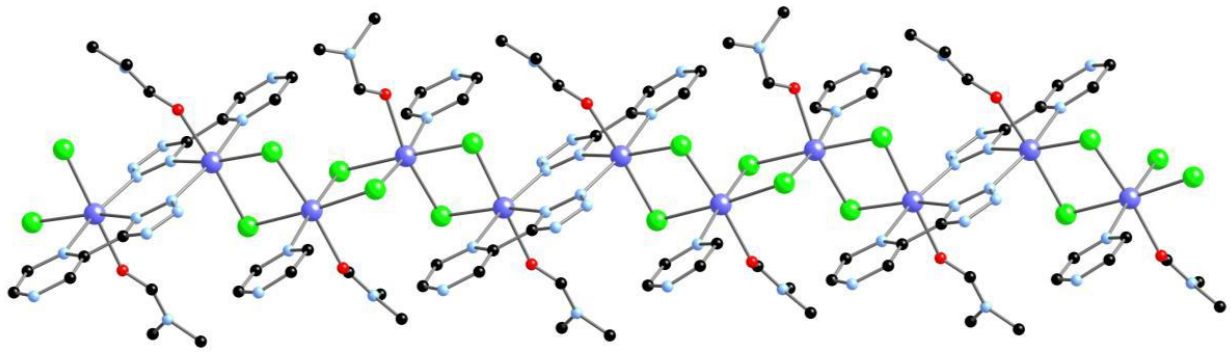

(b)

Figure 4.4: (a) A ball and stick representation of the two-dimensional structure of $[Cd_4Cl_6(prztet)_2(DMF)_4]$ (**5**). (b) The chain substructure of **5**, showing the $\{Co_4Cl_6\}$ building units. Same color scheme as for **Figure 4.3**.

The pyrazine-tetrazolate ligands bridge two cadmium sites from each of two tetranuclear units through N2,N5 donors and chelate to one of these sites through the pyrazine N2 donor. The pyrazine N5 donor is then employed in bonding to an adjacent chain to complete the two-dimensional connectivity. The DMF molecules project from either surface of the layer into the interlamellar space. Dimethylformamide molecules from neighboring layers interdigitate, such that the interlamellar spacing is *ca.* 9.0Å.

As shown in **Figure 4.5a**, the structure of $[Cd_3(N_3)_4(4\text{-pyrtet})_2(H_2O)_2]$ (**6**) adopts a "pillared" layer three-dimensional framework. The structure may be described as $\{Cd_3(N_3)_4(tetrazolate)_2(H_2O)_2\}_n$ layers, running parallel to the *ab* plane, linked through 4-pyrtet buttressing ligands. Within the layer (**Figure 4.5b**), three are two-distinct Cd(II) sites. The first consists of a $\{CdN_6\}$ distorted octahedra defined by two nitrogen donors from $\mu_{1,1,3}$-bridging azide groups in the *trans* orientation, two nitrogen donors of $\mu_{1,1,3}$-bridging azide groups in the *trans* configurations, and two nitrogen atoms from two N2,N3-bridging tetrazolate groups. The

second cadmium site enjoys {CdN_5O} coordination through bonding to a nitrogen donor of a $\mu_{1,1}$-azide group, two nitrogen atoms of $\mu_{1,1,3}$-bridging azide groups, a pyridyl nitrogen, a nitrogen donor of an N3,N4-bridging tetrazolate and an aqua ligand.

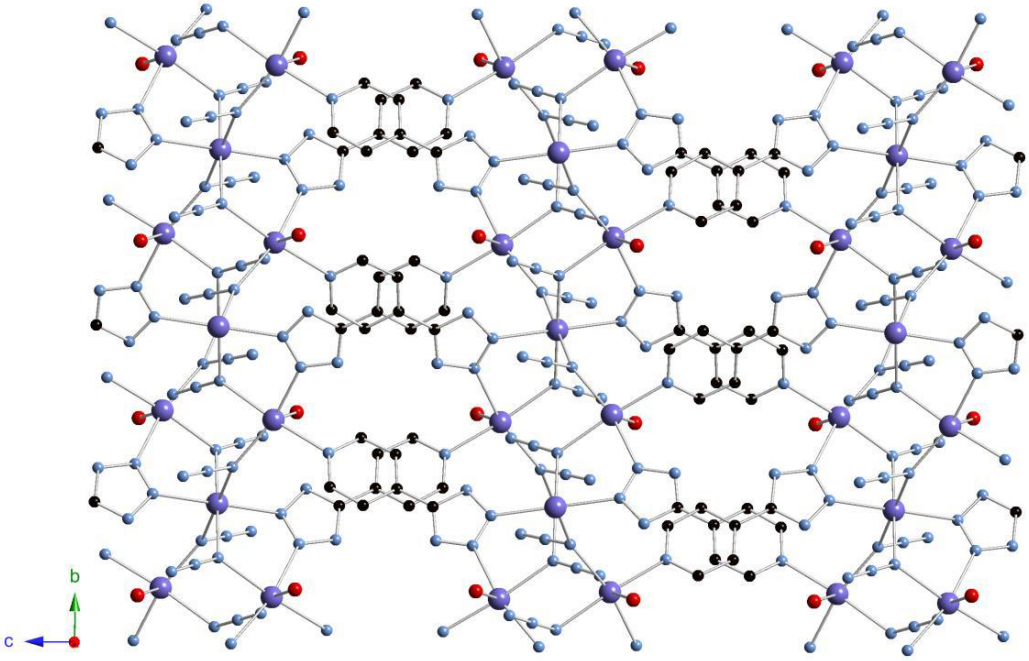

(a)

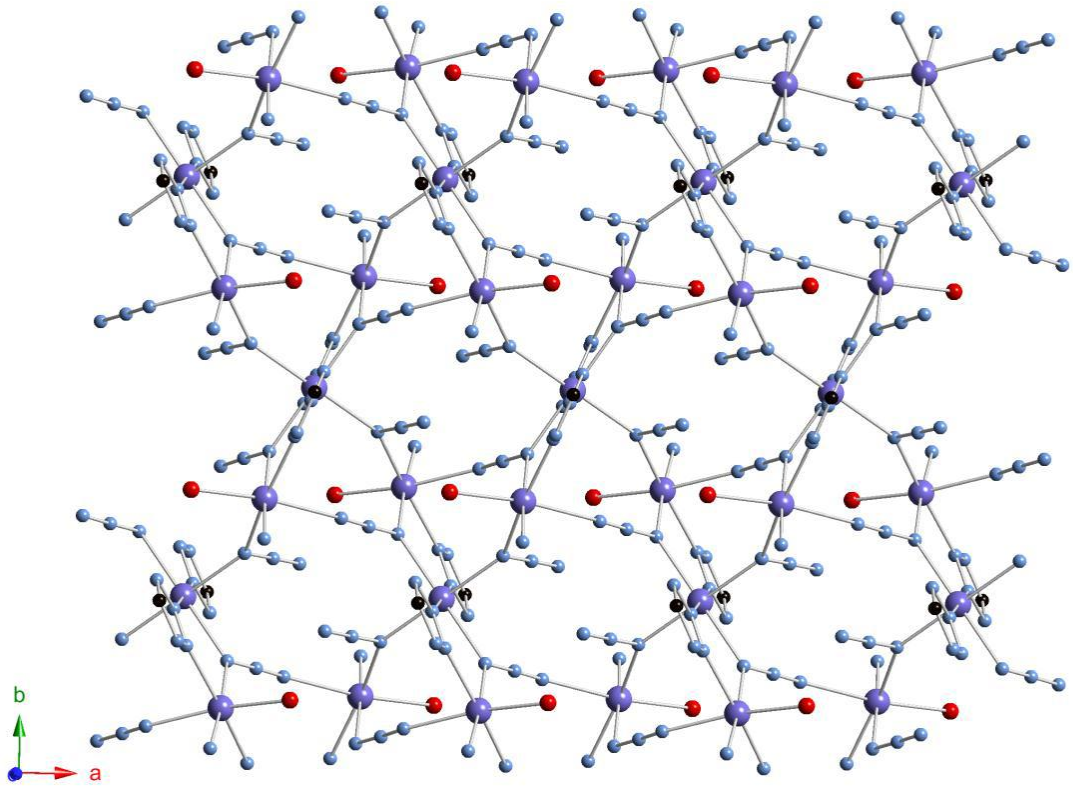

(b)

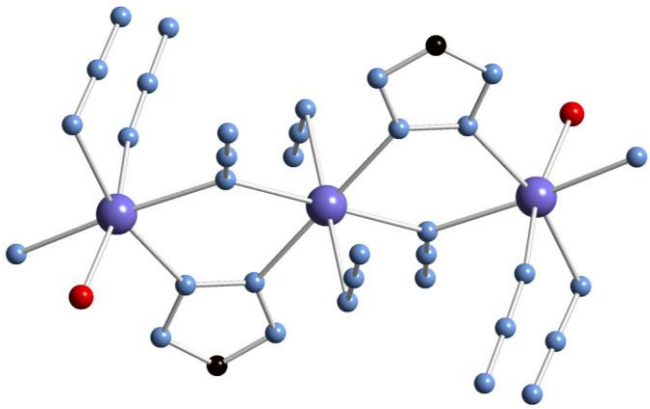

(c)

Figure 4.5: (a) A ball and stick representation of the structure of $[Cd_3(N_3)_4(4\text{-pyrtet})_2(H_2O)_2]$ (**6**) in the *bc* plane, illustrating the "pillared" layer framework of $\{Cd_3(N_3)_4(\text{tetrazolate})_2(H_2O)_2\}_n$ layers linked by the pyrtet buttresses. (b) A view of the $\{Cd_3(N_3)_4(\text{tetrazolate})_2(H_2O)_2\}_n$ layer, viewed in the *ab* plane. (c) The trinuclear secondary building unit of **6**.

As shown in **Figure 4.5c**, the two-dimensional substructure of **6** is constructed from the linking of trinuclear secondary building units (sbu's). Each sbu contains a central $\{CdN_6\}$ site which is bridged to the two peripheral $\{CdN_5O\}$ sites through two $\mu_{1,1,3}$-bridging azido ligands and two N2,N3-bridging tetrazolate moieties. In addition, the $\{CdN_6\}$ center projects two azido groups which link to adjacent cadmium triads in the $\mu_{1,1}$-mode. Each of the azido-groups involved in intratriad bridging also bridges to an adjacent triad, adopting the $\mu_{1,1,3}$-bridging mode. In this fashion, each cadmium triad is linked to four adjacent triads to generate the two-dimensional substructure connectivity. Each triad is also involved in linkages to four 4-pyrtet groups to provide pillaring to two adjacent layers, thus providing three-dimensional connectivity.

4.2.3 Structural Observations

The structural variety of the three cadmium structures of this study reflects the range of coordination possibilities associated with tetrazole ligands bearing functionalized substituents, as well as the influence of secondary anionic components, in this instance chloride or hydroxide. It is noteworthy that the 4-pyridyltetrazole ligand can function analogously to the 4-pyridylpyrazole ligand, an observation consistent with previous speculations on the structural relationships between 1,2,4-triazole and substituted tetrazole and pyrazole ligands.

While one-dimensional structures are relatively uncommon in the transition metal-azolate chemistry, reflecting the bridging capacity of these ligands and their tendency to form higher dimensionality structures, the 1-D structure of [CdCl(2-pyrtet)(DMF)] (**5**) exhibits a $\{M(azolate)\}_n^{n+}$ ribbon substructure similar to those observed in high dimensionality structures. For example, the two-dimensional [Cu(4-pyrtet)]·DMF [46] exhibits an analogous $\{Cu(tetrazolate)\}_n$ ribbon to that of **3**, embedded within the overall network topology. The

N1,N2,N3-bridging mode of tetrazolate based ligands is not uncommon, suggesting that such ribbon motifs will emerge as recurrent structural features in the metal-tetrazolate chemistry.

Incorporation of a secondary anion, such as a halide, a pseudohalide or an oxyanion, into the M/azolate framework can have profound structural consequences.[17,23] For example, the Cd(II)/4-pyridyltetrazolate system exhibits a range of unusual three-dimensional structures for the series $[Cd_4(OH)_2(4\text{-pyrtet})_6(DMF)_4]$, $[Cd_4Cl_3(4\text{-pyrtet})_4(OH)(DMF)_3]$ and $[Cd_5Cl_6(4\text{-pyrtet})(DMF)_2(H_2O)_2]$. In contrast, when the extended, rigid dipodal ligand 4-pyridyltetrazolate is replaced by the chelating pyrazinetetrazolate, the two-dimensional $[Cd_4Cl_6(prztet)_2(DMF)_4]$ (**5**) is obtained. The structures reflect not only the constraints of the substituents on the tetrazolate moiety but also the presence and influence of coordinating solvents such as DMF.

The remarkable range of structural possibilities are related to factors such as the variety of coordination polyhedra available to the metal, variable modes of coordination associated with the tetrazole(ate) ligands, the role of functional substituents on the azolate moiety, the incorporation and coordination preferences of secondary anionic components (X^{n-} or XO_4^{n-}), the often "soft" M-X-M or M-O-X angles, and the variable incorporation of solvent molecules. While such factors guarantee a rich structural diversity, they also presuppose a lack of predictability. The complexity of the structural chemistry of cadmium-azolates is dramatically illustrated by the entries of **Table 4.1**, which summarizes the structural features of a sampling of the vast number of cadmium-triazolate and tetrazolate structure studied to date. The emergence of a number of recurring structural motifs and a continuing expansion of the structure data base may presage a more systematic understanding of the rational design of these materials.

Table 4.1: Structural Characteristics of Selected Cd(II)-triazolates and –tetrazolates.

Compound	Dimensionality	Substructures and Description	Ref.
$[Cd_3(trz)_3F_2(OH)]$	3D	$\{CdN_3F_3\}$ octahedra forming $\{Cd_4F_4\}^{4+}$ and $\{Cd_6(trz)_6F_4(H_2O)_2\}^{2+}$ clusters and $\{Cd_6(trz)_6F_4(H_2O)\}_n^{2n+}$ chains; substructures linked through triazolate ligands.	21
$[Cd_3(trz)_3Br_3]$	3D	$\{CdN_2Br_4\}$ and $\{CdN_3Br_3\}$ octahedra and $\{CdN_4Br\}$ trigonal bipyramids linked into $\{Cd(trz)_2Br_2\}_n^{2n-}$ chains and $\{Cd_3(trz)_2Br_3\}_n^{n+}$ lavers.	21
$[Cd_2(trz)_2Cl_2(H_2O)]$	3D	$\{CdN_4Cl_2\}$ and $\{CdN_2Cl_3O\}$ octahedra linked into $\{Cd(trz)_2Cl\}_n^{n-}$ and $\{Cd(trz)_2Cl_2(H_2O)_2\}_n^{2n-}$ chains.	21
$[Cd_2(trz)_3I]$	3D	$\{Cd(trz)_3\}_n^{n-}$ chains with triply bridging N1, N2 triazolates between metal sites; chains linked through tetrahedral $\{CdN_3I\}$ sites.	21
$[Cd_3(trz)_5(NO_3)(H_2O)$	3D	$\{CdN_6\}$ octahedra in $\{Cd(trz)_3\}_n^{n-}$ chains with triple N1, N2-triazolate bridges; $\{CdN_3O_2\}$ and $\{CdN_4O\}$ trigonal bipyramidal sites bridge the chains.	21
$[Cd_8(trz)_4(OH)_2(SO_4)_5(H_2O)$	3D	$\{CdN_2O_4\}$, $\{CdNO_5\}$ and $\{CdO_6\}$ octahedra from $\{Cd_3(\mu_3\text{-}OH)\}^{5+}$ clusters, $\{Cd_7(trz)_4\}_n^{10n+}$ chains and a $\{Cd_8(SO_4)_5\}_n^{6n+}$ framework; subunits linked by sulfate bridges and N1, N2, N4-triazolate.	21
$[Cd(Htrz)_2(NCS)_2]$	1D	Triazolate bonds exclusively through N4; N, S-thiocyanate bridges	48
$[Cd_2(amtrz)_2$ (aztrz)]	3D	$\{CdN_6\}$ octahedra linked through N1, N3, N1′, N3′ and diazenen N of aztaz and μ_3-N1, N2, N3 amtaz.	49
$[Cd(aztrz)_2(H_2O)]$	3D	$\{CdN_4O_2\}$ octahedra and $\{CdN_4\}$ tetrahedra bridged by N1, N3, N1′,N3′ aztrz.	49
$[Cd_2(2\text{-pytrz})_4(NO_3)_2(H_2O)_2](NO_3)_2$	Molecular	$\{CdN_4O_2\}$ octahedra bridged by N1, N2-triazolate units	50
$[Cd(2\text{-pytrz})_2(dca)_2]$	2D	$\{CdN_6\}$ octahedra linked through dca ligands; N1 monodentate 2-pytrz.	50
$[Cd(2\text{-pytrz})_2(NCS)_2]$	1D	$\{CdN_6\}$ octahedra linked through NCS ligands; monodentate N1-bound 2-pytrz.	50
$[Cd(3\text{-pytrz})_2(NCS)_2H_2O)_2]$	Molecular	$\{CdN_6\}$ octahedra; monodentate pyridyl N bound 3-pytrz .	50
$[Cd(3\text{-pytrz})_2(dca)_2]$	1D	$\{Cd(N_6\}$ octahedra; monodentate N1-bound 3-pytrz.	50
$[Cd_3(3\text{-pytrz})_3(dca)_6]$	3D	$\{CdN(trz)_4N(dca)_2\}$, $\{CdN(trz)_2N(dca)_4\}$, $\{CdN(dca)_6\}$ octahedra giving $\{Cd(dca)_2\}$ layers; N1 and pyridyl N bonding of 3-pytrz.	50
$[Cd(3\text{-pytrz})(SO_4)(H_2O)]$	3D	$\{CdO_4N_2\}$ octahedra giving $\{Cd(SO_4)(H_2O)\}$ layers; N1, pyridyl N- bridging 3-pytrz.	50
$[Cd_3(ptrz)_6(H_2O)_6](ClO_4)_6$	Molecular	Trinuclear unit of $\{CdN_6\}$ and $\{CdN_3O_3\}$ octahedra; N, N2-bonded ptrz.	51
$[Cd_3(dmatrz)_4(SCN)_6]$	2D	$\{CdN_6\}$ and $\{CdN_4S_2\}$ octahedra, forming a trinuclear building unit with N1, N2-triazolate and (NCS)-bridged Cd(II) sites.	52
$[Cd_3(dmatrz)_4(N_3)_6]$	2D	As above with N_3^- replacing NCS^-.	52
$[Cd(3\text{-atrz})(H_2O)_2]SiF_6$	2D	$\{CdN_4O_2\}$ octahedra linked through N1, N4-bonded atrz.	53
$[Cd_3(deatrz)_2Cl_6(H_2O)_2]$	1D	$\{CdCl_4N_2\}$ and $\{CdCl_4NO\}$octahedra in trinuclear building	54

		blocks; N1, N2-bridging deatrz.	
$[Cd_3(deatrz)_4Cl_2(SCN)_4]$	1D	$\{CdN_4Cl_2\}$ and $CdN_4ClS\}$octahedra in trinuclear building units; N1, N2-bridging deatrz.	54
$[Cd_2(deatrz)_2Br_4(H_2O)]$	Molecular	Binuclear complex of $\{CdN_2Br_2O\}$ trigonal bipyramids with N1, N2-building deatrz.	54
$[Cd(dmtrz)Cl_2]$	1D	$\{CdCl_4N_2\}$ octahedra bridged by N1, N2-bound dmtrz.	54
$[Cd_3(dmtrz)_4(SCN)_6]$	2D	$\{CdN_6\}$ and $\{CdN_5S\}$ octahedra in trinuclear units; N1, N2-bridging dmtrz.	54
$[Cd(dmtrz)(SCN)_2]$	1D	Binuclear units of $\{CdN_4S_2\}$ octahedra.	54
$[Cd_3(4\text{-atrz})_4Cl_6]$	1D	$\{CdN_4Cl_2\}$ and $\{CdN_2Cl_4\}$ octahedra in trinuclear building units with N1, N2-bridging 4-atrz.	52
$[Cd_2(2\text{-pytrz})_2Cl_4]$	Molecular	Binuclear unit of chloride bridged $\{CdN_2Cl_3\}$ square pyramids; N4-bound 2-pytrz.	52
$[Cd_3(dpatrz)_4Cl_6]$	Molecular	$\{CdN_4Cl_2\}$ and $\{CdN_3Cl_3\}$ in trinuclear unit with N1, N2-bridging triazolate.	52
$[Cd(4\text{-atrz})_2(SCN)_2]$	1D	$\{CdN_4S_2\}$ octahedra with monodentate N1-bound 4-atrz.	52
[Cd(datrz)I]	2D	$\{CdN_3I\}$ tetrahedra bridged through N1, N2, N-4 bonding datrz.	52
$(R_4N)[Cd_2(3\text{-atrz})_2I_3]$	2D	$\{CdN_4I_2\}$ octahedra and $\{CdN_2I_2\}$ tetrahedra; {Cd(3-artz)I}n chains linked by tetrahedral sites.	55
$[Cd(oxalate)(4\text{-atrz})_2(H_2O)]$	1D	$\{CdN_2O_4\}$ octahedra; monodentate N1 bound atrz.	56
$[Cd(2\text{-abpytrz})(N_3)_2]$	1D	$\{CdN_6\}$ octahedra with terminal N1, pyridyl N chelating abpytrz.	57
$[Cd(4\text{-abpytrz})(Htma)(H_2O)]$	2D	$\{CdN_2O\}(oxalate)_3O(aqua)$ octahedra linked into {Cd(4-abpytrz)} chains through pyridyl N-bonding; chains linked through Htma groups into network.	58
$[Cd(4\text{-abpytrz})(Htma)(H_2O)_2$	1D	$\{CdO(oxalate)_4O(aqua)_2N\}$ pentagonal bipyramids linked through Htma ligands; terminal, monodentate 4-abpytrz.	58
$[Cd(4\text{-abpytrz})(pa)(H_2O)$	2D	$\{CdN_2O(oxalate)_3O(aqua)\}$ octahedra; 4-abpytrz bonds through pyridyl N donors only.	59
$[Cd_2(4\text{-abpytrz})(ip)_2(H_2O)_4$	2D	$\{CdNO(oxalate)_4O(aqua)_2\}$ pentagonal bipyramids and $\{CdNO(oxalate)_3O(aqua)_2\}$ octahedra; 4-abpytrz bonds through pyridyl N donors only; interpenetrated.	59
$[Cd(4\text{-abpytrz})(tp)_2(H_2O)]$	2D	$\{CdN_2O(oxalate)_4O(aqua)\}$ pentagonal bipyramids forming {Cd(oxalate)} chains linked by 4-abpytrz ligands bonding through pyridyl N donors.	59
$[Cd(4\text{-abpytrz})(tp)_2(DMF)]$	2D	As above with $\{CdN_2O(oxalate)_4O(DMF)\}$	59
$[Cd_3(datrz)_6(H_2O)_2]$	3D	$\{CdN_3O(H_2O)_2\}$ trigonal bipyramids and $\{CdN_6\}$ octahedra; $\{Cd_2(datrz)_6\}$ chains are linked by $\{CdN_3O_2\}$ units. N1, N2, N4-bridging mode of datrz.	60
$[Cd_3(datrz)_4F_2]$	3D	$\{CdN_5F\}$ and $\{CdN_4F_2\}$ octahedra; N1, N2, N4 and N1, N2, N4, amino-N-bridging modes.	60
$[Cd_5(datrz)_4X(OH)_2]$, X = Cl, Br	3D	$\{CdN_4Cl_2\}$, $\{CdN_3Cl_2O(OH)\}$ and $\{CdN_3ClO_2\}$ octahedra forming $\{Cd_4O_2Cl_2\}$ clusters.	60
$[Cd_3(datrz)_2(SO_3)_2(H_2O)]$		$\{CdN_2O(sulfite)_3\}$ square pyramids forming $\{Cd_3(SO_3)_2\}$	60

		chains and $\{CdN_2O_4\}$ octahedra.	
$[Cd_3(datrz)_2(MeCO_2)_4]$	2-D	$\{CdN_2O_4\}$ trigonal prismatic and octahedral sites; N1, N2, N4-bound datrz.	60
$[Cd(datrz)(EtCO_2)]$	2D	$\{CdN_3O_2\}$ square pyramids forming $\{Cd(datrz)_2(EtCO_2)_2\}$ binuclear units linked by N1, N2, N4 bridging datrz.	60
$[Cd(Hdatrz)(Bu^tCO_2)]$	2D	$\{CdO_4N_2\}$ octahedra forming $\{Cd(Hdatrz)(BuCO_2)\}$ chains and linked through the $BuCO_2^-$ ligands.	60
$[Cd(Hdatrz)_2(H_2Edta)]$	Molecular	$\{CdN_4O_2\}$ octahedra with monodentate N1-bound datrz.	60
[Cd(3-atrz)Xl], X = Cl, Br	3D	$\{CdN_4X_2\}$ octahedra linked through μN1, N2, N4, Namnio bridging 3atrz into a chiral 3D framework.	61, 62
$[Cd(trtrz)_2]$	3D	$\{CdN_6\}$ octahedra linked through μ_3-bridging trtrz	63
$[Cd(Htrtrz)Br_2]$	1D	$\{CdN_4B4_4\}$ octahedra linked through N1, N2 coordinated Htrtrz	64
$[Cd(Htrtrz)_2(H_2O)_4)]$ SiF_6	Molecular	$\{CdN_2O_4\}$ octahedra	65
$[Cd(btrz)_3](ClO_4)_2$	3D	$\{CdN_6\}$ octahedra linked through N1, N1′-bridging bis-triazole.	66
$[Cd_3(btrz)_8(H_2O)_2](BF_4)_6$	3D	$\{CdN_6\}$ and $\{CdN_4O_2\}$ octahedra linked through N1, N1′-bridging btrz.	66
$[Cd_3(btrz)_8(dca)_2]$ $(BF_4)_4$	3D	As above with the aqua ligands of the $\{CdN_4O_2\}$ octahedra replaced by dca.	66
$[Cd(btrzpyr)_2(NCS)_2]$	1D	$\{CdN_6\}$ octahedra with N1, N1′-bridging btrzpyr.	67
$[Cd(btrzpyr)_2(NO_3)_2]$	2D	$\{CdN_4O_2\}$ octahedra linked by N1, N1′-bridging btrzpyr into a 1D helical substructure.	67
$[Cd(btrzhex)(SCN)_2]$	2D	$\{CdN(triazole)_4N(NCS)_2\}$ octahedra linked through N1, N1′-bridging btrzhex.	68
$[Cd(btrzhex)_3]$	3D	$\{CdN_6\}$ octahedra linked through N1, N1′-bridging bistriazole	68
$[Cd(btrzeth)_2(H_2O)_2]$	2D	$\{CdN_4O_2\}$ octahedra linked through N1, N1′-bridging btrzeth.	69
[Cd(3-bpyrtrz)(SO_4)]	3D	$\{CdN_3O_3\}$ octahedra linked through N1, N2, N(pyridyl)-bridging 3-bpyrtrz.	70
$[Cd(3\text{-}bpyrtrz)(SO_4)(H_2O)_3]$	1D	$\{CdO(aqua)_3O(sulfate)N_2\}$ octahedra linked through N(pyr), N(pyr′)-bridging azole ligands.	70
$[Cd(4\text{-}pyrtrz)_2(dca)_2(H_2O)_2]$	Molecular	$\{CdN(triazole)_2N(dca)_2O_2\}$ octahedra	71
[Cd(4-pyrtrz)(SCN)]	3D	$\{CdN(triazole)_2N(SCN)_2S_2\}$ octahedra forming $\{Cd(SCN)_2\}_n$ layers bridged by N1, N(pyr)-bridging 4-pyrtrz.	71
$[Cd(abpyrtrz)(N_3)_2]$	1D	$\{CdN(triazole)_2N(N_3)_4\}$ octahedra; abpyrtrz chelates through N1, Npyr.	72
$[Cd(tmtrzpyrm)_2(NCS)_2]$	1D	$\{CdN(triazole)_2N(NCS)_2S_2\}$ octahedra linked through NCS-bridges.	73
$[Cd(bmtrzpyrm)(SO_4)(H_2O)_2]$	2D	$\{CdO(aqua)_3O(sulfate)_2N\}$ octahedra; monodentate N1-bound bmtrzpyrm.	74
$[Cd_5(tet)_9(OH)(H_2O)]$	3D	$\{CdN_6\}$, $\{CdN_5O(H)\}$ and $\{CdN_5O(aqua)\}$ octahedra with μ_2, μ_3 and μ_4-bridging tetrazolate ligands.	48
$[Cd_5(atet)_9(NO_3)]$	3D	$\{CdN_6\}$ octahedra linked through μ_3 and μ_4-bridging tetrazolates.	48
$[Cd_{15}(mtet)_{18}(OH)_4(SO_4)_4]$	3D	$\{CdN_6\}$ and $\{CdN_4O(H)O(sulfate)\}$ octahedra giving $\{Cd_3(\mu_3\text{-}OH)$	75

		$(SO_4)(tet)_3$} cluster building blocks.	
$[Cd(3\text{-pyrtet})(N_3)]$	3D	{$CuN(tetrazole)_4N(azole)_2$} octahedra providing {$Cd(pyrtet)(N_3)$} chains linked through azide and tetrazolate ligands; N1, N2, N3, N(pyr)-bridging pyrtet.	76
$[Cd_3(4\text{-pyrtet})(OH)_2Cl_2]$	2D	{$CdN_2Cl_2O_2$} octahedra giving {$Cd_3(OH)_2Cl_2(pyrtet)_2$} cluster building units; N1, N2, Npyr bridging 4-pyrtet.	77
$[Cd(4\text{-pyrtet})_2(H_2O)_2]$	2D	{CdN_4O_2} octahedra; N1, Npyr-bridging 4-pyrtet.	77
$[Cd_4(4\text{-pyrtet})_6(OH)_2(DMF)_4]$	3D	{CdN_5O} and {CdN_4O_2} octahedra forming {$Cd_2(\mu_2\text{-azolate})_3$} binuclear units; N2, N3, Npyr-bridging 4-pyrtet.	78
$[Cd_4(4\text{-pyrtet})_4Cl_3(OH)(DMF)_3]$	3D	{CdN_4Cl_2} and {CdN_3O_2Cl} octahedra in {$Cd_4(4\text{-pyrtet})_4Cl_3(OH)(H_2O)_4$} cluster building units, N2, N3, Npyr-bridging azolate.	78
$[Cd_4(btetb)_4(pyr)_4(H_2O)_4]$	2D	{$CdN(tet)_6$}, $Cd(N(tet)_4$, N(pyr)O} and {$CdN(tet)_2N(pyr)_2O_2$} octahedra; N2, N2′, N3, N3′-bridging btetb.	82
$[Cd\{Cd_3(bta)_3(OH)(H_2O)_6\}_2]$	2D	{$CdN_3O(aqua)_2O(H)$} octahedra forming a trinuclear {$Cd_3(\mu_3\text{-OH})$} building unit; N1, N1′, N2, N2′-bridging bta. {CdN_6} octahedra linking to six different trinuclear units.	83
$[Cd_2(ttetbf)(CH_3OH)_5]$	3D	{CdN_4O_2} and {CdN_3O_3} octahedra in binuclear secondary building units; N1, N2, N2′-bridging ligand.	84
$[Cd_2O(H_2ttetbf)(DMF)_2]$	3D	[CdN_5O} octahedra and {CdN_4O} square pyramids forming tetranuclear {$Cd_4O_2(tet)_8$} building units; N2, N2′, N3, N3′-bridging ligand.	84
$[Cd_2Cl(Httetbf)(DMF)H_2O)]$	3D	{$CdN_4ClO(DMF)$} and {$CdNClO(aqua)$} octahedra forming {$Cd_4O(tet)_8$} tetranuclear s.b.u.	84

Abbreviations, in order of appearance: Htrz = 1, 2, 4-triazole; Hamtrz = 3-amino-1, 2, 4-triazole; H_2aztrz = 3,3′-azobis(1, 2, 4-triazole); 2-pytrz = 4-(pyrid-2-yl)-1, 2, 4-triazole; dca = dicyanamide; 3-pytrz = 4-(pyrid-3-yl)-1, 2, 4-triazole; Hptrz = n-phenol-1, 2, 4-triazole; dmatrz = 4-amino-3, 5-dimethyl-1, 2, 4-triazole; 3-Hatrz = 3-amino-1, 2, 4-triazole; deatrz = 3, 5-diethyl-4-amino-1, 2, 4-triazole; dmtrz = 3, 5-dimethyl-4-amino-1, 2, 4-triazole; 4atrz = 4-amino-1, 2, 4-triazole; 2Hpytrz = 3, 5-di(pyrid-2yl)-1, 2, 4-triazole; dpatrz = 4-amino-3, 5-dipropyl-1, 2, 4-triazole; Hdatrz = 3, 5-diamino-1,2,4-triazole; dmatrz = 4-amino-3, 5-dimethyl-1, 2, 4-triazole; 2-abpytrz = 4-amino-3, 5-di(pyrid-2-yl)-1, 2, 4-triazole; H_2pa = phthalic acid; H_2ip = isophthalic acid; H_2tp = terephthalic acid; Hdatrz = 3, 5-diamino-1, 2, 4-triazole; 3Hatrz = 3-amino-1, 2, 4-triazole; Htrtrz = 4-(1H-1, 2, 4-triazol-3-yl)-1, 2, 4-triazole; btrz = bis(4, 4′-bis-1, 2, 4-triazole); btrzpyr = 2, 6-di-(1,2,4-triazol-4-yl)pyridine; btrzhex = 1, 6-bis(1, 2, 4-triazol-1-yl)hexane; btrzeth = 1, 2-bis(1, 2, 4-triazol-1-yl)ethane; btrzph = 1, 6-bis(1, 2, 4-triazol-1-ylmethyl)benzene; 3-Hbpyrtrz = 3, 5-bis(3-pyridyl)-1, 2, 4-triazole; 4-pyrtrz = 4-(pyrid-4-yl)-1, 2, 4-triazole; abpyrtz = 4-amino-3, 5-bis(pyridin-2-yl)-1, 2, 4-triazole; tmtrzpyrm = 5, 6, 7-trimethyl-[1, 2, 4-triazole(1, 5-pyrimidine)]; bmtrzpyrm = 5, 7-dimethyl[1, 2, 4-triazole(1, 5-pyrimidine)]; Htet = tetrazole; Hatet = 5-aminotetrazole; Hmtet = 5-methyltetrazole; 3-Hpyrtet = 5-(3-pyridyl)tetrazole; 4-Hpyrtet = 5-(3-pyridyl)tetrazole; Htetpyrz = 2-(1H-tetrazol-5-yl)pyrazine; Hpmtet = 5-(pyrimidyl) tetrazole; H_2btetb = 1, 3-bis(2H-tetrazol-5-yl) benzene; H_2bta = bis (5-tetrazolyl) amine; H_4ttetbf = 2, 2′, 7, 7′-tetrakis(2H-tetrazol-5-yl)-9, 9′-spiroli(fluorene).

4.2.4 Magnetism

The temperature dependent magnetic data for compounds **2** and **3** were recorded at magnetic field of H = 1000 Oe in the temperature range of T = 2 - 300 K, in field cooling mode (FC) using a PPMS-Quantum Design system, in the susceptibility ACMS option.

The Curie-Weiss law was used to analyze the magnetic data for compound **2**, assuming one magnetic site. A temperature-independent-paramagnetism (TIP) term was added to the equation to account for the baseline correction. The final expression used for the fitted susceptibility is given in **Equation 1**.

$$\chi = \chi_h + TIP = \frac{Ng^2\mu_B^2 S(S+1)}{3k_B[T-\theta]} + TIP \quad (1)$$

Equation 2 describes the magnetic susceptibility as a function of the effective magnetic moment.

$$\chi = \chi_h + TIP = \frac{\mu_{eff}^2}{8[T-\theta]} + TIP \quad (2)$$

where $\mu_{eff}^2 = g^2 S(S+1)$. The best fit to the data (**Figure 4.6**) gives μ_{eff} = 4.86±0.72 μ_B, ϑ = 2.41±0.24 K, and *TIP* = 0.00216 cm^3/mol with a g-value of 2.51±0.48 and consistent with Co^{2+} ($3d^7$, spin S = 3/2) and a single magnetic center.

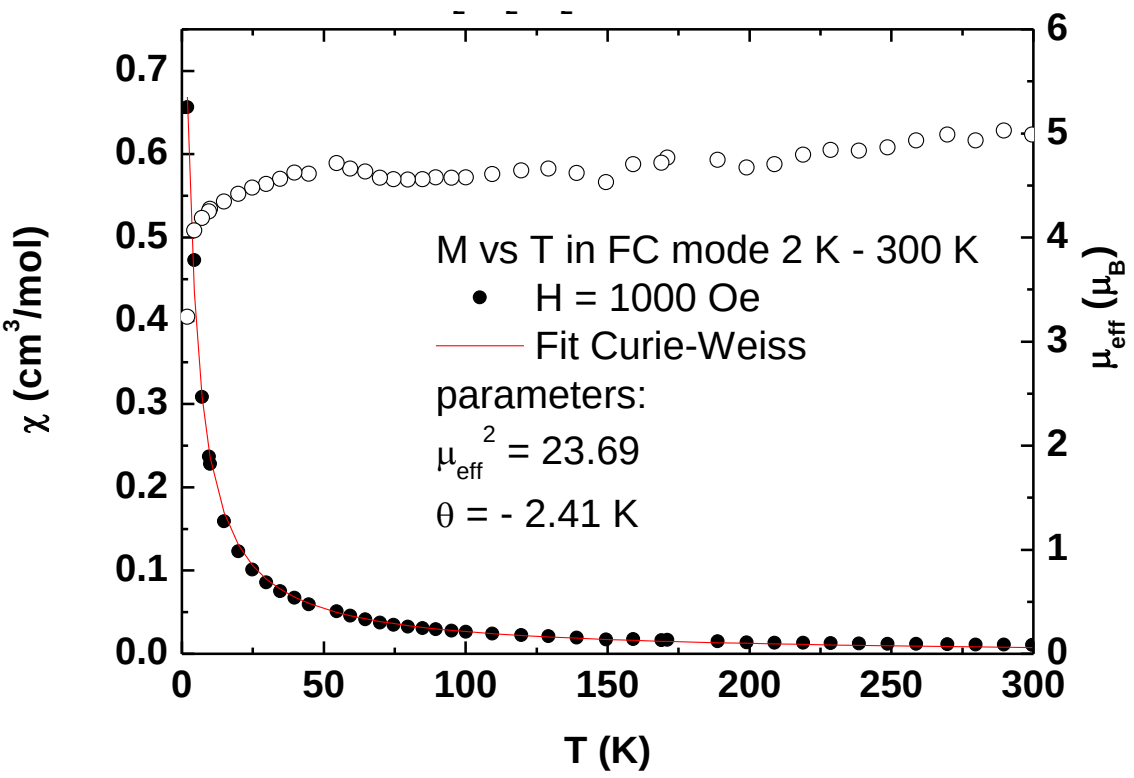

Figure 4.6: The temperature dependence of the magnetic susceptibility χ (filled circles) and of the effective magnetic moment (open circles) of compound **2**. The line through the data represents the fit to **Equation 1**.

The magnetism of compound **3** was also consistent with the Curie-Weiss law for a single spin and conformed to equations 1 and 2. The best fit (Supplementary Figure 71) gave μ_{eff} = 1.80±0.27 μ_B, ϑ = 0.02±0.05 K, and *TIP* = 0.00065 cm^3/mol with a g-value of 2.07± 0.39 which is consistent with a single Cu^{2+} site (d^9, spin S =1/2).

4.3 Conclusions

Hydrothermal chemistry, as well as conventional methods, have been used to prepare a small series of compounds of the Cd(II)/imine-tetrazolate family. The two-dimensional structure of **1** exhibits a network structure with a $\{CdN_4O_2\}$ building unit, in a fashion similar to that observed for the Co(II) and Cu(II) materials **2** and **3**, respectively. However, the cadmium structure contains coordinated hydroxy groups, while the cobalt and copper networks feature

coordinated aqua ligands. This difference is most apparent in the projection of the hydroxy groups into the intralamellar cavities in **1**, in contrast to the aqua ligands of **2** and **3** which project into the interlamellar domain. Compounds **4** and **5** demonstrate the structural consequences of introducing halide coligands and the variety of secondary building units that incorporate into such structures. This observation is reinforced by the unusual structural diversity of Cd(II)-triazolate and Cd(II)-tetrazolate phases. The predictable self-assembly of such materials remains elusive as reaction conditions, coligands and different degrees of aggregation in secondary building units among other factors contribute to the structural chemistry.

4.4 Experimental Section

4.4.1 Materials and General Procedures

The ligands 4-, and 2-pyridyltetrazole and pyrazinetetrazole were prepared by the "click" chemistry approach using zinc catalysis in aqueous solution or by the use of modified montmorillonite K-10.[31-33] All other chemicals were used as obtained without further purification: cadmium nitrate tetrahydrate, cobalt acetate tetrahydrate, copper acetate monohydrate, cadmium chloride hemipentahydrate, N,N-dimethylformamide, and methanol were purchased from Aldrich. All hydrothermal syntheses were carried out in 23 mL poly-(tetrafluoroethylene)-lined stainless steel containers under autogenous pressure. The reactants were stirred briefly, and the initial pH was measured before heating. Water was distilled above 3.0MΩ in-housing using a Barnstead model 525 Biopure distilled water center. The initial and final pH values of each reaction were measured using color pHast sticks.

4.4.1.1 Synthesis of [Cd(4-Hpyrtet)$_2$(OH)$_2$] (1)

A mixture of cadmium nitrate tetrahydrate (93.0 mg, 0.684 mmol), (4-pyridyl)tetrazole (50 mg, 0.342 mmol), and H_2O (10.00 g, 556 mmol) in the mole ratio 2.00:1.00:1626 was stirred briefly before heating to 200°C for 48 hours (initial and final pH values of 3.0 and 2.7, respectively). Clear block like crystals of **1**, suitable for X-ray diffraction, were isolated in 30% yield. Anal. Calcd. for $C_{12}H_{12}CdN_{10}O_2$: C, 32.7; H, 2.72; N, 31.8. Found: C, 38.3; H, 2.62; N, 31.4.

4.4.1.2 Synthesis of [Co(4-pyrtet)$_2$(H$_2$O)$_2$] (2)

A mixture of cobalt acetate tetrahydrate (171 mg, 0.684 mmol), (4-pyridyl)tetrazole (50 mg, 0.342 mmol), and H_2O (10.00 g, 556 mmol) in the mole ratio 2.00:1.00:1626 was stirred briefly before heating to 200°C for 48 hours (initial and final pH values of 3.5 and 3.3, respectively). Clear block crystals of **2**, suitable for X-ray diffraction, were isolated in 50% yield. Anal. Calcd. for $C_{12}H_{12}CoN_{10}O_2$: C, 37.2; H, 3.10; N, 36.2. Found: C, 36.8; H, 2.75; N, 35.9.

4.4.1.3 Synthesis of [Cu(4-pyrtet)$_2$(H$_2$O)$_2$] (3)

A mixture of copper acetate monohydrate (137 mg, 0.684 mmol), (4-pyridyl)tetrazole (50 mg, 0.342 mmol), and H_2O (10.00 g, 556 mmol) in the mole ratio 2.00:1.00:1626 was stirred briefly before heating to 200°C for 48 hours (initial and final pH values of 3.5 and 3.3, respectively). X-ray quality crystals in the form of clear blocks were obtained in 60% yield. X-ray quality crystals in the form of clear blocks were obtained in 60% yield. Anal. Calcd. for $C_{12}H_{12}CuN_{10}O_2$: C, 36.7; H, 3.06; N, 35.2. Found: C, 36.5; H, 3.00; N, 35.5.

4.4.1.4 Syntheses of [CdCl(2-pyrtet)(DMF)] (4) and [$Cd_4Cl_6(prztet)_2(DMF)_4$] (5)

Compounds **4** and **5** were prepared from the room temperature reaction of $Cd(NO_3)_2 \cdot 4H_2O$ and 2-pyridyltetrazole or pyrazinetetrazole in DMF in the mole ratio 2.00 : 1.00 and the addition of a small amount of HCl to induce complete dissolution of the reactants. The solutions were left at room temperature for 14-21 days. Clear block crystals of **4** and **5**, suitable for X-ray diffraction, were isolated in 60% yield. Anal Calcd. for $C_9H_{11}CdClN_6O$: C, 29.4; H, 3.00; N, 22.9. Found: C, 29.6; H, 3.42; N, 22.6. Anal Calcd. for $C_{22}H_{34}Cd_4Cl_6N_{16}O_4$: C, 21.1; H, 2.72; N, 17.9. Found: C, 20.6; H, 2.59; N, 17.4.

4.4.1.5 Syntheses of [$Cd_3(N_3)_4(4\text{-pyrtet})_2(H_2O)_2$ (6)

A solution of cadmium nitrate tetrahydrate (0.619g, 2.0 mmol), 4-pyridinecarbonitrile (0.418g, 4.0 mmol), and sodium azide (0.261g, 4.0 mmol) in 50ml methanol and 75ml water was gently heated with stirring. After 2 h, the mixture was allowed to cool to room temperature and allowed to stand in air at room temperature for several days. Yellow crystals suitable for X-ray diffraction were obtained. Anal. Calcd. for $C_{12}H_{12}Cd_3N_{22}O_2$: C, 17.3; H, 1.44; N, 36.9. Found: C, 17.4; H, 1.32; N, 36.8.

4.4.2 X-Ray Crystallography

Structural measurements were performed on a Bruker-AXS SMART-CCD diffractometer at low temperature (90 K) using graphite-monochromated Mo-Ka radiation (Mo K_α = 0.71073A˚).[34] The data were corrected for Lorentz and polarization effects and absorption using SADABS.[35,36] The structures were solved by direct methods. All non-hydrogen atoms were refined anisotropically. After all of the non-hydrogen atoms had been located, the model was refined against $\mathbf{F}^2$, initially using isotropic and later anisotropic thermal displacement

parameters. Hydrogen atoms were introduced in calculated positions and refined isotropically. Neutral atom scattering coefficients and anomalous dispersion corrections were taken from the *International Tables*, Vol. C. All calculations were performed using SHELXTL crystallographic software packages.[37] Crystallographic details have been summarized in Table 4.2. Selected bond lengths and angles are given in Tables 4.3-4.5.

Table 4.2: Summary of crystal data for the structures of $[Cd(4\text{-}Hpyrtet)_2(OH)_2]$ (**1**) $[Co(4\text{-}pyrtet)_2(H_2O)_2]$ (**2**), $[Cu(4\text{-}pyrtet)_2(H_2O)_2]$ (**3**), $[CdCl(2\text{-}pyrtet)(DMF)]$(**4**), $[Cd_4Cl_6(prztet)_2(DMF)_4]$ (**5**), and $[Cd_3(N_3)_4(4\text{-}pyrtet)_2(H_2O)_2]$ (**6**).

Formula	$C_{12}H_{12}CdN_{10}O_2$	$C_{12}H_{12}CoN_{10}O_2$	$C_{12}H_{12}CuN_{10}O_2$
Formula weight	440.73	387.25	391.87
Crystal System	Monoclinic	Orthorhombic	Orthorhombic
Space group	P2(1)/n	Aba2	Cmca
a (Å)	8.4251(7)	12.6376(7)	12.5645(11)
b (Å)	7.9458(7)	15.9206(9)	15.4031(14)
c (Å)	10.8479(9)	7.5603(4)	8.2773(7)
α (°)	90	90	90
β (°)	95.498	90	90
γ (°)	90	90	90
V ($Å^3$)	722.86(11)	1521.12(14)	1601.9(2)
Z	2	4	4
D_{calc} (mg/m^3)	2.025	1.691	1.625
μ (mm^{-1})	1.546	1.161	1.394
T (K)	98(2)	98(2)	98(2)
Wavelength (Å)	0.71073	0.71073	0.71073
R1	0.0676	0.0226	0.0837
wR2	0.1271	0.0638	0.2095

Formula	$C_8H_{11}CdN_6O$	$C_{22}H_{34}Cd_4Cl_6N_{16}O_4$	$C_6H_6Cd_{1.5}N_{11}O$
Formula weight	367.10	1248.98	416.82
Crystal System	Triclinic	Monoclinic	Orthorhombic
Space group	P-1	P2(1)	Pbca
a (Å)	6.9200(5)	8.3734(6)	7.845(1)
b (Å)	9.7325(7)	18.040(1)	12.664(2)
c (Å)	10.3635(8)	13.762(1)	24.194(3)
α (°)	79.491(1)	90	90
β (°)	86.492(1)	95.546(1)	90
γ (°)	75.524(1)	90	90
V ($Å^3$)	664.39(8)	2069.2(3)	2403.6(5)
Z	2	2	8
D_{calc} (mg/m^3)	1.835	2.005	2.304
μ (mm^{-1})	1.842	2.465	2.693
T (K)	98(2)	98(2)	98(2)
Wavelength (Å)	0.71073	0.71073	0.71073
R1	0.0352	0.0627	0.0155
wR2	0.0936	0.1613	0.0419

Table 4.3: Selected bond lengths and angles for $[Cd(4\text{-}Hpyrtet)_2(OH)_2]$ (1), $[Co(4\text{-}pyrtet)_2(H_2O)_2]$ (2), $[Cu(4\text{-}pyrtet)_2(H_2O)_2]$ (3), [CdCl(2-pyrtet)(DMF)](4).

1		2	
Cd(1)-O(1)	2.316(5)	Co(1)-O(90)	2.040(3)
Cd(1)-O(1)#1	2.316(5)	Co(1)-O(91)	2.120(3)
Cd(1)-N(5)#2	2.364(5)	Co(1)-N(1)#1	2.1577(11)
Cd(1)-N(1)	2.384(5)	Co(1)-N(1)	2.1577(11)
Cd(1)-N(1)#1	2.384(5)	Co(1)-N(4)#2	2.1589(12)
N(5)-Cd(1)#4	2.364(5)	Co(1)-N(4)#3	2.1589(12)
O(1)-Cd(1)-O(1)#1	180.00(11)	O(90)-Co(1)-O(91)	180
N(5)#2-Cd(1)-N(5)#3	180	N(1)#1-Co(1)-N(1)	177.81(10)
N(1)-Cd(1)-N(1)#1	180.000(1)	N(4)#2-Co(1)-N(4)#3	178.19(10)
3		4	
Cu(1)-N(4)#1	2.023(10)	Cd(1)-O(1)	2.305(3)
Cu(1)-N(4)#2	2.023(10)	Cd(1)-N(2)#1	2.345(3)
Cu(1)-N(1)	2.019(9)	Cd(1)-N(5)	2.385(3)
Cu(1)-N(1)#3	2.019(9)	Cd(1)-N(1)	2.409(3)
Cu(1)-O(1)	2.38(2)	Cd(1)-N(3)#2	2.411(3)
Cu(1)-O(1)#3	2.38(2)	Cd(1)-Cl(1)	2.5119(11)
N(1)-Cu(1)-N(1)#3	180	N(1)-Cd(1)-N(3)#2	164.18(10)
N(4)#1-Cu(1)-N(4)#2	180.0(5)	O(1)-Cd(1)-Cl(1)	178.71(7)
O(1)-Cu(1)-O(1)#3	180	N(2)#1-Cd(1)-N(5)	164.41(10)

Table 4.4: Selected bond lengths and angles for $[Cd_4Cl_6(prztet)_2(DMF)_4]$ (**5**).

Cd(1)-N(8)	2.262(10)	N(8)-Cd(1)-N(5)	167.6(4)
Cd(1)-O(4)	2.291(8)	N(4)-Cd(2)-Cl(4)	171.4(2)
Cd(1)-N(7)	2.359(9)	N(7)-Cd(1)-Cl(6)	160.4(3)
Cd(1)-N(5)	2.423(10)	Cl(2)-Cd(2)-Cl(3)	177.96(10)
Cd(1)-Cl(6)	2.542(3)	O(4)-Cd(1)-Cl(5)	176.4(2)
Cd(1)-Cl(5)	2.660(3)	Cl(4)-Cd(3)-Cl(5)	176.12(10)
Cd(2)-O(3)	2.303(10)	N(3)-Cd(3)-Cl(3)	175.6(3)
Cd(2)-N(4)	2.398(11)	O(2)-Cd(3)-Cl(6)	171.2(2)
Cd(2)-Cl(2)	2.594(3)	N(10)-Cd(4)-N(2)	166.3(4)
Cd(2)-Cl(3)	2.596(3)	O(1)-Cd(4)-Cl(2)	179.7(3)
Cd(2)-Cl(4)	2.601(3)	N(1)-Cd(4)-Cl(1)	158.5(2)
Cd(2)-Cl(1)	2.633(3)		
Cd(3)-O(2)	2.318(9)		
Cd(3)-N(3)	2.386(10)		

Cd(3)-Cl(4)	2.588(3)	
Cd(3)-Cl(5)	2.593(3)	
Cd(3)-Cl(3)	2.622(3)	
Cd(3)-Cl(6)	2.637(3)	
Cd(4)-O(1)	2.295(10)	
Cd(4)-N(10)	2.312(9)	
Cd(4)-N(1)	2.315(12)	
Cd(4)-N(2)	2.465(11)	
Cd(4)-Cl(1)	2.540(3)	
Cd(4)-Cl(2)	2.606(3)	

Table 4.5: Selected bond lengths and angles for $[Cd_3(N_3)_4(4\text{-pyrtet})_2(H_2O)_2]$ (**6**).

Cd(1)-N(1)	2.312(1)	N(9)-Cd(1)-N(3)	165.33(4)
Cd(1)-N(9)	2.334(1)	N(1)-Cd(1)-N(6)	174.18(4)
Cd(1)-O(1)	2.338(1)	O(1)-Cd(1)-N(8)	166.34(4)
Cd(1)-N(3)	2.342(1)	N(6)-Cd(2)-N(6)	180.0
Cd(1)-N(6)	2.372(1)	N(4)-Cd(2)-N(4)	180.0
Cd(1)-N(8)	2.406(1)	N(9)-Cd(2)-N(9)	180.0
Cd(2)-N(4)	2.3239(12)		
Cd(2)-N(4)	2.3239(12)		
Cd(2)-N(6)	2.3576(12)		
Cd(2)-N(6)	2.3576(12)		
Cd(2)-N(9)	2.3773(12)		
Cd(2)-N(9)	2.3773(12)		

4.5 Supplementary Materials

Additional material available from the Cambridge Crystallographic Data Centre, CCDC No. CCDC 871439-871444, comprises the final atomic coordinates for all atoms, thermal parameters, and a complete listing of bond distances and angles, for compounds **1-6**, respectively.

4.6 Acknowledgement

This work was supported by a grant from the National Science Foundation, CHE-0907787.

4.7 References

1. Juricek, M.; Kouwer, P.H.J.; Rowan, A.E., *Chem. Commun.*, **2011**, *47*, 8740.
2. Zhoa, H.; Qu, Z.-R.; Ye, H.-Y.; Xiong, R.-G., *Chem. Soc. Rev.*, **2008**, *37*, 84.
3. Beckmann, U.; and Brooker, S., *Coord. Chem. Rev.*, **2003**, *245*, 17.
4. Haasnoot, J.G., *Coord. Chem. Rev.*, **2000**, *200*, 131.
5. Hellyer, R.M.; Larsen, D.S.; and Brooker, S., *Eur. J. Inorg. Chem.*, **2009**, 1162.
6. Zhang J.-P.; and Chen, X.-M., *Chem. Commun.*, **2006**, 1689.
7. Steel, P.J., *Coord. Chem. Rev.*, **1990**, *106*, 227.
8. Potts, K.T., *Chem. Rev.* **1961**, *61*, 87.
9. Dawe, L.N.; and Thompson, L.K., *Dalton Trans.*, **2008**, 3610.
10. Zhang, J.-P.; Lin, Y.-Y.; Huang, X.-C.; and Chen, X.-M., *J. Am. Chem. Soc.*, **2005**, *127*, 5495.
11. Zhang, J.-P.; Zheng, S.-L.; Huang, X.-C.; and Chen, X.-M., *Angew. Chem., Int. Ed.*, **2004**, *43*, 206.
12. Ferrer, S.; Lloret, F.; Bertomeu, I.; Alzuet, G.; Borras, J.; Garcia-Granda, S.; Liu-González, M.; and Haasnoot, J.G., *Inorg. Chem.*, **2002**, *41*, 5821.
13. Zhou, J.-H.; Cheng, R.-M.; Song, Y.; Li, Y.-Z.; Yu, Z.; Chen, X.-T.; Xue, Z.-L.; and You, X.-Z., *Inorg. Chem.*, **2005**, *44*, 8011 and references therein.
14. Zhang, J.-P.; Lin, Y.-Y.; Zhang, W.-X.; and Chen, X.-M., *J. Am. Chem. Soc.*, **2005**, *127*, 14162.
15. Zhang, D.-C.; Lu, W.-G.; Jiang, L.; Feng, X.-L.; and Lu, T.-B., *Cryst. Growth Des.*, **2010**, *10*, 739.

16. Ouellette, W.; Yu, M.H.; O'Connor, C.J.; Hagrman, D.; and Zubieta, J., *Angew. Chem., Int. Ed.*, **2006**, *45*, 3497.

17. Ouellette, W.; Prosvirin, A.V.; Valeich, J.; Dunbar, K.R.; and Zubieta, J., *Inorg. Chem.*, **2007**, *46*, 9067.

18. Ouellette, W.; Galán-Mascarós, J.R.; Dunbar, K.R.; and Zubieta, J., *Inorg. Chem.*, **2006**, *45*, 1909.

19. Ouellette, W.; Prosvirin, A.V.; Chieffo, V.; Dunbar, K.R.; Hudson, B.; and Zubieta, J., *Inorg. Chem.*, **2006**, *45*, 9346.

20. Chesnut, D.J.; Kusnetzow, A.; Birge, R.; and Zubieta, J., *Inorg. Chem.*, **1999**, *38*, 5484.

21. Ouellette, W.; Hudson, B.S.; and Zubieta, J., *Inorg. Chem.*, **2007**, *46*, 4887.

22. Ouellette, W.; Liu, H.; O'Connor, C.J.; and Zubieta, J., *Inorg. Chem.*, **2009**, *48*, 4655.

23. Ouellette W.; and Zubieta, J., *Chem. Commun.*, **2009**, 4533.

24. Ouellette, W.; Prosvirin, A.V.; Whitenack, K.; Dunbar, K.R., and Zubieta, J., *Angew. Chem., Int. Ed.*, **2009**, *48*, 2140.

25. Ouellette, W.; Jones, S.; and Zubieta, J., *CrystEngComm.*, **2011**, 13, 4457

26. Ouellette, W.; Darling, K.; Prosvirin, A.; Whitenack, K.; Dunbar, K.R.; and Zubieta, J., *Dalton Trans.*, **2011**, *40*, 12288.

27. Tahli, A.; Maclaren, J.K.; Boldog, I.; and Janiak, C., Inorg. Chim. Acta **2011**, *374*, 506.

28. Liu, K.; Shi, W.; and Cheng, P., *Dalton Trans.*, **2011**, *40*, 8478.

29. Liu, Q.-K.; Ma, J.-P.; and Dong, Y.-B., *Chem. Commun.*, **2011**, 47, 7185.

30. Xu, Q.-F.; Ge, J.-F.; Zhou, Q.-X., Lu, J.-M.; Ji, S.-J.; Wang, L.-H.; Zhang, Y.; Jin, X.-M.; and Wu, B., *Dalton Trans.*, **2011**, *40*, 2808.

31. (a) Demko, P.Z.; Sharpless, K.B., *J. Org. Chem.*, **2001**, *66*, 7945; (b) Hirno, F.; Demko, P.Z.; Noodleman, L.; and Sharpless, K.B., *J. Am. Chem. Soc.*, **2002**, *124*, 12210.

32. Tao, J.; Ma, Z.-J.; Huang, R.-B.; and Zhang, L.-S., *Inorg. Chem.*, **2004**, *43*, 6133.

33. Chermahini, A.N.; Teimouri, A.; and Moaddeli, A., *Heteroatom Chem.*, **2011**, *22*, 168.

34. SMART, Data Collection Software, version 5.630, Bruker-AXS Inc., Madison, WI, **1997-2002**.

35. SAINT Plus, Date Reduction Software, version 6.45A, Bruker-AXS Inc., Madison, WI, **1997-2002**.

36. Sheldrick, G.M., SADABS, University of Göttingen, Göttingen, Germany, **1996**.

37. SHELXTL PC, version 6.12, Bruker-AXS Inc., Madison, WI, **2002**.

38. Stein, A.; Keller, S.W.; and Mallouk, T.E., Science **1993**, *259*, 1558.

39. Gopalakrishnan, J., Chem. Mater. **1995**, *7*, 1265.

40. Weller, M; and Dann, S.E., Curr. Opin. *Solid State Mater. Sci.*, **1998**, *3*, 137.

41. Gopalakrishnan, J.; Bhuvanesh, N.S.P.; and Rangan, K.K., *Curr. Opin. Solid State Mater. Sci.*, **1996**, *1*, 285.

42. Zubieta, J., Solid state methods, Comprehensive Coordination Chemistry II **2003**, *1*, 697.

43. Tahli, A., et al., Inorganica Chimica Acta **2001**, *374*, 1506-523.

44. He, X.; Zhang, J.; Wu, X.-Y.; and Lu, C.-Z., Inorg. Chim. Acta **2010**, *363*, 1727.

45. Yang, G.; Raptu, R.G.; Safar P., *Cryst. Growth Des.*, **2008**, *8*, 981.

46. Darling, K.; Ouellette, W.; and Zubieta, J., accepted.

47. Liu, K.; Shi, W.; and Cheng, P., *Dalton Trans.*, **2011**, 8475.

48. He, X.; Lu, C.-Z.; and Yuan, D.-Q., *Inorg. Chem.*, **2006**, *45*, 5760.

49. Yin, P.X.; Cheng, J.K.; Li, Z.J.; Zhang, L.; Qin, Y.Y.; Zhang, J.; and Yao, Y.G., *Inorg. Chem.*, **2009**, *48*, 10859.

50. Ding, B.; Yi, L.; Wang, Y.; Cheng, P.; Liao, D.Z.; Yan, S.P.; Jiang, Z.H.; Song, H.B.; and Wang, H.G., *Dalton Trans.*, **2006**, 665.

51. Liu, B.; Xu, L.; Guo, G.C.; and Huang, J.S., *Mol. Struct.*, **2006**, *825*, 79.

52. Zhai, Q.G.; Wu, X.Y.; Chen, S.M.; Lu, C.Z.; and Yang, W.B., *Cryst. Growth Des.*, **2006**, *6*, 2126.

53. Liu, B.; and Zhang, X.C., *Inorg. Chem. Comm.*, **2008**, *11*, 1162.

54. Yi, L.; Ding, B.; Zhao, B.; and Cheng, P., *Inorg. Chem.*, **2004**, *43*, 33.

55. Siddiqui, K.A.; Bolte, M.; and Mehrotra, G.K., *Inorg. Chim. Acta.*, **2010**, *363*, 457.

56. Garcia-Couciero, U.; Castillo, O.; Luque, A.; Garcia-Teran, J.P.; Beobide, G.; and Roman, P., *Eur. J. Chem.*, **2005**, 4280.

57. Meng, Z.S.; Yun, L.; Zhang, W.X.; Hong, C.G.; Herchel, R.; Ou, Y.C.; Leng, J.D.; Peng, M.X.; Lin, Z.J.; and Tong, M.L., *Dalton Trans.*, **2009**, 10284.

58. Du, M.; Jiang, X.J.; and Zhao, X.Z., *Inorg. Chem.*, **2006**, *45*, 3998.

59. Du, M.; Jiang, X.J.; and Zhao, X.J., *Inorg. Chem.*, **2007**, *46*, 3984.

60. R.B. Zhang, R.B.; Li, Z.J.; Qin, Y.Y.; Cheng, J.K.; Zhang, J.; and Yao, Y.G., *Inorg. Chem.*, **2008**, *47*, 4861.

61. Li, W.; Jia, H.P.; Ju, Z.F.; and Zhang, J., *Cryst. Growth Des.*, **2006**, *6*, 2136.

62. Chen, Z.L.; Li, X.L.; and Liang, F.P., *J. Solid State Chem.*, **2008**, *181* 2078.

63. Zhou, W.; Chen, J.; Xu, G.; and Guo, G., *Chem. Comm.*, **2008**, 2762.

64. Zhang, R.; Zhang, J.; Li, Z.; Qin, Y.; and Yao, Y., *Chem. Comm.*, **2008**, 4159.

65. Liu, B.; Zhang, X.C.; and Wang, Y.F., *Inorg. Chem. Comm.*, **2007**, *10*, 199.

66. Huang, Y.Q.; Zhao, X.Q.; Shi, W.; Liu, W.Y.; Chen, Z.C.; Cheng, P.; Liao, D.Z.; and Yan, S.P., *Cryst. Growth Des.*, **2008**, *8*, 3652.

67. Liu, Y.Y.; Huang, Y.Q.; Shi, W.; Cheng, P.; Liao, D.Z.; and Yan, S.P., *Cryst. Growth Des.*, **2007**, 7, 1483.

68. Liu, Y.Y.; Yi, L.; Ding, B.; Huang, Y.Q.; and Cheng, P., *Inorg. Chem. Comm.*, **2007**, 10, 517.

69. Yi, L.; Yang, T.; Lu, T.; and Cheng, P., *Cryst. Growth Des.*. **2005**, *5*, 1215.

70. Xu, Q.F.; Ge, J.F.; Zhou, Q.X.; Lu, J.M.; Ji, S.J.; Wang, L.H.; Zhang, Y.; Jin, X.M.; and Wu, B., *Dalton Trans.*, **2011**, *40*, 2805.

71. Tahli, A.; Maclaren, J.K.; Boldog, I.; and Janiak, C., *Inorg. Chim. Acta.*, **2011**, *374*, 506.

72. Meng, Z.S.; Yun, L.; Zhang, W.X.; Hong, C.G.; Herchel, R.; Ou, Y.C.; Leng, J.D.; Peng, M.X.; Lin, Z.L.; and Tong, M.L., *Dalton Trans.*, **2009**, 10284.

73. Adriaanse, J.H.; Askes, S.H.C.; van Bree, Y.; van Oudheusden, S.; van der Bos, E.D.; Gunay, E.; Mutikainen, I.; Turpeinen, U.; van Albada, G.A.; Haasnoot, J.G.; and Reedijk, J., *Polyhedron*, **2009**, *28*, 3143.

74. Rahmani, A.; Romero, M.A.; Salas, J.G.; Quiros, M.; and deCienfuegos, G.A., *Inorg. Chim. Acta.*, **1996**, *247*, 51.

75. Deng, H.; Qin, Y. C.; Li, Y.H.; Liu, Z.H.; Zeng, R.H.; Zeller, M.; and Batten, S.R., *Chem. Comm.*, **2008**, 2239.

76. Xiong, R.G.; Xue, X.; Zhao, H.; You, X.Z.; Abrahams, B.F.; and Xue, Z., *Angew. Chem. Int. Ed.*, **2002**, *41*, 3800.

77. Xue, X.; Wang, X.S.; Wang, L.Z.; Xiong, R.G.; Abrahams, B.F.; You, X.Z.; Xue, Z.L.; and Che, C.M., *Inorg. Chem.*, **2002**, *41*, 6544.

78. Ouellette, W.; and Zubieta, J., *Chem. Comm.* **2009**, 4533

79. Tao, Y.; Li, J.R.; Yu, Q.; Song, W.-C.; Tong, X.L.; and Bu, X.H., *Cryst. Eng. Comm.*, **2008**, *10*, 699.

80. Li, Z.; Li, M.; Zhou, X.P.; Wu, T.; Li, D.; and Ng, S.W., *Cryst. Growth Des.*, **2007**, *7*, 1992.

81. Rodriguez-Dieguez, A.; Salinas-Castillo, A.; Galli, S.; Masciocchi, N.; Gutierrez-Zorrilla, J.M.; Vitoria, P.; and Colecio, E., *Dalton Trans.*, **2007**, 1821.

82. Jiang, C.; Yu, Z.; Jiao, C.; Wang, S.; Li, J.; Wang, Z.; and Cui, Y., *Eur. J. Inorg. Chem.*, **2004**, 4669.

83. Liu, N.; Yue, Q.; Wang, Y.Q.; Cheng, A.L.; and Gao, E.Q., *Dalton Trans.*, **2008**, 4621.

84. Collins, C.S.; Sun, D.; Liu, W.; Zuo, J.L.; and Zhou, H.C., *J. Mol. Struct.*, **2008**, 890, 163.

Chapter 5: Syntheses, Structural Characterization and Properties of Transition Metal Complexes of 5,5′-(1,4-phenylene)bis(1*H*-tetrazole) (H_2bdt), 5',5''-(1,1'-biphenyl)-4,4'-diylbis(1H-tetrazole) (H_2dbdt), and 5,5′,5″-(1,3,5-phenylene)tris(1*H*-tetrazole) (H_3btt).

5.1 Introduction

Solid state coordination chemistry is concerned with the design of materials that are constructed from metal or metal cluster sites linked through di- or polytopic bridging ligands. The contemporary interest in such materials reflects their diversity of chemical composition and structural complexity, characteristics that result in a range of useful properties, reflected in applications to fields as diverse as catalysis, optical materials, membranes and sorption.[1-22] The inorganic substructures of these hybrid materials are modified through the introduction of organic components that can provide composite or novel physical properties and allow access to a vast domain of potentially multifunctional materials.[23,24]

Organic-inorganic hybrid materials of this type include metal-organic frameworks constructed from metal or metal cluster nodes linked through polyfunctional carboxylate or polypyridyl ligands and the expansive class of prototypical hybrid materials that incorporate organophosphonate ligands.[25-40] These materials have been extensively studied by Yaghi,[41-41] Ferey,[43] Kitagawa,[44] Clearfield[45] and others.[46-49] Other ligand types have also been exploited to afford variable tether lengths, different charge-balance requirements, modified steric constraints, additional functional groups, and appropriate juxtapositions of donor groups. In this respect, the polyazaheteroaromatic ligands of the imidazole, pyrazole, triazole and tetrazole family have witnessed considerable interest because of their ability to bridge multiple metal sites to afford polynuclear compounds, their superexchange capacity reflected in unusual magnetic properties, and their facile modification to provide additional functionality.[50-65] This class of ligands has also been widely used in the design of microporous metal-organic frameworks with significant gas storage properties.[66-70]

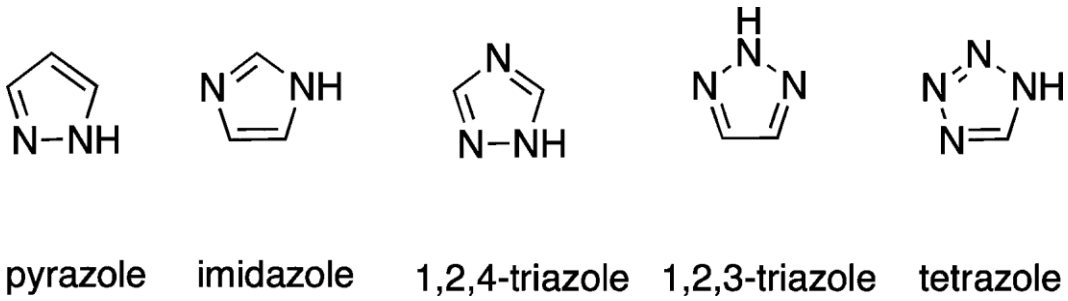

Scheme 1

Our own investigations initially focused on the structural chemistry of metal-triazolates prepared by hydrothermal methods.[71-80] The ease of modification of polyazaheterocyclic ligands led us to explore the naïve design strategy of inserting appropriate tethering groups to expand the coordination domain of the ligand. For example, the bridging ligands 4-(4-pyridyl)pyrazolate and 4-pyridyltetrazolate in N2, N3-bridging mode may be considered expanded analogues of triazolates (**Scheme 2**). Since this approach provided a number of novel materials, this design principle was exploited in the use of polyazaheterocyclic ligands tethered and extended to mimic linear dicarboxylates to provide spatial extension in the construction of frameworks with significant free volume (**Scheme 3**). Examples include complexes of 5,5′-(1,4-phenylene)bis(1*H*-tetrazole) (H_2bdt): the manganese(II) material $[Mn_3(bdt)(dmf)_4(H_2O)_2]$ which exhibits unusually effective hydrogen storage properties and the Co(II) compound $[Co_2(H_{0.67}bdt)_3]$, a microporous framework material exhibiting single-chain magnetism.

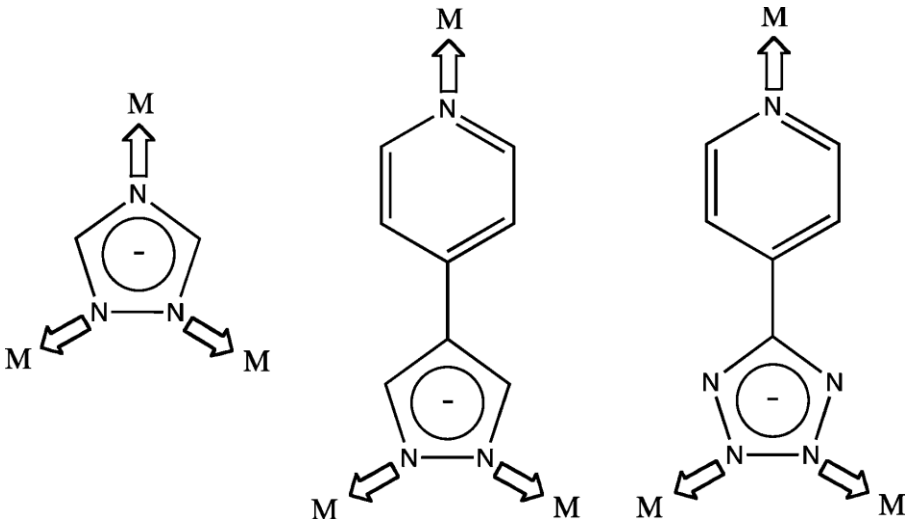

Scheme 2

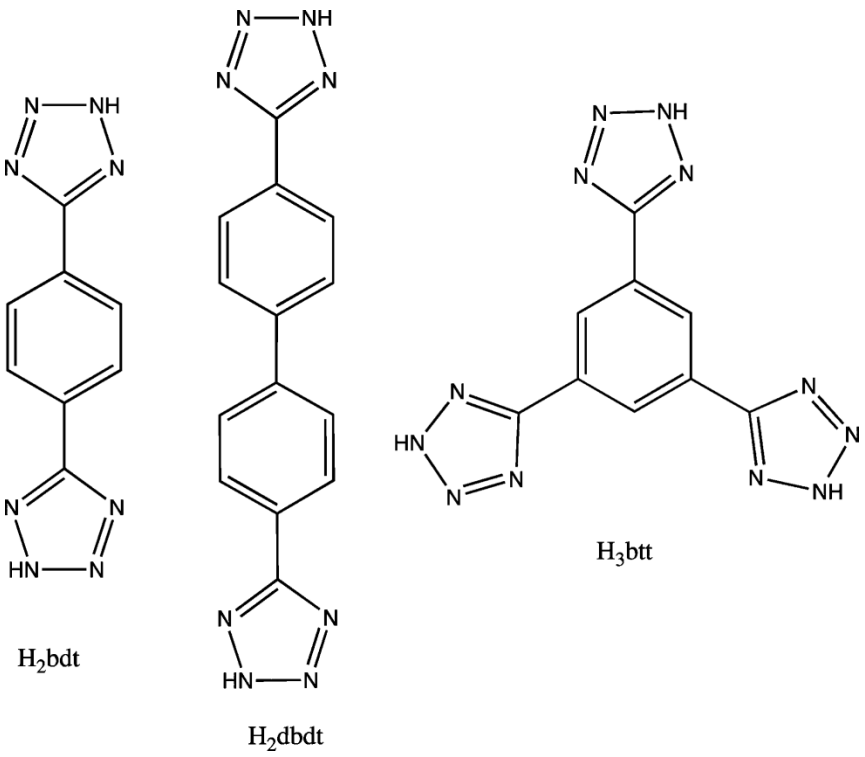

Scheme 3

The effectiveness of the H_2dbt ligand in the construction of framework materials encouraged us to investigate the hydrothermal chemistry with Co(II) under different conditions and to extend our studies to other metals and to the related 5′,5′′-(1,1′-biphenyl)-4,4′-diylbis(1*H*-

tetrazole) (H_2dbdt) and 5,5′,5″-(1,3,5-phenylene)tris(1*H*-tetrazole) (H_3btt) ligands. We report the preparations and structures of a short series of Co(II) frameworks $[Co_5F_2(dbdt)_4(H_2O)_6]\bullet 2H_2O$ (**1**•$2H_2O$), $[Co_4(OH)_2(SO_4)(bdt)_2CH_2O)_4]$ (**2**) and $[Co_3(SO_4)(OH)(btt)(H_2O)_4]\bullet 3H_2O$ (**3**•$3H_2O$); the Ni(II) framework $[Ni_2(H_{0.67}bdt)_3]\bullet 10.5H_2O$ (**4**•$10.5H_2O$); and the Zn(II) and Cd(II) materials [Zn(bdt)] (**5**) and $(Me_2NH_2)_3[Cd_{12}Cl_3(btt)_8(DMF)_{12}]\bullet 12DMF\bullet 5CH_3HO$ (**6**•$12DMF\bullet 5CH_3OH$). The magnetic properties of the cobalt series are also presented.

5.2 Results and Discussion

5.2.1 Syntheses

A useful strategy for securing x-ray quality single crystals is to employ hydrothermal methods. Hydrothermal synthesis has been found to provide a powerful technique for the preparation of organic-inorganic hybrid materials, with retention of the structural elements of the reactants in the final product phases.[91-95] Hydrothermal reactions, typically carried out in the temperature range 120-260 ^oC under autogenous pressure, exploit the self assembly of the product from soluble precursors. The reduced viscosity of water under these conditions enhances diffusion processes so that solvent extraction of solids and crystal growth from solution are favored. Since problems associated with different solubilities of organic and inorganic starting materials are minimized, a variety of precursors may be introduced, as well as a number of organic and/or inorganic structure-directing or charge-balancing reagents from which those of appropriate size, shape and charge[96] may be selected for efficient crystal packing during the crystallization process. Under such nonequilibrium crystallization conditions, metastable kinetic phases rather than the thermodynamic phase may also be isolated.

In this study, we wished to explore the structural consequences of tethering tetrazolate units to provide dipodal ligands with different spacer lengths, H_2bdt and H_2dbdt, and a related

tripodal ligand, H_3btt. Since our previous studies suggested that sulfate provided a charge-compensating anion with a pronounced tendency to incorporate into the frameworks and to provide unusual structural chemistry, we adopted M(II) sulfates as the starting materials. The Co(II) chemistry demonstrated the structural diversity that arises under the complex parameter space of hydrothermal chemistry.

In several cases, HF was added as a "mineralizer", that is, to solubilize the reactants and promote crystal growth. In the case of the reaction of $CoSO_4$•$7H_2O$ with H_2dbdt, the fluoride was incorporated into the framework rather than the sulfate to provide the three-dimensional $[Co_5F_2(dbdt)_4(H_2O)_6]$•$2H_2O$ (**1**•$2H_2O$). In contrast, under basic conditions, the reaction of $CoSO_4$•$7H_2O$ with H_2bdt yields the sulfato phase $[Co_4(OH)_2(SO_4)(bdt)_2(H_2O)_4]$ (**2**). The dramatic influence of minor changes in reaction conditions is illustrated by the isolation of a second sulfato phase under neutral conditions, $[Co_3(OH)(SO_4)(btt)(H_2O)_4]$•$3H_2O$ (**3**•$3H_2O$).

However, under mildly acidic conditions, $CoSO_4$•$7H_2O$ and $NiSO_4$•$6H_2O$ react with H_2bdt to give the materials $[M_2(H_{0.67}bdt)_3]$•xH_2O (M = Ni(**4**) and Co). As noted previously, anion incorporation can be unpredictable in these materials. The reaction of $ZnSO_4$•$7H_2O$ with H_2bdt produces a material of simple composition [Zn(bdt)] (**5**), also with no sulfate incorporation.

Attempts to prepare an analogous Cd(II) species under hydrothermal conditions proved unproductive. However, the reaction of $CdSO_4$ with H_3btt in DMF/MeOH yielded the open-framework material $[Me_2NH_2]_3[Cd_{12}Cl_3(btt)_8(DMF)_{12}]$•12DMF•5MeOH (**6**•12DMF•5MeOH).

5.2.2 Structural Studies

As shown in **Figure 5.1a**, the structure of the cobalt(II)-fluoride derivative $[Co_5F_2(dbdt)_4(H_2O)_6]$•$2H_2O$ (**1**•$2H_2O$) is three-dimensional. The structure is constructed of $\{Co_5F_2(tetrazolate)_4(H_2O)_4\}_\infty$ chains, running parallel to the *c*-axis, with each chain linked to six

adjacent chains through the diphenyl tethers of the dbdt ligands. **Figure 5.1b** illustrates that each chain is constructed from secondary building units (SBU) consisting of pentanuclear $\{Co_5F_2(tetrazolate)_8(H_2O)_6\}$ clusters.

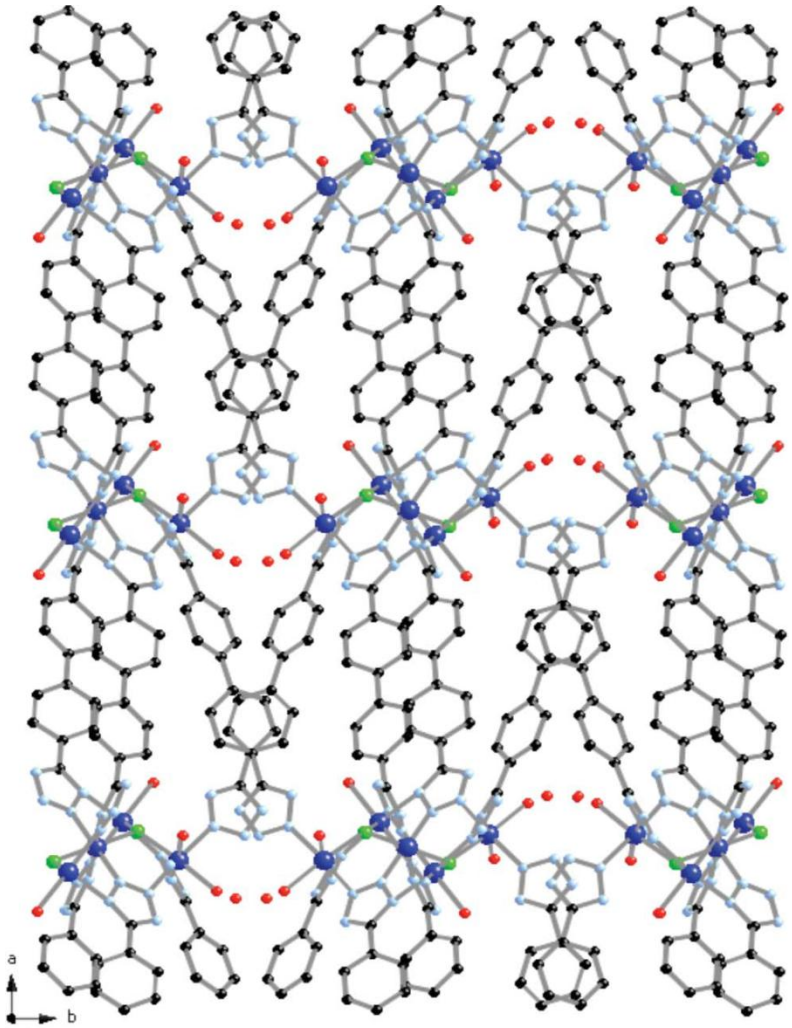

(a)

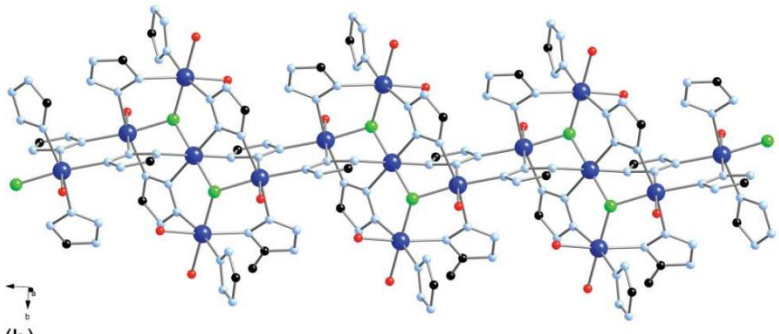

(b)

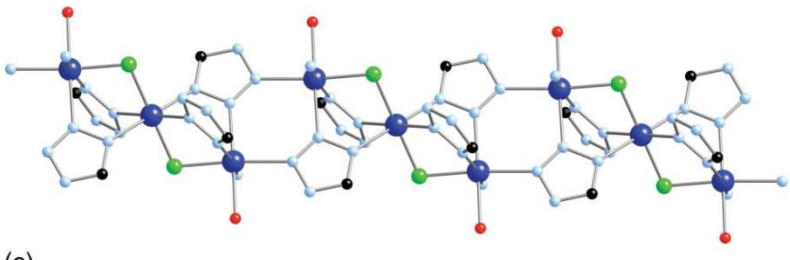

(c)

Figure 5.1: (a) A ball and stick representation of the structure of $[Co_5F_2(dbdt)_4(H_2O)_6]\bullet 2H_2O$ (**1**$\bullet 2H_2O$), viewed normal to the *ab* plane; the water molecules of crystallization are shown as black-edged spheres; Color scheme: cobalt, dark blue spheres; fluorine, green spheres; oxygen, red spheres; nitrogen, light blue spheres; carbon, black spheres. (b) A view of the one-dimensional $\{Co_5F_2(tetrazolate)_4(H_2O)_4\}_\infty$ substructure of **1**. (c) The chain substructure stripped of the peripheral $\{CoN_3FO_2\}$ sites to show the central linear trinuclear substructure and the linking of adjacent triads through triply-bridging tetrazolate groups. Color scheme: cobalt, dark blue spheres; fluorine, green spheres; oxygen, red spheres; nitrogen, light blue spheres; carbon, black spheres.

Within the cluster, there are three crystallographically unique Co(II) sites, linked to a triply bridging fluoride ligand. The pentanuclear grouping may be described as two fluoride bridged cobalt triads, fused at a common cobalt vertex. One cobalt site of the triad exhibits $\{CoN_3FO_2\}$ distorted octahedral coordination through bonding to three tetrazolate nitrogen donors from three dbdt ligands, two oxygen donors of aqua ligands, and the triply bridging fluoride. A second cobalt center enjoys $\{CoN_4FO\}$ coordination involving four tetrazolate nitrogen donors, an aqua ligand and the fluoride, while the third match site exhibits $\{CoN_4F_2\}$ coordination to four tetrazolate groups and two bridging fluorides. Consequently, the triangular subunit $\{Co_3(N,N'\text{-tetrazolate})_3X\}^{+2}$ exhibits the trinuclear core structure common to many metal-triazolate materials, including $[M_3(trz)_3(OH)_3(H_2O)_4]_x$ (M = Ni, Cu) and $[Cu_3(trz)_3(OH)][Cu_2Br_4]$ (trz = triazolate). Within the pentanuclear unit, two tetrazolate units bridge two cobalt centers of one triad and a third cobalt of the adjacent triad, adopting N1,N2,N3-coordination modes. Two tetrazolate groups are engaged exclusively in bridging two metal sites of a single triad, while two other tetrazolate groups bridge two sites of a triad and link to adjacent pentanuclear clusters. The final pair of tetrazolate groups adopt monodentate coordination to the peripheral cobalt sites of the clusters. The linkage pattern of the tetrazolate termini of the dbdt ligands results in two distinct ligand connectivities: the first dbdt ligand bonds to a single cobalt site at one terminus and

bridges two metal sites at the other, while the second dbdt group bridges three cobalt sites at either terminus.

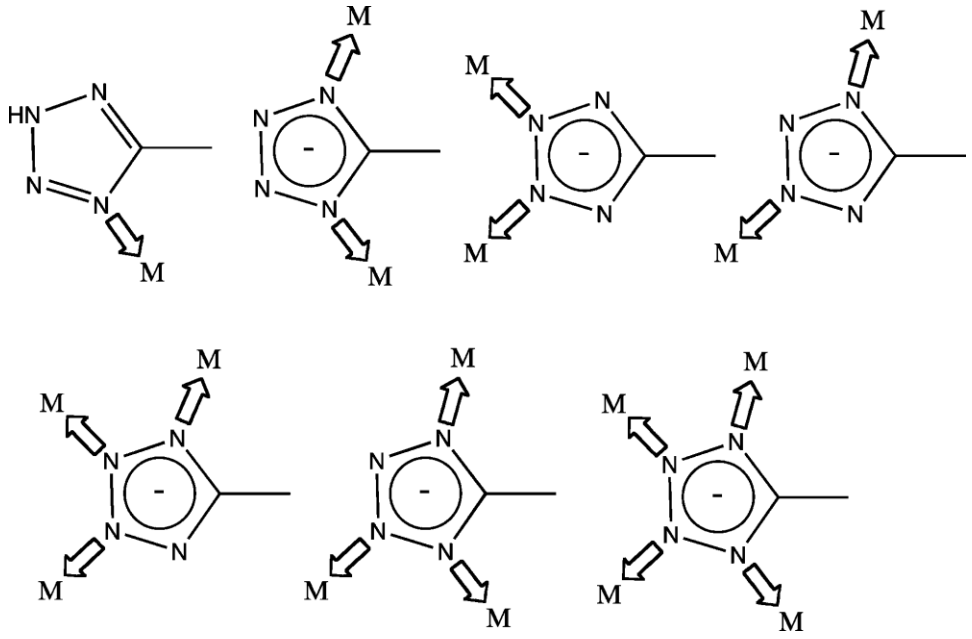

Scheme 4

Further inspection of the chain substructure reveals that the pentanuclear moieties consist of a core of three linearly disposed cobalt centers and two peripheral units, the $\{CoN_3FO_2\}$ sites. As shown in **Figure 5.1(c),** the chain stripped of these latter sites adopts the common pattern of metal sites bridged to each neighbor in the chain through two tetrazolate units. However, in this case, there are both triply-bridging tetrazolate groups and fluoride bridges to complicate the common motif.

The three-dimensional structure of $[Co_4(OH)_2(SO_4)(bdt)_2(H_2O)_4]$ (**2**) is shown in **Figure 5.2a**. The structure may be described as a "buttressed" layer, a structural type characteristic of dipodal ligands with organic tethers such as diphosphonates. In this scheme, the structure consists of $\{Co_4(OH)_2(SO_4)(\text{tetrazolate})_2(H_2O)_4\}_\infty$ layers in the *bc* plane (**Figure 5.2b**), linked through the phenyl groups of the bdt ligand. The network substructure is in turn constructed from

$\{Co_4(OH)_2(tetrazolate)_2(H_2O)_4\}_\infty$ chains, running parallel to the *b* axis, linked through $(SO_4)^{2-}$ chains.

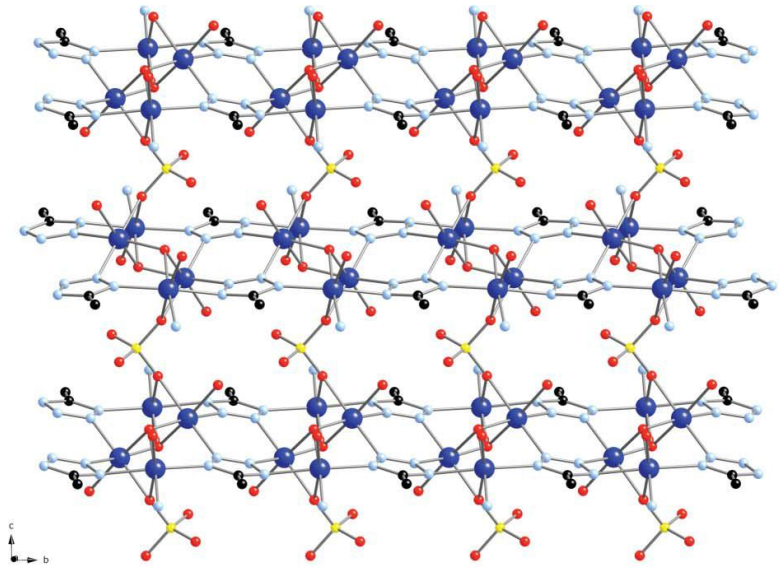

(a)

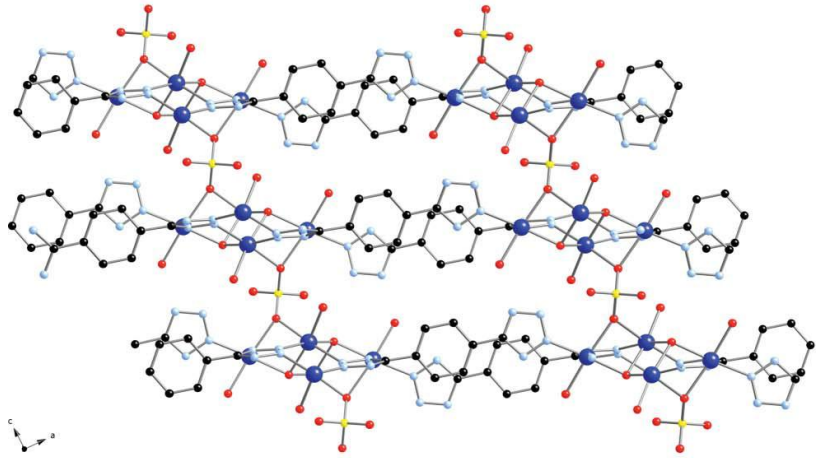

(b)

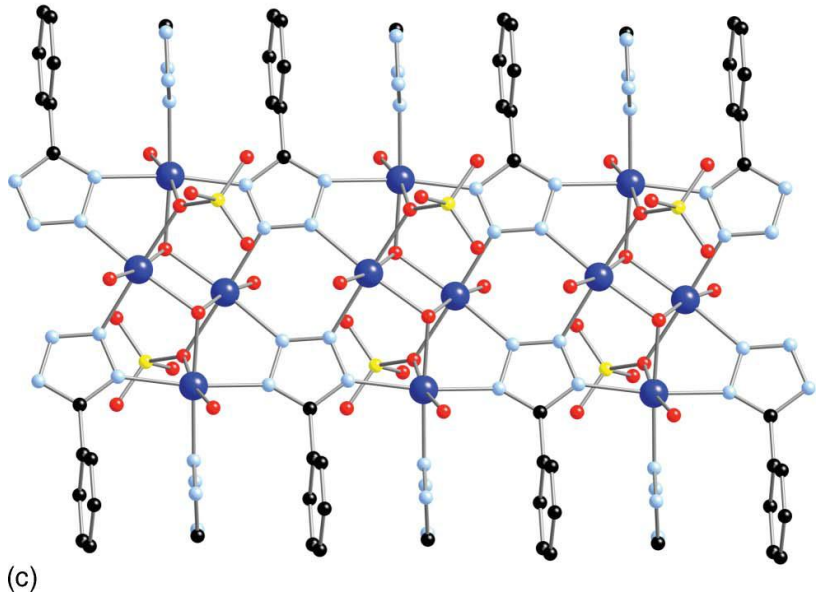

(c)

Figure 5.2: (a) A ball and stick representation of the structure of $[Co_4(OH)_2(SO_4)(bdt)_2(H_2O)_4]$ (**2**) viewed normal to the *ac* plane. Color scheme: as above with yellow spheres for the sulfur. (b) A view of the two-dimensional substructure in the *bc* plane. (c) The one-dimensional substructure, showing the tetranuclear secondary building unit. Color scheme: as above with yellow spheres for the sulfur.

The secondary building unit of these chains is a tetranuclear $\{Co_4(OH)_2SO_4)_2(tetrazolate)_6\}^{4-}$ cluster (**Figure 5.2c**), exhibiting two crystallographically unique cobalt sites: one with meridional $\{CoN_3O_3\}$ coordination to a hydroxy group, a terminal aqua ligand, a sulfate oxygen donor and three tetrazolate nitrogen donors and the second having $\{CoN_2O_4\}$ coordination defined by two hydroxy groups, a sulfate oxygen donor and two tetrazolate nitrogen donors in the *cis* geometry. The tetranuclear core consists of two $\{Co_3(\mu^3\text{-}OH)\}$ triads fused at a common edge. The sulfate groups bridge two cobalt sites of a cluster through a single oxygen donor and bridge to a tetranuclear unit of an adjacent chain. Pairs of cobalt sites in the cluster are linked through N1,N2-bridging tetrazolate ligands, that in turn connect to an adjacent cluster of the chain so as to adopt a quadruply-bridging mode. The two peripheral cobalt centers of each cluster are bound to tetrazolate groups bonding through the N2 site only. Thus, each bdt ligand bonds through four nitrogen donors at one tetrazolate terminus and one at the other.

The structure of $[Co_3(OH)(SO_4)(btt)(H_2O)_4]\bullet 3H_2O$ (**3**$\bullet 3H_2O$), shown in **Figure 5.3a**, is also three-dimensional. The overall structure may be described as $\{Co_3(OH)(SO_4)(tetrazolate)_3\}_\infty$ chains (**Figure 5.3b**) running parallel to the *a* axis, each chain connected to six adjacent chains through the btt ligands whose planes are parallel to the *bc* plane. The chains are constructed from a variant of the common $\{M_3(\mu_3\text{-}X)\}$ cluster, in this case the $\{Co_3(\mu_3\text{-}OH)(SO_4)_2(tetrazolate)_3\}^{2-}$ secondary building unit. The cluster consists of a planar $\{Co_3(tetrazolate)_3\}$ subunit, with the triply-bridging hydroxy ligand displaced 0.2Å from the face of the plane opposite the triply-bridging sulfato ligand. Each tetrazolate unit bridges two cobalt sites of the cluster through the

N2,N3 donors. The sulfate group caps the copper triad in a C_3 symmetric fashion through three oxygen donors. The fourth sulfate oxygen bridges to an adjacent trinuclear unit of the chain. One of the capping oxygen atoms is also involved in bonding to the adjacent cluster, such that the sulfate chelates to this cobalt site and the planes of successive trinuclear units are offset, resulting in a zig-zag pattern along the *a*-direction.

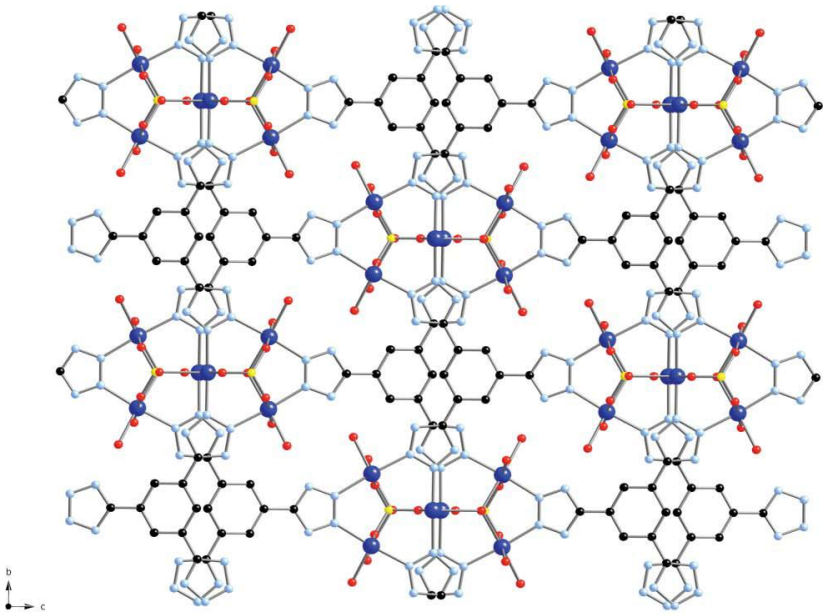

(a)

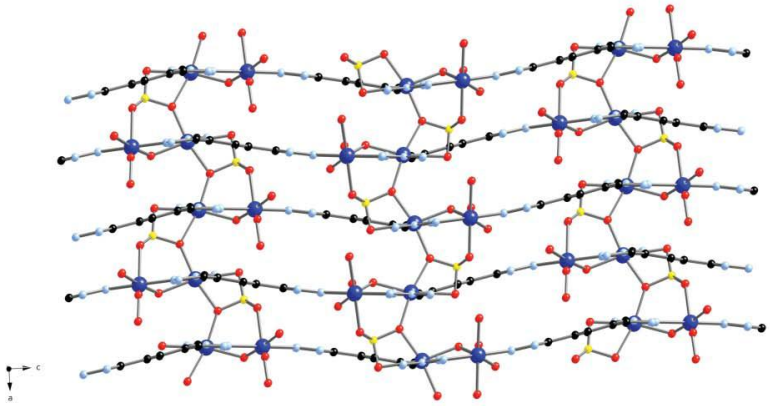

(b)

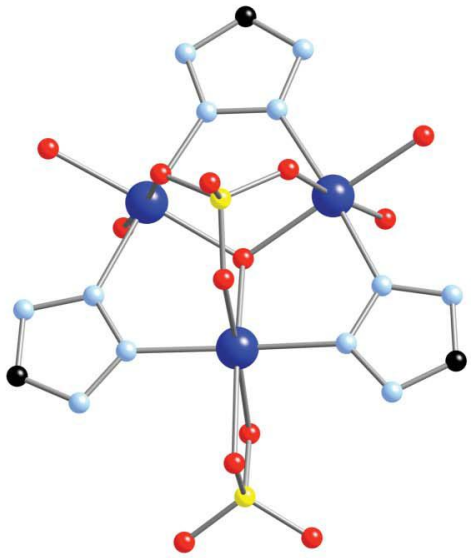

(c)

Figure 5.3: (a) A ball and stick representation of the structure of $[Co_3(OH)(SO_4)(btt)(H_2O)_4]$ (**3**) in the *bc* plane. (b) A view of the structure in the *ac* plane. (c) The trinuclear secondary building unit of **3**.

The connectivity pattern results in two crystallographically unique cobalt sites. One exhibits $\{CoN_2O_4\}$ coordination to nitrogen donors from two tetrazolate groups in a *trans* geometry, the triply-bridging hydroxy ligand, a sulfate oxygen and two aqua ligands. The second site is also $\{CoN_2O_4\}$ with *trans* tetrazolate nitrogen donors, the triply-bridging hydroxy group and sulfate oxygen from the capping sulfate group, but the remaining coordination sites are occupied by oxygen donors of a chelating sulfate.

The structure of the Ni(II) phase $[Ni_2(H_{0,67}bdt)_3]\bullet 10.5H_2O$ (**4**$\bullet 10.5H_2O$) is isomorphous with that of the previously described $[Co_2(H_{0.67}bdt)_3]\bullet 20H_2O$. The structure is a three-dimensional open framework encompassing a large solvent-accessible volume, as shown in **Figures 5.4a** and **b**. The structure is constructed from $\{Ni(tetrazolate)\}_\infty$ chains running parallel to the crystallographic *a* axis and linked through the phenyl tethers of the bdt ligands into the three-dimensional framework. Within the chains, each Ni(II) site adopts distorted octahedral $\{NiN_6\}$ coordination, bonding to nitrogen donors of six bdt ligands. The connectivity within the chain is provided by bridging through the N2 and N3 sites of the tetrazolate group of one terminus of the ligand (**Figure 5.4c**). A single chain is linked to four adjacent chains to provide the three-dimensional connectivity. This bonding pattern also generates the rectangular solvent-occupied cavities parallel to the *a* axis. The chain substructure exhibits a three-bladed paddlewheel motif between metal sites, similar to that previously reported for $[Fe(Htrz)_3](BF_4)_2$ and $[Mn_4(bdt)_3(NO_3)_2(def)_6]$ (Htrz = triazole, def = diethylformamide).[97,48] It is noteworthy that the structure possesses channels of approximate dimensions 12.0 x 9.0Å, corresponding to *ca*. 47% of the unit cell volume, that are occupied by H_2O molecules of crystallization.

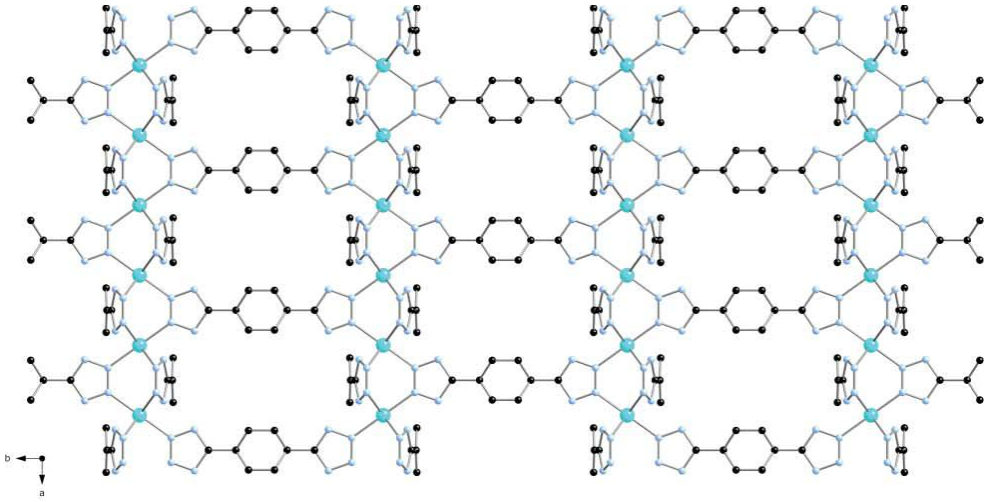

(a)

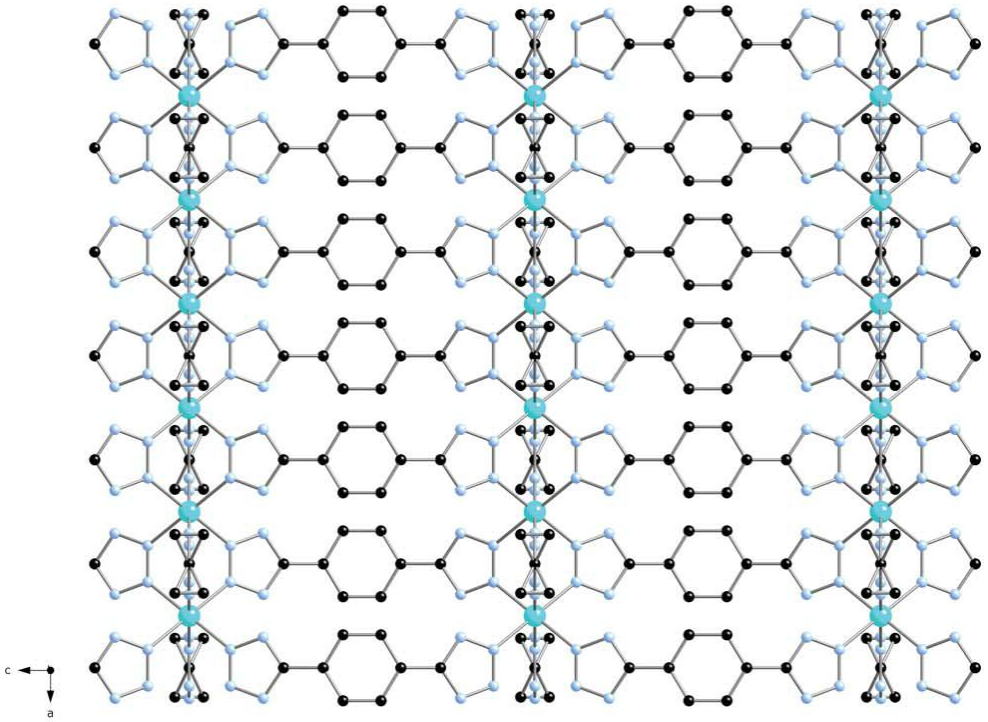

(b)

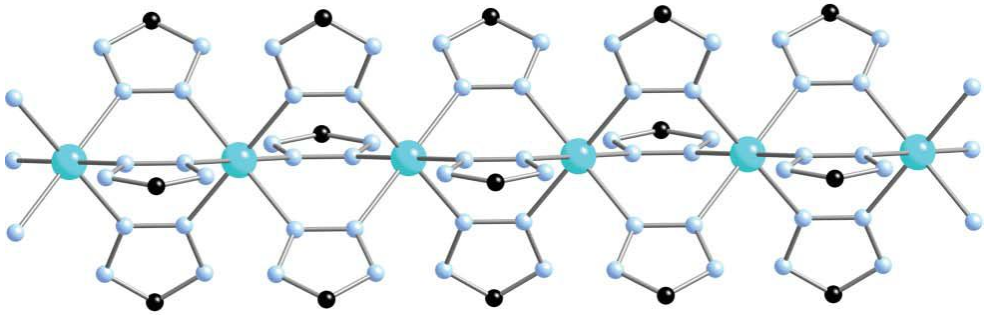

(c)

Figure 5.4: (a) A view of the structure of $[Ni_2(H_{0.67}bdt)_3]\bullet 10.5H_2O$ (**4**$\bullet 10.5H_2O$) in the *ab* plane. Color scheme: as above; nickel, aqua spheres. (b) The structure in the *ac* plane, showing the linking of Ni-tetrazolate chains through the phenyl tethers of the bdt ligands. (c) The $\{Ni_2(tetrazolate)_3\}_\infty$ chain substructure of **4**, showing the six-coordinate Ni(II) sites.

Charge compensation requires that 2/3 of the bdt ligands remain singly protonated in the Hbdt form at the N1 or N4 site. Although the crystallography did not reveal the protonation site due to symmetry and occupation considerations, the IR spectroscopy and the elemental analyses confirmed the absence of other potential charge compensating groups.

As shown in **Figure 5.5a and b**, the three-dimensional framework structure of [Zn(bdt)] (**5**) is constructed from $\{ZnN_4\}$ tetrahedra to generate a material devoid of solvent accessible space. Each Zn(II) site is liked to four adjacent sites through N1, N3-bridging tetrazolate groups (**Figure 5.5c**). However, if the connectivity is expanded to include the distal termini of each of the four bdt ligands associated with a given zinc site, it is apparent that each zinc is bridged to twelve neighboring zinc atoms in a complex connectivity pattern (**Figure 5.5d**). The absence of void space is a consequence of the relative orientations of the axes of the bdt ligands. Rather than radiating outward from a metal node like the spokes of a wheel, the ligands adopt parallel axial dispositions along the *c*-axis. As a result, the void volume is compressed and minimized, while the ligand packing efficiency appears to be maximized.

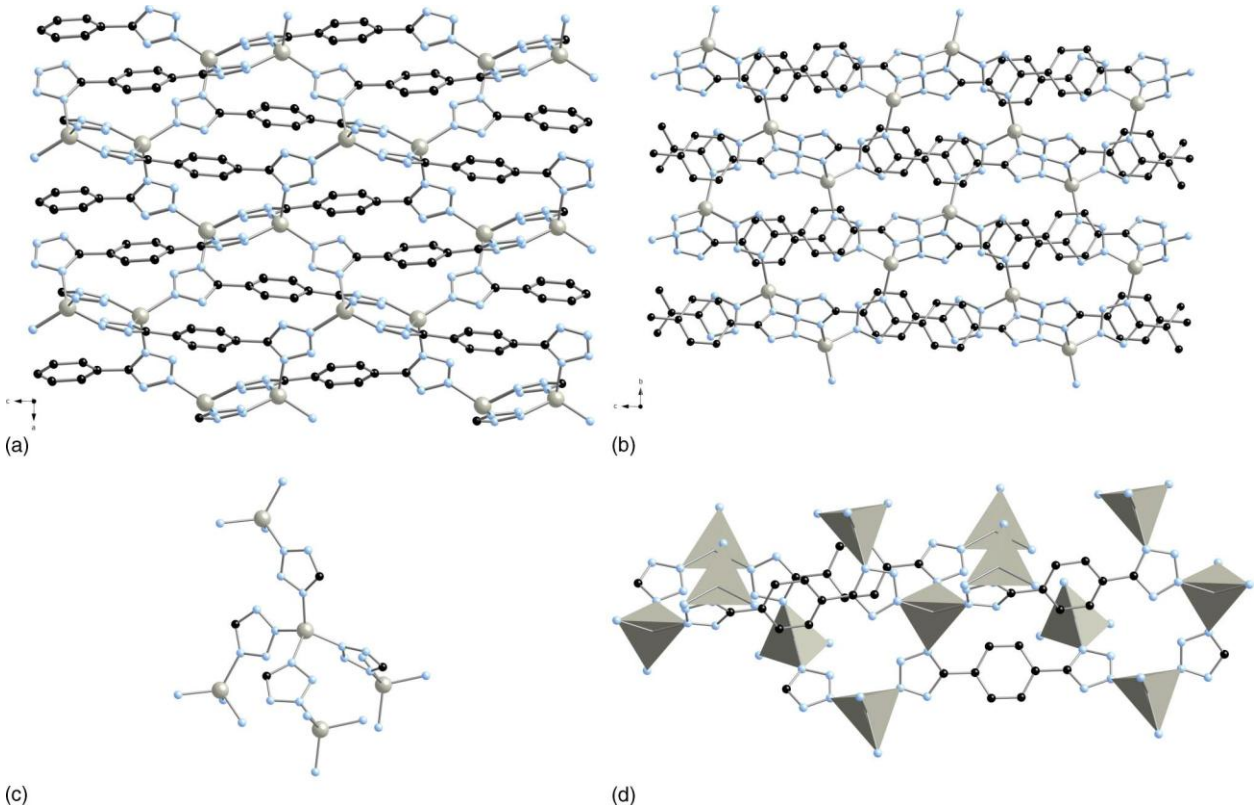

Figure 5.5: (a) Ball and stick representation of the structure of [Zn(bdt)] (**5**) in the *ac* plane; (b) the structure in the *bc* plane. Color scheme: as above; zinc, gray spheres; (c) the bridging of a zinc site to the adjacent four neighbors; (d) a central zinc bridged by the four bdt ligands to twelve zinc neighbors.

Figure 5.6 illustrates the three-dimensional structure of $(Me_2HN_2)_3[Cd_{12}Cl_3(btt)_8(DMF)_{12}]$•12DMF•5MeOH (**6**•12DMF•5MeOH). The structure may be described in terms of the cluster secondary building units $\{Cd_4Cl(tetrazolate)_8(H_2O)_4\}^{1-}$ linked through the phenyl tether of the tripodal btt ligand into a framework structure. As shown in **Figure 5.6b**, each btt ligand bridges six Cd sites two from each of three tetranuclear cadmium clusters, while adopting the N2, N3 coordination mode. In effect, each square planar $\{Cd_4Cl\}^{7+}$ subunit is linked through bdd^{3-} tethers to form the three-dimensional framework of **Figure 5.6a** which is reminiscent of the sodalite cage. The structure is isomorphous with the previously described $[Mn(DMF)_6]_3[(Mn_4Cl)_3(btt)_8(H_2O)_{12}]$•xSol (DMF = dimethylformamide).[84]

Within the tetranuclear cluster, the Cd sites are crystallographically equivalent. The coordination geometry is distorted octahedral and defined by four nitrogen donors from four tetrazolate groups in the equatorial plane and axial chloride and aqua ligands. The central Cl^- adopts a μ_4-coordination mode. Each cluster is associated with tetrazolate termini of eight btt groups, and, consequently, each cluster is linked to eight neighboring clusters by the btt tethers in providing the expansion into three-dimensions.

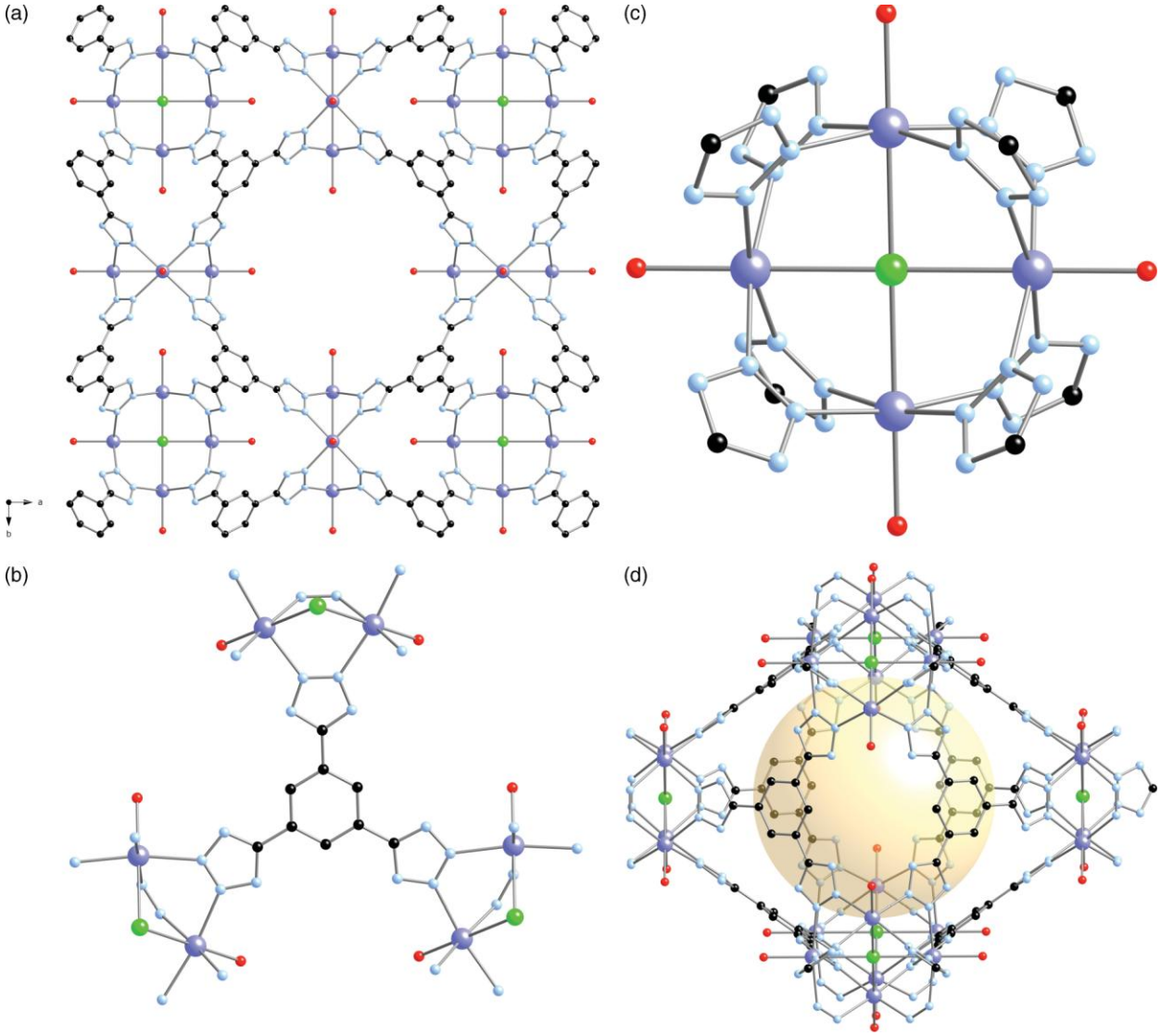

Figure 5.6: (a) Ball and stick representation of the three-dimensional structure of $(Me_2NH_2)_3[Cd_{12}Cl_3(btt)_8(DMF)_{12}]\bullet 12DMF\bullet 5MeOH$ (**6**•12DMF•5MeOH), viewed normal to the *ab* plane; (b) the linking of pairs of Cd sites from three adjacent clusters by the btt ligand; (c) the tetranuclear $\{Cd_4Cl(tetrazolate)_8(H_2O)_4\}^{1-}$ cluster secondary building unit of **6**. Color scheme: Cd, purple spheres; chlorine, green spheres; (d) the cavity centered at the cell origin with the pale orange sphere indicating the void volume.

As shown in **Figure 5.6a**, there are two distinct cavities generated by this connectivity pattern. The first is centered at the cell origin with boundaries defined by six linked clusters, as shown in **Figure 5.6b**. The second consists of channels running parallel to the *c*-axis along (1/2, 1/2, c). The previously reported manganese derivative exhibited $\{Mn(DMF)_6\}^{2+}$ cations as the charge-compensating groups. However, for the Cd(II) analogue **6**, the crystallography was inconsistent with the presence of a heavy atom in the void spaces, and the difference Fourier maps clearly revealed disordered $(Me_2NH_2)^+$ groups occupying the cavities located at the cell origins. The cations are formed in the thermal decomposition of dimethylformamide, which occurs readily under solvothermal conditions. The solvent molecules of crystallization are located in the larger channels.

5.3 Conclusions

Conventional hydrothermal methods were used to prepare a series of materials of the general type M(II)tetrazolate/anion where M(II) = Co, Ni, Zn and Cd. The diverse structural chemistry of these phases reflects several determinants, such as reaction conditions of stoichiometry, pH and temperature, the identity of the anionic component, the coordination preferences of the transition metal cation, the spacer type, and the variations in the tetrazolate coordination mode which can be monodentate, doubly- triply- or quadruply-bridging. In addition, the tetrazolate termini of the dipodal ligand types, H_2bdt and H_2dbdt, can engage in different ligation modes.

A recurrent theme of the structural chemistry of these materials is the presence of embedded transition metal/tetrazolate clusters as architectural motifs. Thus, compound **1** exhibits pentanuclear Co(II) building blocks. Similarly, compounds **2** and **3** manifest tetranuclear and trinuclear Co(II) clusters, respectively. A tetranuclear motif is also observed in the structure of the Cd(II) material **6**. While compound **4** is not constructed from cluster substructures, it does exhibit the common $\{M_2(\mu^2\text{-tetrazolate})_3\}_\infty$ chain as the building block.

As previously noted, variations in hydrothermal reaction conditions can dramatically influence product compositions and structures of organic/inorganic materials. This observation is illustrated by the phases **1-3** and $[Co_2(H_{0.67}bdt)_3]\bullet 20H_2O$ which are all prepared from $CoSO_4\bullet 7H_2O$ under different hydrothermal conditions. The structural variety associated with these phases has encouraged us to pursue the development of materials of the M(II)/tetrazolate/anion family, where the anion is NO_3^-, PO_4^{3-}, MoO_4^{2-} and VO_3^-.

5.4 Experimental Section

5.4.1 Materials and General Procedures

5,5'-(1,4-phenylene)bis(1H-tetrazole) (H_2bdt) was prepared using a literature method.[81] 5',5''-(1,1'-biphenyl)-4,4'-diylbis(1H-tetrazole) (H_2dbdt) was also prepared using literature precedents.[82] 5,5',5''-(1,3,5-phenylene)tris(1H-tetrazole) (H_3btt) was synthesized from 1,3,5-tricyanobenzene[83] using a modified version of the procedure described in ref. 84. All other chemicals were used as obtained without further purification. Cadmium sulfate, cobalt sulfate heptahydrate, nickel sulfate hexahydrate, zinc sulfate heptahydrate, and hydrofluoric acid (99.5%) were purchased from Alfa Aesar. All hydrothermal syntheses were carried out in 23 mL poly-(tetrafluoroethylene)-lined stainless steel containers under autogenous pressure. The reactants were stirred briefly, and the initial pH was measured before heating. Water was

distilled above 3.0MΩ in-housing using a Barnstead model 525 Biopure distilled water center. The initial and final pH of each reaction were measured using color pHast sticks. Infrared spectra were obtained on a Perkin-Elmer 1600 series FTIR spectrometer.

5.4.1.1 Synthesis of $[Co_5F_2(dbdt)_4(H_2O)_6]\bullet 2H_2O$ ($1\bullet 2H_2O$)

A solution of $CoSO_4\bullet 7H_2O$ (0.287 g, 1.02 mmol), 5′,5′′-(1,1′-biphenyl)-4,4′-diylbis (1H-tetrazole) (H_2dbdt) (0.076 g, 0.262 mmol), HF (100 μL, 0.06 mmol) and H_2O (10.00 g, 556 mmol) in the mole ratio 17.0:4.37:1.00:9270 was stirred for 15 min before heating at 200 ^oC for 96 hr. Light red needles of **1** were isolated in 10% yield based on cobalt. Anal Calcd. for $C_{56}H_{48}Co_5F_2N_{32}O_8$: C, 41.2; H, 2.97; N, 27.5. Found: C, 41.8; H, 3.12; N, 27.7.

5.4.1.2 Synthesis of $[Co_4(OH)_2(SO_4)(bdt)_2(H_2O)_4]$ (2)

The pH of a solution of $CoSO_4\bullet 7H_2O$ (0.226 g, 0.804 mmol), 5′,5′′-(1,1′-biphenyl)-4,4′ diylbis(1H-tetrazole) (H_2dbdt) (0.099 g, 0.463 mmol) and H_2O (10.00 g, 556 mmol) in the mole ratio 1.74:1.00:1200 was adjusted to 6.8 by addition of tetrabutylammonium hydroxide. After stirring for 30 min, the solution was heated at 200 ^oC for 42 h. Light brown crystals of **2** were isolated inn 30% yield based on cobalt. Anal Calcd. for $C_8H_9Co_2N_8O_5S_{0.5}$: C, 22.3; H, 218; N, 26.0. Found: C, 22.0; H, 2.10; N, 25.8.

5.4.1.3 Synthesis of $[Co_3(OH)(SO_4)(btt)(H_2O)_4]\bullet 3H_2O$ ($3\bullet 3H_2O$)

A solution of $CoSO_4\bullet 7H_2O$ (0.230 g, 0.818 mmol), 5,5′,5′′-(1,3,5-phenylene)tris(1H-tetrazole) (H_3btt) (0.079 g, 0.280 mmol) and H_2O (10.00 g, 556 mmol) in the mole ratio 2.92:1.00:1990 was heated for 48h at 200 ^oC. Red blocks of **3** were isolated in 60% yield based on cobalt. Anal. Calcd. for $C_9H_{18}Co_3N_{12}O_{12}S$: C: 15.5; H, 2.59; N, 24.2. Found: C, 15.1; H, 2.33; N, 24.3.

5.4.1.4 Synthesis of $[Ni_2(H_{0.67}bdt)_3]\bullet 10.5H_2O$ ($4\bullet 10.5H_2O$)

Tetrabutylammonium hydroxide (0.10 mL) was added to a solution of $NiSO_4\bullet 6H_2O$ (0.216 g, 0.822 mmol), H_2bdt (0.049 g, 0.229 mmol) and H_2O (10.00 g, 556 mmol) in the mole ratio 3.59:1.00:2430 to adjust the pH to 5.1. After heating at 150 ^oC for 48 h, light green crystals of **4** were isolated by mechanical means from an amorphous powder (yield 10% based on nickel). Anal. Calcd. for $C_{24}H_{35}Ni_2N_{24}O_{10.5}$: C, 30.5; H, 3.70; N, 35.6. Found: C, 30.3; H 3.74; N, 35.3.

5.4.1.5 Syntheses of [Zn(bdt)] (5)

The pH of a solution of $ZnSO_4\bullet 7H_2O$ (0.241 g, 0.838 mmol), H_2bdt (0.103 g, 0.481 mmol) and H_2O (10.00 g, 556 mmol) in the mole ratio 1.74:1.00:1160, was adjusted to 7.5 by addition of 0.20 mL of tetrabutylammonium hydroxide. After stirring for 30 min, the solution was heated for 48 h at 200 ^oC. Light tan crystals of **5** were isolated in 65% yield based on zinc. Anal. Calcd. for $C_8H_4N_8Zn$: C, 34.6; H 1.44; N, 40.6. Found: C, 34.5; H, 1.35; N, 40.4.

5.4.1.6 Synthesis of $(Me_2NH_2)_3[Cd_{12}Cl_3(btt)_8(DMF)_{12}]\bullet 12DMF\bullet 5MeOH$ ($6\bullet 12DMF\bullet 5MeOH$)

$CdSO_4$ (0.201 g, 0.964 mmol) was dissolved in 5 mL of methanol. The H_3btt ligand (0.051 g, 0.181 mmol) was dissolved in DMF (5 mL) with mild heating. Upon mixing the solutions, a fine precipitate appeared. Concentrated HCl was added until the solution was clear. After sitting at room temperature for 2 d, the solution was heated at 80 ^oC for 12 h. Upon cooling, colorless crystals of **6** were collected in 20% yield based on cadmium. Anal. Calcd. for $C_{155}H_{236}Cd_{12}Cl_3N_{123}O_{29}$: C, 32.4; H, 4.11; N, 30.0. Found: C, 32.8; H, 4.25; N, 29.8.

5.4.2 X-ray Crystallography

Structural measurements were performed on a Bruker-AXS SMART-CCD diffractometer at low temperature (90 K) using graphite-monochromated Mo Kα radiation ($\lambda_{Mo\ K\alpha}$= 0.71073Å).[85] The data were corrected for Lorentz and polarization effects and absorption using SADABS.[86,87] The structures were solved by direct methods. All non-hydrogen atoms were refined anisotropically. After all of the non-hydrogen atoms were located, the model was refined against F^2, initially using isotropic and later anisotropic thermal displacement parameters. Hydrogen atoms were introduced in calculated positions and refined isotropically. Neutral atom scattering coefficients and anomalous dispersion corrections were taken from the *International Tables*, Vol. C. All calculations were performed using SHELXTL crystallographic software packages.[88] The contributions of the diffused, disordered solvents to the structures of **4** and **6** were subtracted from the observed data by the SQUEEZE method implemented in PLATON.[89,90]

Crystallographic details have been summarized in **Table 5.1**. Atomic positional parameters, full tables of bond lengths and angles, and anisotropic temperature factors are available in the Supporting Material. Selected bond lengths and angles are given in **Table 5.2**.

Table 5.1: Summary of Crystallographic Data for the Structures of $[Co_5F_2(dbdt)_4(H_2O)_6]\bullet 2H_2O$ (**1**•$2H_2O$), $[Co_4(OH)_2(SO_4)(bdt)_2(H_2O)_4]$ (**2**), $[Co_3(SO)_4(OH)(btt)(H_2O)_4]\bullet 3H_2O$ (**3**•$3H_2O$), $[Ni_2(H_{0.67}bdt)_3]\bullet 10.5H_2O$ (**4**•$10.5H_2O$), [Zh(bdt)] (**5**) and $(Me_2NH_2)_3[Cd_{12}Cl_3(btt)_8(DMF)_{12}]\bullet 12DMF\bullet 5MeOH$ (**6**•12DMF•5MeOH).

	1	**2**	**3**	**4**	**5**	**6**
Empirical formula	$C_{56}H_{48}Co_5F_2N_{32}O_8$	$C_{16}H_{18}Co_4N_{16}O_{10}S$	$C_9H_{18}Co_3N_{12}O_{12}S$	$C_3H_{4.38}N_3Ni_{0.25}O_{1.31}$	$C_8H_4N_8Zn$	$C_{3.23}H_{4.92}Cd_{0.25}$ $Cl_{0.0625}N_{2.56}O_{0.60}$
FW	1629.91	862.22	695.20	118.15	277.56	119.62
Cryst system	Monoclinic	Monoclinic	Orthorhombic	Orthorhombic	Orthorhombic	cubic
Space group	$P2_1/c$	$C2/c$	*Pnma*	*Cmmm*	$P2_12_12_1$	$Pm\bar{3}m$
a/Å	14.014(1)	28.828(2)	7.3246(4)	7.5423(9)	8.0626(5)	19.3273(3)
b/Å	25.414(1)	6.4136(5)	13.2240(7)	26.318(3)	8.7291(6)	19.3273
c/Å	8.7031(4)	13.956(1)	22.767(1)	12.539(1)	12.9913(9)	19.3273
α (°)	90.0	90.0	90.0	90.0	90.0	90.0
β (°)	100.240(1)	91.547(2)	90.0	90.0	90.0	90.0
γ (°)	90.0	90.0	90.0	90.0	90.0	90.0
V/Å^3	3050.3(2)	2579.4(3)	2205.2(2)	2488.9(5)	914.3(1)	7219.6(2)
Z	2	4	4	16	4	48
D_c/g cm^{-3}	1.775	2.220	2.094	1.261	2.016	1.321
μ/mm^{-1}	1.424	2.699	2.413	0.824	2.674	0.962
T/K	98(2)	98(2)	98(2)	98(2)	98(2)	98(2)
λ/Å	0.71073	0.71073	0.71073	0.71073	0.71073	0.71073
Total Reflns	31767	13042	21880	12789	9704	69660
Unique Reflns	7420	3211	2793	1699	2281	1789
R_{int}	0.433	0.0318	0.0548	0.0672	0.0385	0.0610
R_1[a]	0.0427	0.0279	0.0431	0.0576	0.0293	0.0375
wR_2[b]	0.1073	0.0656	0.1051	0.1374	0.0699	0.0969
Flack					0.03(2)	

[a] $R_1 = \sum||F_o| - |F_c||/\Sigma|F_o|$; based on reflections with $I > 2\sigma(I)$. [b] w$R_2 = \{\sum[w(F_o^2 - F_c^2)^2]/\sum[w(F_o^2)^2]\}^{1/2}$, based on all data.

Table 5.2: Selected Bond Lengths and Angles of $[Co_5F_2(dbdt)_4(H_2O)_6]\bullet 2H_2O$ (**1**•$2H_2O$), $[Co_4(OH)_2(SO_4)(bdt)_2(H_2O)_4]$ (**2**), $[Co_3(SO)_4(OH)(btt)(H_2O)_4]\bullet 3H_2O$ (**3**•$3H_2O$), $[Ni_2(H_{0.67}bdt)_3]\bullet 10.5H_2O$ (**4**•$10.5H_2O$), [Zh(bdt)] (**5**) and $(Me_2NH_2)_3[Cd_{12}Cl_3(btt)_8(DMF)_{12}]\bullet 12DMF\bullet 5MeOH$ (**6**•12DMF•5MeOH).

Compound **1**		Compound **2**	
Co(1)–N(1)	2.056(2) (×2)	Co(1)–O(3)	2.0754(15)
Co(1)–F(1)	2.0640(17) (×2)	Co(1)–O(90)	2.0817(16)
Co(1)–N(5)	2.132(2) (×2)	Co(1)–N(1)	2.0944(19)
Co(2)–O(90)	2.073(2)	Co(1)–N(8)	2.1190(18)
Co(2)–N(7)	2.090(2)	Co(1)–N(5)	2.1610(19)
Co(2)–F(1)	2.107(2)	Co(1)–O(1)	2.2246(15)
Co(2)–N(9)	2.147(2)	Co(2)–O(3)	2.0419(15)
Co(2)–N(6)	2.151(2)	Co(2)–O(3)	2.0679(15)
Co(2)–N(4)	2.210(2)	Co(2)–O(91)	2.0717(16)
Co(3)–O(92)	2.050(2)	Co(2)–N(6)	2.1297(18)
Co(3)–F(1)	2.082(2)	Co(2)–N(7)	2.1354(18)
Co(3)–O(91)	2.133(2)	Co(2)–O(1)	2.1889(15)
Co(3)–N(14)	2.162(3)		
Co(3)–N(2)	2.174(2)	S(1)–O(1)–Co(2)	130.23(9)
Co(3)–N(12)	2.176(2)	S(1)–O(1)–Co(1)	134.45(9)
Co(2)–O(1)–Co(1)	88.82(5)		
Co(1)–F(1)–Co(3)	113.48(8)	Co(2)–O(3)–Co(2)	95.10(6)
Co(1)–F(1)–Co(2)	104.87(7)	Co(2)–O(3)–Co(1)	120.63(7)
Co(3)–F(1)–Co(2)	122.93(8)	Co(2)–O(3)–Co(1)	96.40(6)

Compound **3**		Compound **4**	
Co(1)–O(2)	2.043(3)	Ni(1)–N(1)	2.096(3) (×2)
Co(1)–O(2)	2.066(3)	Ni(1)–N(3)	2.130(2) (×4)
Co(1)–N(1)	2.074(3)		
Co(1)–N(1)	2.074(3)	Compound **5**	
Co(1)–O(1)	2.078(3)		
Co(1)–O(3)	2.354(3)	Zn(1)–N(5)	1.991(2)
Co(2)–O(91)	2.083(2)	Zn(1)–N(4)	1.993(2)
Co(2)–O(1)	2.087(2)	Zn(1)–N(1)	2.020(2)
Co(2)–N(2)	2.088(3)	Zn(1)–N(8)	2.030(2)
Co(2)–O(90)	2.089(2)		
Co(2)–N(6)#	2.110(2)	Compound **6**	
Co(2)–O(4)	2.157(2)		
Co(1)–O(1)–Co(2)	112.35(8)	Cd(1)–O(1)	2.284(6)
Co(1)–O(1)–Co(2)	112.35(8)	Cd(1)–N(1)	2.315(2)
Co(2)–O(1)–Co(2)	114.5(1)	Cd(1)–N(1)	2.315(2)
S(1)–O(2)–Co(1)	130.5(2)	Cd(1)–N(1)	2.315(2)
S(1)–O(2)–Co(1)	102.1(2)	Cd(1)–N(1)	2.315(2)
Co(1)–O(2)–Co(1)	127.4(1)	Cd(1)–Cl(1)	2.8018(3)
S(1)–O(3)–Co(1)	91.5(2)		
S(1)–O(4)–Co(2)	123.9(1)	Cd(1)–Cl(1)–Cd(1)	90.0
N(2)–N(1)–N(3)	109.8(2)	Cd(1)#4–Cl(1)–Cd(1)	180.0

5.5 Supplementary Materials

Additional material available from the Cambridge Crystallographic Data Centre comprises the final atomic coordinates for all atoms, thermal parameters, and a complete listing of bond distances and angles, for compounds **1-6**, respectively. Copies of this information may be obtained free of charge online at http://pubs.rsc.org/en/Content/ArticleLanding/2011/DT/c1dt11590a.

5.6 Acknowledgments

This work was funded by a grant from the National Science Foundation (CHE-0907787).

5.7 References

1. Chen, B.; Ockwig, N.W.; Millward, A.R.; Contreras, D.S.; and Yaghi, O.M., *Angew. Chem., Int. Ed. Engl.* **2005**, *44*, 4745.
2. Rowsell, J.L.C.; and Yaghi, O.M., *Angew. Chem., Int. Ed. Engl.* **2005**, *44*, 4670.
3. Bradshaw, D.; Claridge, J.B.; Cussen, E.J.; Prior, T.J.; and Rosseinsky, M.J., *Chem. Res.* **2005**, *38*, 273.
4. Rosseinsky, M.J., Microporous and Mesoporous Materials **2004**, *73*, 15.
5. Cingolani, A.; Galli, S.; Masciocchi, N.; Pandolfo, L.; Pettinari, C.; and Sironi, A., *J. Am. Chem. Soc.* **2005**, *127*, 6144.
6. Ohmori, O.; Kawano, M.; and Fujita, M., *Angew. Chem., Int. Ed.* **2005**, *44*, 1962.
7. Lee, E.Y.; Jang, S.Y.; and Suh, M.P., *J. Am. Chem. Soc.* **2005**, *127*, 6374.
8. Noro, S.-I.; Kitagawa, S.; Kondo, M.; and Seki, K., *Angew. Chem., Int. Ed.* **2000**, *39*, 2081.
9. Wang, Z.; Zhang, B.; Kurmoo, M.; Green, M.A.; Fujiwara, H.; Otsuka, T.; and Kobayashi, H., *Inorg. Chem.* **2005**, *44*, 1230.
10. Kim, H.; and Suh, M.P., *Inorg. Chem.* **2005**, *44*, 810.
11. Sudik, A.C.; Millward, A.R.; Ockwig, N.W.; Cote, A.P.; Kim, J.; and Yaghi, O.M., *J. Am. Chem. Soc.* **2005**, *127*, 7110.
12. Kitaura; R.; Kitagawa, S.; Kubtoa, Y.; Kobayashi, T.C.; Kindo, K.; Mita, Y.; Matsuo, A.; Kobayashi, M.; Chang, H.-C.; Ozawa, T.C.; Suzuki, M.; Sakata, M.; and Takata, M., *Science* **2002**, *298*, 2358.
13. Bradshaw, D.; Prior, T.J.; Cussen, E.J.; Claridge, J.B.; and Rosseinsky, M.J., *J. Am. Chem. Soc.* **2004**, *126*, 6106.

14. Kepert, C.J.; Prior, T.J.; and Rosseinsky, M.J., *J. Am. Chem. Soc.* **2000**, *122*, 5158.

15. Halder, G.J.; Kepert, C.J.; Moubaraki, B.; Murray, K.S.; and Cashion, J.D., *Science* **2002**, *298*, 1762.

16. Evans, O.R.; Ngo, H.L.; and Lin, W., *J. Am. Chem. Soc.* **2001**, *123*, 10395.

17. Sanchez, C.; Lebeau, B.; Chaput, F.; and Boilet, J.P., *Advanced Materials* **2003**, *15*, 1969.

18. Evans, O.R.; and Lin, W., *Chem. Mater.* **2001**, *13*, 3009.

19. Jannasch, P., *Curr. Opin. Coll. Inter. Sci.* **2003**, *8*, 96.

20. Javaid, A.; Hughey, M.P.; Varutbangkul, V.; and Ford, D.M., *J. Membrane Sci.* **2001**, *187*, 141.

21. Honma, I.; Nomura, S.; and Nakajima, H., *J. Membrane Sci.* **2001**, *185*, 83.

22. Rowsell, J.L.C.; Millward, A.R.; Park, K.S.; and Yaghi, O.M., *J. Am. Chem. Soc.* **2004**, *126*, 5666.

23. Janiak, C., *Dalton Trans.* **2003**, 2781 and references therein.

24. Mitzi, D.B., *Dalton Trans.* **2001**, 1.

25. S. Kitagawa, S. Noro, Comprehensive Coordination Chemistry II **2004** ,*7*, 231.

26. Yaghi, O.M.; O'Keeffe, M.; Ockwig, N.W.; Chae, H.K.; Eddaoudi, M.; and Kim, J., *Nature* **2003**, *423*, 705.

27. James, S.L.; *Chem. Soc. Rev.* **2003**, *32*, 276.

28. Rao, C.N.R.; Natarajan, S.; and Vaidhyanathan, R., *Angew. Chem., Int. Ed.* **2005**, *43*, 1466.

29. Kitagawa, S.; Kitaura, R.; and Noro, S.-I., *Angew. Chem., Int. Ed.* **2004**, *43*, 2334.

30. Papaefstathiou, G.S.; and MacGillivray, L.R., *Coord. Chem. Rev.* **2003**, *246*, 169.

31. Eddaoudi, M.; Moler, D.B.; Li, H.; Chen, B.; Reineke, T.M.; O'Keeffe, M.; Yaghi, O.M., *Acct. Chem. Res.* **2001**, *34*, 319.

32. Finn, R.C.; Haushalter, R.C.; and Zubieta, J., *Prog. Inorg. Chem.* **2003**, *51*, 421.

33. Vioux, A.; LeBideau, J.; Mutin, P.H.; and Leclercq, D., *Top. Curr. Chem.* **2004**, *232*, 145.

34. Clearfield, A., Current Opinion in Solid State & Materials Science **2003**, *6*, 495.

35. Clearfield, A., *Prog. Inorg. Chem.* **1998**, *47*, 371.

36. Alberti, G., in *Comprehensive Supramolecular Chemistry* Atwood, J.L.; Davies, J.E.D.; MacNicol, D.D.; and Vögtle, F., eds.: Pergamon Press, New York: **1996**, vol. 7, Alberti, G.; and Bein, T., eds. 151.

37. Férey, G., *Chem. Mat.* **2001**, *13*, 3084.

38. Farrusseng, D.; Aguado, S.; and Pinel, C., *Angew. Chem. Int. Ed*., **2009**, *48*, 7502-7513.

39. Zheng, B.; Bai, J.; Duan, J.; Wojtas, L.; Zaworotko, M.J., *J. Am. Chem. Soc*., **2011**, *133*, 748-751.

40. Sumida, K.; Brown, C.R.; Herm, Z.R.; Chavan, S.; Bordiga, S.; and Long, J.R., *Chem. Comm*., **2011**, *47*, 1157-1159.

41. Tranchemontagne, D.J.; Ni, Z.; O'Keefe, M.; and Yaghi, O.M., *Angew. Chem. Int. Ed.*, **2008**, *47*, 5136-5147.

42. Li, Q.; Sue, C.-H.; Basu, S.; Shveyd, A.K.; Zhang, W.; Barin, G.; Fang, L.; Sarjeant, A.A.; Stoddart, J.F.; and Yaghi, O.M., *Angew. Chem. Int. Ed*., **2010**, *49*, 6751-6755.

43. Ferey, G.; Serre, C.; Devic, T.; Maurin, G.; Jobic, H.; Llewellyn, P.L.; De Weireld, G.; Vimont, A.; Daturi, M.; and Chang, J.-S., *Chem. Soc. Rev*., **2011**, *40*, 550-562.

44. Hijikata, Y.; Horike, S.; Sugimoto, M.; Sato, H.; Matsuda, R.; and Kitagawa, S., *Chem. Eur. J.*, **2011**, *17*, 5138-5144.

45. Clearfield, A., *Dalton Trans*., **2008**, 6089-6102.

46. Moulton, B.; and Zaworotko, M.J., Curr. Opinion Solid State & Mater. Sci. **2002**, *6*, 117.

47. Wang, C.; and Lin, W., *J. Am. Chem. Soc*., **2011**, *133*, 4232-4235.

48. Choi, H.J.; Dincă, M.; and Long, J.R., *J. Am. Chem. Soc.* **2008**, *130*, 7848.

49. Eddaoudi, M.; and Eubank, J.F., *Org. Nanostruct.* **2008**, 251.

50. Beckmann, U.; and Brooker, S., *Coord. Chem. Rev.* **2003**, *245*, 17.

51. Haasnoot, J.G., *Coord. Chem. Rev.* **2000**, *200*, 131.

52. Hellyer, R.M.; Larsen, D.S.; Brooker, S., *Eur. J. Inorg. Chem.* **2009**, 1162.

53. Zhang, J.-P.; and Chen, X.-M., *Chem. Commun.* **2006**, 1689.

54. Steel, P.J., *Coord. Chem. Rev.* **1990**, *106*, 227.

55. Potts, K.T.; *Chem. Rev.* **1961**, *61*, 87.

56. Dawe, L.N.; and Thompson, L.K., *Dalton Trans.* **2008**, 3610.

57. Zhang, J.-P.; Lin, Y.-Y.; Huang, X.-C.; and Chen, X.-M., *J. Am. Chem. Soc.* **2005**, *127*, 5495.

58. Zhang, J.-P.; Zheng, S.-L.; Huang, X.-C.; and Chen, X.-M., *Angew. Chem. Int. Ed. Engl.* **2004**, *43*, 206.

59. Ferrer, S.; Lloret, F.; Bertomeu, I.; Alzuet, G.; Borras, J.; Garcia-Granda, S.; Liu-González, M.; and Haasnoot, J.G., *Inorg. Chem.* **2002**, *41*, 5821.

60. Zhou, J.-H.; Cheng, R.-M.; Song, Y.; Li, Y.-Z.; Yu, Z.; Chen, X.-T.; Xue, Z.-L.; and You, X.-Z., *Inorg. Chem.* **2005**, 44, 8011 and references therein.

61. Du, M.; Jiang, X.-J.; and Zhao, X.-J., *Chem. Comm.* **2005**, 5521.

62. Zhang, J.-P.; Lin, Y.-Y.; Zhang, W.-X.; and Chen, X.-M., *J. Am. Chem. Soc.* **2005**, *127*, 14162.

63. Zhang, X.-M.; Zhao, Y.-F.; Wu, H.-S.; Batten, S.R.; and Ng, S.W., *Dalton Trans.*, **2006**, 3170-3178.

64. Zhang, D.-C.; Lu, W.-G.; Jiang, L.; Feng, X.-L.; and Lu, T.-B., *Cryst. Growth Des*., **2010**, *10*, 739-746.

65. Li, Z.; Li, M.; Zhan, S.-Z.; Huang, X.-C.; Ng, S.W.; and Li, D., *Cryst. Eng. Comm.*, **2008**, *10*, 978-980.

66. Demessence, A.; D'Alessandro, D.M.; Foo, M.L.; and Long, J.R., *J. Am. Chem. Soc.*, **2009**, *131*, 8784-8785.

67. Murray, L.J.; Dinca, M.; and Long, J.R., *Chem. Soc. Rev.*, **2009**, *38*, 1294-1314.

68. Dinca, M.; and Long, J.R., *Angew. Chem. Int. Ed*., **2008**, *47*, 6766-6779.

69. Choi, H.J.; Dinca, M.; and Long, J.R., *J. Am. Chem. Soc.*, **2008**, *130*, 7848-7850.

70. Banerjee, R.; Furukawa, H.; Britt, D.; Knobler, C.; O'Keeffe, M.; and Yaghi, O.M., *J. Am. Chem. Soc.*, **2009**, *131*, 3875-3877.

71. Ouellette, W.; Yu, M.H.; O'Connor, C.J.; Hagrman, D.; and Zubieta, J., *Angew. Chem. Int. Ed.* **2006**, *45*, 3497.

72. Ouellette, W.; Prosvirin, A.V.; Valeich, J.; Dunbar, K.R.; and Zubieta, J., *Inorg. Chem.* **2007**, *46*, 9067.

73. Ouellette, W.; Galán-Mascarós, J.R.; Dunbar, K.R.; and Zubieta, J., *Inorg. Chem.* **2006**, *45*, 1909.

74. Ouellette, W.; Prosvirin, A.V.; Chieffo, V.; Dunbar, K.R.; Hudson, B.; and Zubieta, J., *Inorg. Chem.* **2006**, *45*, 9346.

75. Chesnut, D.J.; Kusnetzow, A.; Birge, R.; and Zubieta, J., *Inorg. Chem.* **1999**, *38*, 5484.

76. Ouellette, W.; Hudson, B.S.; and Zubieta, J., *Inorg. Chem.* **2007**, *46*, 4887.

77. Ouellette, W.; Liu, H.; O'Connor, C.J.; and Zubieta, J., *Inorg. Chem.* **2009**, *48*, 4655.

78. Ouellette, W.; and Zubieta, J., *Chem. Commun.* **2009**, 4533.

79. Ouellette, W.; Prosvirin, A.V.; Whitenack, K.; Dunbar, K.R.; and Zubieta, J., *Angew. Chem. Int. Ed.*, **2009**, *48*, 2140-2143.

80. Ouellette, W.; Jones, S.; and Zubieta, J., *Cryst. Eng. Comm.*, **2011**, DOI: 10.1039/c0ce0091a.

81. Maspero, A.; Galli, S.; Masciocchi, N.; and Palmisano, G., *Chem. Lett.*, **2008**, *37*, 956-957.

82. Sumida, K.; Foo, M.L.; Horike, S.; and Long, J.R., *Eur. J. Inorg. Chem*., **2010**, 3739-3744.

83. Hill, M.; Mahon, M.F.; and Molloy, K.C., *J. Chem. Soc., Dalton Trans.* **1996**, 1857-1865.

84. Dinca, M.; Dailly, A.; Liu, Y.; Brown, C.R.; Neumann, D.; Long, J.R., *J. Am. Chem. Soc.*, **2006**, *128*, 16876.

85. *SMART, Data Collection Software*, version 5.630; Bruker-AXS Inc.: Madison, WI, **1997-2002**.

86. *SAINT Plus, Date Reduction Software*, version 6.45A; Bruker-AXS Inc.: Madison, WI, **1997-2002**.

87. Sheldrick, G.M., *SADABS*; University of Göttingen: Göttingen, Germany, **1996**.

88. *SHELXTL PC*, version 6.12; Bruker-AXS Inc.: Madison, WI **2002**.

89. Spek, A.L., PLATON, A Multipurpose Crystallographic Tool, Utrecht University, Utrecht, The Netherlands, **2008**.

90. Spek, A.L., *J. Appl. Crystalllogr*., **2003**, *36*, 7-13.

91. Stein, A.; Keller, S.W.; and Mallouk, T.E., *Science* **1993**, *259*, 1558.

92. Gopalakrishnan, J., *Chem. Mater.* **1995**, *7*, 1265.

93. Weller, M.; and Dann, S.E., Current Opinions Solid State Mater. Sci. **1998**, *3*, 137.

94. Gopalakrishnan, J.; Bhuvanesh, N.S.P.; and Rangan, K.K., *Current Opinions Solid State Mater. Sci.* **1996**, *1*, 285.

95. Zubieta, J., Solid state methods, hydrothermal in *Comprehensive Coordination Chemistry II* **2003**, *1*, 697.

96. Maggard, P.A.; and Boyle, P.D., *Inorg. Chem.* **2003**, *42*, 4250.

97. Verelst, M.; Sommier, L.; Lecante, P.; Mosset, A.; and Kahn, O., *Chem. Mater.* **1998**, *10*, 980.

Chapter 6: Hydrothermal Synthesis and Structures of Materials of the M(II)/Tetrazole/Sulfate Family (M(II) = Co, Ni, Cu; tetrazole = 2-, 3-and 4-Pyridyltetrazole and Pyrazinetetrazole)

6.1 Introduction

Solid state coordination chemistry focuses on the rational design of materials for technological applications based on molecular scale composites of inorganic and organic components.[1] Such materials exhibit a vast compositional range and significant structural complexity that allow applications in fields ranging from heavy construction to molecular electronics.[2-23]

To further emphasize the pioneer work referenced in Chapter 1, organic-inorganic hybrid compounds of this type include materials constructed from metal or metal cluster nodes linked through polyfunctional carboxylates, polypyridyl linkers and organophosphonate ligands.[24-39] Such materials have been extensively explored by Clearfield,[40] Ferey,[41] Kitagawa,[42,43] Yaghi[44] and others.[45-48]

Another class of bridging ligands that have been exploited in the construction of complex organic-inorganic architectures are the polyazaheterocyclic compounds, of which 1,2,4-triazole and tetrazole are characteristic (**Scheme 1**). These ligands exhibit not only the ability to bridge multiple metal sites to afford polynuclear and extended structures, but also superexchange properties that provide unusual magnetic behaviors and a facility of modification to allow introduction of additional functionality.[49-61]

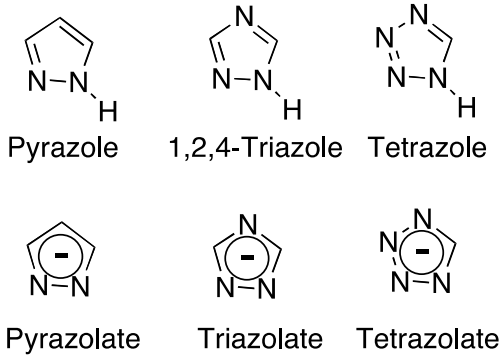

Scheme 1

Our investigations have focused on the structural chemistry of metal-triazolate and metal-tetrazolate frameworks prepared by hydrothermal methods.[62-75] In the course of these studies, we noted that the modified polyazaheterocyclic ligands 4-(4-pyridyl)pyrazolate and 4-pyridyltetrazolate in the N2,N3 bridging mode function as expanded analogues of 1,2,4-triazolate (**Scheme 2**). This observation motivated us to examine the structural consequences of modification of the pyridyl nitrogen donor location and the substitution of a pyrazine group for the pyridyl substituent (**Scheme 3**).

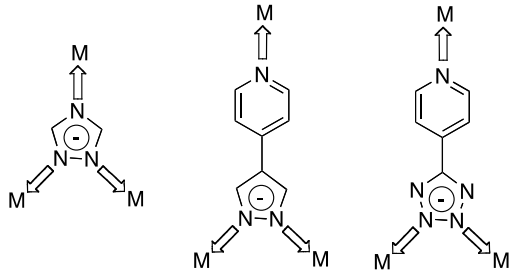

Scheme 2

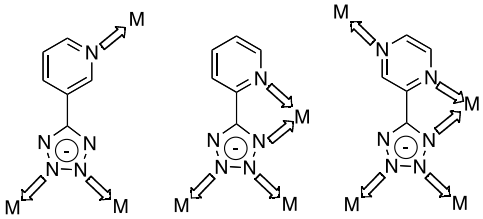

Scheme 3

We have also noted that introduction of coordinating anions in expanding from the metal/polyazaheterocyclic ligand system to the metal/polyazaheterocyclic ligand/anion system dramatically influences the structures and properties of the composite materials. The structural influences were most pronounced when the anion is sulfate. Encouraged by these results, we have investigated the hydrothermal and structural chemistry of cobalt (II), nickel (II), and copper(II) sulfate with 2-, 3-, and 4-pyridyltetrazole and pyrazinetetrazole. Herein we report the structures of several Co(II), Ni(II), and Cu(II) composite materials including:

$[Co(prztet)_2(H_2O)_2]\cdot 0.5H_2O$ (**1**•$0.5H_2O$), $[Co_2(4\text{-pyrtet})(SO_4)(OH)(H_2O)]\bullet 1.5H_2O$ (**2**•$1.5H_2O$), $[Co_4(prztet)_6(SO_4)(H_2O)_2]$ (**3**), $[Co_3F_2(SO_4)(3\text{-pyrtet})_2(H_2O)_4]$ (**4**), $[Ni_3F_2(SO_4)(3\text{-pyrtet})_2(H_2O)_4]$ (**5**), $[Ni_5(3\text{-pyrtet})_4(SO_4)_2(OH)_2\ (H_2O)_2]\bullet 0.5H_2O$ (**6**•$0.5H_2O$), $[Cu_3(OH)(H_2O)_3(3\text{-pyrHtet-}O)_3(SO_4)]$ (**7**), $[Cu_3(OH)_2(H_2O)_3(3\text{-pyrtet})_2(SO_4)]$ (**8**), $(Me_2NH_2)[Cu(2\text{-pyrtet})(SO_4)]$ (**9**) and $[Cu_4(pyrztet)_6(H_2O)_2(SO_4)]$ (**10**) (pyrHtet = pyridyltetrazole; pyrzHtet = pyrazinetetrazole).

6.2 Results and Discussion

6.2.1 Syntheses

Hydrothermal synthesis is an effective method for the preparation of x-ray quality single crystals of coordination polymers. In the temperature domain of conventional hydrothermal methods, the reactants are solubilized while retaining their structural features in the product phases.[83-87] Hydrothermal reactions, typically carried out in the temperature range 120-260 ^oC under autogenous pressure, exploit the self assembly of the product from soluble precursors. The reduced viscosity of water under these conditions enhances diffusion processes so that solvent extraction of solids and crystal growth from solution are favored. Since problems associated with different solubilities of organic and inorganic starting materials are minimized, a variety of precursors may be introduced, as well as a number of organic and/or inorganic structure-directing or charge-balancing reagents from which those of appropriate size, shape and charge may be selected for efficient crystal packing during the crystallization process. Under such nonequilibrium crystallization conditions, metastable kinetic phases rather than the thermodynamic phase may also be isolated.

While hydrothermal reactions generally retain the structural integrity of the ligand components, *in situ* modification of ligands is not uncommon.[88] In the case of compound **7**, the 3-pyridyltetrazole ligand has been hydroxylated at the α-carbon of the pyridine ring to form a

covalent hydrate, presumably in a Gillard type reaction.[89] Similarly, the synthesis of compound **9** produces the $Me_2NH_2^+$ cation from the decomposition of the tetrazole fragment of ligands. Addition of $Me_2NH_2^+$ to the reaction mixture significantly increases the product yield.

6.2.2 Structural Studies

The molecular structure of $[Co(prztet)_2(H_2O)_2]\cdot 0.5H_2O$ (**1**·$0.5H_2O$) is shown in **Figure 6.1**. The distorted octahedral $\{CoN_4O_2\}$ geometry is defined by the pyrazine and N1 tetrazolate nitrogen donors of two chelating pyrazinetetrazolate ligands in the equatorial plane, with the axial positions occupied by the aqua ligands. Hydrogen bonding between the aqua ligands and the N4-tetrazolate nitrogen atoms of neighboring molecules with O···N distances of 2.803 Å stabilizes the structure.

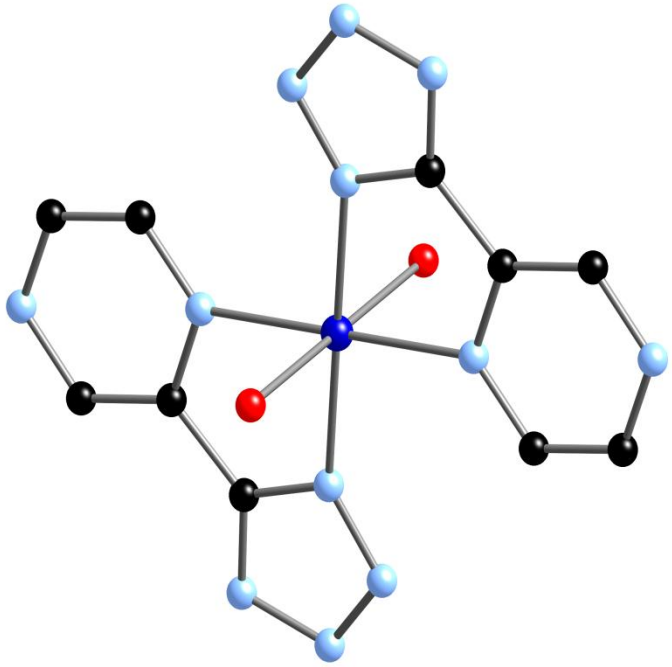

Figure 6.1: Ball and stick representation of the structure of molecular $[Co(prztet)_2(H_2O)_2]\cdot 0.5H_2O$ (**1**$\cdot 0.5H_2O$). Color scheme: cobalt, blue spheres; sulfur, yellow spheres; oxygen, red spheres; nitrogen, light blue spheres; carbon, black spheres. The color scheme is used throughout.

As shown in **Figure 6.2**, the structure of $[Co_2(4\text{-pyrtet})(SO_4)(OH)(H_2O)]\bullet 1.5H_2O$ (**2**$\bullet 1.5H_2O$) is two-dimensional. The network is constructed from $\{Co_2(tetrazolate)(SO_4)(OH)H_2O)\}_n$ chains linked through the pyridyl substituents of the 4-pyridyltetrazolate ligands. The chain exhibits the common $\{M_3(azole)_3(OH)\}^{2+}$ motif as a secondary building unit. These Co(II) triads share two Co sites with neighboring triads to generate the chain of hydroxy bridged cobalt centers. Each triad is capped by a sulfato group which shares a vertex with each of the three cobalt sites of the triad. The fourth oxygen is pendant and projects into the interlamellar domain.

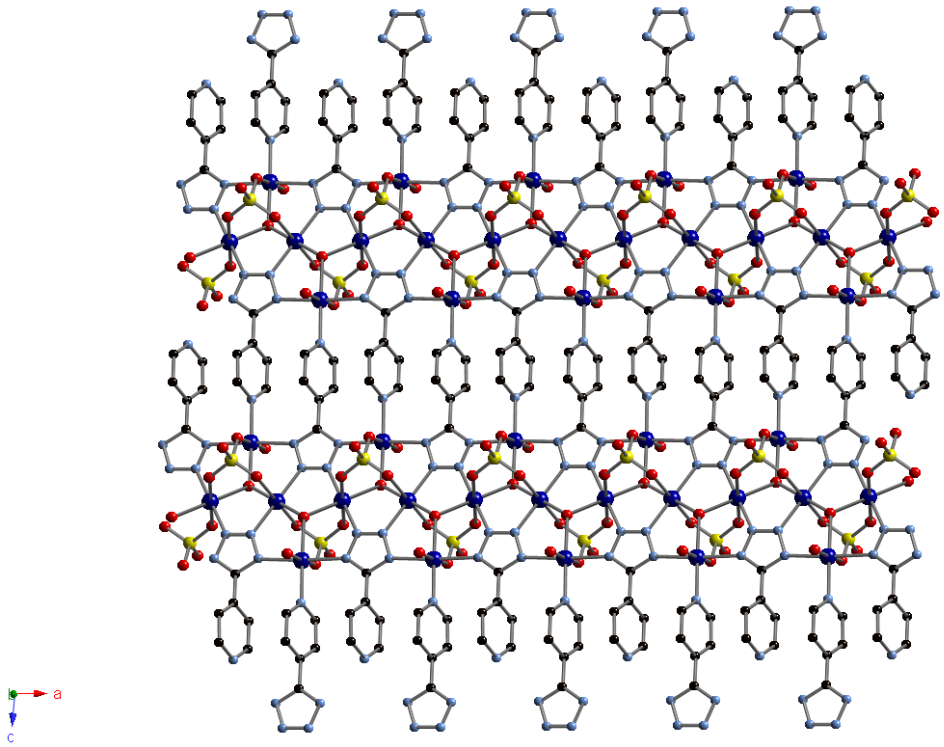

Figure 6.2: Ball and stick representation of the two-dimensional structure of $[Co_2(4\text{-pyrtet})(SO_4)(OH)(H_2O)]\bullet 1.5H_2O$ (**2**$\bullet 1.5H_2O$) in the ac plane.

The tetrazolate subunits adopt the tetradentate mode, bridging four cobalt sites from three adjacent triads. There are two distinct cobalt sites. The first forms the central backbone of the ribbon in an infinite zig-zag $\{Co\text{-}O(H)\}_n$ chain and exhibits $\{CoO_4N_2\}$ coordination through bonding to two tetrazolate nitrogen donors, two *trans* μ_3-hydroxy groups, and two sulfate oxygens. The peripheral cobalt sites exhibit $\{CoN_3O_3\}$ coordination, bonding to two azolate nitrogen atoms, one pyridyl nitrogen, one sulfato oxygen donor, a hydroxy group and a terminal aqua ligand that projects into the interlamellar domain.

The structure of the $\{Co_2(tetrazolate)(SO_4)(OH)(H_2O\}_n$ chain of **2** is similar to that of the chain substructure of the previously reported $[Co_2(SO_4)(OH)(tryphCO_2H)]$ with the exceptions of substitutions of a pyridyl nitrogen and an aqua ligand of the peripheral cobalt sites of **2** by a carboxylate oxygen from the carboxyphenyl-tetrazolate ligand and a sulfato oxygen, respectively, in the latter. The sulfato group of the latter compound bridges adjacent $\{Co_2(SO_4)(OH)(trzphCO_2H)\}_n$ layers to generate overall three-dimensional connectivity. The structures of these $[Co_2(azolate)(SO_4)(OH)(H_2O)_x]$ materials (azolate = 4-pyrtet, x = 1; azolate = $trzphCO_2H$, x = 0) suggest that the $\{M_3(azolate)_3(OH)\}_n$ ribbon is a recurrent theme in the structural chemistry of the transition metal-azolate phases. The water molecules of crystallization occupy the interlamellar region and engage in hydrogen bonding to the sulfato oxygen and the aqua ligand that project into this domain.

The pyrazine-tetrazolate material $[Co_4(prztet)_6(SO_4)(H_2O)_2]$ (**3**), shown in **Figure 6.3**, is three-dimensional and constructed from $\{Co_4(prztet)_6(H_2O)\}^{2+}$ networks linked through sulfato groups. The cobalt-azolate layers run parallel to the crystallographic *ab* plane and are constructed from tetranuclear $\{Co_4(tetrazolate)_6\}^{2+}$ secondary building units. Pairs of Co(II) sites within these tetrads are bridged by two N1,N2 bound tetrazolate groups, with the exterior

{Co_2N_4} planes of the tetrad at right angle to the {Co_2N_4} interior plane. The N2 nitrogen atoms of the pyrazine substituents chelate to the cobalt sites of a given tetrad, while the N5-pyrazine nitrogen donors bridge to adjacent tetrads to provide the two-dimensional connectivity for the cobalt-azolate substructure. Each tetrad is linked to six adjacent SBUs in the layer. These layers are in turn connected through sulfato groups along the *c*-direction. Each sulfato ligand is bidentate, thus projecting two pendant oxygen atoms. The sulfate groups serve to buttress the cobalt-pyrazine-tetrazolate layers and with the aqua ligands occupy the interlamellar region of the structure.

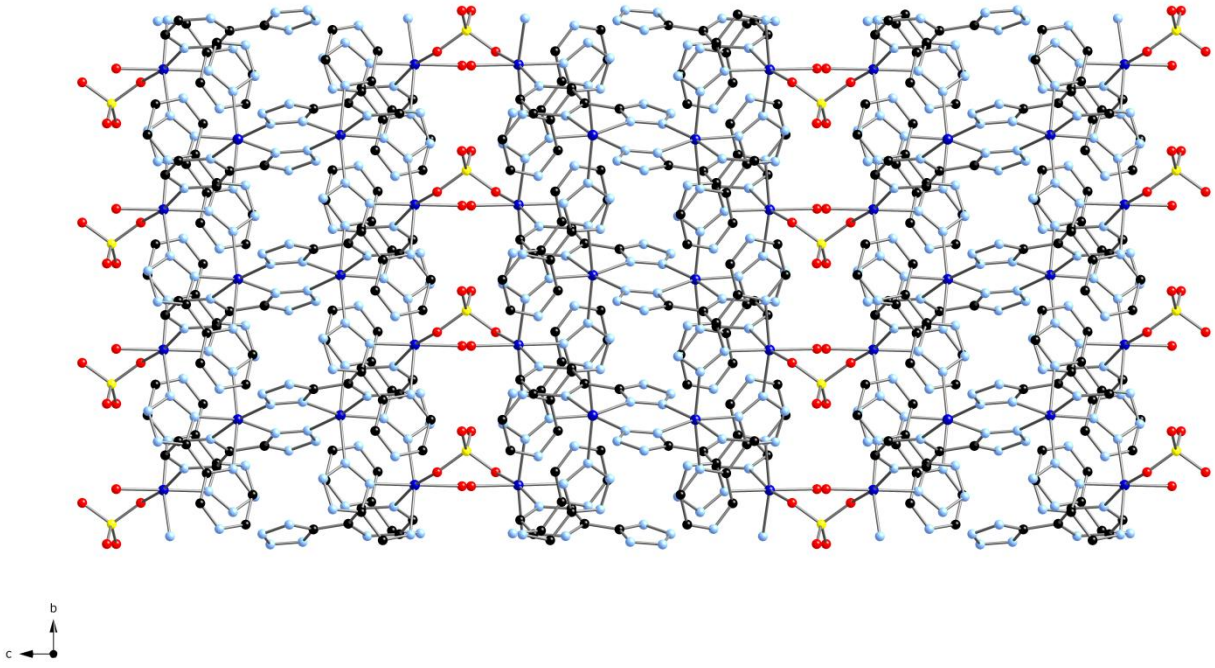

(a)

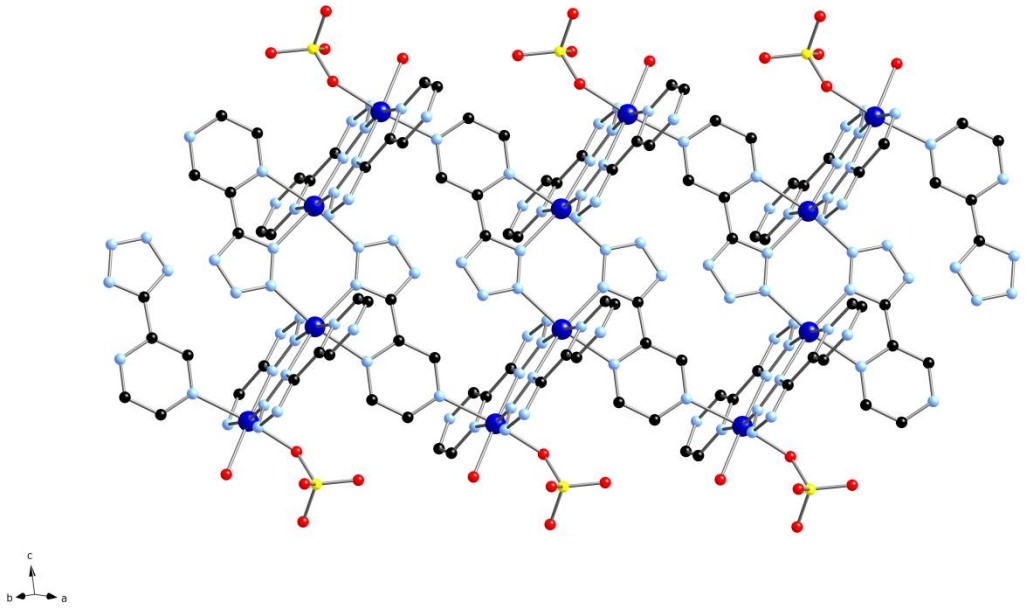

(b)

Figure 6.3: (a) Ball and stick representation of the three-dimensional structure of $[Co_4(prztet)_6(SO_4)(H_2O)_2]$ (**3**). (b) Ball and stick representation of the tetranuclear secondary building unit of **3**.

There are two distinct cobalt geometries. The first is a distorted octahedral $\{CoN_6\}$ site that bonds to four tetrazolate nitrogen donors from four prztet ligands and to two pyrazine nitrogen atoms from two chelating prztet ligands. The second cobalt site exhibits $\{CoN_4O_2\}$ coordination, bonding to two tetrazolate nitrogen donors, two pyrazine nitrogens, a sulfato oxygen and a terminal aqua ligand.

The prztet ligands adopt two distinct coordination modes. The first involves bridging two interior cobalt sites of a tetrad in bridging, chelating mode through the tetrazolate N1,N2 donors and the pyrazine N2 donor of two prztet ligands. A second set of ligands bridges each peripheral cobalt site to a central metal center through two similar bonding patterns at each terminal pair of

metal sites. Consequently, each prztet ligand bridges two cobalt sites of a given tetrad and connects to an adjacent tetrad through the pyrazine N5 donor.

The structure of the fluoride containing derivative $[Co_3F_2(SO_4)(3\text{-pyrtet})_2(H_2O)_4]$ (**4**), shown in **Figure 6.4**, is two-dimensional. The structure exhibits a variant of the common trinuclear building block, in this case $\{Co_3F_2(SO_4)(azolate)_2\}$. There are two cobalt coordination geometries within the triad. Two sites exhibit $\{CoF_2O_2N_2\}$ distorted octahedral geometry, defined by the nitrogen donor of a N2,N3 bridging tetrazolate group, the pyridyl nitrogen of 3-pyridyl substituent, the μ^3-fluoride, a μ^2-fluoride, an oxygen from a capping sulfato group, and an aqua ligand. The second metal site exhibits $\{CoFO_3N_2\}$ coordination to two tetrazolate nitrogen donors, the μ^3-fluoride, two *cis*-aqua ligands, and an oxygen from the sulfato ligand. The fourth vertex of the sulfato group is uncoordinated and directed toward the centroid of an adjacent triad with an O···F distance of 2.820 Å. Each triad SBU is linked to four adjacent triads through the 3-pyridyltetrazolate ligands to establish the three-dimensional connectivity.

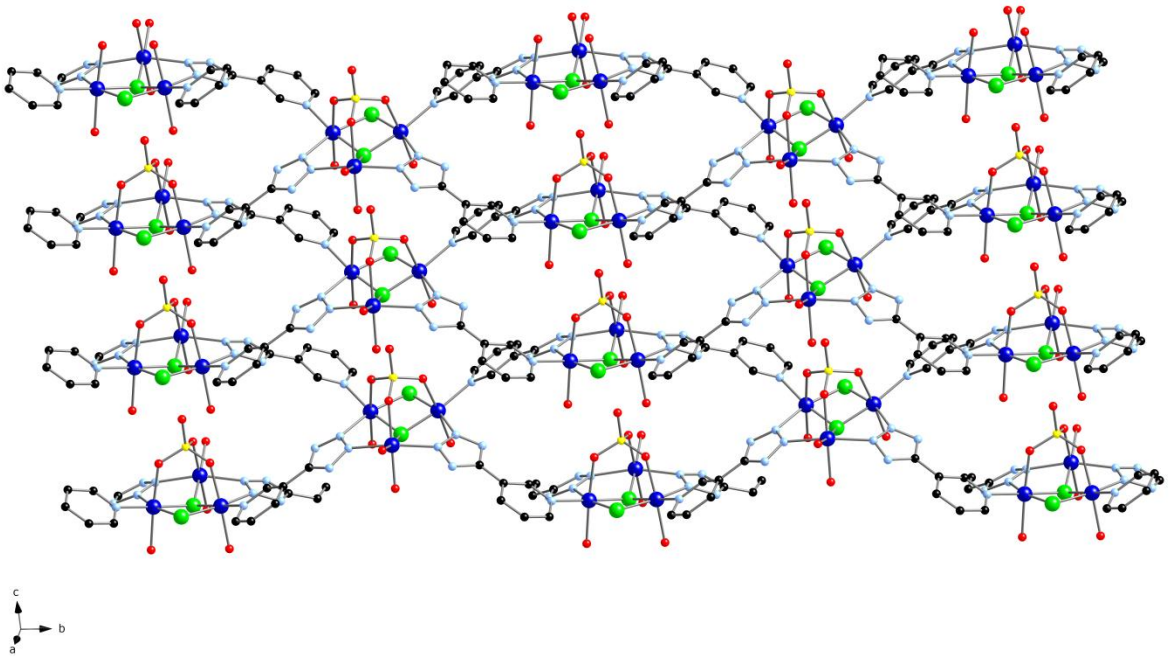

Figure 6.4: Ball and stick representation of the two dimensional structure of $[Co_3F_2(SO_4)(3\text{-pyrtet})_2(H_2O)_4]$ (**4**) in the bc plane.

The nickel analogue $[Ni_3F_2(SO_4)(3\text{-pyrtet})_2(H_2O)_4]$ (**5**) is isostructural with the cobalt analogue **4** (**Figure 6.5**). The structure exhibits the anticipated contraction in bond lengths for the nickel analogue as a result of the contraction of the covalent radius upon moving to the right of the transition series from Co to Ni.

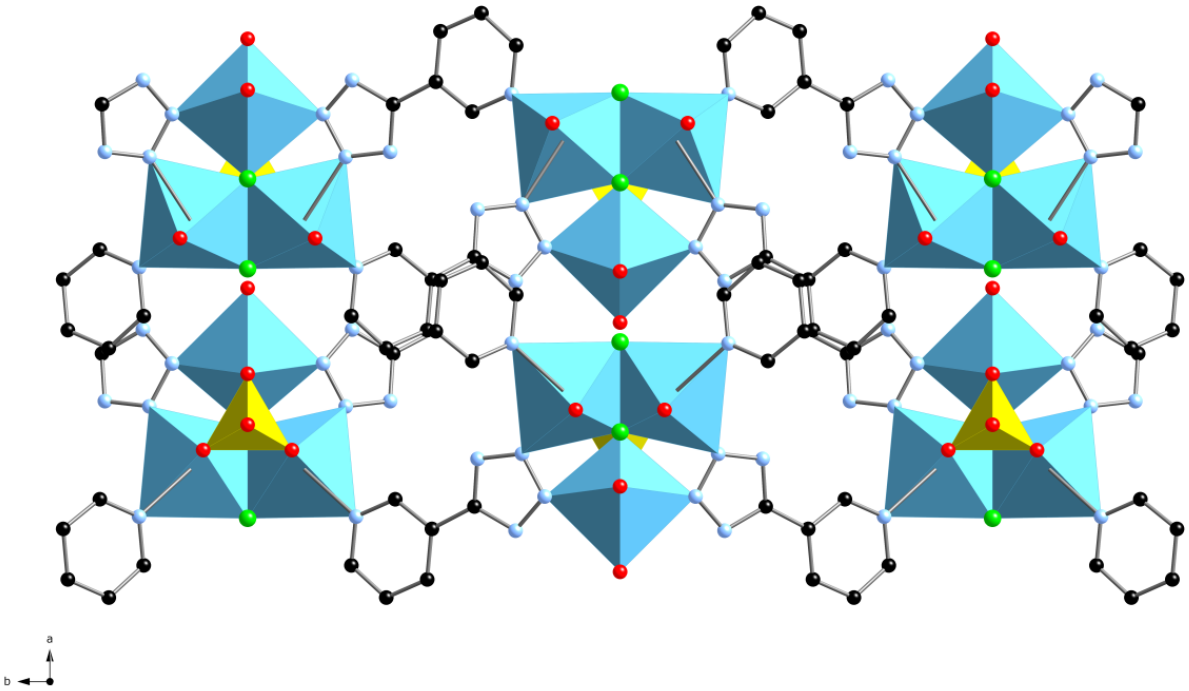

Figure 6.5: Mixed polyhedral and ball and stick representation of the two dimensional structure of $[Ni_3F_2(SO_4)(3\text{-pyrtet})_2(H_2O)_4]$ (**5**) in the ab plane. Color scheme: nickel, aqua octahedra; sulfur, yellow tetrahedra; oxygen, red spheres; nitrogen, light blue spheres; carbon, black spheres. The color scheme is used throughout.

As shown in **Figure 6.6**, the three-dimensional structure of $[Ni_5(3\text{-pyrtet})_4(SO_4)_2(OH)_2(H_2O)_2]\bullet H_2O$ (**6**•$0.5H_2O$) is constructed from pentanuclear SBUs. The structure is best described as $\{Ni_5(\text{tetrazolate})_4(SO_4)_2(OH)_2\}_n$ layers in the *ac* plane connected through the pyridyl arms of the 3-pyridyltetrazolate ligands.

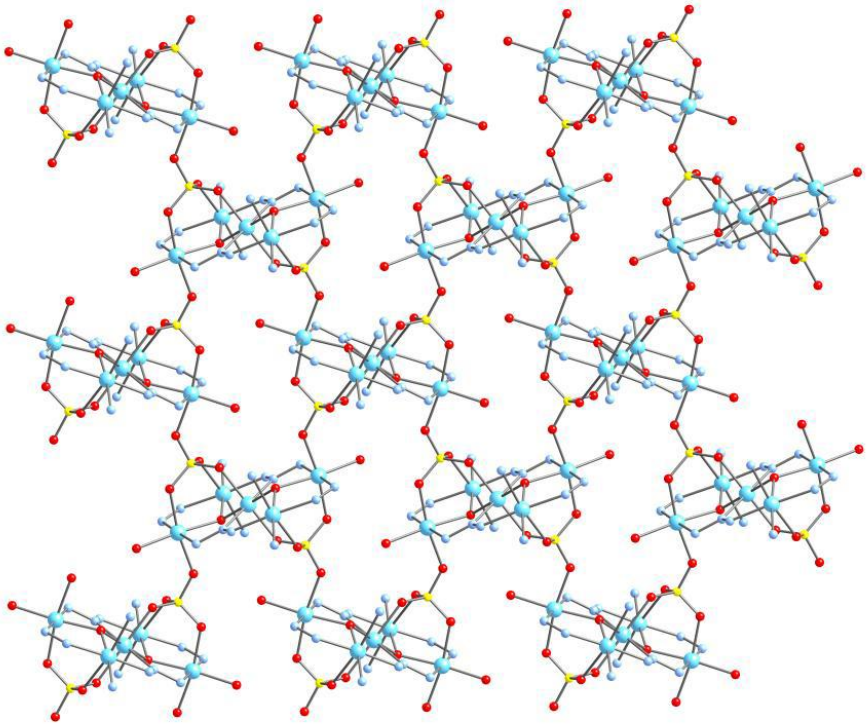

(a)

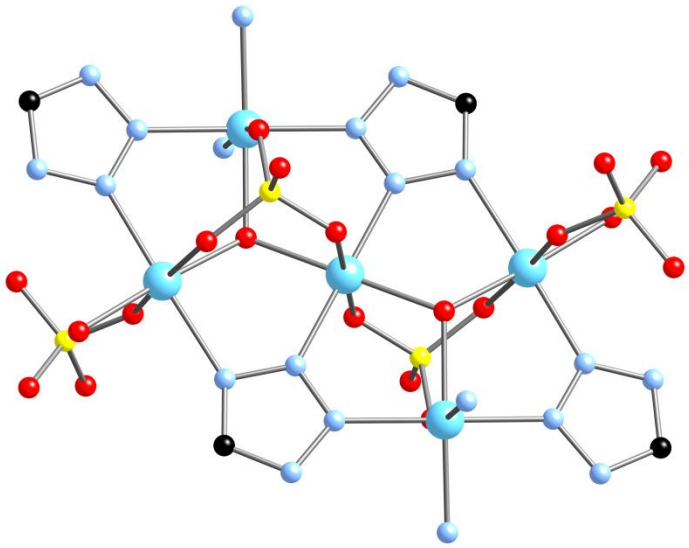

(b)

Figure 6.6: (a) Ball and stick representation of the structure of $[Ni_5(3\text{-pyrtet})_4(SO_4)_2(OH)_2\ (H_2O)_2]\bullet 0.5H_2O$ (**6**$\bullet 0.5H_2O$) with 3-pyridyltetrazole ligands omitted to illustrate $[Ni_5SO_4)_2(OH)_2(H_2O)_2]^{4-}$ layers. (b) The pentanuclear building units of **6**.

The pentanuclear SBU is constructed from two of the recurring $\{M_3(\mu^3\text{-OH})(\text{azolate})_3\}^{2+}$ building units sharing a common edge. Each pentanuclear unit is associated with four sulfato groups: two capping nickel triads through three oxygen donors and two bonding to the unit through a single oxygen donor. There are three distinct nickel coordination environments. The central nickel of the pentanuclear unit bonds to two tetrazolate nitrogen donors, two sulfato oxygens from two SO_4 groups, and two μ^3-hydroxy groups. A pair of nickel sites exhibit $\{NiO_2N_4\}$ coordination to two tetrazolate nitrogen donors, two pyridyl nitrogens, a sulfato oxygen and the μ^3-hydroxy group. The final pair of nickel centers possesses $\{NiO_4N_2\}$ coordination, defined by two tetrazolate nitrogens, the oxygen donor of a capping sulfato ligand, an oxygen from a second sulfato group, the μ^3-hydroxy ligand, and an aqua group.

The pentanuclear SBUs are linked in the *bc* plane through the sulfato ligands and one set of 3-pyridyltetrazolate ligands. Three-dimensional connectivity is achieved through bridging of adjacent networks along the *a*-direction by the second group of 3-pyridyltetrazolate ligands.

As shown in **Figure 6.7**, the structure of $[Cu_3(OH)(H_2O)_3(3\text{-pyrHtet-O})_3(SO_4)]$ (**7**) is a neutral trinuclear molecular species. The compound contains the common $\{M_3(\mu^3\text{-OH})\}^{5+}$ unit previously described for $[M_3(trz)_3(OH)_3(H_2O)_4]$ (M=Cu, Ni),[66,67] $[Cu_3(OH)(trz)_3][Cu_2Br_4]$,[66] $\{[Cu_3O(OH)(trz)_2]_3Cl_2(H_2C_3N_3O_3)\}$,[91] $[Cu_4(trz)_3]OH$,[69] $[Cu_6^{II}Cu_2^{I}(trz)_6(SO_4)_3(OH)_2(H_2O)]$,[69] $[Co_3(OH)(SO_4)(btt)(H_2O)_4]$,[63] and $[Fe_3(OH)(Htrz)_3(HSO_4)(SO_4)_2]$[67] (trz = triazolate, btt = 5,5′,5′′-(1,3,5-phenylene)tris(1H-tetrazole)). The copper sites exhibit '4+2' Jahn-Teller distorted geometry with the equatorial plane defined by two nitrogen donors from two N1,N2-bridging

tetrazolate ligands, the μ^3-OH group, and a hydroxyl oxygen of the hydroxy-pyridyl group of the ligand; the axial sites are occupied by a sulfate oxygen and an aqua ligand.

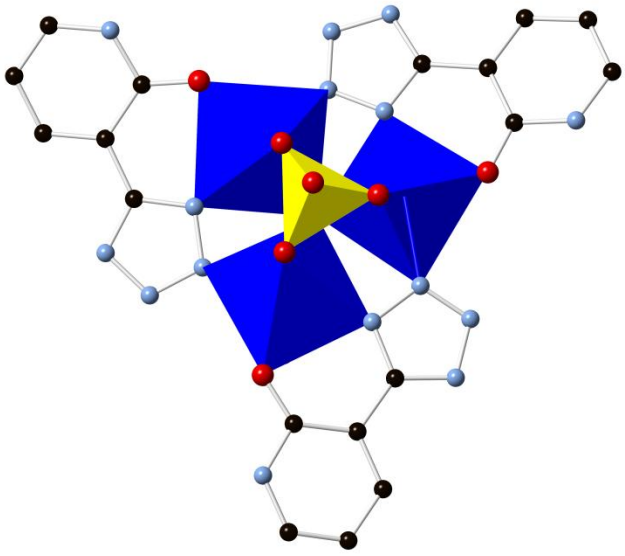

Figure 6.7: Mixed polyhedral and ball and stick representation of the structure of $[Cu_3(OH)(H_2O)_3(3\text{-pyrHtet-}O)_3(SO_4)]$ (**7**). Color scheme: copper, blue polyhedra; sulfur, yellow tetrahedra; oxygen, red spheres; nitrogen, light blue spheres; carbon, black spheres. The color scheme is used throughout.

Each hydroxypyridyltetrazolate ligand bridges two copper sites through N1,N2 donors and chelates to a site through additional coordination through the hydroxyl group. The sulfato ligand shares an oxygen vertex with each copper site, having the fourth oxygen uncoordinated and projecting toward a neighboring cluster.

An unusual feature of the structure of **7** is the presence of the hydroxylated form of the ligand. The *in situ* hydroxylation of pyridine based ligands in hydrothermal reactions in the presence of copper or molybdenum has been noted previously and appears to be a recurrent theme of the chemistry.[80] The final difference Fourier map clearly reveals the pyridyl nitrogen

as a protonation site. Consequently, the ligand is present as the singly negatively charged 2-hydroxy-3-Hpyridyl tetrazole, $\{N_4C\text{-}C_5NHO\}^-$.

The structure of the two-dimensional material $[Cu_3(OH)_2(H_2O)_3(3\text{-pyrtet})_2(SO_4)]$ (**8**) is shown in **Figure 6.8**. The layer is constructed from trinuclear $\{Cu_3(OH)_2(H_2O)_3(SO_4)\}^{2+}$ clusters linked through the 3-pyrtet ligands in the *ac* plane. While the trinuclear cluster exhibits the common $\{Cu_3(\mu^3\text{-OH})\}^{5+}$ core also found in compound **8**, the detailed structure is quite distinct. In contrast to the cluster of **8** which exhibits three six coordinate Cu sites corner-sharing at a single μ^3-OH vertex, the cluster of **9** offers a pair of edge-sharing pseudo-octahedral sites and a square pyramid site corner-sharing at the μ^3-OH group. Each '4+2' site exhibits an equatorial plane occupied by a tetrazolate nitrogen, a pyridyl nitrogen, the μ^3-OH group and a μ^2-OH ligand while the axial positions are defined by a sulfato oxygen and an aqua ligand. The '4+1' axially distorted site exhibits a basal plane occupied by two tetrazolate nitrogen donors, the μ^3-OH group, and an aqua ligand; the apical site is defined by a sulfato oxygen.

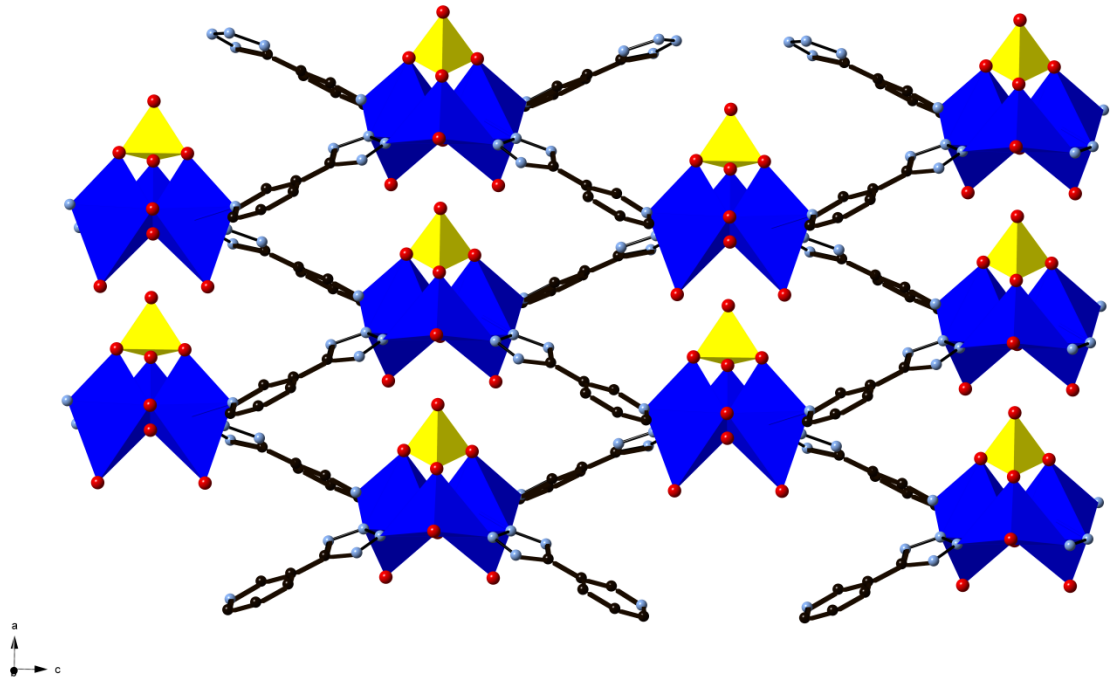

Figure 6.8: Mixed polyhedral and ball and stick representation of the structure of $[Cu_3(OH)_2(H_2O)_3(3\text{-pyrtet})_2(SO_4)]$ (**8**) in the *ac* plane.

Each trinuclear unit is associated with four 3-pyrtet ligands. Two bridge through N2,N3 sites between a six coordinate and the five coordinate copper sites, while the other two employ pyridyl nitrogens bound to the six coordinate copper sites. The 3-pyrtet groups project outward from the trinuclear core and link each cluster to four adjacent clusters in the plane. The clusters are aligned in the plane such that the S-O vectors of the uncoordinated sulfato oxygens lie within the plane approximately parallel to the *a*-axis. As a result of this alignment, the aqua ligands of the five coordinate copper sites project into the interlamellar domains.

While the structure of $(Me_2NH_2)[Cu(2\text{-pyrtet})(SO_4)]$ (**9**) is also two-dimensional as shown in **Figure 6.9**, it does not share the common $\{M_3(\mu^3\text{-OH})\}^{5+}$ motif. The secondary building unit in this case is a binuclear $\{Cu_2(2\text{-pyrtet})\}^{2+}$ group which is linked to four adjacent binuclear units through sulfato groups.

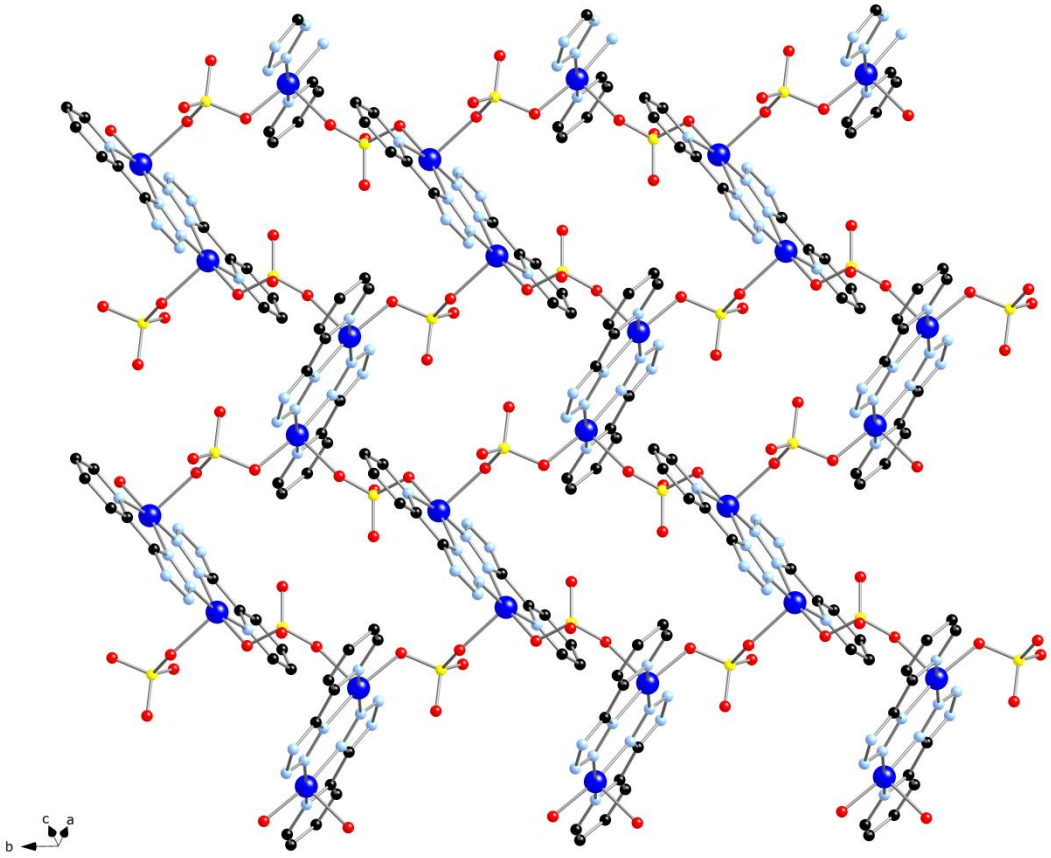

(a)

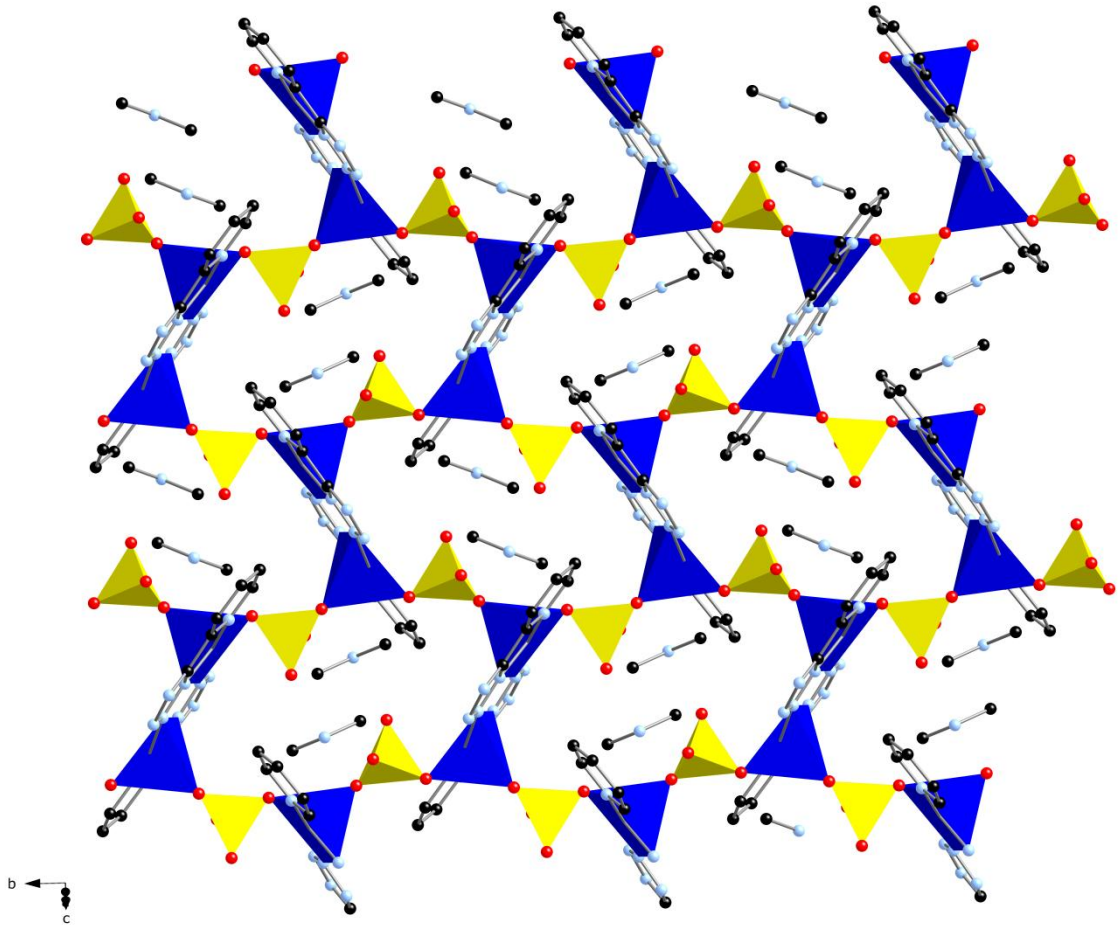

(b)

Figure 6.9: (a) Ball and stick representation of the two-dimensional structure of the $[Cu(2\text{-pyrtet})(SO_4)]_n^{n-}$ network of **9**. (b) Polyhedral representation of the layer structure of **9**, showing the locations of the $(Me_2NH_2)^+$ cations in the intralamellar cavities.

The copper sites exhibit '4+1' square pyramidal geometry with the basal plane defined by the N1 and pyridyl nitrogens of a chelating 2-pyrtet ligand, the N2 donor of a second 2-pyrtet ligand and a sulfato oxygen; the apical site is occupied by an oxygen from a second sulfato group. Each 2-pyrtet ligand bridges two copper sites through N1,N2 donors and chelates to one of these sites through the pyridyl donor. The location of the pyridyl nitrogen adjacent to the

carbon 5 site favors the chelate bonding mode rather than the bridging mode between secondary building units.

Each sulfato group bridges two adjacent binuclear units, bonding to a basal site in one and an apical site in the second. Each sulfato group projects an uncoordinated oxygen into an intralamellar cavity and a second toward the interlamellar domains.

The interlayer separation between the mean planes is *ca*. 12.5Å. Since the 2-pyridyltetrazolate ligands are oriented normal to the planes, their projection into the interlamellar domain renders the packing of layers relatively dense. As a consequence, the $Me_2NH_2^+$ cations nestle in the layers just above and below the twenty-two membered {-O-S-O-Cu-N-N-Cu-O-S-O-Cu}$_2$ rings that fuse to form the core of the layer structure of **9**.

The structure of the pyrazine derivative [Cu_4(pyrztet)$_6$(H_2O)$_2$(SO_4)] (**10**) is three-dimensional (**Figure 6.10**). The structure consists of {Cu_4(tetrazolate)$_6$(H_2O)$_2$(SO_4)}$_n$ chains, running approximately along the crystallographic *c*-axis, each linked through the pyrztet ligands to four adjacent chains to provide the three-dimensional expansion.

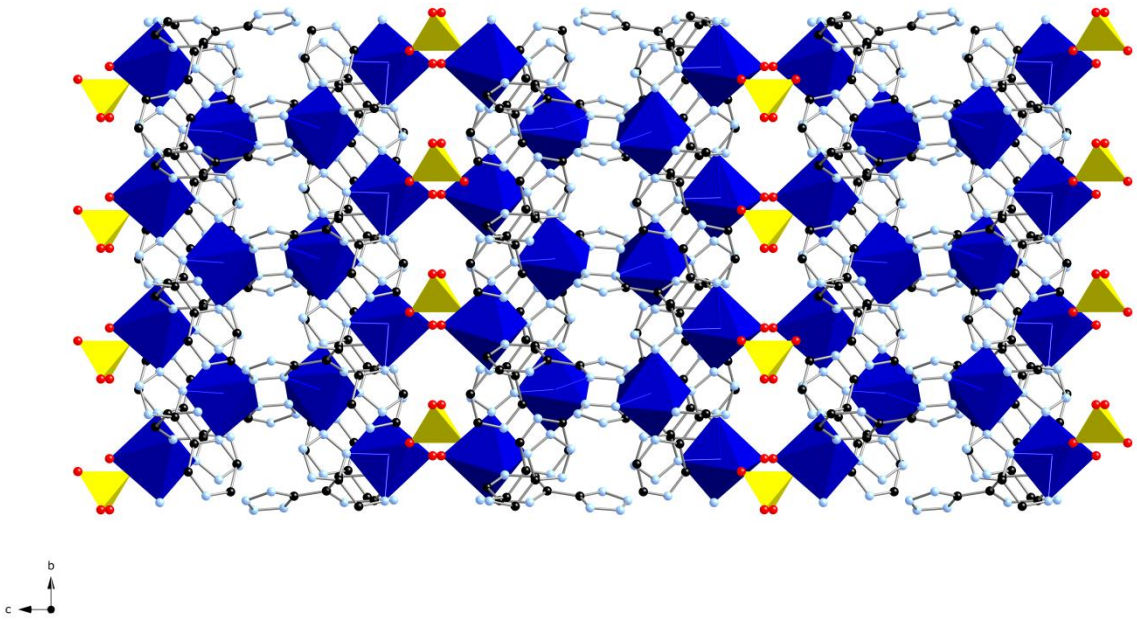

(a)

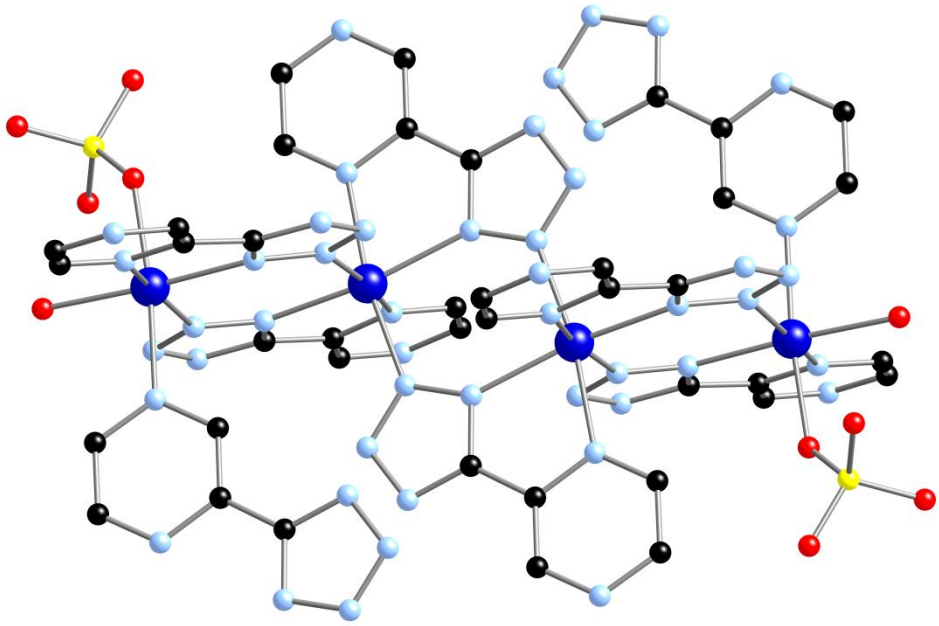

(b)

Figure 6.10: (a) Mixed polyhedral and ball and stick representation of the structure of $[Cu_4(pyrztet)_6(H_2O)_2(SO_4)]$ (**10**) in the *bc* plane. (b) Ball and stick representation of the tetranuclear secondary building unit of **10**.

The secondary building unit of the chain is the tetranuclear $\{Cu_4(pyrztet)_8(H_2O)_2(SO_4)_2\}$ unit shown in **Figure 6.10b**. There are two distinct Cu(II) environments within the non-linear tetranuclear unit. The interior pair of copper sites exhibit distorted $\{CuN_6\}$ geometry. Each of these copper sites participates in bonding to four pyrztet ligands. Two pyrztet ligands provide N1,N2 bridging between the copper centers to provide the common $\{Cu_2(tet)_2\}$ coordination unit. In addition, these pyrztet ligands chelate to the central copper sites through a pyrazine nitrogen donor. These nitrogen donors adopt a meridional orientation about the copper sites. The remaining coordination sites are occupied by two tetrazolate nitrogen donors from pyrztet ligands that bridge each central copper center to a peripheral copper site through the common bis-N1,N2 tetrazolate motif. One of these pyrztet ligands chelates to the central copper site through a pyrazine nitrogen donor while the second chelates to a peripheral copper center.

6.2.3 Structural Observations

The array of architectures and substructures observed for M(II)/azolate materials of **Table 6.1** reflects several determinants, such as reaction conditions of stoichiometry, pH, temperature, and the range of coordination possibilities associated with tetrazole ligands. This is further enhanced by the introduction of auxiliary coordinating anions, whether simple halides X^- or pseudohalides (such as CN^-) or oxyanions such as sulfate and phosphate. For example, sulfato groups can function in a variety of coordination modes, including bidentate, tridentate and tetradentate geometries as noted by the structures of this work. The incorporation of aqua and hydroxide ligands which can serve as terminal or bridging groups also contributes to lack of predictability for such structures. In fact, compounds **2**, **6-8,** and **10** exhibit the presence of sulfato, hydroxy and aqua ligands. In the case of **4** and **5**, the hydroxy groups have been replaced by fluoride, further complicating the compositional and structural chemistry.

Furthermore, the sulfate phases of this study may be considered topologically metastable since the structural variations arise from the apparently promiscuous condensation of the metal polyhedra and the sulfato tetrahedra, as suggested by the soft M-O-S angles of the structures.

Table 6.1: Selected structural characteristics of representative compounds of the type M(II)/azolate/SO_4^{2-}.

Compound	Azolate, L	Dimensionality	Coord. Geom.	Substructures	Ref.
$[M_5(L)_2(SO_4)_4(OH)_2]$ M = Mn, Fe	triazole	3D	octahedral	chains of M(II) pentanuclear clusters linked through sulfato groups	65
$[Cu_8(L)_6(SO_4)_3(OH)_2(H_2O)$	triazole	3D	sq. planar; sq. pyramidal	two-dimensional $\{Cu_4(L)_3(OH)\}_n$ with embedded $\{Cu_3(\mu_3\text{-}OH)(L)_3\}^{2+}$ clusters	143
$Zn_2(L)(SO_4)(OH)]$	triazole	3D	octahedral	$\{Zn_3(\mu_3\text{-}OH)\}^{5+}$ clusters and $\{Zn_2(SO_4)(OH)\}_n$ layers	71
$Cd_8(OH)_2(L)_4(SO_4)_5(H_2O)$	triazole	3D	octahedral	$\{Cd_3(\mu_3\text{-}OH)\}^{5+}$ clusters, $\{Cd_7(L)_4\}^{10n+}$ chains, $\{Cd_8(SO_4)_5\}_n$ frameworks	71
$Fe(OH)(HL)_3(HSO_4)(SO_4)_2$	triazole	3D	octahedral	trinuclear $\{Fe_3(\mu_3\text{-}OH)(HL)_3\}^{5+}$	67
$[Co_4(OH)_2(SO_4)(L)_2(H_2O)_4]$	1,4 bistetrazole benzene	3D	octahedral	$\{Co_4(HO)_2(SO_4)(L)_2(H_2O)_4$ layers with embedded $\{Co_4(OH)_2(L)_2(H_2O)_4\}$ chains	63
$[Co_3(OH)(SO_4)(L)(H_2O)_4]$	1,3,5 tritetrazole benzene	3D	octahedral	$\{Co_3(OH)(SO_4)(L)_3\}$ chains with $\{Co_3(\mu_3\text{-}OH)(SO_4)_2(L)_3\}^{2-}$ clusters	63
$[Cu_3(OH)(H_2O)_3(L)_3(SO_4)$	3-hydroxy pyridyl Tetrazole	mol.	octahedral	trinuclear $\{Cu_3(\mu_3\text{-}OH)(L)_3\}^{2+}$	this work
$[Cu_3(OH)(H_2O)_3(L)_3(SO_4)]$	3-pyridyl Tetrazole	2D	octahedral	trinuclear $\{Cu_3(\mu_3\text{-}OH)(L)_3\}^{2+}$	this work
$[Cu_3(OH)(H_2O)_3(L)_3(SO_4)]$	2-pyridyl Tetrazole	2D	octahedral	binuclear $\{Cu_2(L)\}^{2+}$	this work
$[Co_2(4\text{-pyrtet})(SO_4)(OH)(H_2O)]$	4-pyridyl tetrazole	2D	octahedral	$\{Co_2(L)(SO_4)(OH)(H_2O)\}_n$ chains of $\{Co_3(\mu_3\text{-}OH)(L)_3\}^{2+}$ building units	this work
$[Co_4(prztet)_6(SO_4)(H_2O)_2]$	pyrazine tetrazole	3D	octahedral	$\{Co_4(L)_6(H_2O)\}_n^{2+n}$ networks	this work
$[M_3F_2(SO_4)(3\text{-pyrtet})_2(H_2O)_4]$ M = Co, Ni	3-pyridyl tetrazole	3D	octahedral	$\{Co_3F_2(SO_4)(L)_2\}$ triads	this work
$[Ni_5(3\text{-pyrtet})_4(SO_4)_2(OH)_2(H_2O)_2]$	3-pyridyl tetrazole	3D	octahedral	$\{Ni_5(\text{tetrazolate})_4(SO_4)_2(OH)_2\}_n$ layers $(Ni_3(\mu_3\text{-}OH)(L)_3\}^{2+}$ building units	this work

The peripheral copper sites exhibit distorted $\{CuN_4O_2\}$ geometry. This coordination is defined by two tetrazolate donors from the bis-N1,N2 pyrztet ligands and the pyrazine nitrogen of the chelating pyrztet in a meridional arrangement, while the remaining coordination sites are occupied by an aqua ligand, a sulfato oxygen donor and a pyrazine nitrogen donor from a pyrztet

ligand directed toward an adjacent chain. The copper sites of compound **10** do not exhibit the pronounced Jahn-Teller induced '4+2' axial distortion observed for compounds **7-9**.

6.2.3.1 The {$M_3(\mu_3$-O(H)} Cores

The triangular {$M_3(\mu_3$-OH)} core of complexes **7** and **8** is a recurrent theme of the structural chemistry of Cu(II) and other transition metal. The {$M_3(\mu_3$-OH)} and {$M_3(\mu_3$-O)} cores have been described for systems with peripheral ligands such as pyrazole[92-109] and triazole[110-123] and homo- and heterometallic examples include {$Cu(II)_3$}, {$V(IV)_3$}, {$Cr(III)_3$}, {$Co(II)_3$)}, {$Fe(III)_3$}, {$Ni(III)_3$} and {$Cr(III)_2Fe(III)$}.[124-132] The {$M_3(\mu^3$-F} cluster of complexes **4** and **5**, however, has not been reported previously in the literature.

Table 6.2: Compounds containing common variants of the $\{M_3(\mu^3\text{-}OH)\}^{n+}$ building unit.

Building Unit	Bridging Ligand	Coordination Geometry	Coligand	M-μ_3O bond lengths	Ref
$[Cu_3(O)(L_3)Cl_3]^{2-}$	Pyrazolate	square planar	Cl^-	1.987	A
$[Cu_3(OH)(L_3)Cl_3]^-$	Pyrazolate	square planar	Cl^-	1.989	B
$[Fe_3(O)(4\text{-}O2N\text{-}L)_6Cl_3]^{2+}$	Pyrazolate	Octahedral	Cl^-	1.885, 1.894	C
$Mn_7(OH)_2(L)_8(CH_3O_2)_4$	Triazolate	octahedral and square pyramidal	$CH_3O_2^-$	2.0988	D
$[Cu_3(OH)(L1)_3(L2)_3]^{2+}$	pyrazolate and pyridine	octahedral and square pyramidal		1.999	E
$Cd_8(OH)_2(L)_4(SO_4)_5(H_2O)$	Triazolate	Octahedral	SO_4^{2-}	2.186-2.320	F
$Cu_3(OH)_3(L)_3(H_2O)_4$	Triazolate	Octahedral	H_2O	2.036	G
$Fe_3(OH)(HL)_3(HSO_4)(SO_4)_2$	Triazole	Octahedral	SO_4^{2-}	2.0847	D
$Ni_3(OH)(L)_3(OH)_2(H_2O)_4$	Triazolate	Octahedral	H_2O	2.041	D
$Cu_3(OH)_3(L)_3(DMF)_4$	4-pyridyl Tetrazolate	Octahedral	OH^-/DMF	2.005	H
$Co_3(OH)(SO_4)(L)_3(H_2O)_4$	1,4 bistetrazolate Benzene	Octahedral	H_2O/SO_4^{2-}	2.078	I
$[Cu_3(OH)(L)_3(H_2O)_3]^{2+}$	acetylaminotriazolate	square pyramidal	H_2O	1.983-2.043	J
$Cu_3(OH)(H_2O)_3(L)_3(SO_4)$	3-hydroxy pyridyl Tetrazolate	Octahedral	SO_4^{2-}	1.932	this work
$Cu_3(OH)_2(H_2O)_3(L)_2(SO_4)$	3-pyridyl tetrazolate	Octahedral	SO_4^{2-}	1.94	this work
$Co_3(L)_3(PO_4)$	4-pyridyl tetrazolate	Octahedral	PO_4^{3-}	2.128	K

References: (a) Angaridis, P. A.; Baran, P.; Boca, R.; Cervantes-Lee, F.; Haase, W.; Mezei, G.; Raptis, R. G.; Werner, R. *Inorg. Chem.* **2002**, *41*, 2219; (b)Liu, J.C.; Guo, G.-C.; Huang, J.-S.; You, X.-Z. *Inorg. Chem.* **2003**, *42*, 235. Ferrer, S.; Lloret, F.; Bertomeu, I.; Alzulet, G.; Borra´s, J.; Garcı´a-Granda, S.; Liu-Gonza´lez, M.; Haasnoot, J. G. *Inorg. Chem.* **2002**, *41*, 5821; (c)Dalice Pin˜ ero, D.; Raptis, R. G.; Renz, F.; Sanakis, Y.; *Inorg. Chem.* **2007**, *46*, 10981-10989; (d) Ouellette,W.; Prosvirin,A.V.; Valeich,J.; Dunbar K. R.; Zubieta J. *Inorg. Chem*. **2007**, *46*, 9067-9082; (e) Rivera-Carrillo,M.; Chakraborty, I.; Mezei,G.;Webster, R. D.; Raptis, R. G. I*norg. Chem.* **2008**, *47*, 7644-7650; (f) Ouellette W.; Hudson, B. S.; Zubieta J. *Inorg. Chem.* **2007**, *46*, 9075-9077; (g) Ouellette W.; Yu, M. H.; O'Connor, C.J.; Zubieta, J. *Angew. Chem. Int. Ed*. **2006**, *45*, 3497 –3500; (h) Ouellette, W.; Liu, H.; O'Connor, J.; Zubieta, J. *Inorg. Chem.* **2009**, *48*, 4655-4657; (i) Ouellette, W; Darling, K.; Prosvirin, A.; Whitenack, K.; Dunbar, K. R.; Zubieta, J. *Dalton Trans.*, **2011**, *40*, 12288; (j) Ferrer, S.; Lloret, F.; Pardo, E.; Liu-Gonzalez, M. L.; Garcia-Granda, S. Inorg. Chem. **2012**, *51*, 985-1001; (k) K. Darling, J. Zubieta, unpublished results.

In the specific instances of azolate N,N′-bridging ligand types about the $\{M_3(\mu_3\text{-}O(OH)\}$ core, a variety of additional peripheral or capping ligands may be accommodated, as shown in **Figure 6.11.** Furthermore, there is considerable variability of the M-O bond distances within the triad. Potentially bridging coligands such as capping sulfato- or phosphato-groups, can also provide spatial expansion to generate extended architectures. The number and diversity of compounds featuring these triangulo cores reflect the versatility of the unit in accommodating bridging and other peripheral ligands.

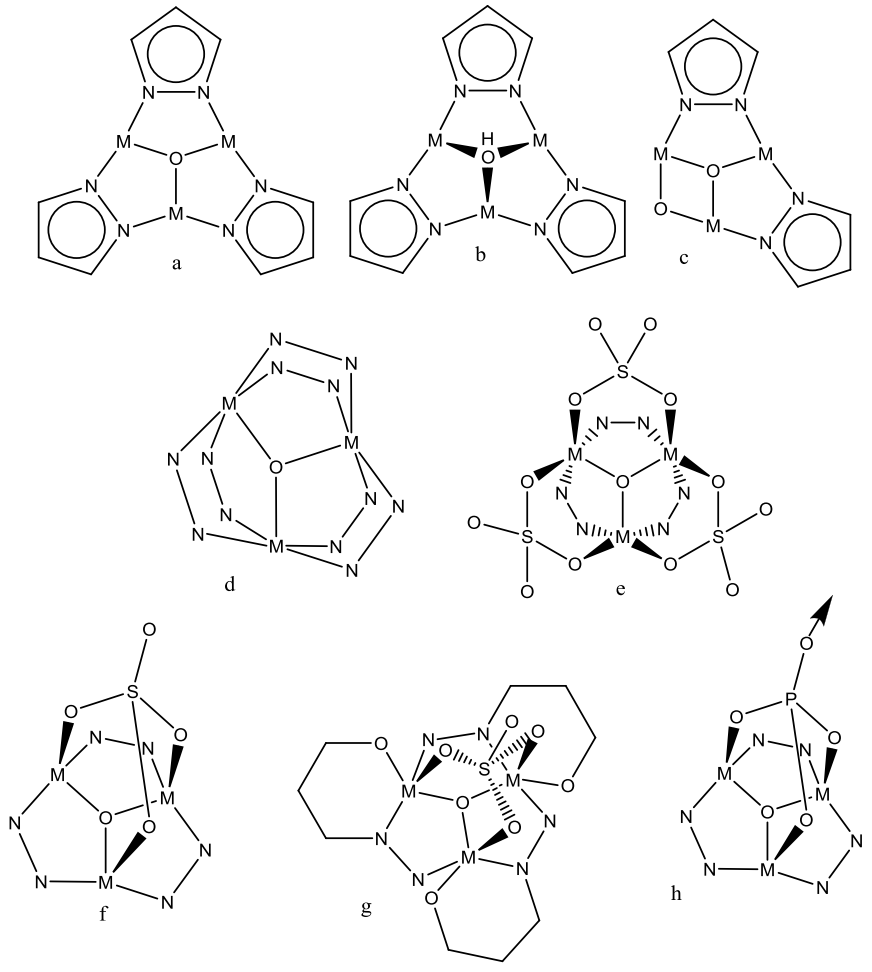

Figure 6.11: Common azolate bridged triads. (a, b) The prototypical $\{M_3(\mu_3\text{-}O)\}$ and $\{M_3(\mu_3\text{-}OH)\}$cluster types. (c) A variant of the $\{M_3(\mu_3\text{-}O)\}$ cluster featuring a peripheral μ_2-oxo group. (d) The $\{M_3(\mu_3\text{-}O)\}$ cluster with two additional doubly bridging N1, N2 azolates. (e) Incorporation of sulfate anion as an additional bridging ligand to the trinuclear core. (f) Sulfate as a capping anion to the $\{M_3(\mu_3\text{-}OH)\}$ structural motif. (g)

The structural building unit of compound **1** of this study. (h) $\{M_3(\mu_3\text{-}O)\}$ cluster variant with phosphate as a capping ligand with the fourth oxo group of the phosphate anion providing extension of the cluster motif into a chain structure.

6.2.4 Magnetism

Magnetic susceptibility measurements of complexes **3, 4** and **5** were performed on polycrystalline samples of compound at 1000 Oe over the temperature range 2-300 K (**Figure 6.12**). The value of χT for **3** at 300 K is 11.7 emu·mol^{-1} K, which is close to the expected value for four Co(II) ions (S = 3/2, g = 2.5). It decreases monotonically to a value 3.6 emu·mol^{-1} K at 2 K. The temperature dependence of $1/\chi$ between 300 and 20 K approximates Curie-Weiss behavior with C = 12.3 emu·mol^{-1} K and θ = -14 K. The decrease of χT upon cooling and negative sign of the Curie-Weiss constant is due to superposition of antiferromagnetic interactions and spin-orbit coupling of Co(II) ions.

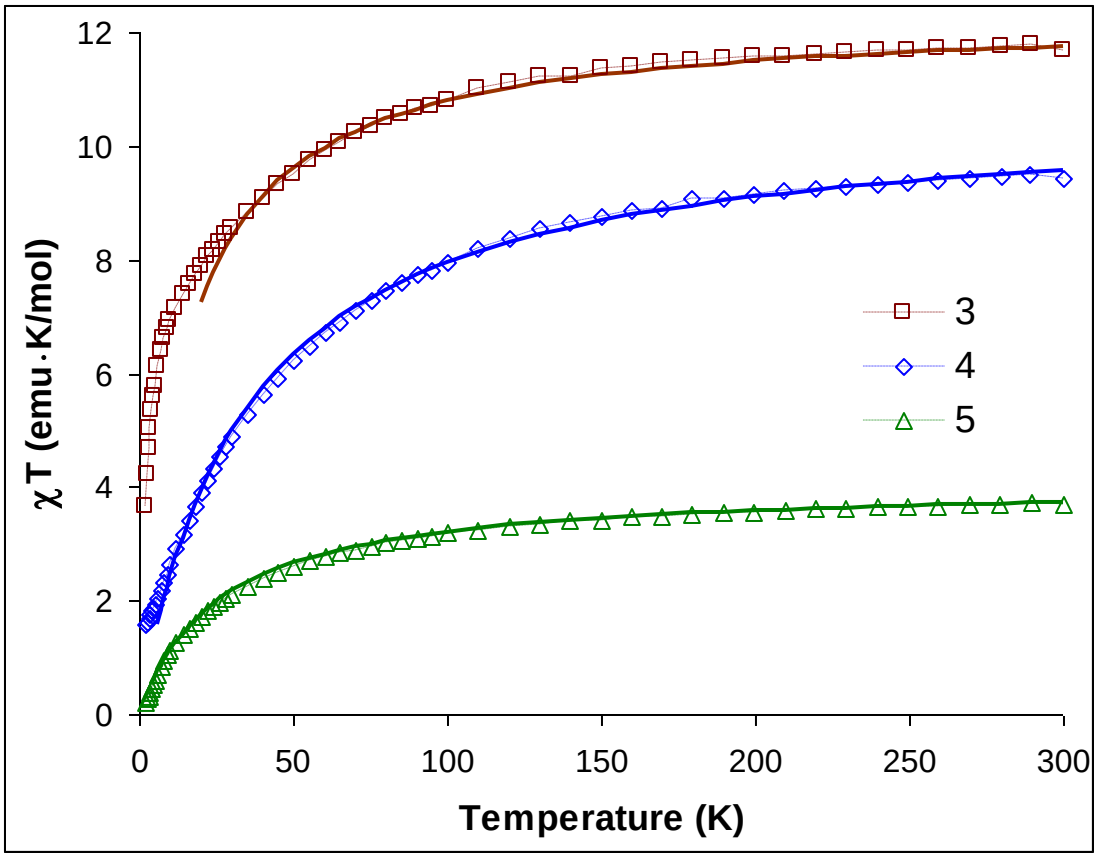

Figure 6.12: Temperature dependence of the χT product for compounds **3**, **4** and **5**. The solid lines correspond to Curie-Weiss law.

The value of χT for **4** at 300 K is 9.5 emu·mol^{-1} K, which is close to the expected value for three Co(II) ions (S = 3/2, g = 2.6). It constantly decreases to a value 1.6 emu·mol^{-1} K at 2 K. The temperature dependence of 1/χ between 300 and 5 K approximates Curie-Weiss behavior with C = 10.6 emu·mol^{-1} K and θ = -34 K. The decrease of χT upon cooling and negative sign of the Curie-Weiss constant is due to superposition of antiferromagnetic interactions and spin-orbit coupling of Co(II) ions.

The value of χT for **5** at 300 K is 3.7 emu·mol^{-1} K, which is close to the expected value for three Ni(II) ions (S = 1, g = 2.25). It constantly decreases to a value 0.2 emu·mol^{-1} K at 2 K. The temperature dependence of 1/χ between 300 and 6 K approximates Curie-Weiss behavior

with C = 4.05 emu·mol^{-1} K and θ = -26 K. The decrease of χT upon cooling and negative sign of the Curie-Weiss constant is due to superposition of antiferromagnetic interactions and spin-orbit coupling of Ni(II) ions. No AC signal or magnetic ordering were found.

The magnetic properties of compounds **7** and **8** have been studied and the results are presented. The magnetic behavior of the {$Cu_3(\mu_3$-O(H)} core has been extensively studied[133-138] with an extensive review of the field being provided by Ferrer, et.al.[133] The compounds have been found to exhibit strong antiferromagnetic and, in most cases, antisymmetric exchange.

The unit cells of compounds **7** and **8** consist of a Cu(II) triangle as the dominant magnetic unit. The values for χT at 300 K are 0.82 and 0.88 emu•mol^{-1} K per trimer for compounds **7** and **8**, respectively. These numbers are less than the expected values for three Cu(II)-ions ($3\chi_{Cu}T$ = 1.125 cm^3 mol^{-1} K, S = 1/2) (**Figure 6.13**). The χT values decrease in a continuous fashion from room temperature and reach a plateau at ~60 K and finally decrease to 0.21 and 0.37 emu•mol^{-1} K at 2 K. The temperature dependence of $1/\chi$ between 300 and 60 K approximates Curie-Weiss behavior with C = 1.37 emu•mol^{-1} K, θ = -200 K and C = 1.45 emu•mol^{-1} K, θ = -190 K for compounds **7** and **8,** respectively. These values indicate antiferromagnetic interactions between Cu(II) centers. As a first approximation, it is often assumed that the three metal ions are essentially structurally equivalent, such that $J = J_1 = J_2 = J_3$ and $g = g_1 = g_2 = g_3$ and the spin Hamiltonian $H_{iso} = -J(S_1 \cdot S_2 + S_2 \cdot S_3 + S_1 \cdot S_3)$ can be used to describe the magnetic interactions.[139-143] An attempt to use this approach, however, failed to reproduce the low-temperature decrease in χT. Different J and g values for the different magnetic centers do not improve the fit and lead to over-parameterization.

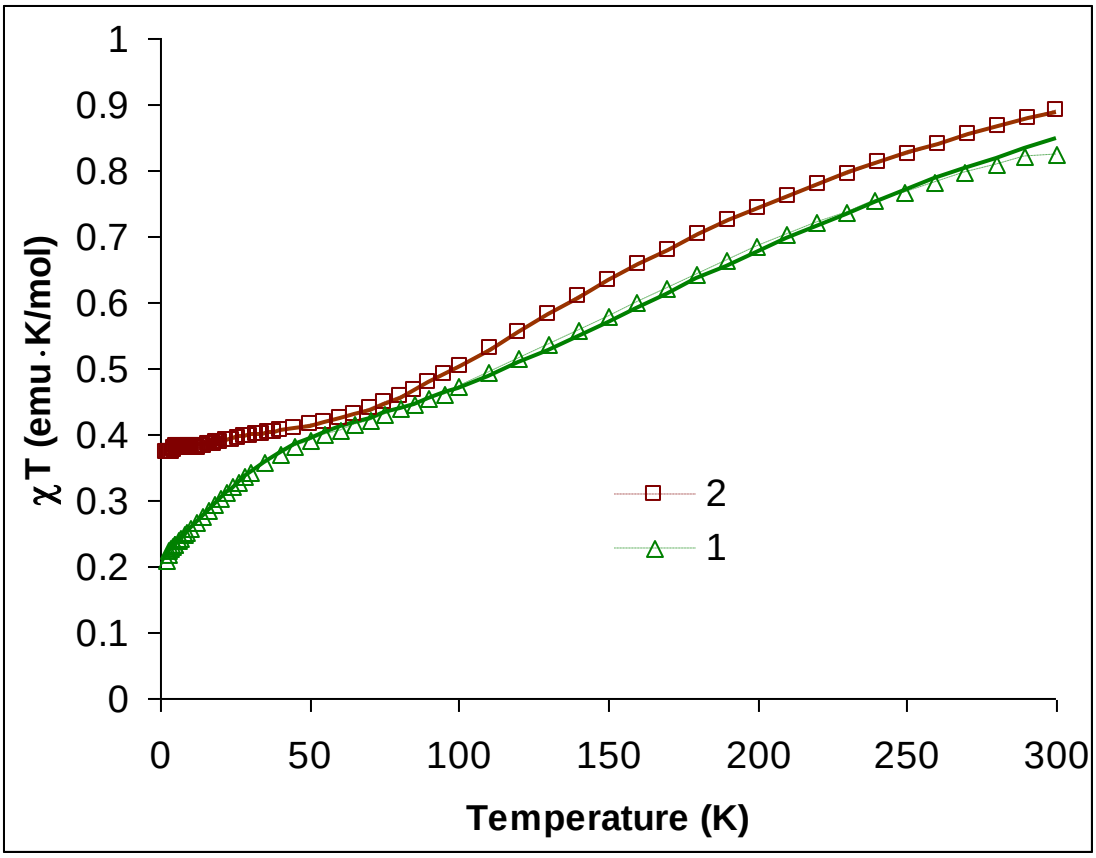

Figure 6.13: The temperature dependence of χT for **7** (green) and **8** (red). The solid lines correspond to the best fit obtained with **Equation 1**.

Another approach was used [133-138] assuming a strong contribution of antisymmetric exchange. For fitting experimental data of compounds **7** and **8** we used the Hamiltonian:

$$H = H_{iso} + H_{ASE} + H_{Zeem} \quad (1)$$

$$H_{iso} = -J(S_1S_2 + S_2S_3) - jS_1S_3 \quad (2)$$

$$H_{AS} = G_Z[S_1 \times S_2 + S_2 \times S_3 + S_3 \times S_1] \quad (3)$$

$$H_{Zeem} = g_{||}\beta(S_{1Z} + S_{2Z} + S_{3Z})H_Z + g_{\perp}\beta[(S_{1X} + S_{2X} + S_{3X})H_X + (S_{1Y} + S_{2Y} + S_{3Y})H_Y \quad (4)$$

where H_{iso} is a Hamiltonian for isotropic exchange for an isosceles triangle with parameters $J = J_{12} = J_{23}$ and $j = J_{13}$; H_{AS} is an axial Hamiltonian for antisymmetric exchange with G_Z parallel to the C_3 axis and $G_{\perp} = 0$; H_{Zeem} is an axial Hamiltonian for the Zeeman interaction with $g_{||} = g_{1z} =$

$g_{2z} = g_{3z}$ and $g_{\perp} = g_{1x} = g_{2x} = g_{3x} = g_{1y} = g_{2y} = g_{3y}$. The exact analytical expression for the magnetic susceptibility χ can be found in the article by Ferrer and coworkers.[133]

The magnetic data were fitted over the entire temperature range of 2-300 K with the parameters J = -184.2 cm^{-1}, j = -171 cm^{-1}, G_Z = 19.9 cm^{-1}, $g_{||}$ = 2.35, $g_{\perp}$ = 2.14 for compound **7** and J = -140.8 cm^{-1}, j = -109.6 cm^{-1}, G_Z = 8.8 cm^{-1}, $g_{||}$ = 2.28, $g_{\perp}$ = 2.03 for compound **8.** All of the derived values are in good agreement to those reported for similar compounds.[133-143] The difference between J and j for compound **8** is much larger than that for compound **7** because of the large difference in the Cu-O-Cu angles of compound **8**. A symmetrical magnetic core of compound **7** with Cu-O-Cu angle θ = 115º gives a predictable magnetic exchange parameter J. Using the empirical formula J = 13.65θ + 1385 from reference 133, the magnetic exchange parameter was estimated to be J = 186.75 cm^{-1}.

6.3 Conclusions

Hydrothermal methods have been used to prepare a series of crystalline materials of the general type Co(II), NI(II), and Cu(II)/substituted tetrazole/SO_4^{2-}. The structural chemistry reflects the coordination preferences of the substituted tetrazole ligand: 3-and 4-pyridyltetrazole bridges metal or metal cluster nodes; 2-pyridyltetrazole adopts a chelating modality through a tetrazole nitrogen and a pyridyl nitrogen; and pyrazine tetrazole adopts both chelating and bridging roles.

A recurrent theme of the extended structures of such materials is the presence of embedded metal(II)/tetrazolate clusters as architectural motifs. The structures of compounds **2-10** are constructed from a variety of clusters acting as secondary building units. Compounds **2**, **4** and **5** exhibit variants of the common trinuclear core $\{M_3(\mu_3\text{-}X)\}^{+5}$ (X = F, OH^-), while **3** is constructed from tetranuclear subunits and **5** from a novel pentanuclear core. The structures of **7**

and **8** exhibit the common $\{Cu_3(\mu^3\text{-}OH)\}^{5+}$ trinuclear secondary building block, while the structures of **3**, **9** and **10** exhibit the persistent $\{Cu_2(\mu^2\text{-tetrazolate})_2\}$ building block. Compounds **2**, **4** and **5** exhibit variants of the common trinuclear core $\{M_3(\mu_3\text{-}X)\}^{+5}$ (X = F, OH^-), while **3** and **10** are constructed from tetranuclear subunits and **5** from a novel pentanuclear core.

It is also noteworthy that hydrothermal conditions promoted *in situ* ligand reactions leading to the hydroxylation of 3-pyridyltetrazole in compound **7** and to ligand decomposition in **9** to provide $Me_2NH_2^+$ cations.

The magnetic behavior of the compounds of this study may be contrasted with the magnetic characteristics of materials of other M(II)/polyazaheterocyclic materials with trinuclear and pentanuclear cores.[143] Such materials often exhibit strong antiferromagnetic and, in many cases, antisymmetric exchange. The Curie-Weiss behavior reflects the structural details of these materials which suggest poor overlap between the magnetic orbitals within the cluster units.

The structural variety and range of magnetic properties of the phases of this study suggests that a rich magneto-structural chemistry can be developed for compounds of the general type M(II)/substituted tetrazole/anion where M(II) = Mn, Fe, Co, Ni and Cu and the anion is NO_3^-, SO_4^{2-}, PO_4^{3-}. MoO_4^{2-}, VO_3^- or ReO_4^-.

6.4 Experimental Section

6.4.1 Materials and General Procedures

The ligands 2-, 3- and 4-pyridyltetrazole and pyrazinetetrazole were prepared by the "click" chemistry approach using zinc catalysis in aqueous solution or by the use of modified montmorillonite K-10.[76-78] All other chemicals were used as obtained without further purification. Copper sulfate and hydrofluoric acid (99.5%) were purchased from Alfa Aesar. All hydrothermal syntheses were carried out in 23 mL poly-(tetrafluoroethylene)-lined stainless steel

containers under autogenous pressure. The reactants were stirred briefly, and the initial pH was measured before heating. Water was distilled above 3.0MX in-housing using a Barnstead model 525 Biopure distilled water center. The initial and final pH values of each reaction were measured using color pHast sticks. Infrared spectra were obtained on a Perkin–Elmer 1600 series FTIR spectrometer.

6.4.1.1 Synthesis of $[Co(prztet)_2(H_2O)_2]\bullet 0.5H_2O$ ($1\bullet 0.5H_2O$)

A mixture of cobalt sulfate heptahydrate (193 mg, 0.684 mmol), 4-pyridyltetrazole (50 mg, 0.342 mmol), and H_2O (10.00 g, 556 mmol) in the mole ratio 2.00:1.00:1626 was stirred briefly before heating to 120°C for 48 hours. Dark pink block crystals of **1**, suitable for X-ray diffraction, were isolated in 40% yield. IR (KBr pellet, cm^{-1}): 3435(b), 1528(m), 1074(m), 1085(s), 1034(s), 1118(m), 874(m) 839(w), 688(m).

6.4.1.2 Synthesis of $[Co_2(4\text{-}pyrtet)(SO_4)(OH)(H_2O)]\bullet 1.5H_2O$ ($2\bullet 1.5H_2O$)

A mixture of cobalt sulfate heptahydrate (193 mg, 0.684 mmol), 4-pyridyltetrazole (50 mg, 0.342 mmol), and H_2O (10.00 g, 556 mmol) in the mole ratio 2.00:1.00:1626 was stirred briefly before heating to 170°C for 48 hours. Pink needle crystals of **2**, suitable for X-ray diffraction, were isolated in 20% yield. 3476(b), 3196(w), 2414(w), 1582(s), 1542(s), 1454(m), 1202(m), 1045(m), 987(m), 638(w).

6.4.1.3 Synthesis of $[Co_4(prztet)_6(SO_4)(H_2O)_2]$ (3)

A mixture of cobalt sulfate heptahydrate (193 mg, 0.684 mmol), 4-pyridyltetrazole (51 mg, 0.342 mmol), and H_2O (10.00 g, 556 mmol) in the mole ratio 2.00:1.00:1626 was stirred briefly before heating to 150°C for 48 hours. Orange block crystals of **3**, suitable for X-ray

diffraction, were isolated in 50% yield. IR (KBr pellet, cm^{-1}): 3422(b), 3005(s), 1625(s), 1425(m), 1401(m), 1157(m), 1105(m), 965(m), 678(w).

6.4.1.4 Synthesis of $[Co_3F_2(SO_4)(3\text{-pyrtet})_2(H_2O)_4]$ (4)

A mixture of cobalt sulfate heptahydrate (193 mg, 0.684 mmol), 3-pyridyltetrazole (50 mg, 0.342 mmol), 400µL HF (11.6 mmol) and H_2O (10.00 g, 556 mmol) in the mole ratio 2.00:1.00:33.9:1626 was stirred briefly before heating to 180°C for 48 hours. Purple block crystals of **4**, suitable for X-ray diffraction, were isolated in 30% yield. IR (KBr pellet, cm^{-1}): 3401(b), 1623(s) 1510(s), 1472(m), 1199(m), 1104(m), 834(s), 742(m).

6.4.1.5 Synthesis of $[Ni_3F_2(SO_4)(3\text{-pyrtet})_2(H_2O)_4]$ (5)

A mixture of nickel sulfate heptahydrate (192 mg, 0.684 mmol), 3-pyridyltetrazole (50 mg, 0.342 mmol), 300µL HF (8.7 mmol) and H_2O (10.00 g, 556 mmol) in the mole ratio 2.00:1.00:25.4:1626 was stirred briefly before heating to 180°C for 48 hours. Purple block crystals of **5**, suitable for X-ray diffraction, were isolated in 30% yield. IR (KBr pellet, cm^{-1}): 3402(b), 1577(s) 1482(s), 1423(m), 1257(m), 1084(m), 811(s), 720(m), 597(m).

6.4.1.6 Synthesis of $[Ni_5(3\text{-pyrtet})_4(SO_4)_2(OH)_2(H_2O)_2]\bullet 0.5H_2O$ (6•0.5H_2O)

A mixture of nickel sulfate heptahydrate (192 mg, 0.684 mmol), 3-pyridyltetrazole (50 mg, 0.342 mmol), and H_2O (10.00 g, 556 mmol) in the mole ratio 2.00:1.00:1626 was stirred briefly before heating to 150°C for 48 hours. Dark blue block crystals of **6**, suitable for X-ray diffraction, were isolated in 20% yield. IR (KBr pellet, cm^{-1}): 3454(b), 1433(m), 1138(m), 1077(s), 1054(s), 1022(m), 965(m) 822(w), 703(m).

6.4.1.7 Synthesis of $[Cu_3(OH)(H_2O)_3(3\text{-pyrHtet-}O)_3(SO_4)]$ (7)

A mixture of $Cu(SO_4)\cdot 5H_2O$ (171 mg, 0.684 mmol), 5-(3-pyridyl)tetrazole (50 mg, 0.342 mmol), HF (400µL) and H_2O (10.00 g, 556 mmol) in the mole ratio 2.00:1.00:0.58:1626 was stirred briefly before heating to 200°C for 48 hours (initial and final pH values of 1.1 and 1.0, respectively). Dark green block crystals of **7**, suitable for X-ray diffraction, were isolated in 50% yield. Anal. Cald. for $C_{18}H_{19}Cu_3N_{15}O_{11}S$: C, 25.6; H, 2.25; N, 24.9. Found: C, 25.2; H, 2.17; N, 24.8. IR (KBr pellet, cm^{-1}): 3415(b), 1428(m), 1144(m), 1095(s), 1062(s), 1018(m), 973(m) 819(w), 698(m).

6.4.1.8 Synthesis of $[Cu_3(OH)_2(H_2O)_3(3\text{-pyrtet})_2(SO_4)]$ (8)

A mixture of $Cu(SO_4)\cdot 5H_2O$ (171 mg, 0.684 mmol), 5-(3-pyridyl)tetrazole (50 mg, 0.342 mmol), and H_2O (10.00 g, 556 mmol) in the mole ratio 2.00:1.00:1626 was stirred briefly before heating to 135°C for 48 hours (initial and final pH values of 2.5 and 2.3, respectively). Dark blue block crystals of **8**, suitable for X-ray diffraction were isolated in 80% yield. Anal. Cald. for $C_{12}H_{16}Cu_3N_{10}O_9S$: C, 21.6; H, 2.40; N, 21.0. Found: C, 21.7; H, 2.55; N, 20.8. IR (KBr pellet, cm^{-1}): 3481(b), 3086(w), 2924(w), 1602(s), 1571(s), 1514(m), 1162(m), 1095(m), 1054(m), 618(w).

6.4.1.9 Synthesis of $[Me_2NH_2]$ $[Cu(2\text{-pyrtet})(SO_4)]$ (9)

The reaction of a solution of $Cu(SO_4)\cdot 5H_2O$ (183 mg, 0.732 mmol), 5-(2-pyridyl)tetrazole (55 mg, 0.377 mmol), dimethylammonium chloride (31 mg, 0.380 mmol), and H_2O (10.00 g, 556 mmol) in the mole ratio 2.00:1.00:1.00:1475 at 120°C for 64 h (initial and final pH values of 3.0 and 3.5, respectively) provided blue crystals of 3 in 55% yield. Anal. Cald. for $C_8H_{12}CuN_6O_4S$: C, 27.3; H, 3.41; N, 23.9; Found: C, 27.2; H, 3.27; N, 23.7. IR (KBr pellet, cm^{-1}): 3456(b), 2975(s), 1638(s), 1465(m), 1411(m), 1177(m), 1045(m), 945(m), 625(w).

6.4.1.10 Synthesis of $[Cu_4(pyrztet)_6(H_2O)_2(SO_4)]$ (10)

A mixture of $Cu(SO_4)\cdot 5H_2O$ (171 mg, 0.684 mmol), 2-tetrazole 5-yl pyrazine (52 mg, .342 mmol), and H_2O (10.00 g, 556 mmol) in the mole ratio 2.00:1.00:1626 was stirred briefly before heating to 135°C for 48 hours (initial and final pH values of 2.5 and 2.3, respectively). Dark blue block crystals of **4**, suitable for X-ray diffraction were isolated in 10% yield. Anal. Cald. for $C_{30}H_{22}Cu_4N_{36}O_6S$; C, 28.4; H, 1.73; N, 39.7. Found: C, 28.2; H, 1.89; N, 39.6. IR (KBr pellet, cm^{-1}): 3340(b), 1617(s) 1472(s), 1403(m), 1262(m), 1134(m), 802(s), 730(m), 597(m).

6.4.2 X-Ray Crystallography

Structural measurements were performed on a Bruker-AXS SMART-CCD diffractometer at low temperature (90 K) using graphite-monochromated Mo-K_α radiation (Mo K_α = 0.71073A°).[79] The data were corrected for Lorentz and polarization effects and absorption using SADABS.[80,81] The structures were solved by direct methods. All non-hydrogen atoms were refined anisotropically. After all of the non-hydrogen atoms had been located, the model was refined against $\mathbf{F}^2$, initially using isotropic and later anisotropic thermal displacement parameters. Hydrogen atoms were introduced in calculated positions and refined isotropically. Neutral atom scattering coefficients and anomalous dispersion corrections were taken from the *International Tables*, Vol. C. All calculations were performed using SHELXTL crystallographic software packages.[82]

Crystallographic details have been summarized in Tables 6.3 to 6.6. Atomic positional parameters, full tables of bond lengths and angles, and anisotropic temperature factors are available in the Supplementary Materials. Selected bond lengths and angles are given in Tables 6.4 and 6.6. Full tables of crystal parameters and experimental conditions, atomic positional

parameters and isotropic temperature factors, bond lengths and angles, anisotropic temperature factors, hydrogen atom coordinates, and torsion angles for **1–10** are available as Supplementary Materials.

Table 6.3: Summary of crystal data for the structures of $[Co(prztet)_2(H_2O)_2] \cdot 0.50\ H_2O$ (**1**), $[Co_2(4\text{-pyrtet})\ (SO_4)(OH)(H_2O)] \bullet 1.5H_2O$ (**2**$\bullet 1.5H_2O$), $[Co_4(prztet)_6(SO_4)(H_2O)_2]$ (**3**), $[Co_3F_2(SO_4)(3\text{-pyrtet})_2(H_2O)_4]$ (**4**), $[Ni_3F_2(SO_4)(3\text{-pyrtet})_2(H_2O)_4]$ (**5**), and $[Ni_5(3\text{-pyrtet})_4(SO_4)_2(OH)_2\ (H_2O)_2] \bullet 0.5\ H_2O$ (**6**$\bullet 0.5\ H_2O$).

Compound	**1**	**2**	**3**
Empirical formula	C10 H11 Co1 N12 O2.5	C6 H10 Co2 N5 O7.5 S1	C30 H22 Co4 N36 O6 S
Formula weight	389.23	420.09	1250.63
Temperature	98(2) K	98(2) K	98(2) K
Wavelength	0.71073 Å	0.71073 Å	0.71073 Å
Crystal system	Monoclinic	Triclinic	Monoclinic
Space group	C2/c	P-1	C2/c
Unit cell dimensions	a = 18.1688(15) Å	a = 6.7621(4) Å	a = 12.5253(12) Å
	b = 12.9055(10) Å	b = 8.0573(4) Å	b = 11.4852(11) Å
	c = 7.1092(6) Å	c = 13.2355(7) Å	c = 29.628(3) Å
	α= 90°.	α= 72.8670(10)°.	α= 90°.
	β= 102.997(2)°.	β= 89.4680(10)°.	β= 100.792(2)°.
	γ = 90°.	γ = 74.8760(10)°.	γ = 90°.
Volume	1624.2(2) Å3	663.47(6) Å3	4186.7(7) Å3
Z	4	1	4
Density (calculated)	1.702 Mg/m3	2.093 Mg/m3	1.984 Mg/m3
Absorption coefficient	1.104 mm-1	2.703 mm-1	1.704 mm-1
Final R indices [I>2sigma(I)]	R1 = 0.0342, wR2 = 0.0876	R1 = 0.0278, wR2 = 0.0775	R1 = 0.0567, wR2 = 0.1135
Compound	**4**	**5**	**6**
Empirical formula	C12 H16 Co3 F2 N10 O8 S	C12 H16 F2 N10 Ni3 O8 S	C24 H23 N20 Ni5 O12.5 S2
Formula weight	676.22	674.49	1148.21
Temperature	98(2) K	98(2) K	98(2) K
Wavelength	0.71073 Å	0.71073 Å	0.71073 Å
Crystal system	Orthorhombic	Orthorhombic	Monoclinic
Space group	Pnma	Pnma	P2(1)/c
Unit cell dimensions	a = 13.7639(6) Å	a = 13.6609(7) Å	a = 13.9261(11) Å
	b = 20.6295(9) Å	b = 20.4183(11) Å	b = 10.9466(9) Å
	c = 7.3285(3) Å	c = 7.2862(4) Å	c = 12.5532(10) Å
	α= 90°.	α= 90°.	α= 90°.
	β= 90°.	β= 90°.	β= 111.371(2)°.
	γ = 90°.	γ = 90°.	γ = 90°.
Volume	2080.87(15) Å3	2032.36(19) Å3	1782.1(2) Å3
Z	4	4	1
Density (calculated)	2.158 Mg/m3	2.204 Mg/m3	2.142 Mg/m3
Absorption coefficient	2.551 mm-1	2.942 mm-1	2.806 mm-1
Final R indices [I>2sigma(I)]	R1 = 0.0239, wR2 = 0.0621	R1 = 0.0241, wR2 = 0.0595	R1 = 0.0391, wR2 = 0.0745

Table 6.4: Selected bond lengths and angles for $[Co(prztet)_2(H_2O)_2] \cdot 0.50\ H_2O$ (**1**), $[Co_2(4\text{-pyrtet})(SO_4)(OH)(H_2O)] \bullet 1.5H_2O$ (**2**•1.5H_2O), $[Co_4(prztet)_6(SO_4)(H_2O)_2]$ (**3**), $[Co_3F_2(SO_4)(3\text{-pyrtet})_2(H_2O)_4]$ (**4**), $[Ni_3F_2(SO_4)(3\text{-pyrtet})_2(H_2O)_4]$ (**5**), and $[Ni_5(3\text{-pyrtet})_4(SO_4)_2(OH)_2\ (H_2O)_2] \bullet H_2O$ (**6**•0.5 H_2O).

1		2		3	
Co(1)-N(1)	2.0937(15)	Co(1)-O(90)	2.0097(17)	Co(1)-O(1)	2.038(3)
Co(1)-O(90)	2.1023(14)	Co(1)-O(1)	2.0430(16)	Co(1)-N(7)	2.099(3)
Co(1)-N(5)	2.1233(15)	Co(1)-N(5)	2.1240(18)	Co(1)-N(1)	2.119(3)
N(1)-Co(1)-N(1)	180	Co(1)-O(5)	2.1439(14)	Co(1)-O(90)	2.145(3)
O(90)-Co(1)-O(90)	180	Co(1)-N(4)	2.2561(18)	Co(1)-N(13)	2.172(3)
N(5)-Co(1)-N(5)	180	Co(1)-N(3)	2.2884(18)	Co(1)-N(11)	2.181(3)
		Co(2)-N(2)	2.0796(18)	Co(2)-N(17)	2.097(3)
		Co(2)-O(5)	2.0813(14)	Co(2)-N(8)	2.113(3)
		Co(2)-O(2)	2.1029(15)	Co(2)-N(18)	2.117(3)
		Co(3)-O(5)	2.0569(14)	Co(2)-N(2)	2.123(3)
		Co(3)-N(1)	2.0857(18)	Co(2)-N(14)	2.174(3)
		Co(3)-O(3)	2.1344(15)	Co(2)-N(5)	2.202(3)
		O(90)-Co(1)-O(1)	176.69(7)	N(7)-Co(1)-O(90)	177.04(12)
		N(5)-Co(1)-O(5)	178.00(6)	N(1)-Co(1)-N(11)	167.37(12)
		N(4)-Co(1)-N(3)	176.11(6)	N(8)-Co(2)-N(5)	169.61(12)
		N(2)-Co(2)-N(2)	180	N(18)-Co(2)-N(2)	165.78(12)
		O(5)-Co(2)-O(5)	180	N(17)-Co(2)-N(14)	170.90(12)
		N(1)-Co(3)-N(1)	180.00(5)		
		O(2)-Co(2)-O(2)	180		
		O(5)-Co(3)-O(5)	180		
		O(3)-Co(3)-O(3)	180.00(8)		

4		5		6	
Co(1)-F(1)	2.0263(14)	Ni(1)-F(1)	2.0014(15)	Ni(1)-O(6)	2.025(2)
Co(1)-O(91)	2.0274(19)	Ni(1)-O(90)	2.013(2)	Ni(1)-N(6)	2.054(3)
Co(1)-O(90)	2.0838(19)	Ni(1)-O(91)	2.049(2)	Ni(1)-N(1)	2.064(3)
Co(1)-O(1)	2.1095(17)	Ni(1)-O(1)	2.0703(18)	Ni(1)-N(10)	2.079(3)
Co(1)-N(1)	2.1331(15)	Ni(1)-N(1)	2.0857(15)	Ni(1)-N(5)	2.181(3)
Co(2)-F(1)	2.0633(9)	Ni(1)-N(1)	2.0857(15)	Ni(1)-O(1)	2.184(2)
Co(2)-O(92)	2.0662(13)	Ni(2)-F(1)	2.0205(9)	Ni(2)-O(6)	2.018(2)
Co(2)-O(3)	2.0794(13)	Ni(2)-N(5)	2.0414(15)	Ni(2)-O(6)	2.019(2)
Co(2)-N(5)	2.0917(14)	Ni(2)-O(2)	2.0522(13)	Ni(2)-N(2)	2.023(3)
Co(2)-F(2)	2.0990(10)	Ni(2)-O(92)	2.0574(15)	Ni(2)-N(2)	2.023(3)
Co(2)-N(2)	2.1382(15)	Ni(2)-F(2)	2.0633(10)	Ni(2)-O(4)	2.070(2)
		Ni(2)-N(2)	2.0885(16)	Ni(2)-O(4)	2.070(2)
		F(1)-Ni(1)-O(90)	174.92(8)	Ni(3)-O(3)	2.055(2)
		O(91)-Ni(1)-O(1)	178.31(8)	Ni(3)-O(90)	2.058(3)
		O(2)-Ni(2)-O(92)	178.06(6)	Ni(3)-O(6)	2.059(2)
		N(1)-Ni(1)-N(1)	165.66(9)	Ni(3)-O(2)	2.067(2)
		F(1)-Ni(2)-N(5)	173.04(5)	Ni(3)-N(7)	2.076(3)
				Ni(3)-N(3)	2.166(3)
				N(6)-Ni(1)-N(1)	176.05(12)
				O(6)-Ni(1)-N(10)	173.02(11)
				N(5)-Ni(1)-O(1)	169.43(10)
				O(6)-Ni(2)-O(6)	179.999(1)
				N(2)-Ni(2)-N(2)	179.998(1)
				O(4)-Ni(2)-O(4)	180
				O(90)-Ni(3)-O(6)	175.13(10)
				O(3)-Ni(3)-O(2)	170.63(10)

Table 6.5: Summary of crystal data for the structures of $[Cu_3(OH)(H_2O)_3(3\text{-pyrHtet-O})_3(SO_4)]$ (**7**), $[Cu_3(OH)_2(H_2O)_3(3\text{-pyrtet})_2(SO_4)]$ (**8**), $(Me_2NH_2)[Cu(2\text{-pyrtet})(SO_4)]$ (**9**), and $[Cu_4(pyrztet)_6(H_2O)_2(SO_4)]$ (**10**).

Compound	7	8	9	10
FW	884.2	667.04	351.86	1250.93
Crystal System	Trigonal	Orthorhombic	Monoclinic	Monoclinic
Space group	P-3	Pnma	P2(1)/n	C2/c
a (Å)	14.929(2)	13.721(5)	11.3959(9)	12.5217(18)
b (Å)	14.929(2)	20.601(8)	10.4591(8)	11.4818(17)
c (Å)	7.2554(15)	7.034(3)	12.0996(9)	29.605(4)
α (°)	90	90	90	90
β (°)	90	90	117.506(10)	100.758
γ (°)	120	90	90	90
V ($Å^3$)	1400.4(4)	1988.3(14)	12.7914(17)	4181.5(11)
Z	2	4	4	4
D_{calc} (mg/m^3)	2.002	2.235	1.827	2.022
μ (mm-1)	2.42	3.362	1.895	2.155
T (K)	98(2)	98(2)	98(2)	98(2)
Wavelength (Å)	0.71073	0.71073	0.71073	0.71073
$R1 = \sum\|\|F_o\| - \|F_c\|\|/\sum\|F_o\|$	0.0438	0.05	0.0446	0.0594
$wR2= [\sum[w(F_o^2 - F_c^2)^2]/\sum w(F_o^2)^2]^{1/2}$	0.1761	0.1357	0.0979	0.1714

Table 6.6: Selected Bond Lengths [Å] and Angles (deg) for $[Cu_3(OH)(H_2O)_3(3\text{-pyrHtet-}O)_3(SO_4)]$ (**7**), $[Cu_3(OH)_2(H_2O)_3(3\text{-pyrtet})_2(SO_4)]$ (**8**), $(Me_2NH_2)[Cu(2\text{-pyrtet})(SO_4)]$ (**9**) and $[Cu_4(pyrztet)_6(H_2O)_2(SO_4)]$ (**10**) .

7		**9**	
Cu(1)-N(1)	1.932(6)	Cu(1)-O(1)	1.954(2)
Cu(1)-O(1)	1.959(6)	Cu(1)-N(4)#1	1.995(2)
Cu(1)-N(2)#1	1.979(7)	Cu(1)-N(2)	2.012(2)
Cu(1)-O(2)	2.001(2)	Cu(1)-O(3)#2	2.192(2)
Cu(1)-O(3)	2.400(6)	Cu(1)-(O2)	2.8041
Cu(1)-O(4)	2.391(7)	Cu(1)-N(1)	2.037(2)
N(1)-Cu(1)-N(2)#1	175.6(3)	N(4)#1-Cu(1)-N(1)	170.96(10)
O(1)-Cu(1)-O(2)	175.5(3)	O(1)-Cu(1)-N(2)	166.01(9)
O(4)-Cu(1)-O(3)	172.2(2)		
8		**10**	
Cu(1)-O(1)	1.940(3)	Cu(1)-N(12)	2.162(4)
Cu(1)-O(2)	1.974(3)	Cu(1)-N(18)	2.183(4)
Cu(1)-N(1)	1.988(4)	Cu(1)-O(1)	2.028(3)
Cu(1)-N(2)	2.056(4)	Cu(1)-N(7)	2.098(4)
Cu(1)-O(5)	2.454	Cu(1)-N(1)	2.126(4)
Cu(1)-O(7)	2.477	Cu(1)-O(3)	2.149(4)
Cu(2)-O(6)	2.842	Cu(2)-N(13)	2.093(4)
Cu(2)-O(1)	1.933(4)	Cu(2)-N(8)	2.116(4)
Cu(2)-O(3)	1.938(5)	Cu(2)-N(14)	2.118(4)
Cu(2)-N(3)	2.038(4)	Cu(2)-N(2)	2.127(4)
Cu(2)-O(4)	2.137(5)	Cu(2)-N(17)	2.171(4)
N(3)-Cu(2)-N(3)#1	160.4(2)	Cu(2)-N(5)	2.203(4)
O(2)-Cu(1)-N(2)	163.96(14)	N(1)-Cu(1)-N(18)	167.32(16)
O(1)-Cu(2)-O(3)	172.78(19)	O(1)-Cu(1)-N(12)	170.78(16)
O(1)-Cu(1)-N(1)	175.19(16)	N(7)-Cu(1)-O(3)	177.27(16)
		N(8)-Cu(2)-N(5)	169.63(16)
		N(14)-Cu(2)-N(2)	165.48(17)
		N(13)-Cu(2)-N(17)	170.83(16)

6.5 Supplementary Materials

Additional material available from the Cambridge Crystallographic Data Centre, CCDC No. CCDC 881492-881497, comprises the final atomic coordinates for all atoms, thermal parameters, and a complete listing of bond distances and angles, for compounds **1-10**, respectively.

6.6 Acknowledgements

This work was funded by a grant from the National Science Foundation (CHE-0907787). KRD thanks the National Science Foundation for funds to purchase the SQUID magnetometer and sponsorship of personnel (AP).

6.7 References

1. Janiak, C., *Dalton Trans.* **2003**, 2781 and references therein.
2. Chen, B.; Ockwig, N.W.; Millward, A.R.; Contreras, D.S.; and Yaghi, O.M., *Angew. Chem., Int. Ed*. **2005**, *44*, 4745.
3. Rowsell, J.L.C.; and Yaghi, O.M., *Angew. Chem., Int. Ed*. **2005**, *44*, 4670.
4. D. Bradshaw, D.; Claridge, J.B.; Cussen, E.J.; Prior, T.J.; and Rosseinsky, M.J., *Acc. Chem. Res*. **2005**, *38*, 273.
5. Rosseinsky, M.J., *Microporous Mesoporous Mater*. **2004**, *73*, 15.
6. Cingolani, A.; Galli, S.; Masciocchi, N.; Pandolfo, L.; Pettinari, C.; and Sironi, A., *J. Am. Chem. Soc*. **2005**, *127*, 6144.
7. Ohmori, O.; Kawano, M.; and Fujita, M., *Angew. Chem., Int. Ed*. **2005**, *44*, 1962.
8. Lee, E.Y.; Jang, S.Y.; and Suh, M.P., *J. Am. Chem. Soc*. **2005**, *127*, 6374.
9. Noro, S.-I.; Kitagawa, S.; Kondo, M.; and Seki, K., *Angew. Chem., Int. Ed*. **2000**, *39*, 2081.
10. Wang, Z.; Zhang, B.; Kurmoo, M.; Green, M.A.; Fujiwara, H.; Otsuka, T.; and Kobayashi, H., *Inorg. Chem*. **2005**, *44*, 1230.
11. Kim, H.; and Suh, M.P., *Inorg. Chem*. **2005**, *44*, 810.
12. Sudik, A.C.; Millward, A.R.; Ockwig, N.W.; Cote, A.P.; Kim, J.; and Yaghi, O.M., *J. Am. Chem. Soc*. **2005**, *127*, 7110.
13. Kitaura, R.; Kitagawa, S.; Kubtoa, Y.; Kobayashi, T.C.; Kindo, K.; Mita, Y.; Matsuo, A.; Kobayashi, M.; Chang, H.-C.; Ozawa, T.C.; Suzuki, M.; Sakata, M.; and Takata, M., *Science* **2002**, *298*, 2358.

14. Bradshaw, D; Prior, T.J.; Cussen, E.J.; Claridge, J.B.; and Rosseinsky, M.J., *J. Am. Chem. Soc*. **2004**, *126*, 6106.

15. Kepert, C.J.; Prior, T.J.; and Rosseinsky, M.J., *J. Am. Chem. Soc*. **2000**, *122*, 5158.

16. Halder, G.J.; Kepert, C.J.; Moubaraki, B.; Murray, K.S.; and Cashion, J.D., *Science* **2002**, *298*, 1762.

17. (a) Ngo, H.L.; Hu, A.; and Lin, W., *J. Mol. Catal. A: Chem*. **2004**, *215*, 177; (b) Evans, O.R.; Ngo, H.L.; and Lin, W., *J. Am. Chem. Soc*. **2001**, *123*, 10395.

18. Sanchez, C.; Lebeau, B.; Chaput, F.; and Boilet, J.P., *Adv. Mater*. **2003**, *15*, 1969.

19. Evans, O.R.; and Lin, W., *Chem. Mater*. **2001**, *13*, 3009.

20. Jannasch, P., Curr. Opin. Colloid Interface Sci. **2003**, *8*, 96.

21. Javaid, A.; Hughey, M.P.; Varutbangkul, V.; and Ford, D.M., *J. Membr. Sci*. **2001**, *187*, 141.

22. Honma, I.; Nomura, S.; and Nakajima, H., *J. Membr. Sci*. **2001**, *1*, 185.

23. Rowsell, J.L.C.; Millward, A.R.; Park, K.S.; and Yaghi, O.M., *J. Am. Chem. Soc*. **2004**, *126*, 5666.

24. Kitagawa, S.; and Noro, S., *Compr. Coord. Chem*. II **2004**, *7***,** 231.

25. Yaghi, O.M.; O'Keeffe, M.; Ockwig, N.W.; Chae, H.K.; Eddaoudi, M.; and Kim, J., *Nature* **2003**, *423*, 705.

26. James, S.L., *Chem. Soc. Rev*. **2003**, *32*, 276.

27. Rao, C.N.R.; Natarajan, S.; and Vaidhyanathan, R., *Angew. Chem., Int. Ed*. **2005**, *43*, 1466.

28. Kitagawa, S.; Kitaura, R.; and Noro, S.-I., *Angew. Chem., Int. Ed*. **2004**, *43*, 2334.

29. Papaefstathiou, G.S.; and MacGillivray, L.R., *Coord. Chem. Rev*. **2003**, *246*, 169.

30. Eddaoudi, M.; Moler, D.B.; Li, H.; Chen, B.; Reineke, T.M.; O'Keeffe, M.; Yaghi, O.M., *Acc. Chem. Res*. **2001**, *34*, 319.

31. Finn, R.C.; Haushalter, R.C.; and Zubieta, J., *Prog. Inorg. Chem*. **2003**, *51*, 421.

32. Vioux, A.; LeBideau, J.; Mutin, P.H.; and Leclercq, D., *Top. Curr. Chem*. **2004**, 232, 145.

33. Clearfield, A., Curr. Opin. Solid State Mater. Sci. **2003**, *6*, 495.

34. Clearfield, A., *Prog. Inorg. Chem*. **1998**, *47*, 371.

35. Alberti, G. in *Comprehensive Supramolecular Chemistry*, J.L. Atwood, J.E.D. Davies, D.D. MacNicol and F. Vogtle, ed., Pergamon Press, New York, **1996** vol. 7, G. Alberti, T. Bein, ed. 151.

36. Ferey, G., *Chem. Mater*. **2001**, *13*, 3084.

37. Farrusseng, D.; Aguado, S.; Pinel, C., *Angew. Chem., Int. Ed*. **2009**, *48*, 7502–7513.

38. Zheng, B.; Bai, J.; Duan, J.; Wojtas, L.; and Zaworotko, M.J., *J. Am. Chem. Soc*. **2011**, *133*, 748.

39. Sumida, K.; Brown, C.R.; Herm, Z.R.; Chavan, S.; Bordiga, S.; and Long, J.R., *Chem. Commun*. **2011**, *47*, 1157.

40. Metal phosphonate chemistry, A. Clearfield and K.D. Demadis, eds., RSC Publishing, Cambridge, UK, **2012**.

41. Ferey, G.; Serre, C.; Devic, T.; Maurin, G.; Jobic, H.; Llewellyn, P.L.; De Weireld, G.; Vimont, A.; Daturi, M.; and Chang, J.-S., *Chem. Soc. Rev*. **2011**, *40*, 550.

42. Hijikata, Y.; Horike, S.; Sugimoto, M.; Sato, H.; Matsuda, R.; and Kitagawa, S., *Chem.–Eur. J*. **2011**, *17*, 5138.

43. Noro, S.; and Kitagawa, S., in *Supramolecular Chemistry of Organic-Inorganic Hybrid Materials*, K. Rurack and R. Martinez-Manez, ed., **2010**, 235.

44. Bloch, E.D.; Britt, D.; Lee, C.; Doonan, C.J.; Uribe-Romo, F.J.; Furukawa, H.; Long, J.R.; and Yaghi, O.M., *J. Am. Chem. Soc*. **2010**, *132*, 14382

45. Moulton, B.; and Zaworotko, M.J., *Curr. Opin. Solid State Mater. Sci*. **2002**, *6*, 117.

46. Wang, C.; and Lin, W., *J. Am. Chem. Soc.* **2011**, *133*, 4232–4235.

47. Choi, H.J.; Dinca; and Long, J.R., *J. Am. Chem. Soc.* **2008**, *130*, 7848.

48. Sava, D.F.; Kravtsov, V. Ch.; Nouar, F.; Wojtas, L.; Eubank, J.F.; and Eddaoudi, M., *J. Am. Chem. Soc.* **2008**, *130*, 3768.

49. Beckmann, U.; and Brooker, S., *Coord. Chem. Rev*. **2003**, *245*, 17.

50. Haasnoot, J.G., *Coord. Chem. Rev*. **2000**, *200*, 131.

51. Hellyer, R.M.; Larsen, D.S.; and Brooker, S., *Eur. J. Inorg. Chem*. **2009**, 1162.

52. Zhang, J.-P.; and Chen, X.-M., *Chem. Commun*. **2006,** 1689.

53. Steel, P.J., *Coord. Chem. Rev*. **1990**, *106*, 227.

54. Potts, K.T., *Chem. Rev*. **1961**, *61*, 87.

55. Dawe, L.N.; and Thompson, L.K., *Dalton Trans*. **2008**, 3610.

56. Zhang, J.-P.; Lin, Y.-Y.; Huang, X.-C.; and Chen, X.-M., *J. Am. Chem. Soc*. **2005**, *127*, 5495.

57. Zhang, J.-P.; Zheng, S.-L.; Huang, X.-C; and Chen, X.-M., *Angew. Chem., Int. Ed*. **2004**, *43*, 206.

58. Ferrer, S.; Lloret, F.; Bertomeu, I.; Alzuet, G.; Borras, J.; Garcia-Granda, S.; Liu-González, M.; and Haasnoot, J.G., *Inorg. Chem*. **2002**, *41*, 5821.

59. Zhou, J.-H.; Cheng, R.-M.; Song, Y.; Li, Y.-Z.; Yu, Z.; Chen, X.-T.; Xue, Z.-L.; and You, X.-Z., *Inorg. Chem*. **2005**, *44*, 8011 and references therein.

60. Zhang, J.-P.; Lin, Y.-Y.; Zhang, W.-X.; and Chen, X.-M., *J. Am. Chem. Soc*. **2005**, *127*, 14162.

61. Zhang, D.-C.; Lu, W.-G.; Jiang, L.; Feng, X.-L.; and Lu, T.-B., *Cryst. Growth Des*. **2010**, *10*, 739.

62. Ouellette, W.; Jones, S.; and Zubieta, J., *CrystEngComm*. **2011**, *13*, 4457.

63. Ouellette, W.; Darling, K.; Prosvirin, A.; Whitenack, K.; Dunbar, K.R.; and Zubieta, J., *Dalton Trans.* **2011**, *40*, 12288.

64. Hagrman, P.J.; Bridges, C.; Greedan, J.E.; Zubieta, J., *J. Chem. Soc. Dalton Trans.* **1999**, 2901.

65. Hagrman, D.; and Zubieta, J., *Chem. Commun.* **1998**, 2005.

66. Ouellette, W.; Yu, M.H.; O'Connor, C.J.; Hagrman, D.; and Zubieta, J., *Angew. Chem., Int. Ed*. **2006**, *45*, 3497.

67. Ouellette, W.; Prosvirin, A.V.; Valeich, J.; Dunbar, K.R.; and Zubieta, J., *Inorg. Chem*. **2007**, *46*, 9067.

68. Ouellette, W.; Galán-Mascarós, J.R.; Dunbar, K.R.; and Zubieta, J., *Inorg. Chem*. **2006**, *45*, 1909.

69. Ouellette, W.; Prosvirin, A.V.; Chieffo, V.; Dunbar, K.R.; Hudson, B.; and Zubieta, J., *Inorg. Chem*. **2006**, *45*, 9346.

70. Chesnut, D.J.; Kusnetzow, A.; Birge, R.; and Zubieta, J., *Inorg. Chem*. **1999**, *38*, 5484.

71. Ouellette, W.; Hudson, B.S.; and Zubieta, J., *Inorg. Chem*. **2007**, *46*, 4887.

72. Ouellette, W.; Liu, H.; O'Connor, C.J.; and Zubieta, J., *Inorg. Chem*. **2009**, *48*, 4655.

73. Ouellette, W.; and Zubieta, J., *Chem. Commun*. **2009**, 4533.

74. Ouellette, W.; Prosvirin, A.V.; Whitenack, K.; Dunbar, K.R.; and Zubieta, J., *Angew. Chem., Int. Ed.* **2009**, *48*, 2140.

75. Ouellette, W.; Jones, S; and Zubieta, J., *CrystEngComm*. 2011, *13*, 4457.

76. (a) Demko, P.Z.; and Sharpless, K.B., *J. Org. Chem.* **2001**, *66*, 7945; (b) Hirno, F.; Demko, P.Z.; Noodleman, L.; and Sharpless, K.B., *J. Am. Chem. Soc.* **2002**, *124*, 12210.

77. Tao, J.; Ma, Z.-J.; Huang, R.-B.; and Zhang, L.-S., *Inorg. Chem.* **2004**, *43*, 6133.

78. Chermahini, A.N.; Teimouri, A.; and Moaddeli, A., *Heteroatom Chem.* **2011**, *22*, 168.

79. SMART, Data Collection Software, version 5.630, Bruker-AXS Inc., Madison, WI, **1997-2002**.

80. SAINT Plus, Date Reduction Software, version 6.45A, Bruker-AXS Inc., Madison, WI, **1997-2002**.

81. G.M. Sheldrick, SADABS, University of Göttingen, Göttingen, Germany, **1996**.

82. SHELXTL PC, version 6.12, Bruker-AXS Inc., Madison, WI, **2002**.

83. Stein, A.; Keller, S.W.; Mallouk, T.E., *Science* **1993**, *259*, 1558.

84. Gopalakrishnan, J., *Chem. Mater*. **1995**, *7*, 1265.

85. Weller, M.; and Dann, S.E., *Curr. Opin. Solid State Mater. Sci*. **1998**, *3*, 137.

86. Gopalakrishnan, J.; Bhuvanesh, N.S.P.; and Rangan, K.K., *Curr. Opin. Solid State Mater. Sci*. **1996**, *1*, 285.

87. Zubieta, J., Solid state methods, hydrothermal in, *Comprehensive Coordination Chemistry II* **2003**, *1*, 697.

88. Zhang, X.-M., *Coord. Chem. Rev.* **2005**, *249*, 1201.

89. Gillard, R.D., *Coord. Chem. Rev.* **1975**, *16*, 67.

90. Bugalho, S.C.S.; Macoas, E.M.S.; Cristiano, M.L.S.; and Fausto, R., *Phys. Chem. Chem. Phys.* **2001**, *3*, 3541.

91. Huang, X.-C.; Luo, W.; Shen, X.-F.; Lin, X.-J.; and Li, D., *Chem. Commun.* **2008**, 3995.

92. Rivera-Carrillo, M.; Chakraborty, I.; and Raptis., R.G., *Cryst. Growth Des*. **2010**, *10*, 2606.

93. Di Nicola, C.; Garau, F.; Monari, M.; Pandolfo, L.; Pettinari, C.; and Pettinari, R., *Cryst. Growth Des.* **2010**, *10*, 3120.

94. Li, H.-X.; Ren, Z.-G.; Liu, D.; Chen, Y.; Lang, J.-P.; Cheng, Z.-P.; Zhu, X.-L.; and Abrahams, B. F., *Chem. Commun.* **2010**, *46*, 8430.

95. Zhou, Q.-J.; Liu, Y.-Z.; Wang, R.-L.; Fu, J.-W.; Xu, J.-Y.; and Lou, J.-S., *J. Coord. Chem.* **2009**, *62*, 311.

96. Contadi, S.; Di Nicola, C.; Garau, F.; Karabach, Y. Yu.; Martins, L.M.D.R.S.; Monari, M.; Pandolfo, L.; Pettinari, C.; and Pombeiro, A.J.L., *Dalton Trans*. **2009**, 4928.

97. Rivera-Carrillo, M.; Chakraborty, I.; Mezei, G.; Webster, R.D.; and Raptis, R.G., *Inorg. Chem.* **2008**, *47*, 7644.

98. Casarin, M.; Cingolani, A.; di Nicola, C.; Falcomer, D.; Monari, M.; Pandolfo, L.; and Pettinari, C., *Cryst. Growth Des*. **2007**, *7*, 676.

99. Mezei, G.; McGrady, J.E.; and Raptis, R.G., *Inorg. Chem*. **2005**, *44*, 7271.

100. Casarin, M.; Corvaja, C.; di Nicola, C.; Falcomer, D.; Franco, L.; Monari, M.; Pandolfo, L.; Pettinari, C.; and Piccinelli, F., *Inorg. Chem*. **2005**, *44*, 6265.

101. Mezei, G.; Rivera-Carrillo, M.; and Raptis, R.G., *Inorg. Chim. Acta* **2004**, *357*, 3721.

102. Casarin, M.; Corvaja, C.; di Nicola, C.; Falcomer, D.; Franco, L.; Monari, M.; Pandolfo, L.; Pettinari, C.; Piccinelli, F.; and Tagliatesta, P., *Inorg. Chem*. **2004**, *43*, 5865.

103. Shen, W.-Z.; Yi, L.; Cheng, P.; Yan, S.-P.; Liao, D.-Z.; and Jiang, Z.-H., *Inorg. Chem. Commun.* **2004**, *7*, 819.

104. Boca, R.; Dlhan, L.; Mezei, G.; Ortiz-Peŕez, T.; Gaptis, R.; Telser, J., *Inorg. Chem*. **2003**, *42*, 5801

105. Angaridis, P.A.; Baran, P.; Boca, R.; Cervantes-Lee, F.; Haase, W.; Mezei, G.; Raptis, R.G.; and Werner, R., *Inorg. Chem*. **2002**, *41*, 2219.

106. Kamiyama, A.; Kajiwara, T.; and Ito, T., *Chem. Lett*. **2002**, 980.

107. Angaroni, M.; Ardizzoia, G.A.; Beringhelli, T.; La Monica, G.; Gatteschi, D.; Masciocchi, N.; and Moret, M.J., *Chem. Soc., Dalton Trans*. **1990**, 3305.

108. Sakai, K.; Yamada, Y.; Tsubomura, T.; Yabuki, M.; and Yamaguchi, M., *Inorg. Chem.* **1996**, *35*, 522.

109. Hulsbergen, F.B.; ten Hoedt, R.W.M.; Verschoor, J.; Reedijk, J.; and Spek, A.L.J., *J. Chem. Soc., Dalton Trans*. **1983**, 539.

110. Wu, X.-Y.; Kuang, X.-F.; Zhao, Z.-G.; Chen, S.-C.; Xie, Y.-M.; Yu, R.-M.; and Lu., C.-Z., *Inorg. Chim. Acta* **2010**, *363*, 1236.

111. Wang, Y.; Cheng, P.; Song, Y.; Liao, D.-Z.; and Yan., S.-P., *Chem. Eur. J.* **2007**, *13*, 8131.

112. Zhai, Q.; Wu, X.; Chen, S.; Chen, L.; Lu C., *Inorg. Chim. Acta* **2007**, *360*, 3484.

113. Ferrer, S.; Aznar, E.; Lloret, F.; Castiñeiras, A.; and Liu-Gonzaĺez, M., *Inorg. Chem*. **2007**, *46*, 372.

114. Lider, E.V.; Peresypkina, E.V.; Smolentsev, A.I.; Elokhina, N.; Yaroshenko, T.I.; Virovets, A.V.; Ikorskii, V.N.; and Lavrenova, L.G., *Polyhedron* **2007**, *26*, 1612.

115. Ding, B.; Yi, L.; Cheng, P.; Liao, D.-Z.; and Yan, S.-P., *Inorg. Chem*. **2006**, *45*, 5799.

116. Bichay, M.; Fronabarger, J.W.; Gilardi, R.; Butcher, R.J.; Sanborn, W.B.; Sitzmann, M.E.; and Williams, M. D., *Tetrahedron Lett*. **2006**, *47*, 6663.

117. Lysenko, A.B.; Govor, E.V.; Krautscheid, H.; and Domasevitch, K.V., *Dalton Trans*. **2006**, 3772.

118. Zhai, Q.-G.; Lu, C.-Z.; Chen, S.-M.; Xu, X.-J.; and Yang., W.-B., *Cryst. Growth Des*. **2006**, *6*, 1393.

119. Virovets, A.V.; Podberezskaya, N.V.; and Lavrenova, L.G., *J. Struct. Chem*. **1997**, *38*, 532.

120. Liu, J.-C.; Guo, G.-C.; Huang, J.-S.; and You, X.-Z., *Inorg. Chem*. **2003**, *42*, 235.

121. Ferrer, S.; Lloret, F.; Bertomeu, I.; Alzuet, G.; Borraś, J.; García- Granda, S.; Liu-Gonzaĺez, M.; and Haasnoot, J., *Inorg. Chem*. **2002**, *41*, 5821.

122. Ferrer, S.; Haasnoot, J.G.; Reedijk, J.; Müller, E.; Biagini-Cingi, M.; Lanfranchi, M.; Manotti-Lanfredi, A. M.; and Ribas, *J. Inorg. Chem*. **2000**, *39*, 1859.

123. Zhou, J.-H.; Cheng, R.-M.; Song, Y.; Li, Y.-Z.; Yu, Z.; Chen, X.-T.; Xue, Z.-L.; and You, X.-Z., *Inorg. Chem*. **2005**, *44*, 8011.

124. Koper, P.; Mrozinski, J.; Dolezal, K.; Langer, V.; Boca, R.; Bienko, A.; and Pochaba, A., *Eur. J. Inorg. Chem*. **2009**, 5475.

125. Piñero, D.; Baran, P.; Boca, R.; Herchel, R.; Klein, M.; Raptis, R. G.; Renz, F.; and Sanakis, Y., *Inorg. Chem*. **2007**, *46*, 10981.

126. Figuerola, A.; Tangoulis, V.; Ribas, J.; Hartl, H.; Brudgam, I.; Maestro, M.; and Diaz, C., *Inorg. Chem*. **2007**, *46*, 11017.

127. Tsukerblat, B.; Tarantul, A.; and Muller, A., *Inorg. Chem*. **2007**, *46*, 161.

128. Psycharis, V.; Raptopoulou, C.P.; Boudalis, A.K.; Sanakis, Y.; Fardis, M.; Diamantopoulos, G.; and Papavassiliou, G., *Eur. J. Inorg. Chem*. **2006**, 3710.

129. Boudalis, A.K.; Sanakis, Y.; Dahan, F.; Hendrich, M.; and Tuchagues, J.P., *Inorg. Chem*. **2006**, *45*, 443.

130. Berry, J.F.; Cotton, F.A.; Liu, C.Y.; Lu, T.B.; Murillo, C.A.; Tsukerblat, B.S.; Villagran, D.; and Wang, X.P., *J. Am. Chem. Soc*. **2005**, *127*, 4895.

131. Sanakis, Y.; Macedo, A.L.; Moura, I.; Papaefthymiou, V.; and Punk, E., J. *Am. Chem. Soc*. **2000**, 122, 11855.

132. Gatteschi, D.; Sessoli, R.; Plass, W.; Müller, A.; Krickemeyer, E.; Meyer, J.; Sölter, D.; and Adler, P., *Inorg. Chem*. **1996**, *35*, 1926.

133. Ferrer, S.; Lloret, F.; Pardo, E.; Clemente-Juan, J.M.; Liu-Gonzalez, M.; and Garcia-Granda, S., *Inorg. Chem*. **2012**, *51*, 985.

134. (a) Afrati, T.; Dendrinou-Samara, C.; Raptopoulou, C.; Terzis, A.; Tangoulis, V.; Kessissoglou, D.P., *Dalton Trans*. **2007**, 5156.

135. Liu, X.; de Miranda, M.P.; McInnes, E.J.L.; Kilner, C.A.; and Halcrow, M.A., *J. Chem. Soc., Dalton Trans*. **2004**, 59.

136. Yoon, J.; Mirica, L.M.; Stack, T.D.P.; and Solomon, E.I., *J. Am. Chem. Soc*. **2004**, *126*, 12586.

137. Tsukerblat, B.S.; Kuyavskaya, B.Y.; Belinskii, M.I.; Ablov, A.V.; Novotortsev, V.M.; and Kalinnikov, V.T., *Theor. Chim. Acta* **1975**, *38*, 131.

138. Moriya, T., *Phys. Rev. Lett*. **1960**, *4*, 228.

139. Ferrer, S.; Lloret, F.; Bertomeu, I.; Alzuet, G.; Borras, J.; Garcia-Granda, S.; Liu-Gonzalez, M.; and Haasnoot, J.G., *Inorg. Chem.* **2002**, *41*, 5821-5830.

140. Maeyer, J.T.; Johnson, T.J.; Smith, A.K.; Borne, B.D.; Pike, R.D.; Pennington, W.T.; Krawiec, M.; and Rheingold, A.L., *Polyhedron* **2003**, *22*, 419.

141. Bacchi, A.; Carcelli, M.; Pelizzi, G.; Solinas, C.; and Sorace, L., *Inorg. Chim. Acta* **2006**, *359*, 2275.

142. Kong, D.; Li, Y.; Ouyang, X.; Prosvirin, A.V.; Zhao, H.; Ross, Jr., J.R.; Dunbar, K.D.; and Clearfield, A., *Chem. Mater.* **2004**, *16*, 3020.

143. Ouellette, W.; Prosvirin, A.V.; Chieffo, V.; Dunbar, K.R.; Hudson, B.; and Zubieta, J., *Inorg. Chem.* **2006**, *45*, 9346.

Chapter 7: Solid State Coordination Chemistry of Metal-Azolate Compounds: Structural Consequences of Incorporation of Phosphate Components in the Co(II)/4-Pyridyltetrazolate/Phosphate System

7.1 Introduction

As stated in Chapter 1 of this work, metal organic frameworks are enjoying widespread contemporary interest by virtue of their applications in areas of catalysis, optical materials, membranes, and sorption.[1-22] The diversity of the properties of these materials reflects a vast compositional range, and provides potential for design of novel functional materials where properties from both the inorganic and organic realms can combine in a complimentary fashion.[23,24] This combination of features unique to both the inorganic and organic components can lead to unusual structures with novel properties and provides an avenue for design of potentially multifunctional materials.

In such a design, metal atoms or clusters serve as nodes from which flexible organic ligands act as tethers. A variety of organic linkers have been investigated, with materials featuring carboxylate and pyridine tethers showing the most significant development.[25-40] In designing multifunctional materials, it can be advantageous to investigate the coordination chemistry of ligands exhibiting an ability to bridge metal ions to afford polynuclear compounds, such as the polyazaheteroaromatic family of which pyrazole, imidazole, triazole, and their derivatives are representative. Recent investigations of the coordination compounds of azole-containing linkers have resulted in complexes that exhibit interesting properties due to the ability of the azolate ligand to bridge multiple metal centers in a bi-, tri-, and tetradentate modes.[41-61]

As an extension of these studies, materials of the M(II)/azolate/X system have recently been explored (where M(II)= Ni, Cu, Co, Mn, etc.; azolate = triazole and tetrazole, and X = a variety of anionic components including halides, pseudohalides, SO_4^{2-}, MO_4^{n-}, $Mo_xO_y^{n-}$, etc.).[62-75] In the course of these studies, it was found that the identity of the anion can have dramatic effects on the structure and properties of the composite material, specifically when the anion was

SO_4^{2-}. These results encouraged us to continue our investigations into the structural chemistry of systems featuring PO_4^{3-}, a structural analog of sulfate, as a coordinating anion. The structures of two three-dimensional materials $[Co_3(4\text{-pt})_3(PO_4)]$ (**1**) and $[Co_3(H_2O)_4(4\text{-pt})_2(HOPO_3)_2]$ (**2**) are reported (4-Hpt = 5-(4-pyridyl)tetrazole).

7.2 Results and Discussions

7.2.1 Syntheses

Compounds were synthesized using conventional hydrothermal methods, which are routinely applied in the isolation of organic-inorganic composite materials. At these temperature ranges, typically 120-250°C, the reactants are solubilized while retaining their structural features in the product phases, exploiting the self assembly of products from these soluble precursors.[83-87] Under these crystallization conditions, problems associated with different solubilities of organic and inorganic starting materials are minimized, allowing for introduction of a variety of different organic and/or inorganic precursors, as well as organic and/or inorganic structure-directing or charge-balancing reagents. Such conditions may also allow for the isolation of kinetic rather than thermodynamically favored products.

Both **1** and **2** were isolated as minor components from polycrystalline mixtures whose major phase was the previously described $[Co_2(OH)(PO_4)]$.[88,89] Attempts to prepare pure samples of **1** and **2** by modifying stoichiometries, changes in reaction temperature and varying pH proved unsuccessful. Consequently, pure samples for elemental analyses and magnetic susceptibility studies could be obtained.

7.2.2 Structural Studies

As shown in **Figure 7.1**, the structure of $[Co_3(4\text{-pt})_3(PO_4)]$ is a three-dimensional framework constructed from $\{Co_3(PO_4)\}_n^{3n+}$ chains linked through 4-pyridyltetrazolate ligands. The chain substructures (**Figure 7.1b**) consist of triangular trinuclear units of distorted $\{CoO_3N_3\}$ octahedra fused through corner-sharing interactions at the phosphate groups (**Figure 7.1c**). Each phosphate ligand provides a μ^3-oxygen donor at the center of a cobalt triad, while the remaining three oxygen atoms of the tetrahedron each bridge a cobalt of a given triad to a cobalt of a neighboring cluster. Consequently, each phosphate group links six cobalt sites of two triads. The resulting $\{Co_3(PO_4)\}_n^{3n+}$ substructure exhibits three parallel $\{\text{-Co-O-Co-}\}_n$ chains, with alternating short-long Co-O distances of 2.015 Å and 2.504 Å, respectively. Pairs of cobalt centers of the triad are bridged by N1,N2-bonded tetrazolate groups, and, in addition, each cobalt bonds to a pyridyl nitrogen of the 4-pt ligand. As a result of this connectivity pattern, each cobalt triad coordinates to six 4-pt ligands, and each $\{Co_3(PO_4)\}_n^{3n+}$ chain bridges to six adjacent chains. The cobalt sites adopt the meridional $\{CoO_3N_3\}$ configuration.

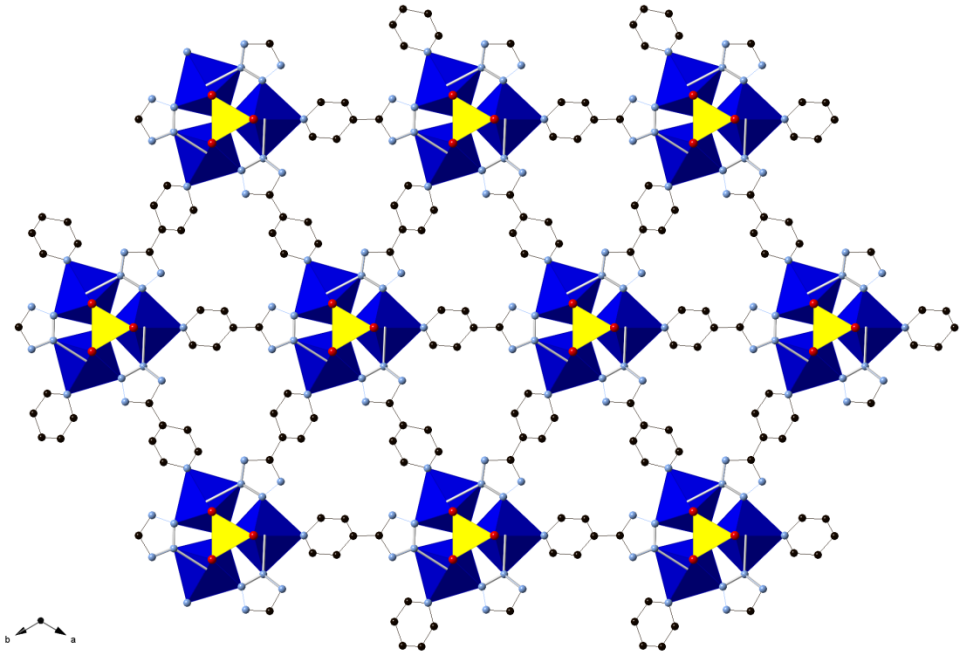

(a)

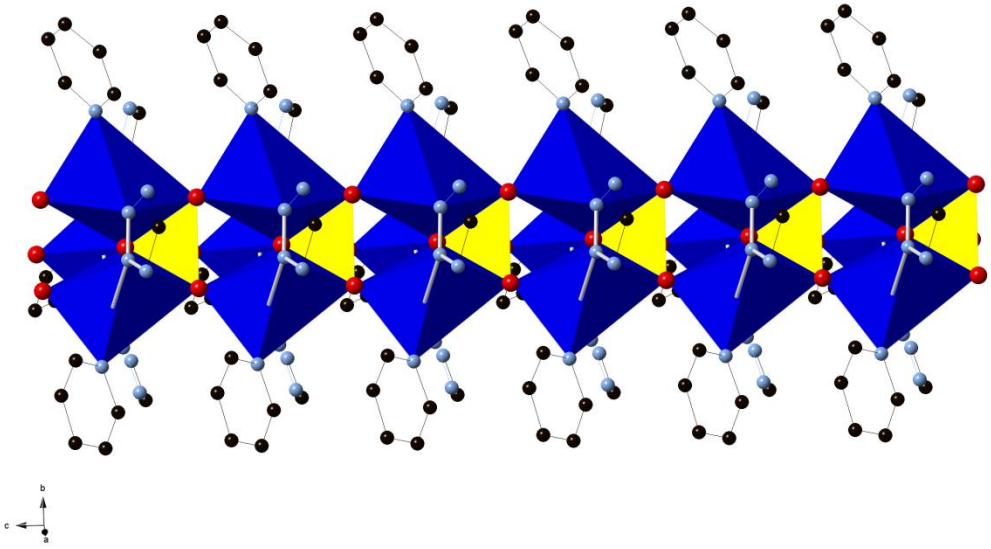

(b)

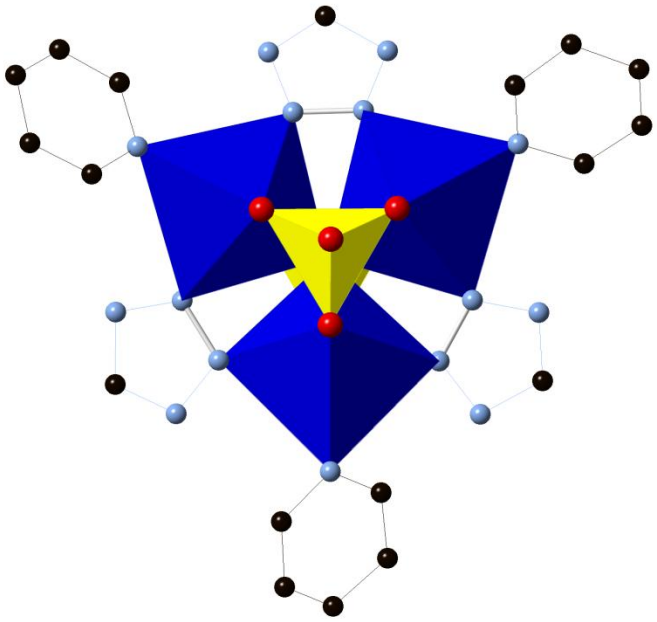

(c)

Figure 7.1: (a) A mixed polyhedral and ball-and-stick representation of the three-dimensional structure of $[Co_3(4\text{-pt})_3(PO_4)]$ (**1**) in the *ab* plane. (b) a view of the $\{Co_3(PO_4)\}_n^{3n+}$ chain substructure of **1**. (c) the trinuclear secondary building unit of **1**.

The structure of the second phase $[Co_3(H_2O)_4(4\text{-pt})_2(HOPO_3)_2]$ (**2**), shown in **Figure 7.2**, is also three-dimensional. However, in this instance, the structure is constructed from cobalt(II)-hydrogen phosphate layers, linked through the 4-pt ligands into the overall framework. As illustrated in **Figure 7.2b**, each layer contains $\{Co_3(H_2O)_4\}^{6+}$ linear trinuclear secondary building units. Each of these triads is linked to four adjacent clusters through $\{HOPO_3\}^{2-}$ tetrahedra, each of which bridges two Co sites of a given triad and one of an adjacent triad and projects a pendant {P-OH} group into an intralamellar cavity. Adjacent pairs of cobalt centers in a triad are bridged by N1,N2-coordinated 4-pt ligands, and the terminal cobalt sites also bond to pyridyl nitrogen donors. The central cobalt atom of the linear triad exhibits $\{CoO_4N_2\}$ coordination geometry through bonding to two phosphate oxygen donors, two *trans*-situated

tetrazolate nitrogen donors from two 4-pt ligands and two *trans*-bridging aqua ligands. In contrast, the peripheral cobalt sites exhibit *cis*-{CoO_4N_2} geometry, bonding to two phosphate oxygen donors, a tetrazolate N-donor, a pyridyl N-donor, and bridging and terminal aqua ligand.

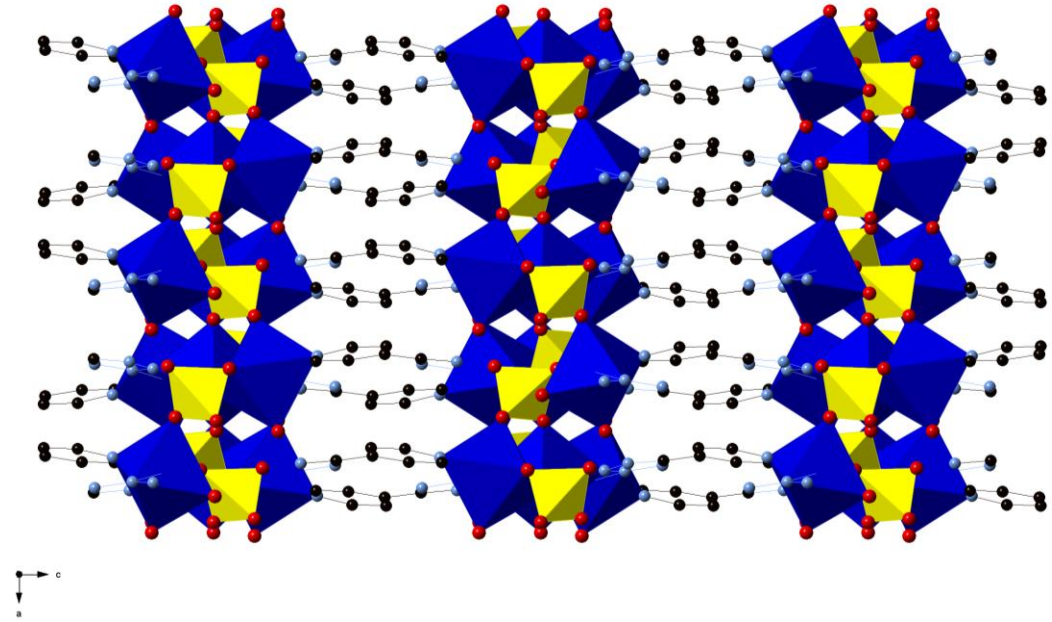

(a)

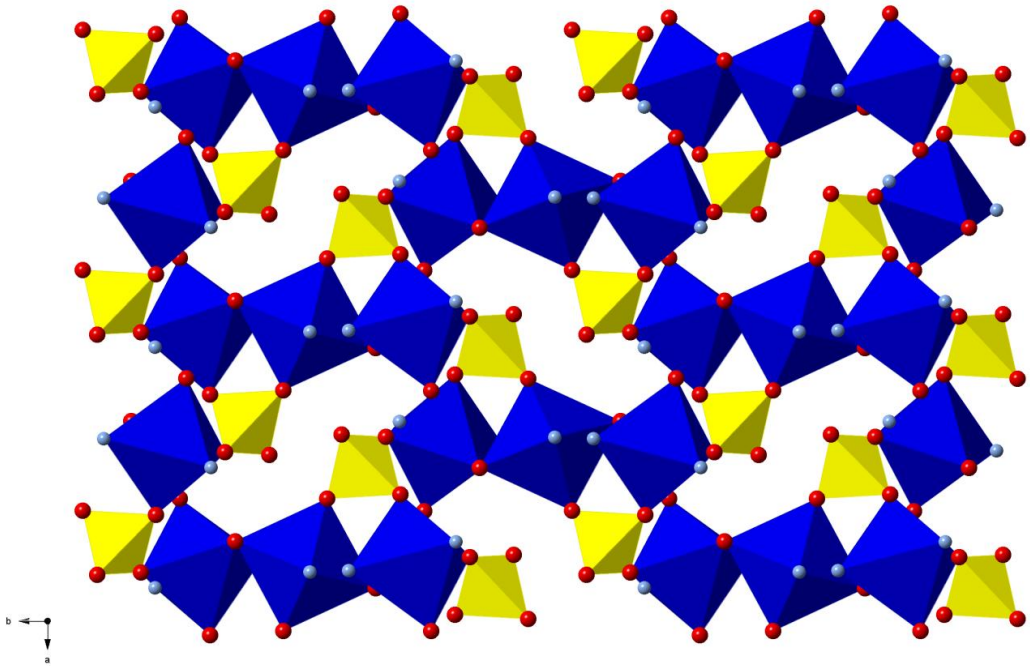

(b)

Figure 7.2: (a) A mixed polyhedral and ball-and-stick representation of the three-dimensional structure of $[Co_3(H_2O)_4(4\text{-pt})_2(HOPO_3)_2]$ (**2**). (b) A view of the inorganic cobalt-phosphate layer of **2**.

7.2.3 General Structural Observations

A recurrent theme of the structural chemistry of the general system M(II)tetrazolate/anion where M(II) = Co, Ni, Cu, etc. is the presence of embedded transition metal/tetrazolate clusters as architectural motifs. In the case of the compounds of this study, both exhibit trinuclear Co(II) building blocks; however, it should be noted that these substructures are quite distinct. In the case of **1** a triangular trinuclear core is observed, while **2** is composed of linear building units, revealing a structural diversity dependent upon hydrothermal reaction conditions and starting materials.

Furthermore, the trinuclear $\{M_3(\mu_3\text{-}O_{phospahte})\}$ core of complex **1** is a new variant of a common structural motif seen in similar systems with cobalt and other transition metals. These $\{M_3(\mu_3\text{-}OH)\}$ and $\{M_3(\mu_3\text{-}O)\}$ cores have been described for systems with azolate N,N′-bridging ligand types with examples including: $\{Cu(II)_3\}$, $\{V(IV)_3\}$, $\{Cr(III)_3\}$, $\{Co(II)_3)\}$, $\{Fe(III)_3\}$, $\{Ni(III)_3\}$ and $\{Cr(III)_2Fe(III)\}$ [90-96] and entries of **Table 7.1**.[67,71,75,95-103]

Table 7.1: Selected structural features of representative metal-azolate compounds containing common variants of the $\{M_3(\mu^3\text{-}O(H))\}^{n+}$ building unit.

Building Unit	Azolate Bridging Ligand, L	Dimension-ality	Coordination Geometry	Coligand	M-μ_3-O bond lengths, Å	ref
$Cu_3(O)(L_3)Cl_3$	pyrazolate	molecular	square planar	Cl^-	1.987	97
$Cu_3(OH)(L_3)Cl_3$	pyrazolate	molecular	square planar	Cl^-	1.989	98
$[Fe_3(O)(4\text{-}O_2N\text{-}L)_6Cl_3]^{2+}$	pyrazolate	molecular	Octahedral	Cl^-	1.885, 1.894	99
$Mn_7(OH)_2(L)_8(CH_3O_2)_4$	triazolate	3-D	octahedral and square pyramidal	$CH_3O_2^{2-}$	2.0988	100
$[Cu_3(OH)(L1)_3(L2)_3]^{2+}$	pyrazolate and pyridine	molecular	octahedral and square pyramidal		1.999	67
$Cd_8(OH)_2(L)_4(SO_4)_5(H_2O)$	triazolate	3-D	Octahedral	SO_4^{2-}	2.186-2.320	71
$Zn_2(L)(SO_4)(OH)$	triazolate	3-D	Octahedral	SO_4^{2-}	2.043	71
$Cu_3(OH)_3(L)_3(H_2O)_4$	triazolate	3-D	Octahedral	H_2O	2.036	66
$Fe_3(OH)(HL)_3(HSO_4)(SO_4)_2$	triazole	3-D	Octahedral	SO_4^{2-}	2.0847	100
$Ni_3(OH)(L)_3(OH)_2(H_2O)_4$	triazolate	3-D	Octahedral	H_2O	2.041	100
$Cu_3(OH)_3(L)_3(DMF)_4$	4-pyridyl tetrazolate	3-D	Octahedral	OH^-/DMF	2.005	72
$Co_3(OH)(SO_4)(L)_3(H_2O)_4$	1,3,5 tritetrazolate benzene	3-D	Octahedral	H_2O/SO_4^{2-}	2.078	101
$Co_4(OH)_2(SO_4)_2(L)_6$	1,4 bistetrazolate benzene	3-D	Octahedral	H_2O/SO_4^{2-}	2.075	101
$[Cu_3(OH)L_3(H_2O)_3]^{2+}$	acetylaminotriazolate	molecular	square pyramidal	H_2O	1.983-2.043	102
$Cu_3(OH)(H_2O)_3(L)_3(SO_4)$	3-hydroxy pyridyl tetrazolate	molecular	Octahedral	H_2O/SO_4^{2-}	1.932	75
$Cu_3(OH)_2(H_2O)_3(L)_2(SO_4)$	3-pyridyl tetrazolate	2-D	Octahedral	H_2O/SO_4^{2-}	1.94	75
$Co_2(L)(SO_4)(OH)(H_2O)$	4-pyridyl tetrazolate	2-D	Octahedral	H_2O/SO_4^{2-}	2.043	103
$M_3F_2(SO_4)(L)_2(H_2O)_4$ M= Co, Ni	3-pyridyl tetrazolate	2-D	Octahedral	H_2O/SO_4^{2-}	2.026 (Co) 2.001 (Ni)	103
$Co_3(L)_3(PO_4)$	4-pyridyl tetrazolate	3-D	Octahedral	PO_4^{3-}	2.128	this work

A variety of additional potentially bridging coligands such as capping sulfato- or phosphato-groups may be accommodated, as shown in **Figure 7.3**, which provide spatial expansion to generate extended architectures. In the case of complex **1**, phosphate provides not

only a μ^3-oxygen donor at the center of a cobalt triad, but also three bridging oxygen atoms of the tetrahedron so that each phosphate bridges to six cobalt centers from neighboring triads, a structural variant new to the library of $\{M_3(\mu_3\text{-}O)\}$ cores.

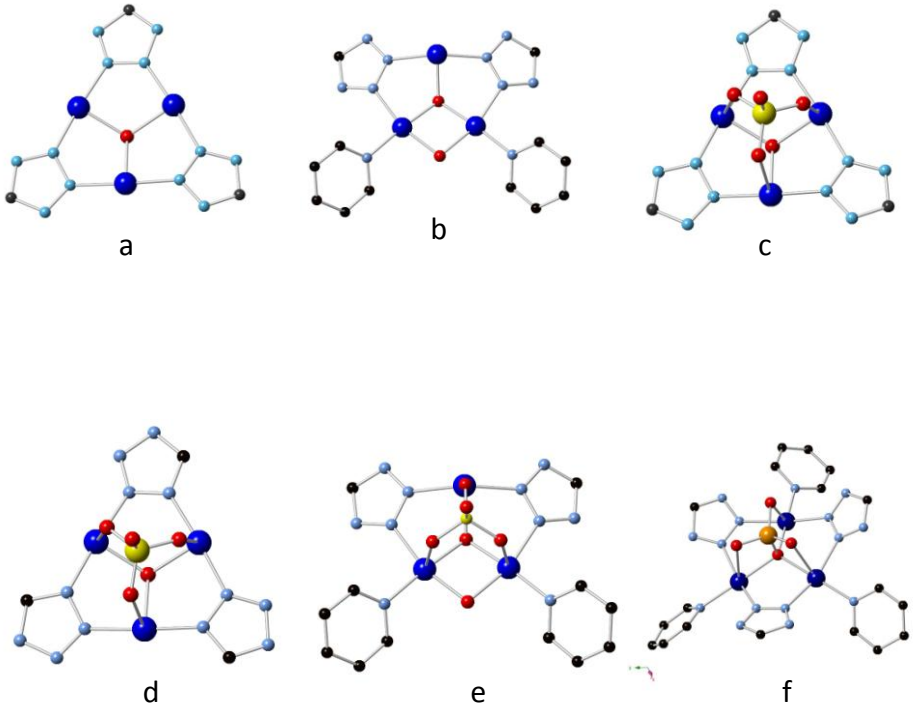

Figure 7.3: The variety of tetrazole bridged triads (a, b) Variants of the typical $M_3(\mu\text{-}O)$ cluster. (c) Incorporation of sulfate anion as a capping ligand in the trinuclear core. (d,e) The triad cores of $[Cu_3(OH)_3(H_2O)_3(3\text{-pyrHtet-}O)_3(SO_4)]$ and $[Cu_3(OH)_2(H_2O)_3(3\text{-pyrtet})_2(SO_4)]$ (f) The building unit of **1**, where phosphate provides a μ^3-oxygen donor at the center of a cobalt triad.

The number and diversity of compounds featuring these trinuclear cores reflect the versatility of the unit in accommodating peripheral and capping ligands. We are encouraged by these results to pursue the development of materials of the M(II)/tetrazolate/anion family, with polyoxoanions such as AsO_4^{3-}, MoO_4^{2-}, $Mo_xO_y^{n-}$, and VO_3^-.

7.3 Conclusions

Hydrothermal methods have been exploited in the preparation of two cobalt(II) phosphate phases incorporating 4-pyridyltetrazolate as an organic component, resulting in isolation of two novel three-dimensional structures of $[Co_3(4\text{-pt})_3(PO_4)]$ (**1**) and $[Co_3(H_2O)_4(4\text{-pt})_2(HOPO_3)_2]$ (**2**). The structure of **1** exhibits a recurrent structural building block, the $\{M_3(\mu_3\text{-o})\}$ subunit, most commonly encountered as the $\{M_3(\mu_3\text{-oxo})\}$ and $\{M_3(\mu_3\text{-hydroxo})\}$ moieties. In the case of compound **1**, this subunit is present as part of an inorganic $\{Co_3(PO_4)\}_n^{3n+}$ chain. The expansion into three-dimensions is accomplished through the bridging dipodal 4-pyridyltetrazolate ligands.

In contrast, the structure of **2** is the pillared layer variant, constructed from $\{Co_3(H_2O)_4(HOPO_3)_2\}_n^{2n+}$ layers, linked through buttressing 4-pyridyltetrazolate ligands. The structural variety encountered for this compositionally simple system reflects a number of structural determinants. Most prominent among these are the variable protonation possibilities for the $H_xPO_4^{3-x}$ component, the structural influences of aqua coordination, and the flexibility of the M-O-P bond angle. While allowing a rich structural chemistry, such factors render the chemistry rather unpredictable, such that the extensive hydrothermal parameter space requires continuing exploration. A more systematic understanding of the complex chemistry will evolve as the structural data base for these systems expands.

7.4 Experimental Section

7.4.1 General Considerations

All chemicals were used as obtained without further purification: cobalt(II) phosphate hydrate, cobalt (II) acetate tetrahydrate, and phosphoric acid were purchased from Aldrich. 5-(4-pyridyl)tetrazole was prepared by prepared by the "click" chemistry approach using zinc

catalysis in aqueous solution or by the use of modified montmorillonite K-10.[76-78] All hydrothermal syntheses were carried out in 23 mL poly-(tetrafluoroethylene)-lined stainless steel containers under autogenous pressure. The reactants were stirred briefly, and the initial pH was measured before heating. Water was distilled above 3.0MΩ in-housing using a Barnstead model 525 Biopure distilled water center. The initial and final pH values of each reaction were measured using color pHast sticks.

7.4.1.1 Synthesis of $[Co_3(4\text{-pt})_3PO_4]$ (1)

A mixture of $Co_3(PO_4)_2 \cdot xH_2O$ (85.5 mg, 0.234 mmol), 5-(4-pyridyl)tetrazole (34.4 mg, .236 mmol), and H_2O (10.00g, 556mmol) in the mole ration 1.00:1.00:2360 was stirred briefly before heating to 180°C for 48 hours (initial and final pH values of 3.2 and 2.8 respectively). Purple crystals of **1**, suitable for X-ray diffraction were isolated in 10% yield. IR (KBr pellet, cm^{-1}): 3065(w), 1626(s), 1557(w), 1454(m), 1380(w), 1237(w), 1227(w), 1077(s), 1013(s), 923(s), 845(m), 758(s), 732(m), 719(m), 579(s), 543(w).

7.4.1.2 Synthesis of $[Co_3(4\text{-pt})_2(H_2O)_4(PO_4H)_2]$ (2)

A mixture of $Co(C_2H_3O_2)_2$ (41.2mg, 0.165 mmol), 5-(4-pyridyl)tetrazole (34.4 mg, .236 mmol), H_2O (10.00g, 556mmol), and H_3PO_4 (50µL 0.860mmol), in the mole ratio 1.42:1.00:3.64:2360 was stirred briefly before heating to 200°C for 48 hours (initial and final pH values of 2.3 and 2.1 respectively). Purple crystals of **2**, suitable for X-ray diffraction were isolated in 5-10% yield. IR (KBr pellet, cm^{-1}): 3498(b), 12294(w), 1110(m), 1012(m), 874(w), 756(m) 581(m), 530(w), 458(w).

7.4.2 X-Ray Crystallography

Structural measurements were performed on a Bruker-AXS SMART-CCD diffractometer

at low temperature (90 K) using graphite-monochromated Mo-K_α radiation (Mo K_α = 0.71073A°).[79] The data were corrected for Lorentz and polarization effects and absorption using SADABS.[80,81] The structures were solved by direct methods. All non-hydrogen atoms were refined anisotropically. After all of the non-hydrogen atoms had been located, the model was refined against $\mathbf{F}^2$, initially using isotropic and later anisotropic thermal displacement parameters. Hydrogen atoms were introduced in calculated positions and refined isotropically. Neutral atom scattering coefficients and anomalous dispersion corrections were taken from the *International Tables*, Vol. C. All calculations were performed using SHELXTL crystallographic software packages.[82]

Crystallographic details have been summarized in **Table 7.2**. Selected bond lengths and angles are given in **Table 7.3**. Full tables of crystal parameters and experimental conditions, atomic positional parameters and isotropic temperature factors, bond lengths and angles, anisotropic temperature factors, hydrogen atom coordinates, and torsion angles for **1** and **2** are available as Supplementary Materials. ORTEP plots of the metal coordination spheres and ligand atoms are also available.

Table 7.2: Summary of crystal data for the structures of $[Co_3(4\text{-pt})_3(PO_4)]$(**1**) and $[Co_3(H_2O)_4(4\text{-pt})_2(HOPO_3)_2]$(**2**).

Compound	**1**		**2**	
Empirical formula	C18 H12 Co3 N15 O4 P		C12 H18 Co3 N10 O12 P2	
Formula weight	710.19		733.09	
Temperature	98(2) K		98(2) K	
Wavelength	0.71073 Å		0.71073 Å	
Crystal system	Trigonal		Orthorhombic	
Space group	R3		PBCA	
Unit cell dimensions	a = 22.202(2) Å	□= 90°.	a = 6.9683(8) Å	□= 90°.
	b = 22.202(2) Å	□= 90°.	b = 14.1302(16) Å	□= 90°.
	c = 4.3536(9) Å	□ = 120°.	c = 22.426(3) Å	□ = 90°.
Volume	1858.4(5) $Å^3$		2208.1(5) $Å^3$	
Z	3		4	
Density (calculated)	1.904 Mg/m^3		2.205 Mg/m^3	
Absorption coefficient	2.111 mm^{-1}		2.461 mm^{-1}	
Final R indices [I>2sigma(I)]	R1 = 0.0542, wR2 = 0.1444		R1 = 0.0302, wR2 = 0.0762	
R indices (all data)	R1 = 0.0639, wR2 = 0.1477		R1 = 0.0373, wR2 = 0.0824	

Table 7.3: Selected bond lengths (Å) and angles (°) for $[Co_3(4\text{-pt})_3(PO_4)]$(**1**) and $[Co_3(H_2O)_4(4\text{-pt})_2(HOPO_3)_2]$(**2**).

Compound	**1**		**2**
Co(1)-O(2)	2.019(5)	Co(1)-O(1)	2.0145(15)
Co(1)-N(5)	2.104(6)	Co(1)-O(6)	2.0786(15)
Co(1)-N(1)	2.108(6)	Co(1)-O(5)	2.1170(17)
Co(1)-N(6)	2.110(6)	Co(1)-N(5)	2.1339(18)
Co(1)-O(1)	2.130(2)	Co(1)-N(2)	2.1669(19)
N(1)-Co(1)-O(1)	179.0(2)	Co(1)-O(4)	2.2748(15)
N(5)-Co(1)-N(6)	159.6(2)	Co(2)-O(2)	2.0155(15)
		Co(2)-O(4)	2.1384(15)
		Co(2)-N(1)	2.1414(19)
		O(1)-Co(1)-O(5)	175.64(6)
		N(1)-Co(2)-N(1)	180.00(9)
		N(5)-Co(1)-O(4)	173.37(6)
		O(2)-Co(2)-O(2)	180
		O(4)-Co(2)-O(4)	179.999(1)
		O(6)-Co(1)-N(2)	167.47(7)

7.5 Acknowledgement

This work was funded by a grant from the National Science Foundation (CHE-0907787).

7.6 Supplementary Materials

Additional material available from the Cambridge Crystallographic Data Centre, CCDC No. CCDC 885477 and 885478, comprises the final atomic coordinates for all atoms, thermal parameters, and a complete listing of bond distances and angles, for compounds **1** and **2**, respectively.

7.7 References

1. Chen, B.; Ockwig, N.W.; Millward, A.R.; Contreras, D.S.; Yaghi, O.M., *Angew. Chem., Int. Ed. Engl.*, **2005**, *44*, 4745.
2. Rowsell, J.L.C.; and Yaghi, O.M., *Angew. Chem., Int. Ed. Engl.*, **2005**, *44*, 4670.
3. Bradshaw, D.; Claridge, J.B.; Cussen, E.J.; Prior, T.J.; and Rosseinsky, M.J., *Chem. Res.*, **2005**, *38*, 273.
4. Rosseinsky, M.J., Microporous and Mesoporous Materials, **2004**, *73*, 15.
5. Cingolani, A.; Galli, S.; Masciocchi, N.; Pandolfo, L.; Pettinari, C.; Sironi, A., *J. Am. Chem. Soc.*, **2005**, *127*, 6144.
6. Ohmori, O.; Kawano, M.; and Fujita, M., *Angew. Chem., Int. Ed.*, **2005**, *44*, 1962.
7. Lee, E.Y.; Jang, S.Y.; and Suh, M.P., *J. Am. Chem. Soc.*, **2005**, *127*, 6374.
8. Noro, S.-I.; Kitagawa, S.; Kondo, M.; and Seki, K., *Angew. Chem., Int. Ed.*, **2000**, *39*, 2081.
9. Wang, Z.; Zhang, B.; Kurmoo, M.; Green, M.A.; Fujiwara, H.; Otsuka, T.; and Kobayashi, H., *Inorg. Chem.*, **2005**, *44*, 1230.
10. Kim, H.; and Suh, M.P., *Inorg. Chem.*, **2005**, *44*, 810.
11. Sudik, A.C.; Millward, A.R.; Ockwig, N.W.; Cote, A.P.; Kim, J.; and Yaghi, O.M., *J. Am. Chem. Soc.*, **2005**, *127*, 7110.
12. Kitaura, R.; Kitagawa, S.; Kubtoa, Y.; Kobayashi, T.C.; Kindo, K.; Mita, Y.; Matsuo, A.; Kobayashi, M.; Chang, H.-C.; Ozawa, T.C.; Suzuki, M.; Sakata, M.; and Takata, M., *Science*, **2002**, *298*, 2358.
13. Bradshaw, D.; Prior, T.J.; Cussen, E.J.; Claridge, J.B.; and Rosseinsky, M.J., *J. Am. Chem. Soc.*, **2004**, *126*, 6106.

14. Kepert, C.J.; Prior, T.J.; and Rosseinsky, M.J., *J. Am. Chem. Soc.*, **2000**, *122*, 5158.

15. Halder, G.J.; Kepert, C.J.; Moubaraki, B.; Murray, K.S.; and Cashion, J.D., *Science*, **2002**, *298*, 1762.

16. Ngo, H.L.; Hu, A.; and Lin, W., *J. Mol. Catal. A*, **2004**, *215*, 177.

17. Sanchez, C.; Lebeau, B.; Chaput, F.; and Boilet, J.P., *Advanced Materials*, **2003**, *15*, 1969.

18. Evans, O.R.; and Lin, W., *Chem. Mater.*, **2001**, *13*, 3009.

19. Jannasch, P., *Curr. Opin. Coll. Inter. Sci.*, **2003**, *8*, 96.

20. Javaid, A.; Hughey, M.P.; Varutbangkul, V.; and Ford, D.M., *J. Membrane Sci.*, **2001**, *187*, 141.

21. Honma, I.; Nomura, S.; and Nakajima, H., *J. Membrane Sci.*, **2001**, *185*, 83.

22. Rowsell, J.L.C.; Millward, A.R.; Park, K.S.; and Yaghi, O.M., *J. Am. Chem. Soc.*, **2004**, *126*, 5666.

23. Janiak, C., *Dalton Trans.*, **2003**, 2781 and references therein.

24. Mitzi, D.B., *Dalton Trans.*, **2001**, 1.

25. Kitagawa, S.; and Noro, S., *Comprehensive Coordination Chemistry II*, **2004**, *7*, 231.

26. Yaghi, O.M.; O'Keeffe, M.; Ockwig, N.W.; Chae, H.K.; Eddaoudi, M.; and Kim, J., *Nature*, **2003**, *423*, 705.

27. James, S.L., *Chem. Soc. Rev.*, **2003**, *32*, 276.

28. Rao, C.N.R.; Natarajan, S.; and Vaidhyanathan, R., *Angew. Chem., Int. Ed.*, **2005**, *43*, 1466.

29. Kitagawa, S.; Kitaura, R.; and Noro, S.-I., *Angew. Chem., Int. Ed.*, **2004**, *43*, 2334.

30. Papaefstathiou, G.S.; and MacGillivray, L.R., *Coord. Chem. Rev.*, **2003**, *246*, 169.

31. Eddaoudi, M.; Moler, D.B.; Li, H.; Chen, B.; Reineke, T.M.; O'Keeffe, M.; and Yaghi, O.M., *Acct. Chem. Res.*, **2001**, *34*, 319.

32. Finn, R.C.; Haushalter, R.C.; and Zubieta, J., *Prog. Inorg. Chem.*, **2003**, *51*, 421.

33. Vioux, A.; LeBideau, J.; Mutin, P.H.; and Leclercq, D., *Top. Curr. Chem.*, **2004**, *232*, 145.

34. Clearfield, A., Current Opinion in Solid State & Materials Science, **2003**, *6*, 495.

35. Clearfield, A., *Prog. Inorg. Chem.*, **1998**, *47*, 371.

36. Alberti, G., in *Comprehensive Supramolecular Chemistry* Atwood, J.L.; Davies, J.E.D.; MacNicol, D.D.; and Vögtle, F., eds.: Pergamon Press, New York: vol. 7 **1996** Alberti, G.; and Bein, T., eds. 151.

37. Férey, G., *Chem. Mat.*, **2001**, *13*, 3084.

38. Farrusseng, D.; Aguado, S.; and Pinel, C., *Angew. Chem. Int. Ed*., **2009**, *48*, 7502-7513.

39. Zheng, B.; Bai, J.; Duan, J.; Wojtas, L.; and Zaworotko, M.J., *J. Am. Chem. Soc*., **2011**, *133*, 748-751.

40. Sumida, K.; Brown, C.R.; Herm, Z.R.; Chavan, S.; Bordiga, S.; and Long, J.R., *Chem. Comm*., **2011**, *47*, 1157-1159.

41. Beckmann, U.; and Brooker, S., *Coord. Chem. Rev*., **2003**, *245*, 17.

42. Haasnoot, J.G., *Coord. Chem. Rev*., **2000**, *200*, 131.

43. Hellyer, R.M.; Larsen, D.S.; and Brooker, S., *Eur. J. Inorg. Chem*., **2009**, 1162.

44. Zhang, J.-P.; and Chen, X.-M., *Chem. Commun*., **2006**, 1689.

45. Steel, P.J., *Coord. Chem. Rev*., **1990**, *106*, 227.

46. Potts, K.T., *Chem. Rev*., **1961**, *61*, 87.

47. Dawe, L.N.; and Thompson, L.K., *Dalton Trans*., **2008**, 3610.

48. Zhang, J.-P.; Lin, Y.-Y.; Huang, X.-C.; and Chen, X.-M., *J. Am. Chem. Soc*., **2005**, *127*, 5495.

49. J.-P. Zhang, J.-P.; Zheng, S.-L.; Huang, X.-C.; and Chen, X.-M., *Angew. Chem., Int. Ed*., **2004**, *43*, 206.

50. Ferrer, S.; Lloret, F.; Bertomeu, I.; Alzuet, G.; Borras, J.; Garcia-Granda, S.; Liu-González, M.; and Haasnoot, J.G., *Inorg. Chem*., **2002**, *41*, 5821.

51. Zhou, J.-H.; Cheng, R.-M.; Song, Y.; Li, Y.-Z.; Yu, Z.; Chen, X.-T.; Xue, Z.-L.; and You, X.-Z., *Inorg. Chem*., **2005**, *44*, 8011 and references therein.

52. Zhang, J.-P.; Lin, Y.-Y.; Zhang, W.-X.; and Chen, X.-M., *J. Am. Chem. Soc*., **2005**, *127*, 14162.

53. Zhang, D.-C.; Lu, W.-G.; Jiang, L.; Feng, X.-L.; and Lu, T.-B., *Cryst. Growth Des*., **2010**, *10*, 739.

54. Ouellette, W.; Jones, S.; and Zubieta, J., *CrystEngComm*., **2011**, *13*, 4457.

55. Ouellette, W.; Darling, K.; Prosvirin, A.; Whitenack, K.; Dunbar, K.R.; and Zubieta, J., *Dalton Trans.*, **2011**, *40*, 12288.

56. Hagrman, P.J.; Bridges, C.; Greedan, J.E.; and Zubieta, J., *J. Chem. Soc. Dalton Trans.*, **1999**, 2901.

57. Hagrman, D.; and Zubieta, J., *Chem. Commun.*, **1998**, 2005.

58. Ouellette, W.; Yu, M.H.; O'Connor, C.J.; Hagrman, D.; and Zubieta, J., *Angew. Chem., Int. Ed*., **2006**, *45*, 3497.

59. Ouellette, W.; Prosvirin, A.V.; Valeich, J.; Dunbar, K.R.; and Zubieta, J., *Inorg. Chem*., **2007**, *46*, 9067.

60. Ouellette, W.; Galán-Mascarós, J.R.; Dunbar, K.R.; and Zubieta, J., *Inorg. Chem*., **2006**, *45*, 1909.

61. Ouellette, W.; Prosvirin, A.V.; Chieffo, V.; Dunbar, K.R.; Hudson, B.; and Zubieta, J., *Inorg. Chem*., **2006**, *45*, 9346.

62. Ouellette, W.; Jones, S.; and Zubieta, J., *CrystEngComm*., **2011**, *13*, 4457.

63. Ouellette, W.; Darling, K.; Prosvirin, A.; Whitenack, K.; Dunbar, K.R.; and Zubieta, J., *Dalton Trans.*, **2011**, *40*, 12288.

64. Hagrman, P.J.; Bridges, C.; Greedan, J.E.; and Zubieta, J., *J. Chem. Soc. Dalton Trans.*, **1999**, 2901.

65. Hagrman, D.; and Zubieta, J., *Chem. Commun.*, **1998**, 2005.

66. Ouellette, W.; Yu, M.H.; O'Connor, C.J.; Hagrman, D.; and Zubieta, J., *Angew. Chem., Int. Ed*., **2006**, *45*, 3497.

67. Ouellette, W.; Prosvirin, A.V.; Valeich, J.; Dunbar, K.R.; and Zubieta, J., *Inorg. Chem*., **2007**, *46*, 9067.

68. Ouellette, W.; Galán-Mascarós, J.R.; Dunbar, K.R.; and Zubieta, J., *Inorg. Chem*., **2006**, *45*, 1909.

69. Ouellette, W.; Prosvirin, A.V.; Chieffo, V.; Dunbar, K.R.; Hudson, B.; and Zubieta, J., *Inorg. Chem*., **2006**, *45*, 9346.

70. Chesnut, D.J.; Kusnetzow, A.; Birge, R.; and Zubieta, J., *Inorg. Chem*., **1999**, *38*, 5484.

71. Ouellette, W.; Hudson, B.S.; and Zubieta, J., *Inorg. Chem*., **2007**, *46*, 4887.

72. Ouellette, W.; Liu, H.; O'Connor, C.J.; and Zubieta, J., *Inorg. Chem*., **2009**, *48*, 4655.

73. Ouellette, W.; and Zubieta, J., *Chem. Commun*., **2009**, 4533.

74. Ouellette, W.; Prosvirin, A.V.; Whitenack, K.; Dunbar, K.R.; and Zubieta, J., *Angew. Chem., Int. Ed.*, **2009**, *48*, 2140.

75. Darling, K.; Ouellette, W.; and Zubieta, J., *Cryst. Growth Des.*, **2012**. Accepted.

76. (a) Demko, P.Z.; and Sharpless, K.B., *J. Org. Chem.*, **2001**, 66, 7945.

77. Tao, J.; Ma, Z.-J.; Huang, R.-B.; and Zhang, L.-S., *Inorg. Chem.*, **2004**, *43*, 6133.

78. Chermahini, A.N.; Teimouri, A.; and Moaddeli, A., *Heteroatom Chem.*, **2011**, *22*, 168.

79. SMART, Data Collection Software, version 5.630, Bruker-AXS Inc., Madison, WI, **1997-2002**.

80. SAINT Plus, Date Reduction Software, version 6.45A, Bruker-AXS Inc., Madison, WI, **1997-2002**.

81. Sheldrick, G.M., SADABS, University of Göttingen, Göttingen, Germany, **1996**.

82. SHELXTL PC, version 6.12, Bruker-AXS Inc., Madison, WI, **2002**.

83. Stein, A.; Keller, S.W.; and Mallouk, T.E., *Science*, **1993**, *259*, 1558.

84. Gopalakrishnan, J., *Chem. Mater.*, **1995**, *7*, 1265.

85. Weller, M.; and Dann, S.E., *Curr. Opin. Solid State Mater. Sci.*, **1998**, *3*, 137.

86. Gopalakrishnan, J.; Bhuvanesh, N.S.P.; and Rangan, K.K., *Curr. Opin. Solid State Mater. Sci.*, **1996**, *1*, 285.

87. Zubieta, J., Solid state methods, hydrothermal in, *Comprehensive Coordination Chemistry II*, **2003**, *1*, 697.

88. Harrison, W.T.A.; Vaughey, J.T.; Dussack, L.L.; Jacobson, A.J.; Martin, T.G.; and Stucky, G.D., *J. Solid State Chem.*, **1995**, *114*, 151.

89. Rojo, J.M.; Mesa, J.L.; Lezama, L.; Pizarro, J.L.; Arriotua, M.I.; Fernandez, J.R.; Barberis, G.E.; and Rojo, T., *Phsy. Rev.*, **2002**, *66*, 094406.

90. Figuerola, A.; Tangoulis, V.; Ribas, J.; Hartl, H.; Brudgam, I.; Maestro, M.; and Diaz, C., *Inorg. Chem.*, **2007**, *46*, 11017.

91. Tsukerblat, B.; Tarantul, A.; and Muller, A., *Inorg. Chem.*, **2007**, *46*, 161.

92. Psycharis, V.; Raptopoulou, C.P.; Boudalis, A.K.; Sanakis, Y.; Fardis, M.; Diamantopoulos, G.; and Papavassiliou, G., *Eur. J. Inorg. Chem.*, **2006**, 3710.

93. Boudalis, A.K.; Sanakis, Y.; Dahan, F.; Hendrich, M.; and Tuchagues, J.P., *Inorg. Chem.*, **2006**, *45*, 443.

94. Berry, J.F.; Cotton, F.A.; Liu, C.Y.; Lu, T.B.; Murillo, C.A.; Tsukerblat, B.S.; Villagran, D.; and Wang, X.P., *J. Am. Chem. Soc*., **2005**, *125*, 4895.

95. Sanakis, Y.; Macedo, A.L.; Moura, I.; Papaefthymiou, V.; and Punk, E., *J. Am. Chem. Soc*., **2000**, *122*, 11855.

96. Gatteschi, D.; Sessoli, R.; Plass, W.; Müller, A.; Krickemeyer, E.; Meyer, J.; Sölter, D.; and Adler, P., *Inorg. Chem*., **1996**, *35*, 1926.

97. Angaridis, P.A.; Baran, P.; Boca, R.; Cervantes-Lee, F.; Haase, W.; Mezei, G.; Raptis, R.G.; and Werner, R., *Inorg. Chem.*, **2002**, *41*, 2219.

98. Liu, J.C.; Guo, G.-C.; Huang, J.-S.; and You, X.-Z., *Inorg. Chem.*, **2003**, *42*, 235.

99. Ferrer, S.; Lloret, F.; Bertomeu, I.; Alzulet, G.; Borra´s, J.; Garcı´a-Granda, S.; Liu-Gonza´lez, M.; Haasnoot, J.G., *Inorg. Chem.*, **2002**, *41*, 5821.

100. Dalice Piñero, D.; Raptis, R.G.; Renz, F.; and Sanakis, Y., *Inorg. Chem.*, **2007**, *46*, 10981.

101. Rivera-Carrillo, M.; Chakraborty, I.; Mezei, G.; Webster, R.D.; and Raptis, R.G., I*norg. Chem.*, **2008**, *47*, 7644.

102. Ouellette, W.; Darling, K.; Prosvirin, A.; Whitenack, K.; Dunbar, K.R.; and Zubieta, J., *Dalton Trans.*, **2011**, *40*, 12288.

103. Ferrer, S.; Lloret, F.; Pardo, E.; Liu-Gonzalez, M.L.; and Garcia-Granda, S., *Inorg. Chem.*, **2012**, *51*, 985.

104. Darling, K.; Ouellette, W.; Prosvirin, A.; Walter, S.; Dunbar, K.R.; and Zubieta, J., unpublished results.

Chapter 8: Conclusion

8.1 Conclusion

The scope of this research encompasses the detailed investigation of the design, synthesis, and structural influence of a secondary anionic component on the structure and connectivity of hybrid organic-inorganic materials of the M(I,II)/polyazaheterocycle/anion system where the anion is F^-, Cl^-, I^-, OH^-, SO_4^{2-}, or PO_4^{3-}. The structural versatility of this family of compounds is a reflection of the many structural determinants at play. These include factors such as: (i) the variety of coordination polyhedra available to the metal, (ii) variable modes of coordination associated with the azole(ate) ligands, (iii) the role of functional substituents on the azolate moiety, (iv) the incorporation and coordination preferences of secondary anionic components (X^{n-} or XO_m^{n-}) and (v) the variable incorporation of solvent molecules. In addition, it has been demonstrated that hydrothermal reaction conditions of stoichiometry, pH, and temperature can influence the identity of the products. While a number of recurring structural motifs have been observed, the remarkable array of structures of materials of this study underlines the difficulty in predicting product composition and the challenge in rational design of framework materials.

8.2 The Structural Chemistry of the M(I,II)/Polyazaheterocycle/Anion System

In an attempt to systematically explore the structural variety of and accumulate a structural data base for materials of the type M(I,II)/Polyazaheterocycle/Anion where the transition metal cation is Co^{2+}, Ni^{2+}, $Cu^{2+/+}$, Cd^{2+}, or Zn^{2+} and the anion is F^-, Cl^-, I^-, OH^-, SO_4^{2-}, or PO_4^{3-}, we have focused on the structural influences of: (i) the coordination preferences of the metal cation, (ii) the identity of the azole-containing tethering ligand, and (iii) the introduction of a secondary charge compensating anionic component or solvent molecule.

8.3 Azolate Moiety Variation

The exploitation of polyazaheteroaromatic ligands as templating and structure directing agents in hybrid materials is a relatively well known strategy. 1,2,4-triazole, specifically, has proved to be an attractive ligand for the design of hybrid materials due to its ability to bridge multiple metal centers through the N1, N2, and N4 positions of the ligand, resulting in a rich structural chemistry and expanded dimensonality of the products. In addition, triazole's ease of derivitization can also provide a route for the design of tethering ligands with multiple functionality**.** As an extension of a structural study of the M(I,II)/triazole system, we have focused on the structural chemistry of materials featuring 4-pyridyl tetrazole, which can be considered an extended analog of triazole, as well as the structural consequences of modification of the pyridyl nitrogen donor, substitution of the pyridyl substituent for a pyrazine or carboxylate group, and insertion of a tethering group to expand the coordination domain of the ligand.

8.3.1 Variability in Bridging Modes

The N1, N2 bridging mode is the most common for 1,2,4-triazole and analogous bridging modes have been observed for many of the tetrazolate-containing materials of this study. It should be noted; however, that the additional nitrogen donors of the derivatized tetrazolate linker ligands of this work allow for a variety of different bridging modes. For instance, the pyridyltetrazole (ate) ligand has been shown to adopt a variety of coordination and bridging modes ranging from monodentate terminal to bridging through one pyridyl and four tetrazolate nitrogen donors.

For example, while $[CuCl_2(4\text{–Hpyrtet})] \cdot 0.5H_2O$ contains prototypical N2,N3 tetrazole-bridged copper sites mentioned previously, the pyrazine-tetrazole derivative, $[H_2en]_{0.5}[CuCl_2(prztet)]$, contains copper sites bridged by N1,N2 nitrogen donors of the

tetrazolate units. A third and less common dinucleating coordination mode, N1,N4 bridging, has also been observed in the structural chemistry of tetrazole containing compounds, where repulsive influences can be minimized. Tetrazole's additional nitrogen donor atoms allows it to bridge multiple metal centers, as evidenced by the structure of [CdCl(2-pyrtet)(DMF)], where the ligand adopts a tridentate bridging mode in which each 4-pyrtet ligand bridges three Cd sites through N1,N2,N3-coordination and chelates to one of these sites through additional coordination of the pyridyl nitrogen. The N1,N2,N3-bridging mode of tetrazolate based ligands is not uncommon and the resulting ribbon motifs contained in [CdCl(2-pyrtet)(DMF)] is a recurrent structural feature in the metal-tetrazolate chemistry **(see Figure 8.1a)**. Lastly, in an even more complicated example, the structure of $[Co_2(4\text{-pyrtet})(SO_4)(OH)(H_2O)]1.5H_2O$ ($1.5H_2O$) adopts the tetradentate mode, where all four nitrogen donors from the tetrazolate subunits bridge four cobalt sites, resulting in an extended chain substructure linked into two dimensional layers through a fifth nitrogen from the pyridyl arms of the ligand **(see Figure 8.1b)**.

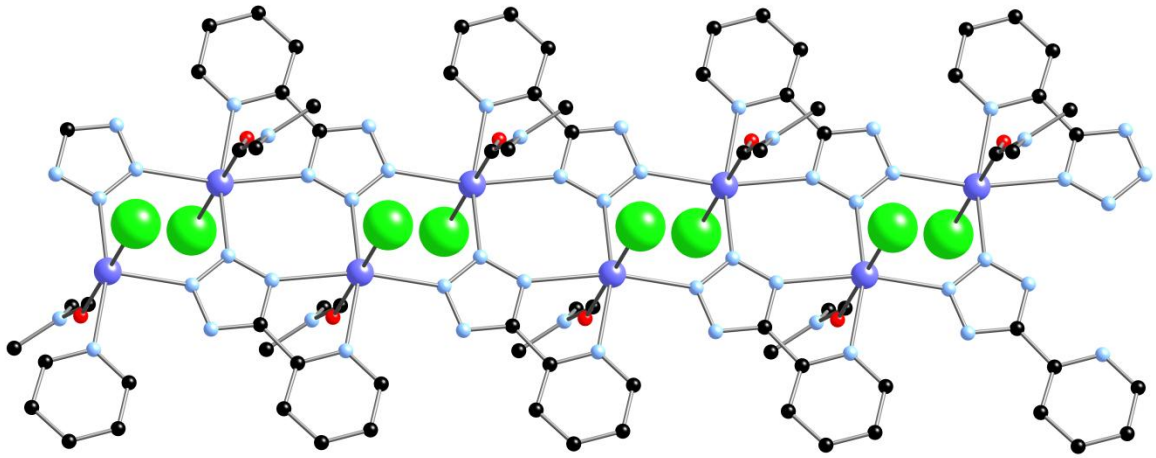

(a)

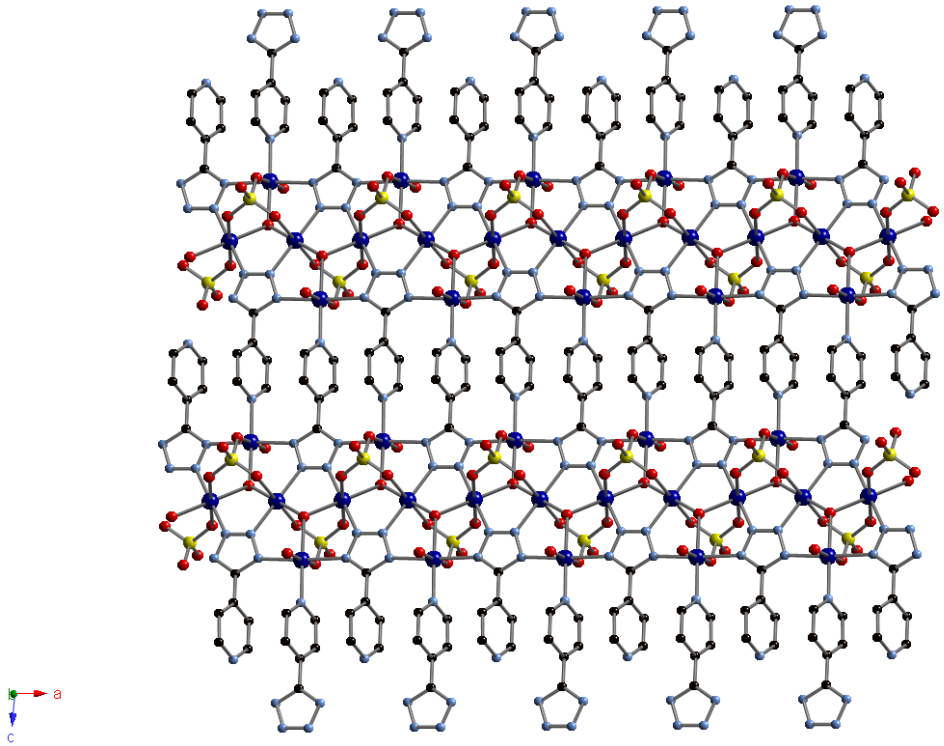

(b)

Figure 8.1: (a) The one-dimensional structure of [CdCl(2-pyrtet)(DMF)]. Color scheme: Cd shown as blue spheres, Cl as large light green spheres, oxygen, red; nitrogen, light blue; carbon black. (b) Ball and stick representation of the two-dimensional structure of $[Co_2(4\text{-pyrtet})(SO_4)(OH)(H_2O)]\bullet 1.5H_2O$ in the ac plane. Color scheme: cobalt, blue spheres; sulfur, yellow spheres; oxygen, red spheres; nitrogen, light blue spheres; carbon, black spheres.

8.3.2 Addition of Functionalized Substituents

Polyazaheterocyclic ligands are quite attractive in their facility of modification to allow introduction of additional functionality. The observation that the modified polyazaheterocyclic ligands 4-(4-pyridyl)pyrazolate and 4-pyridyltetrazolate in the N2,N3 bridging mode can function as expanded analogues of 1,2,4-triazolate motivated us to examine the structural consequences of modification of the pyridyl nitrogen donor location and the replacement of a pyrazine group for a pyridyl or carboxylate substituent. It has been determined that this introduction of additional functional groups unto the azolate ligand can result in unexpected

products often showing increased complexity and dimensionality. The structural consequences of derivitazation of tetrazole containing ligands is shown in the coordination chemistry of transition metal sulfates with 2-, 3-, and 4-pyridyltetrazole and pyrazinetetrazole.

In this structural study of materials of the M(II)/polyazahetercycle/SO_4^{2-} family where M(II) is either nickel or cobalt, recurrent structural trends were observed. For structures containing 3-, and 4- pyridyltetrazole, bridging of metal centers or nodes through the pyridyl arms of the tethering ligands is observed in $[Co_2(4\text{-pyrtet})(SO_4)(OH)(H_2O)]1.5H_2O$ ($1.5H_2O$), $[Co_3F_2(SO_4)(3\text{-pyrtet})_2(H_2O)_4]$, and $[Ni_3F_2(SO_4)(3\text{-pyrtet})_2(H_2O)_4]$ **(see Figure 8.2a)**. In the pyrazine-tetrazole derivative $[Co_4(prztet)_6(SO_4)(H_2O)_2]$; however, the ligand participates in both bridging and chelating coordination of the cobalt metal centers through four nitrogens from each ligand. In this case, The N2 nitrogen atoms of the pyrazine substituents chelate to the cobalt sites, while the N5-pyrazine nitrogen donors bridge to adjacent metal sites to provide two-dimensional connectivity for the cobalt-azolate substructure where each tetrad is linked to six adjacent building units in the layer **(see Figure 8.2b)**.

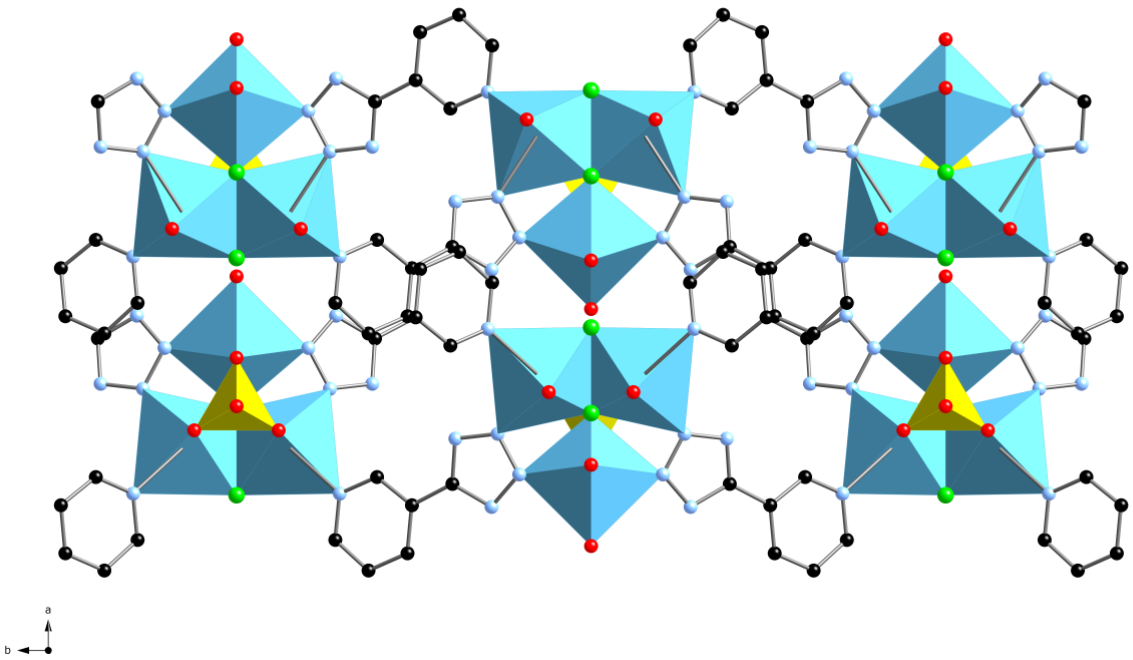

(a)

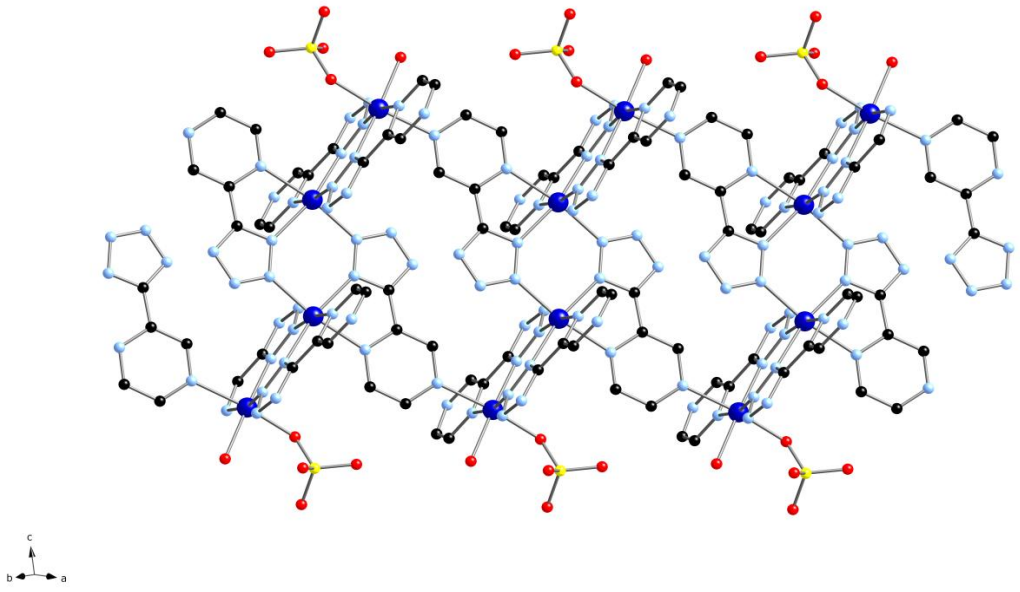

(b)

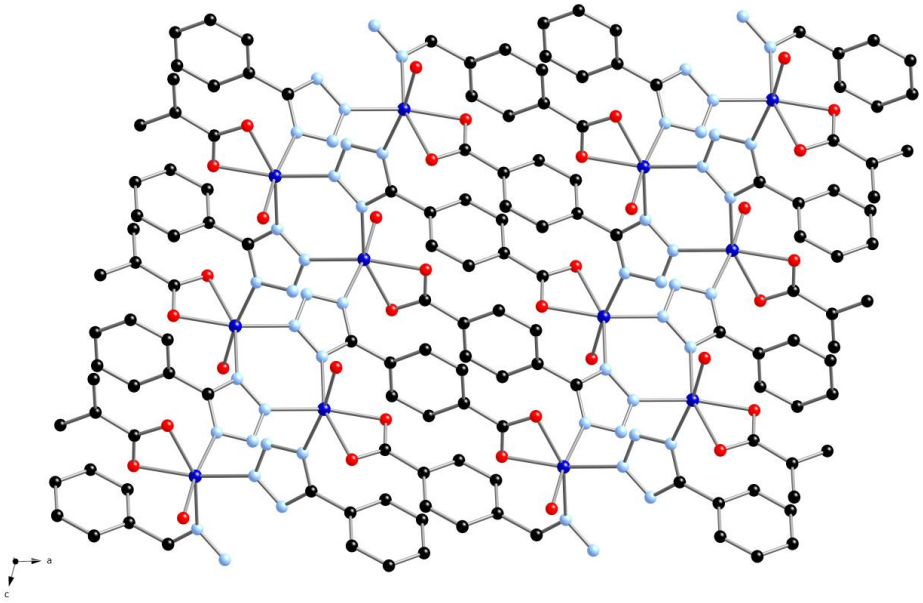

(c)

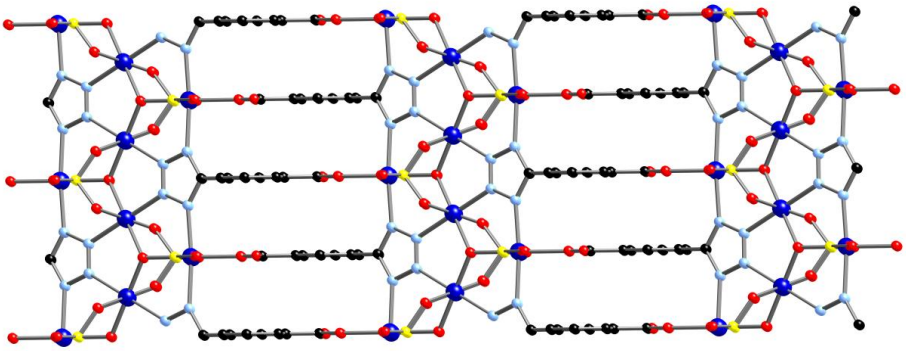

(d)

Figure 8.2: (a) Mixed polyhedral and ball and stick representation of the two dimensional structure of $[Ni_3F_2(SO_4)(3\text{-pyrtet})_2(H_2O)_4]$ in the ab plane. Color scheme: nickel, aqua octahedra; sulfur, yellow tetrahedra; oxygen, red spheres; nitrogen, light blue spheres; carbon, black spheres. (b) Ball and stick representation of the three-dimensional structure of $[Co_4(prztet)_6(SO_4)(H_2O)_2]$. Color scheme: cobalt, blue spheres; sulfur, yellow spheres; oxygen, red spheres; nitrogen, light blue spheres; carbon, black spheres. (c) A view of the structure of $[Co(4\text{-trzphCO}_2)(H_2O)]$, normal to the *ac* plane, showing the pillaring of the {Co(tetrazolate)} layers through the ($-C_6H_5CO_2^-$) substituents to establish the overall three-dimensional connectivity. Color scheme: cobalt, dark blue spheres; oxygen, red spheres; nitrogen, blue spheres; carbon, black spheres. (d) The linking of the $\{Co_2(tetrazolate)(OH)(SO_4)\}_n$ layers through ($-C_6H_5CO_2H$) groups into a pillared layer. Color scheme: cobalt, dark blue spheres; oxygen, red spheres; nitrogen, blue spheres; carbon, black spheres.

In a similar study of compounds featuring copper (II) as the transition metal cation, analogous structural motifs are observed. The coordination preferences of the substituted tetrazole ligand in $[Cu_3(OH)_2(H_2O)_3(3\text{-pyrtet})_2(SO_4)]$ is such that 3-pyridyltetrazole bridges metal or metal cluster nodes. In contrast, 2-pyridyltetrazole adopts a chelating modality through a tetrazole nitrogen and a pyridyl nitrogen in $(Me_2NH_2)[Cu(2\text{-pyrtet})(SO_4)]$. Finally, in the structure of $[Cu_4(\text{pyrztet})_6(H_2O)_2(SO_4)]$, pyrazine tetrazole again adopts both chelating and bridging roles, resulting in a complex $\{Co_4(\text{prztet})_6(H_2O)\}$ layer constructed from tetranuclear $\{Co_4(\text{tetrazolate})_6\}^{2+}$ secondary building units.

Because functionalizing tetrazole with a pyridyl or pyrazine substituent provided products with an increased structural complexity, we also investigated other functionalized tetrazoles, including 3- and 4-carboxyphenyltetrazole. As previously noted , 4-pyridyltetrazolate can function in the N2,N3-bridging mode to provide an expanded analogue to the triazolate ligand. The 4-carboxyphenyl-tetrazolate ligand could in principle provide a similar connectivity pattern; however, in this study the coordination modes adopted are quite different and result in novel and unexpected structural types.

For instance, in the structure of $[Co(3\text{-trzph}CO_2)]$, the $\text{trzph}CO_2^{2-}$ ligand bonds to four cobalt sites, two through the N1,N4 donors of the tetrazolate group and two through the carboxylate oxygen donors in an *anti-syn* coordination mode. In the case of $[Co(4\text{-trzph}CO_2)(H_2O)]$, the $\text{trzph}CO_2^{2-}$ ligands bridge three cobalt sites through the N1,N2,N4 positions of the tetrazolate terminus, while the carboxylate functionality serves as a bidentate chelator for the cobalt centers **(see Figure 8.2c)**. Lastly, in $[Co_2(SO_4)(OH)(3\text{-trzph}CO_2H)]$, tetrazolate groups bridge four cobalt sites and the carboxyl group is monodentate and protonated at the pendant oxygen **(see Figure 8.2d)**.

8.3.3 Variation in Tether Length of Polyazaheterocyclic Ligands

In a study to further explore a design strategy of inserting tethering groups to expand the coordination domain of the tetrazole-containing ligand, dipodal ligands with different spacer lengths, 5,5”-(1,4-phenylene)bis(1H-tetrazole) (= bdt), 5’5”-(1.1’-biphenyl)-4,4”-diylbis(1H-tetrazole) (= dbdt), and 5,5”,5”-(1,3,5-phenylene)tris(1H-tetrazole) (=btt) were exploited in an attempt to provide increased spatial expansion of the products. In the hydrothermal chemistry of the Co(II) series, three phases were isolated: $[Co_5F_2(dbdt)_4(H_2O)_6]\cdot 2H_2O$, $[Co_4(OH)_2(SO_4)(bdt)_2(H_2O)_4]$, and $[Co_3(OH)(SO_4)(btt)(H_2O)_4]\cdot 3H_2O$ where the structures are all three-dimensional and consist of cluster-based secondary building units.

In the case of $[Co_5F_2(dbdt)_4(H_2O)_6]\cdot 2H_2O$, the structure consists of cobalt chains connected via the dbdt ligands by a linkage in which the first dbdt ligand bonds to a single cobalt site at one terminus and bridges two metal sites at the other, while the second dbdt group bridges three cobalt sites at either terminus, connecting each chain to six adjacent chains. In contrast, the structure of $[Co_4(OH)_2(SO_4)(bdt)_2(H_2O)_4]$ adopts a buttressed layer motif, characteristic of other dipodal organic tethering ligands of the diphosphonates where the terminal ends of the bdt ligands bridge four cobalt centers. Lastly, the structure of $[Co_3(OH)(SO_4)(btt)(H_2O)_4]\cdot 3H_2O$ again consists of cobalt chains connected to six adjacent chains via the btt ligands; however, in this case the ligand adopts the protypical N1,N2, bridging mode, illustrating the variety of different ligation modes that can result in changes in the spacer length and symmetry of these di- or tripodal ligands.

8.4 Introduction of Anionic Component

An array of architectures and substructures are observed for M(II)/azolate materials and this is further enhanced by the introduction of auxiliary coordinating anions, whether simple

halides X^- or pseudohalides (such as CN^-) or oxyanions such as sulfate and phosphate. The synergism of bridging azolates and the observed effectiveness of the anionic components in adopting bridging modes provide complex, highly dimensional materials and suggests the need for a paralleled investigation of the structural consequences of the introduction of a variety of different charge balancing subunits. As such, a series of materials featuring anions including F^-, Cl^-, I^-, OH^-, SO_4^{2-}, or PO_4^{3-} were synthesized, where the incorporation of secondary anion components can have dramatic and unpredictable structural consequences on the products due to the tendency of these anionic components to adopt a variety of different coordination modes.

8.4.1 Structural Significance of Coordinating Anions

In a study focused on the copper/pyridyltetrazole system in the presence of a variety of anions, the parent compound, $[Cu(3\text{-pyrtet})_2]$, is composed of isolated square planar copper atoms, linked into a two dimensional layer through the tetrazolate ligand. The result of introducing coordinating anions is revealed in the structures of a series of compounds featuring copper and pyridyltetrazolate ligands with a variety of different anions. In the structure of $[CuCl_2(4\text{-Hpyrtet})]\cdot 0.5H_2O$, chloride anions serve to bridge copper octahedra into a chain substructure **(see Figure 8.3a)**. In replacing chloride with iodine as in the structure of $[Cu_2I_2(4\text{-Hpyrtet})]$, the μ^3-bridging iodine donors generate a substructure of $\{CuI\}_n$ layers **(see Figure 8.3b).** Lastly, the incorporation of sulfate into the structure of $[Cu_3(OH)_2(H_2O)_3(3\text{-pyrtet})_2(SO_4)]$ has dramatic structural consequences where triangular trinuclear $\{Cu_3(OH)_2(H_2O)_3(SO_4)\}^{2+}$ building units are observed **(see Figure 8.3c)**. It should be noted that sulfate containing materials in general in materials of the type M(II)/azolate/SO_4^{2-}, feature this $\{Cu_3(\mu^3\text{-}OH)\}^{5+}$ core as a recurrent structural motif where sulfato ligands cap the triad via coordination to an oxygen vertex of each copper site, having the fourth oxygen uncoordinated.

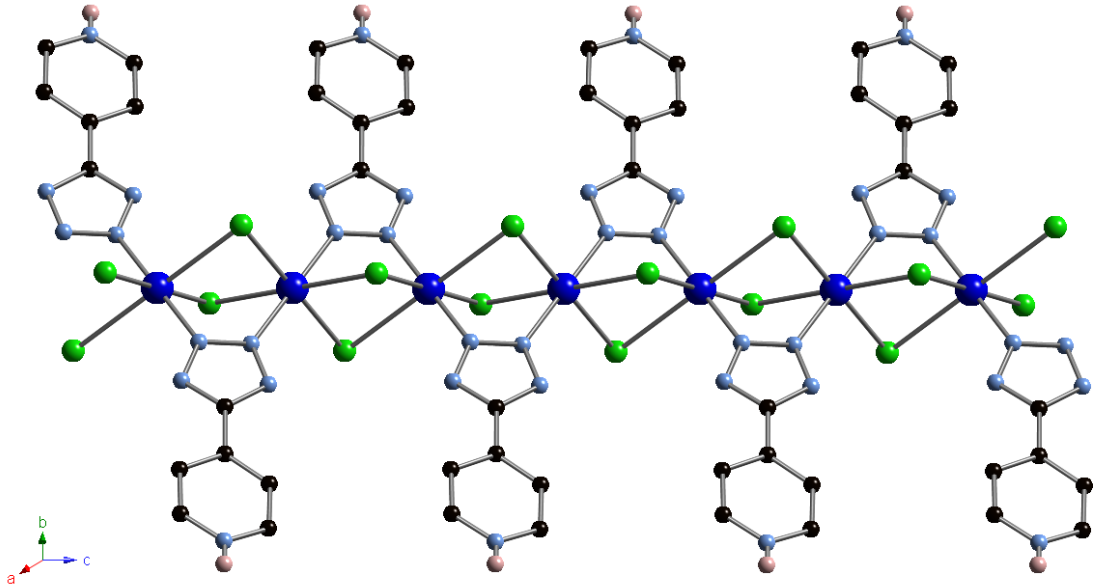

(a)

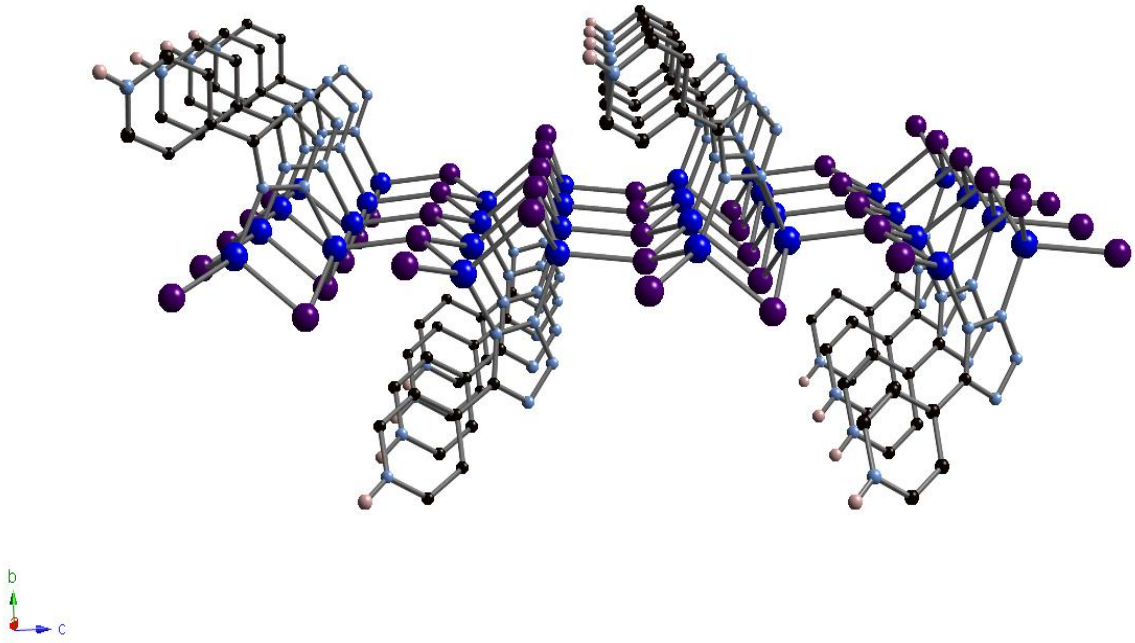

(b)

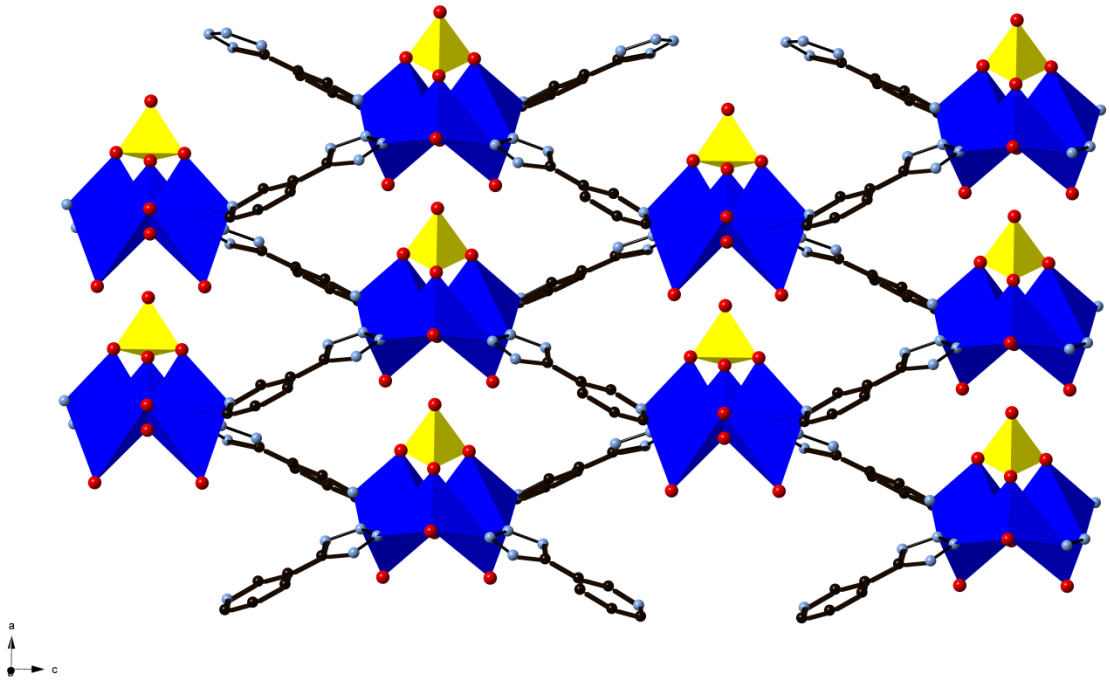

(c)

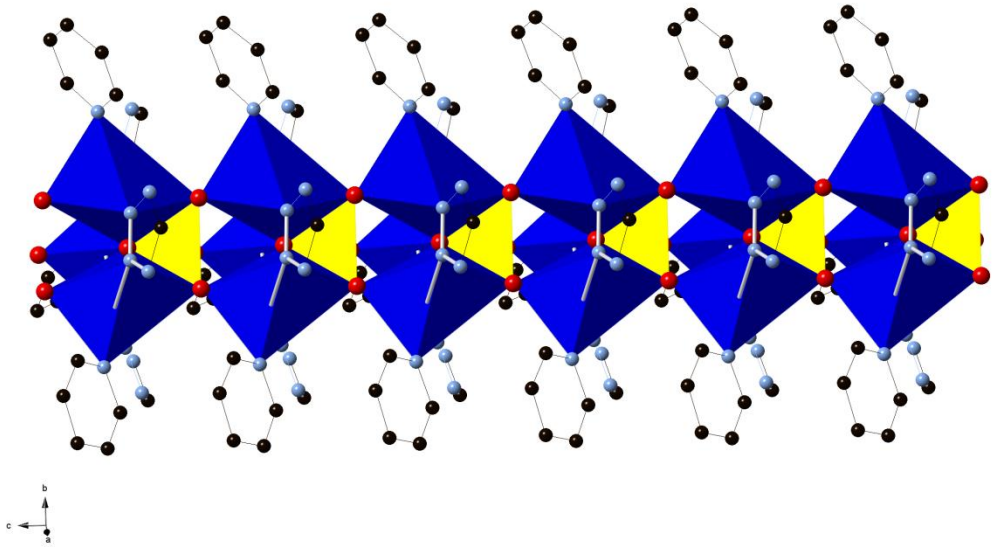

(d)

Figure 8.3: (a) The one-dimensional structure of $[CuCl_2(4\text{-Hpyrtet})]\cdot 0.5H_2O$. Chlorine atoms shown as green spheres; the hydrogen atom bound to the pyridyl nitrogen shown as a pink sphere; copper, dark blue spheres; nitrogen, light blue spheres; carbon, black spheres. (b) A view of the two-dimensional structure of $[Cu_2I_2(4\text{-Hpyrtet})]$. Iodide atoms shown as purple spheres; the hydrogen atom bound to the pyridyl nitrogen shown as a pink sphere; copper, dark blue spheres; nitrogen, light blue spheres; carbon, black spheres. (c) Mixed polyhedral and ball and stick representation of the structure of $[Cu_3(OH)_2(H_2O)_3(3\text{-pyrtet})_2(SO_4)]$. Color scheme: copper, blue polyhedra; sulfur, yellow tetrahedra; oxygen, red spheres; nitrogen, light blue spheres; carbon, black spheres. (d) A view of the $\{Co_3(PO_4)\}_n^{3n+}$ chain substructure. Color scheme: copper, blue polyhedra; phosphorous, yellow tetrahedra; oxygen, red spheres; nitrogen, light blue spheres; carbon, black spheres.

While sulfate often adopts this capping motif, in a study of the M(II)/azole/SO_4^{2-} family of compounds, sulfato groups can show a variety of bridging modes, including bidentate, tridentate and tetradentate geometries as observed in the structures of $[Co_4(prztet)_6(SO_4)(H_2O)_2]$, . $[Co_2(4\text{-pyrtet})(SO_4)(OH)(H_2O)]\cdot 1.5H_2O$, and $[Ni_5(3\text{-pyrtet})_4(SO_4)_2(OH)_2\ (H_2O)_2]\cdot H_2O$, respectively. An added factor contributing to the structural variety of this family of compounds is the incorporation of aqua and hydroxide ligands which can serve as terminal or bridging groups. $Co_2(4\text{-pyrtet})(SO_4)(OH)(H_2O)]\cdot 1.5H_2O$ and $[Ni_5(3\text{-pyrtet})_4(SO_4)_2(OH)_2\ (H_2O)_2]\cdot H_2O$ exhibit the presence of sulfato, hydroxy and aqua ligands. In the case of $[Co_3F_2(SO_4)(3\text{-pyrtet})_2(H_2O)_4]$, the hydroxy groups have been replaced by fluoride, further complicating the compositional and structural chemistry.

The dramatic effects that SO_4^{2-} has on the structure and properties of the composite material encourages investigation into the structural chemistry of systems featuring PO_4^{3-}, a structural analog of sulfate, as a coordinating anion. In a study replacing sulfate with phosphate, two novel three-dimensional structures of $[Co_3(4\text{-pt})_3(PO_4)]$ and $[Co_3(H_2O)_4(4\text{-pt})_2(HOPO_3)_2]$ were synthesized. The first exhibits a variation the same recurrent structural building block, the $\{M_3(\mu_3\text{-o})\}$ subunit, most commonly encountered as the $\{M_3(\mu_3\text{-oxo})\}$ and $\{M_3(\mu_3\text{-hydroxo})\}$ moieties as in the sulfate containing materials of this study. In this case; however, the trinuclear

subunit is present as part of a structurally complex inorganic $\{Co_3(PO_4)\}_n^{3n+}$ chain **(see Figure 8.3d)**. The second structure is also composed of trinuclear units that extend into $\{Co_3(H_2O)_4(HOPO_3)_2\}_n^{2n+}$ layers, linked through buttressing 4-pyridyltetrazolate ligands. In both cases, the variable protonation possibilities for the $H_xPO_4^{3-x}$ component, and the flexibility of the M-O-P bond angle results in a rather unpredictable chemistry.

8.4.2 Embedded Metal/Azolate Clusters

A recurrent theme of the structural chemistry of the materials of this study is the presence of embedded transition metal/tetrazolate clusters as architectural motifs, with the identity of the anion acting as a significant structural determinant. The range of component substructures of this study further reinforces this observation through a variety of cluster, chain, and layered structural motifs. As noted previously, in the absence of coordinating anion [Cu(3-pyrtet)$_2$] is composed of isolated square planar copper atoms, whereas introduction of either chloride or iodide into the parent compound results in copper chain and layered substructures, respectively, in which bridging anions enhance the complexity of the products in both instances. This is further illustrated by the rather complicated structure of $[Co_2(4\text{-pyrtet})(SO_4)(OH)(H_2O)]\ 1.5H_2O$ which is constructed from $\{Co_2(\text{tetrazolate})(SO_4)(OH)H_2O)\}_n$ chains as a secondary building unit. In this case, the chain itself is composed of another building unit, the common $\{M_3(\text{azole})_3(OH)\}^{2+}$ cluster motif in which each cobalt triad is capped by a sulfato group **(see Figure 8.4)**.

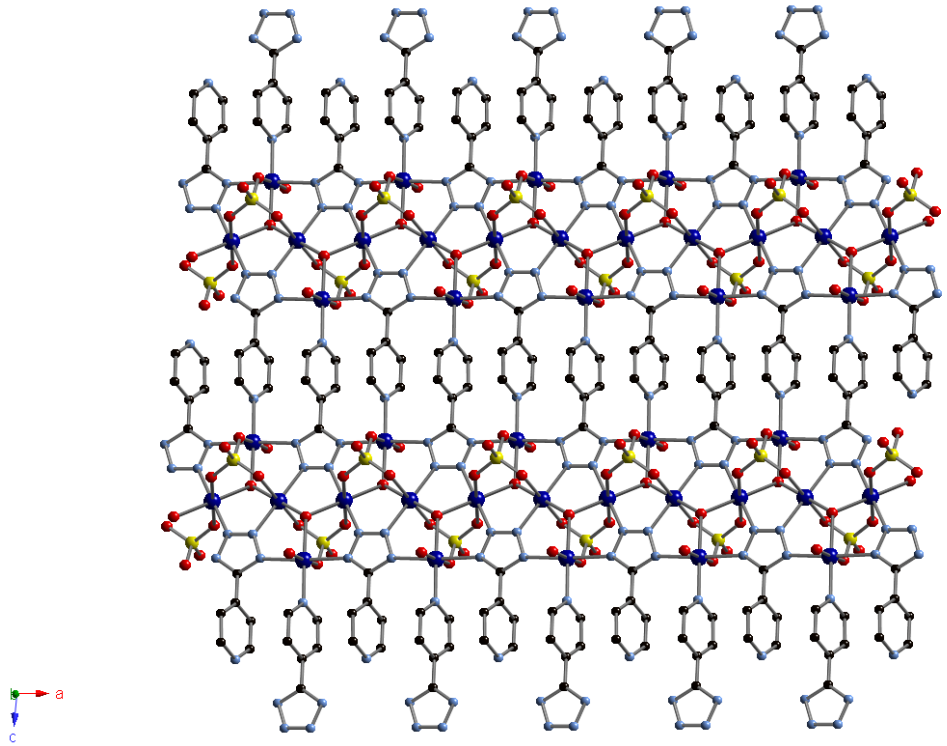

Figure 8.4: Ball and stick representation of the two-dimensional structure of $[Co_2(4\text{-pyrtet})(SO_4)(OH)(H_2O)]\bullet 1.5H_2O$ in the ac plane. Color scheme: cobalt, blue spheres; sulfur, yellow spheres; oxygen, red spheres; nitrogen, light blue spheres; carbon, black spheres.

The variety in cluster and chain substructures is apparent in the building units observed in a series of materials of the general type M(II)/tetrazolate/anion featuring dipodal ligands where M(II) = Co, Ni, Zn and Cd. $[Co_5F_2(dbdt)_4(H_2O)_6]\cdot 2\ H_2O$ is three-dimensional and exhibits a chain structure that is constructed from secondary building units of pentanuclear $\{Co_5F_2(tetrazolate)_8(H_2O)_6\}$ clusters. Similarly, $[Co_4(OH)_2(SO_4)(bdt)_2(H_2O)_4]$ and $[Co_3(OH)(SO_4)(btt)(H_2O)_4]\cdot 3H_2O$ manifest tetranuclear and trinuclear Co(II) clusters, respectively. In $[Co_4(OH)_2(SO_4)(bdt)_2(H_2O)_4]$ the tetranuclear core consists of two $\{Co_3(\mu^3\text{-}OH)\}$ triads fused at a common edge and the trinuclear building units of $[Co_3(OH)(SO_4)(btt)(H_2O)_4]\cdot 3H_2O$ grow to $\{Co_3(OH)(SO_4)(tetrazolate)_3\}_\infty$ chains. A tetranuclear motif is also observed in the structure of $(Me_2HN_2)_3[Cd_{12}Cl_3(btt)_8(DMF)_{12}]\cdot 12\ DMF\cdot 5MeOH$.

Finally, in the absence of coordinating anion, the structure of $[Co_2(H_{0.67}bdt)_3] \cdot 20\ H_2O$ is not constructed from cluster substructures but instead features the common $\{M_2(\mu^2\text{-tetrazolate})_3\}_\infty$ chain as a building block, further illustrating the dramatic structural consequences of coordinating anions.

8.5 Structural Trends and Properties

In the study of materials of the M(II)/tetrazolate/anion family, a wide array of structures was realized. The ability of azolate-containing anions to bridge multiple metal centers, combined with a variety of potential coordination modes adopted by the anionic component and the role of the cation itself, provides a library of structures with often complex connectivity and high dimensionality. While this limited library precludes a more complete systematic analysis, a number of recurrent structural trends have been realized including a variety of cluster, chain, and layered structural motifs .

As noted previously, one recurrent structural theme of the materials of this study is embedded transition metal/tetrazole clusters as architectural motifs where such clusters include bi-, tri-, tetra-, and pentanuclear building blocks. Variants of the common trinuclear $\{M_3(\mu_3\text{-}OH)\}$ core, specifically, are a consistent structural trend of this study. In this triad, azolate N,N′-bridging ligands coordinate to the $\{M_3(\mu_3\text{-}O(OH)\}$ core and a variety of additional peripheral or capping ligands may also be accommodated. The variability of the M-O bond distances within the triad combined with bridging anionic coligands such as capping sulfato- or phosphato-groups, results in a diversity of compounds featuring these triangulo cores and reflects the versatility of the unit in accommodating bridging and other peripheral ligands **(see Figure 8.5)**.

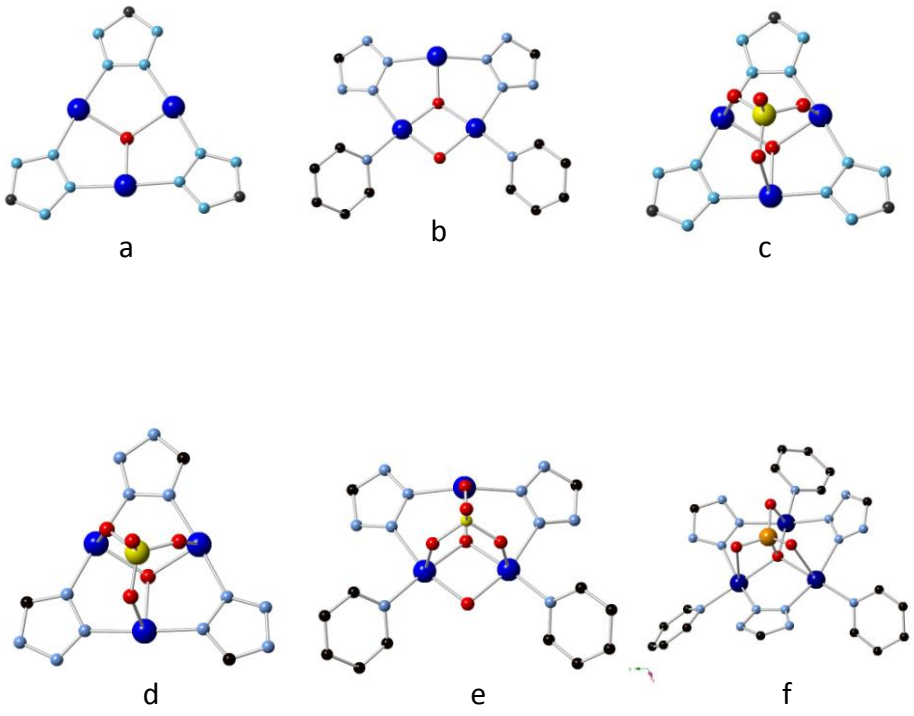

Figure 8.5: Tetrazole bridged triads as a common structural building unit. (a, b) Variants of the typical $M_3(\mu\text{-}O)$ cluster. (c) Incorporation of sulfate anion as a capping ligand in the trinuclear core. (d,e) The triad cores of $[Cu_3(OH)_3(H_2O)_3(3\text{-pyrHtet-}O)_3(SO_4)]$ and $[Cu_3(OH)_2(H_2O)_3(3\text{-pyrtet})_2(SO_4)]$ (f) The building unit of $[Co_3(4\text{-pt})_3(PO_4)]$, where phosphate provides a μ^3-oxygen donor at the center of a cobalt triad.

In addition, the $\{M_3(azole)_3(OH)\}^{2+}$ motif often manifests itself as subunits of secondary building units. For instance, in the structure of $[Co_2(4\text{-pyrtet})(SO_4)(OH)(H_2O)]1.5H_2O$ ($1.5H_2O$), $\{Co_2(tetrazolate)(SO_4)(OH)H_2O)\}_n$ chains exhibit the common $\{M_3(azole)_3(OH)\}^{2+}$ triads where each unit shares two Co sites with neighboring triads to generate the chain of hydroxy bridged cobalt centers. Similarly, in the structure of $[Ni_5(3\text{-pyrtet})_4(SO_4)_2(OH)_2(H_2O)_2]H_2O$ ($0.5H_2O$), the observed pentanuclear SBUs are constructed from two of the recurring $\{M_3(\mu^3\text{-}OH)(azolate)_3\}^{2+}$ building units sharing a common edge.

While cores featuring $\mu^3\text{-}OH^-$ and $\mu^3\text{-}O^{2-}$ ions are the most common, some $\mu^3\text{-}Cl^-$, $\mu^3\text{-}Br^-$, $\mu^3\text{-}OMe^-$ clusters have been described as well.[16-19] The $\{M_3(\mu^3\text{-}F\}$ cluster of $[Co_3F_2(SO_4)(3\text{-pyrtet})_2(H_2O)_4]$ and the isostructural $[Ni_3F_2(SO_4)(3\text{-pyrtet})_2(H_2O)_4]$, where the μ^3-oxo is replaced

by a μ^3-fluoride; however, has not been reported previously in the literature. In addition, in $[Co_3(4\text{-pt})_3(PO_4)]$, the $\{M_3(\mu^3\text{-O})(azolate)_3\}^{3+}$ subunit is present as part of an inorganic $\{Co_3(PO_4)\}_n^{3n+}$ chain where each triangular trinuclear unit is fused through corner-sharing interactions at the phosphate groups. Each phosphate ligand provides the μ^3-oxygen donor at the center of a cobalt triad, while the remaining three oxygen atoms of the tetrahedron each bridge a cobalt of a given triad to a cobalt of a neighboring cluster. What results is a rather complicated and interesting structural variant new to the library of $\{M_3(\mu_3\text{-O})\}$ cores and continues to be the subject of further study.

8.6 Future Work

The structural diversity of the materials of this study has encouraged us to pursue the development of materials of the M(II)/tetrazolate/anion family, where the anion is PO_4^{3-}, AsO_4^{3-}, MoO_4^{2-}, $Mo_xO_y^{n-}$, and VO_3^-. Preliminary studies of phosphate containing compounds $[Co_3(4\text{-pt})_3(PO_4)]$ and $[Co_3(H_2O)_4(4\text{-pt})_2(HOPO_3)_2]$ suggest that the variable protonation possibilities for the $H_xPO_4^{3-x}$ component, the structural influences of aqua coordination, and the flexibility of the M-O-P bond angle provides a number of structural determinants different from sulfate-containing materials. As AsO_4^{3-} can be considered an extended analog of phosphonate anion, the coordination chemistry of materials featuring arsonate are currently under investigation in a hope that a more systematic understanding of the complex chemistry will evolve as the structural data base for these systems expands.

Preliminary work on the consequences of introduction of $Mo_xO_y^{n-}$ is also under investigation in which the $Mo_xO_y^{n-}$ component, whether a cluster or oligomer, serves as an extended anion. Polyoxometalate clusters, in general, provide a chemically robust and structurally diverse scaffold upon which cationic building units can be constructed. In materials

of this study, metal oxide clusters are embedded in metal/tetrazolate cationic components where the anion serves as a structural directing agent in that the clusters must be accommodated within the cationic networks. For materials of the type M(II)/tetrazolate/anion, where the transition metal is Cu(II) and the tetrazolate ligand is 4, or 2- pyridyl tetrazole or pyrazine teterazole, the octamolybdate cluster, $Mo_8O_{26}^{4-}$ is a recurring structural motif. For example, the structure of $\{Cu_7(pyz)_5\}\{Mo_8O_{26}\}\cdot 2H_2O$ **(see Figure 8.6a)** is constructed from $Mo_8O_{26}^{4-}$ clusters and a $\{Cu_7(pyz)_5\}^{4+}$ network where the cluster is embedded within a three dimensional copper/tetrazolate framework that features both Cu(I) and Cu(II) copper sites **(see Figure 8.6b)**.

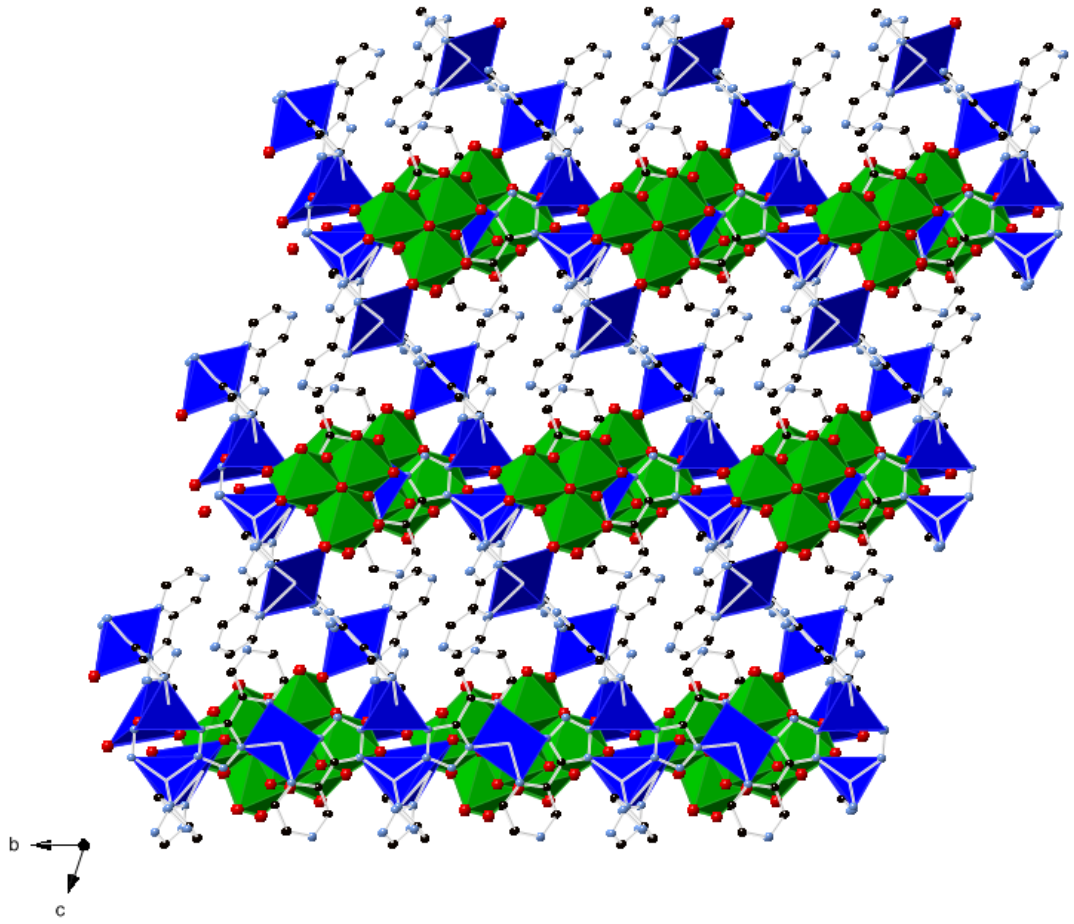

(a)

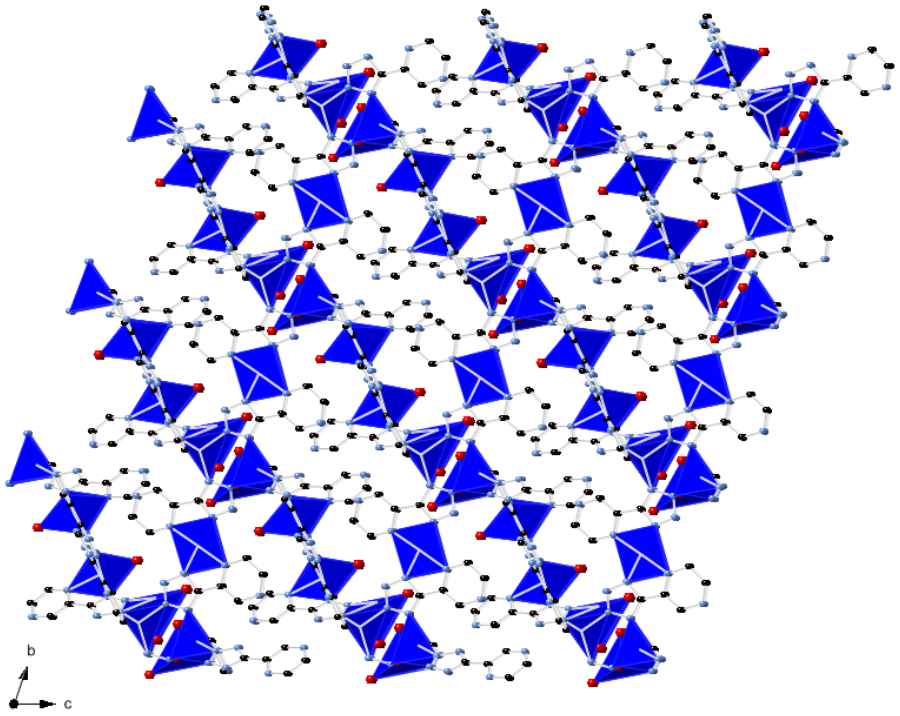

(b)

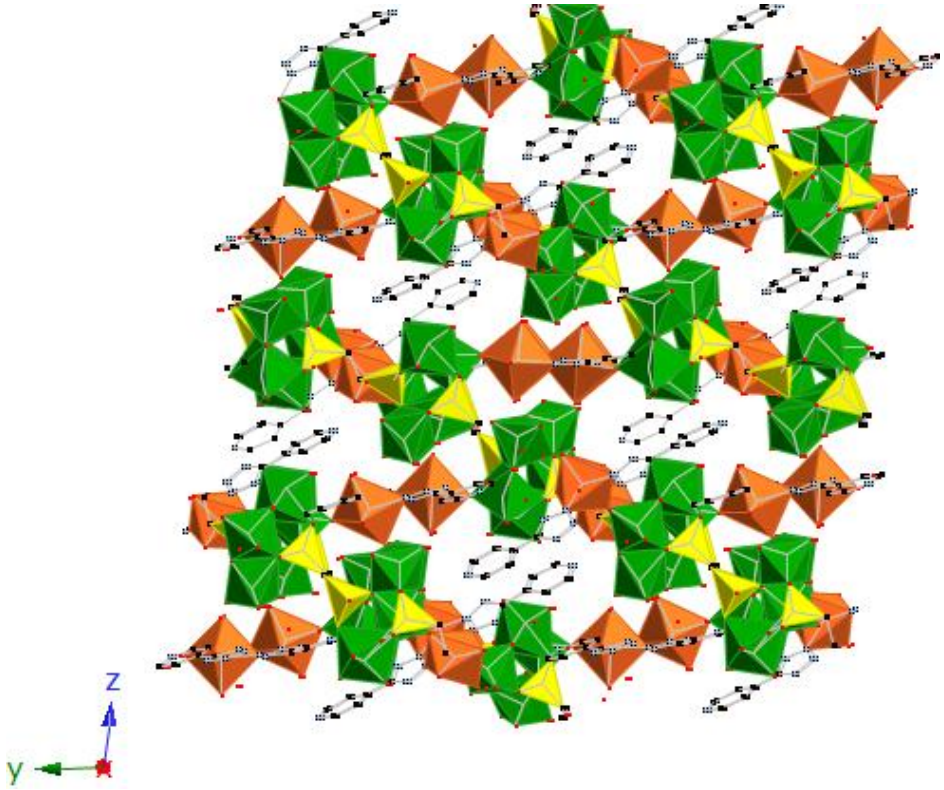

(c)

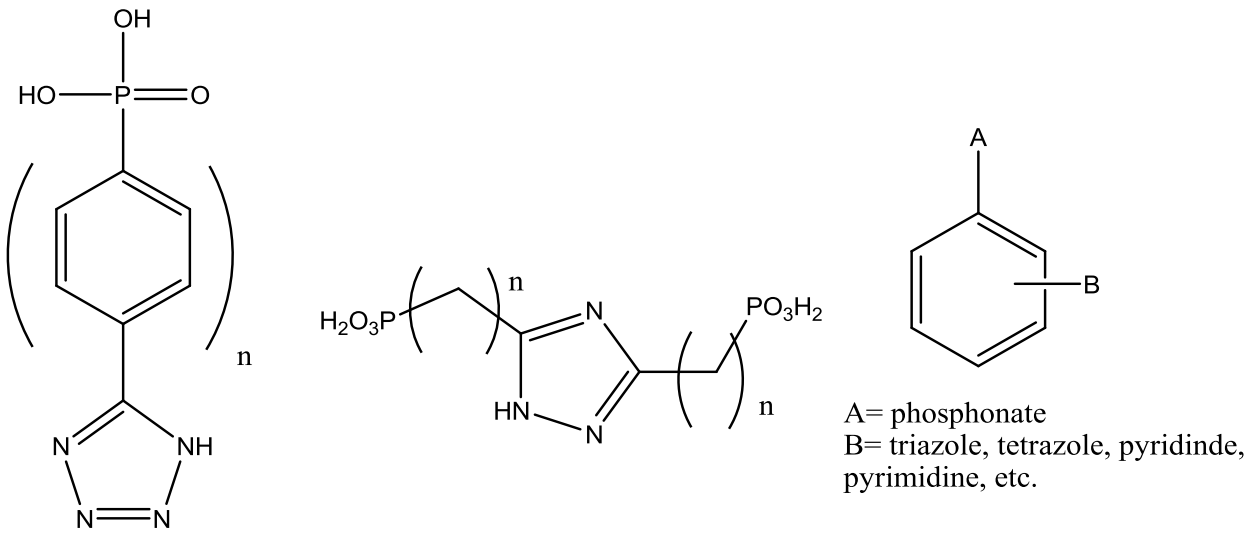

(d)

Figure 8.6: (a) The three dimensional structure of $\{Cu_7(pyz)_5\}\{Mo_8O_{26}\}\cdot 2H_2O$. Color scheme: copper, blue polyhedra; phosphorous, yellow tetrahedra; molybdenum, green polyhedra; oxygen, red spheres; nitrogen, light blue spheres; carbon, black spheres. (b) The three dimensional $\{Cu_7(pyz)_5\}^{4+}$ network. Color scheme: copper, blue polyhedra; phosphorous, yellow tetrahedra; molybdenumb, green polyhedra; oxygen, red spheres; nitrogen, light blue spheres; carbon, black spheres. (c) The three dimensional structure of $[\{Co_2(4\text{-}HPT)_2(H_2O)_6\}_3\ \{Mo_5O_{15}\{(O_3P(CH_2)PO_3)\}_3]\cdot 8H_2O$. Color scheme: cobalt, orange octahedra; phosphorous, yellow tetrahedra; molybdenumb, green polyhedra; oxygen, red spheres; nitrogen, light blue spheres; carbon, black spheres. (d) The bifunctional ligand, 4-(1H-tetrazol-5-yl)phenylphosphonic acid, and other representative multifunctional ligands.

Incorporation of diphosphonic acid ligands is also under investigation. In this case, the protypical chain motif of the type $\{Mo_5O_{15}(O_3PR)_2\}^{4-}$ is present as building units upon which metal/tetrazolate units are constructed. The result is a dramatically different structural chemistry in which the three dimensional copper/tetrazolate framework is instead replaced by cationic copper/tetrazolate triad units. In the case of $[\{Co_2(4\text{-}HPT)_2(H_2O)_6\}_3\ \{Mo_5O_{15}\{(O_3P(CH_2)PO_3)\}_3]\cdot 8H_2O$, the overall three dimensional structure is composed of $\{Mo_5O_{15}(O_3PR)_2\}^{4-}$ chains decorated by $\{Co_2(4\text{-}HPT)_2(H_2O)_6\}^{4+}$ units that coordinate to

adjacent chains **(see Figure 8.6c)**. A paralleled investigation of materials featuring different tetrazolate ligands and a variety of transition metal cations is currently under investigation.

Finally, introduction of modified azolate ligands into hybrid materials may also be explored. Innovative and multifunctional ligands can be designed where denticity, tether length, flexibility, and symmetry of the ligand may be varied. In addition, dipodal ligands may be synthesized with different donor groups so as to introduce the potential for bridging different transition metal or metal oxide sites into the products. In such a design, polyazaheteroaromatics, carboxylates, phosphates, or a combination of functional groups may be considered in an attempt to introduce multiple building blocks into a single material **(see Figure 8.6d)**. For example, the ligand 4-(1H-tetrazol-5-yl) phenylphosphonic acid contains tetrazolate and phosphonate functionalities at either terminus**.** In this design, different coordination preferences of each donor group are exploited in an attempt to construct a material that incorporates transition metal and metal oxide nodes at the tetrazolate and phosphonate termini respectively. The combination of a tetrazolate and phosphonate functionality into one single unit could bridge the gap between the growing fields of tetrazolate and phosphonate chemistry.

8.7 Final Considerations

In general, as the structural complexity of a material increases, so does its functionality. With this in mind, we have employed hydrothermal and solvothermal methods in an attempt to synthesize a variety of hybrid organic-inorganic materials of the type M(II)/tetrazolate/anion. The structural versatility of these materials reflects a number of structural determinants, including (i) the identity of the metal cation, (ii) the coordination preferences of the ligand, (iii) the presence of a secondary anion, and the (iv) hydrothermal reaction conditions themselves.

The small number of parameters surveyed in this study has resulted in a rich structural chemistry and while a number of structural motifs have been indentified, understanding of both synthetic conditions as well as design strategies of solid state materials remains rudimentary. General design strategies have been identified in the recurring structural trends reported in this study and by further adding to the library of hybrid organic-inorganic materials, it is hoped that an understanding of the mechanisms governing these complex systems may be attained. It is by this effort that we seek to one day predict products based upon rational design strategy so as to tune materials for applications such as sorption, catalysis, optical properties, and magnetism.

8.8 References

1. Ouellette, W.; Jones, S.; and Zubieta, J., *CrystEngComm*., **2011**, *13*, 4457.
2. Ouellette, W.; Darling, K.; Prosvirin, A.; Whitenack, K.; Dunbar, K.R.; and Zubieta, J., *Dalton Trans.*, **2011**, *40*, 12288.
3. Ouellette, W.; Yu, M.H.; O'Connor, C.J.; Hagrman, D.; and Zubieta, J., *Angew. Chem., Int. Ed*., **2006**, *45*, 3497.
4. Ouellette, W.; Prosvirin, A.V.; Valeich, J.; Dunbar, K.R.; and Zubieta, J., *Inorg. Chem*., **2007**, *46*, 9067.
5. Ouellette, W.; Galán-Mascarós, J.R.; Dunbar, K.R.; and Zubieta, J., *Inorg. Chem*., **2006,** *45*, 1909.
6. Ouellette, W.; Prosvirin, A.V.; Chieffo, V.; Dunbar, K.R.; Hudson, B.; and Zubieta, J., *Inorg. Chem*., **2006**, *45*, 9346.
7. Ouellette, W.; Hudson, B.S.; and Zubieta, J., *Inorg. Chem*., **2007**, *46*, 4887.
8. Ouellette, W.; Liu, H.; O'Connor, C.J.; and Zubieta, J., *Inorg. Chem*., **2009**, *48*, 4655.
9. Ouellette, W.; and Zubieta, J., *Chem. Commun*., **2009**, 4533.
10. Ouellette, W.; Prosvirin, A.V.; Whitenack, K.; Dunbar, K.R.; and Zubieta, J., *Angew. Chem., Int. Ed.*, **2009**, *48*, 2140.
11. Darling, K.; Ouellette, W.; Prosvirin, A.; and Zubieta, J., Polyhedron, **2012**, accepted.
12. Darling, K.; Ouellette, W.; O'Connor, C.; and Zubieta, J.; Inorg. Chim. Acta, **2012**, accepted.
13. Darling, K.; Ouellette, W.; and Zubieta, J., Inorg. Chim. Acta, **2012**, accepted.
14. Darling, K.; Ouellette, W.; Tomlinski, S.; and Zubieta, J., Inorg. Chim. Acta, **2012**, accepted.

15. Darling, K.; Ouellette, W.; and Zubieta, J., Inorg. Chim. Acta, **2012**, accepted.

16. Angaridis, P.A.; Baran P.; Boca, R.; Cervantes-Lee, F.; Haase, W.; Mezei, G.; Raptis, R.G.; and Werner, R., *Inorg. Chem.* **2002**, *41*, 2219.

17. Liu, X.; de Miranda, M.P.; McInnes, E.J.L.; Kilner, C.A.; and Halcrow, M.A., *Dalton Trans.*, **2004**, 59.

18. Mezei, G.; Raptis, R.G.; and Telser, J., *Inorg. Chem.*, **2006**, *45*, 8841.

19. Afrati, T.; Dendrinou-Samara, C.; Raptopoulou, C.; Terzis, A.; Tangoulis, V.; and Kessissoglou, D.P., *Dalton Trans.*, **2007**, 5156.

Kari Darling

Syracuse University, Department of Chemistry
111 College Place
Syracuse, NY 13244-4100
(315) 443-3731

3 Iris Ct Apt L
Acton, MA 01720
(315) 863-2355
kadarlin@syr.edu

Education

Ph.D., Chemistry, Syracuse University, Syracuse, NY
Expected graduation date: Dec 2012

Advisor: Professor Jon Zubieta

B.S., Chemistry, Lake Superior State University, Sault Ste. Marie, MI

Advisor: Judy Westrick

Work Experience

2012-present	Chemistry Instructor, Lexington High School
	Supervisor: Whitney Hagins
2009-2012	Graduate Research Assistant, Syracuse University
	Advisor: Dr. Jon Zubieta
2010-2012	X-ray Lab Administrator, Bruker-AXS D8 Advance
2008-2010	Teaching Assistant, Syracuse University
	Honors General Chemistry laboratory (2 semesters)

2007	Research Experience for Undergraduates, University of California, Santa Barbara
2006	Research Experience for Undergraduates, University of Kentucky

Publications

"A bimetallic oxide network constructed from oxomolybdoarsonate clusters and copper(II)-tetrapyridylpyrazine building blocks." Darling, Kari; Burkholder, Eric M.; Pellizzeri, Steven; Nanao, Max; Zubieta, Jon *Inorganic Chemistry Communications* (2011), 14(11), 1745-1748.

"Solid state coordination chemistry of the copper(II)/pyridyl- and pyrazine-tetrazole/sulfate system." Darling, Kari; Ouellette, Wayne; Prosvirin, Andrey; Dunbar, Kim; Zubieta, Jon. *Crysa. Growth and Design*. Accepted 2012.

"Hydrothermal synthesis and structures of materials of the M(II)/tetrazole/sulfate family (M(II) = Co, Ni; tetrazole = 3-and 4-pyridyltetrazole and pyrazinetetrazole)." Darling, Kari; Ouellette, Wayne; Prosvirin, Andrey; Dunbar, Kim; Zubieta, Jon. *Polyhedron*. Accepted 2012.

"One and two dimensional coordination polymers of substituted tetrazoles with cadmium." Darling, Kari; Ouellette, Wayne; Zubieta, Jon. *Inorganica Chemica Acta*. Accepted 2012.

"Solid state coordination chemistry of metal-azolate compounds: structural consequences of incorporation of phosphate components in the Co(II)/4-pyridyltetrazolate/phosphate System." Darling, Kari; Ouellette, Wayne; Zubieta, Jon. *Inorganica Chemica Acta*. Accepted 2012.

"One , two and three dimensional copper pyridyl-tetrazoles: the effects of anion incorporation." Darling, Kari; Ouellette, Wayne; Zubieta, Jon. *Inorganica Chemica Acta*. Accepted 2012.

"Hydrothermal chemistry of polyoxometalates and copper pyridyl building blocks." Darling, Kari; Zubieta, Jon. *Inorganic Chemistry Comumications.* Submitted 2012

"Solid state coordination chemistry of Cobalt(II) with Carboxyphenyltetrazoles." Ouellette, Wayne; Darling, Kari; Zubieta, Jon. *Inorganica Chemica Acta*. Accepted 2012.

"Syntheses, structural characterization and properties of transition metal complexes of 5,5'-(1,4-phenylene)bis(1H-tetrazole) (H_2bdt), 5',5''-(1,1'-biphenyl)-4,4'-diylbis(1H-tetrazole) (H_2dbdt) and 5,5',5''-(1,3,5-phenylene)tris(1H-tetrazole) (H_3btt)." Ouellette, Wayne; Darling, Kari; Prosvirin, Andrey; Whitenack, Kelly; Dunbar, Kim R.; Zubieta, Jon. *Dalton Transactions* (2011), 40(45), 12288-12300